

Wnt signalling in prostate cancer stem-like cells

Dr Reena Davda, MBChB, MRCP, PGCert HE, FRCR, PGDip Onc

Submitted for the degree of Doctor of Medicine by Research MD(Res) to
University College London

February 2018

Declaration

I, Reena Davda, confirm that the work presented in this thesis is my own, except the sequencing which was performed as a service. Where information has been derived from other sources, I confirm that this has been indicated in the thesis.

Abstract

The work reported in this thesis describes the characterisation of cell derived colonies from cancer cell lines and mechanisms of a key signalling pathway within these. PC3 cells were cultured at clonal density and resultant colony formation objectively described. Wnt signalling was investigated in colony types using a live $[Ca^{2+}]_i$ assay. Exploratory work regarding ion channel gene and protein expression in 3 prostate cancer cell lines was performed. Preliminary investigation on the effects of MPRC (membrane potential regulating compounds) was performed using a cell proliferation assay. PC3 prostate cancer cells form distinct colonies with different morphologies. These different colony types can be characterised using quantitative parameters such as cell density and percentage cellularity, unlike previously employed visual only characteristics. PC3 cells form two types of colonies from a single cell. In this thesis these are termed holo/meroclones and paraclones. Cells within both colony types respond to Wnt activation, demonstrated by a response in free intracellular calcium $[Ca^{2+}]_i$. In addition, there is a suggestion of increased expression of, and translocation into the nucleus of the transcription factor co-activator β -catenin again in response to both Wnt 5A and Wnt 9B in both colony types. The characteristics of Wnt induced calcium release vary between different types of colonies. This is the first report of Wnt mediated $[Ca^{2+}]_i$ release in response to both Wnt 5A and Wnt 9B in different PC3 colony types and the first report suggestive of β -catenin translocation following Wnt activation in colonies derived from stem-like cells.

Contents

List of Figures.....	7
List of Tables.....	11
Chapter 1: Introduction.....	15
1.1 The Prostate.....	15
1.2 Prostate cancer.....	17
1.3 Stem cells and cancer stem cells.....	18
1.3.1 Stem cells.....	18
1.3.2 Adult stem cells.....	18
1.3.3 Prostate stem cells.....	19
1.3.4 Cancer stem cells and prostate cancer stem cells.....	22
1.3.5 Prostate cancer cell line colonies.....	23
1.4 Wnt Signalling.....	26
1.4.1 Categorisation of Wnt pathways.....	26
1.4.2 Pathways of Wnt Signalling - The canonical (β -catenin) Wnt pathway.....	28
1.4.3 Pathways of Wnt signalling : The non - β -catenin mediated pathways.....	54
1.4.4 Pathways of Wnt signalling - A convergent Wnt pathway.....	58
1.5 Wnt signalling and cancer.....	59
1.5.1 De-regulated Wnt signalling and cancer.....	59
1.5.2 Wnt and solid cancers other than colorectal cancer.....	61
1.6 Wnt signalling in stem and cancer stem cells.....	69
1.6.1 Wnt in stem cells.....	69
1.7 Experimental aims.....	72
1.7.1 Hypothesis.....	72
1.7.2 Key objectives.....	73
Chapter 2: Materials and methods.....	74
2.1 Cell culture.....	74
2.1.1 Cell counting using a haemocytometer.....	74
2.2 Clonal expansion.....	75
2.2.1 Clonal expansion in 6 well plates.....	75
2.2.2 Clonal expansion with cells grown on FluoroDishes.....	75
2.3 Live cell free intracellular calcium ($[Ca^{2+}]_i$) imaging of colonies.....	76
2.4 Cell proliferation assays.....	77
2.5 Immunocytochemistry.....	78
2.5.1 Cell fixation.....	78

2.5.2	Cell staining	78
2.5.3	Imaging using confocal microscopy	79
2.6	Polymerase Chain Reaction (PCR)	79
2.6.1	Primer design	79
2.6.2	RNA extraction	80
2.6.3	Reverse transcription of RNA into cDNA	80
2.6.4	PCR	81
2.6.5	Agarose gel electrophoresis	83
2.6.6	Sequencing	83
Chapter 3:	PC3 prostate cancer colony formation and characterisation	85
3.1	Introduction	85
3.1.1	Hypothesis	86
3.1.2	Objectives	86
3.2	Materials and methods	87
3.2.1	Characterisation of colonies	87
3.2.2	Expression of stem cell genes in different populations of PC3 cells	87
3.2.3	Live cell calcium imaging and data analysis	88
3.2.4	Immunocytochemistry for β -catenin	90
3.2.5	Imaging and analysis of β -catenin immunostaining	91
3.3	Results	92
3.3.1	Colony formation	92
3.3.2	Expression of stem cell genes in different populations of PC3 cells	101
3.3.3	Wnt induced $[Ca^{2+}]_i$ release in PC3 cell line derived colonies	104
3.3.4	Expression of β -catenin in colonies with and without Wnt treatment and co-localisation of β -catenin in the nucleus	125
3.4	Discussion	135
3.4.1	Colony formation by PC3 cells	135
3.4.2	Stem cell gene expression in prostate cancer cell line colonies	137
3.4.3	Differential response to Wnts in cells of holo/meroclones and cells of paraclones	138
3.4.4	Expression and co-localisation of β -catenin in different colony types	141
3.5	Chapter 3 Conclusions	142
Chapter 4:	Expression of ion channels in prostate cancer cell lines and PC3 colonies	144
4.1	Introduction	144
4.1.1	Hypothesis	158
4.1.2	Objectives	158
4.2	Materials and methods	159

4.2.1	Ion channel genes	159
4.2.2	Immunostaining for ion channel proteins	165
4.2.3	Assessment of MPRCs on proliferation of cancer cell lines in whole populations of cells.....	166
4.3	Results	169
4.3.1	Characterisation of ion channel gene expression in 3 prostate cancer cell lines	169
4.3.3	Effect of treatment of MPRCs on proliferation of a population of PC3 cells	187
4.4	Discussion.....	193
4.4.1	Expression of ion channel genes.....	194
4.4.2	Effect of MPRCs on cell proliferation	195
4.5	Chapter 4 Conclusions.....	196
Chapter 5: Discussion and conclusions.....		199
5.1	Summary of findings	199
5.2	Wnt signalling in PC3 colonies	200
5.3	Ion channels and cancer	202
5.4	Ion channels in prostate cancer cell lines and cancer stem cells	202
5.5	MPRCs as a therapy	205
5.6	Further research.....	205
5.7	Conclusions.....	207
References.....		208

List of Figures

Figure 1. Anatomy of male reproductive system (from (http://www.salisbury.nhs.uk))	15
Figure 2. Zones of the prostate gland and incidence of hyperplasia, high grade intra-prostatic neoplasia and cancer occurring within these zones.	16
Figure 3. Adult stem cell hierarchy and the process of self-renewal of a stem cell and the process of differentiation through cell division into cells of distinct lineage.	19
Figure 4. Image showing 3 morphologically different colony types formed from culture of single cell plated PC3 cells.....	23
Figure 5. Colony morphologies observed in prostate cancer cell lines DU145 and LNCaP.	25
Figure 6. Figure summarising inactive canonical signalling (left) and active canonical signalling with target genes under the transcriptional regulation of the β -catenin (right).....	54
Figure 7. Plotted waveform of intensity ratio against time obtained for one cell taken as a region of interest.....	89
Figure 8. Image of 2 distinct PC3 cell colonies formed after 10 days culture at clonal density.....	93
Figure 9. Sequential imaging using incucyte™ live image acquisition system showing colony formation by a single cell over a 10 period.....	94
Figure 10. Representative colony imaged using a bright field microscope.....	96
Figure 11. Histogram showing the distribution of PC3 colony diameters.....	99
Figure 12. Agarose gel electrophoresis of PCR products from holo/meroclones (a) and paraclones (b).	103

Figure 13. A holo/meroclone imaged for intensities of (a) Fluo-4 and (b) Furared with a selection of cells sampled as regions of interest for analysis.	105
Figure 14. Changing intensity of Fluo-4 in cells of a holo/meroclone colony over time following treatment with Wnt5A.	106
Figure 15. Intensity ratio of Fluo-4 : furared in a single cell region of interest against time following wnt treatment with a gaussian fit curve.	107
Figure 16. Numbers of cells within holo/meroclones and paraclones demonstrating a wnt induced free intracellular calcium release $[Ca^{2+}]_i$ following treatment with Wnt 5A and Wnt 9B.	110
Figure 17. $[Ca^{2+}]_i$ response rise time (a), dwell time (b), fall time (c), duration primary response (d), and duration total response (e) in holo/meroclones compared to in paraclones following treatment with Wnt 5a (left column) and Wnt 9b (right column).	115
Figure 18. Calcium response rise time (a), dwell time (b), fall time (c), duration primary response (d), and duration total response (e) following treatment with Wnt 5a compared to Wnt 9b in holo/meroclones (left) and paraclones (right).	120
Figure 19. Experiments conducted as negative controls using no primary antibody and a flurophore secondary antibody (Cy 5 goat anti-mouse IgG) counter stained with DAPI (blue) show that there was no non-specific binding of the secondary antibody.	126
Figure 20. Immunocytochemistry shows presence of β -catenin in PBS treated cells of PC3 holo/meroclones.	128
Figure 21. Immunocytochemistry on cells of PC3 holo/meroclones shows strong staining of β -catenin, and suggests increased nuclear β -catenin following treatment with Wnt 5A.	129

Figure 22. Immunocytochemistry on cells of PC3 holo/meroclones shows strong staining of β -catenin and suggests increased nuclear β -catenin following treatment with Wnt 9B ligand.	130
Figure 23. Immunocytochemistry shows presence of β -catenin in PBS treated control cells of PC3 paraclones.	132
Figure 24. Immunocytochemistry on cells of PC3 paraclones shows strong staining of β -catenin, and suggests increased nuclear β -catenin following treatment with Wnt 5A.	133
Figure 25. Immunocytochemistry on cells of PC3 paraclones shows significant staining of β -catenin, and suggests increased nuclear β -catenin following treatment with Wnt 9B ligand.	134
Figure 26. Two PC3 colonies in a colony forming assay.	136
Figure 27. Agarose gel electrophoresis images from PC3 cell pcr reactions.	170
Figure 28. Immunocytochemistry and optimisation of primary antibody demonstrating expression of KNCK-1 in PC3 cells.	179
Figure 29. Immunocytochemistry and optimisation of primary antibody demonstrating expression of ORAI-3 in PC3 cells.	180
Figure 30. Immunocytochemistry showing expression of KCNK-1 (green) in PC3 cells of a holo/meroclone colony.	181
Figure 31. Immunocytochemistry showing expression of KCNK-1 (green) in PC3 cells of a paraclone colony.	182
Figure 32. Immunocytochemistry showing expression of ORAI-3 (green) in PC3 cells of a holo/meroclone colony.	183
Figure 33. Immunocytochemistry showing expression of ORAI-3 (green) in PC3 cells of a paraclone colony.	184

Figure 34. Immunocytochemistry showing negative controls with lack of flurophore secondary antibody signal in absence of primary antibody in a PC3 holo/meroclone and PC3 paraclone. 186

Figure 35. Graph showing the % confluence against time of population of PC3 cells when treated with isradipine or DMSO control. 188

Figure 36. Graph showing the % confluence against time of population of PC3 cells when treated with amlodipine or DMSO control. 190

Figure 37. Graph showing the % confluence against time of PC3 cells when treated with cadmium chloride or DMSO control. 191

Figure 38. Graph showing the confluence % against time of PC3 cells when treated with isradipine 100 μm , isradipine 10 μm and isradipine 5 μm or DMSO control. 193

List of Tables

Table 1. Survival of PC3 cell colonies.	24
Table 2. Putative target genes under the transcriptional regulation of the B-catenin co-transcription factor.	33
Table 3. Wnt signalling in solid cancers.	62
Table 4. Mixture composition used for reverse transcription reactions.	80
Table 5. Reaction mixture made up in each tube for PCR reaction.	81
Table 6. Programme for thermal cycler.	82
Table 7. Antibodies and dilution used for β -catenin immunocytochemistry.	91
Table 8. Characteristics of colonies formed by PC3 Cells.	98
Table 9. Colony diameter; subjective morphology; % cellularity and the arc sin of these values for a random selection of 13 colonies observed and analysed at day 10 of culture.	101
Table 10. Summary of expression of 4 stem cell genes: BM1, OCT 4, BCRP and HSOX in cells of holo/meroclones and paraclones with 3 experimental repeats.	102
Table 11. Response of cells within holo/meroclones and paraclones to Wnt 5A and Wnt 9B.	109
Table 12. Summary of the rise, dwell and fall times for $[Ca^{2+}]_i$ of cells within holo/meroclones and paraclones in response to Wnt 5A and Wnt 9B presented as mean \pm SE.	111
Table 13. Expression of ion channel genes in solid cancers.	145
Table 14. Summary of ion channel genes known to be associated with malignancy and characterised further in this study.	155

Table 15. Calcium channel blockers, their physiological effect and clinical indications.	156
Table 16. Oligonucleotide sequences designed for PCR of ion channel genes, and expected size for each product.	160
Table 17. Concentrations of primary antibody anti-ORAI-3 tested in optimisation process for immunocytochemistry.	165
Table 18. Concentrations of primary antibody anti-KCNK1 tested in optimisation process for immunocytochemistry.	166
Table 19. MPRCs used in cell proliferation experiments and their molecular formula, mass, structure and concentrations tested in proliferation experiments.	167
Table 20. Gene expression in the three cell lines PC3, DU145 AND LNCaP, performed in triplicate in 3 cell passages.	173
Table 21. Summary of identified ion channel genes in 3 prostate cancer cell lines.	176
Table 22. Ion channel genes expressed in all 3 cell lines PC3, LNCaP and DU145 and confirmed on sequencing.	177

Abbreviations

°C	Degree Celsius
µg	Microgram
µl	Microliter
BSA	Bovine serum albumin
DAPI	4',6-diamidino-2-phenylindole
Fz	Frizzled
PC3	Human prostate adenocarcinoma cell line
PFA	Paraformaldehyde
PIN	Prostatic intraepithelial neoplasia
Wnt	derived from <i>Drosophila wingless</i> and <i>int-1</i>

Acknowledgements

I would like to express my sincere gratitude to Dr Aamir Ahmed and Professor John Masters for their supervision, guidance and help during this project. I am grateful to Dr Christopher Thrasivoulou of UCL Imaging Facility for his help with immunochemistry and confocal microscopy. I am also grateful to all my colleagues in the laboratory for their help, support and friendship during this project.

I am thankful for the support of my family. Lastly, I am extremely grateful to the Prostate Cancer Research Centre charity for funding this project and without their support this project would not be possible.

Chapter 1: Introduction

1.1 The Prostate

The prostate is a small gland forming part of the male reproductive system. The function of the prostate gland is to produce secretions which form constituents of semen. The prostate gland lies beneath the bladder and anterior to the rectum as shown in Figure 1.

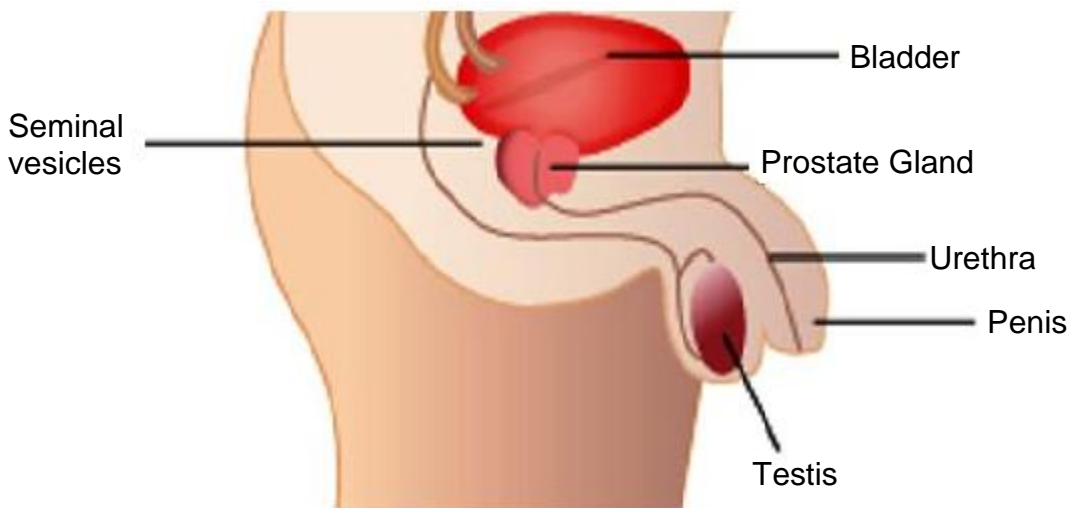
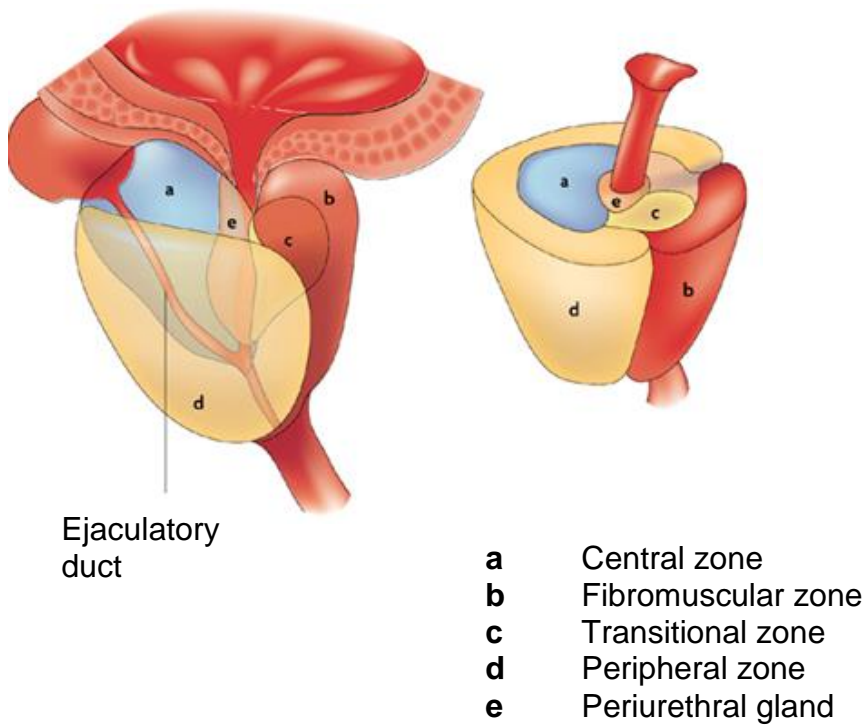


Figure 1. Anatomy of male reproductive system (From (<http://www.salisbury.nhs.uk>))

The prostate gland has been divided into different anatomical lobes or zones (Griffiths, 1889; Walker, 1904). The former consists of the anterior lobe (or isthmus), posterior lobe, lateral lobes and median lobe. Zones include the peripheral zone, the central zone, the transition zone and the anterior zone (McNeal, 1988). As shown in Figure 2, the majority of prostate cancers are thought to occur in the peripheral zone, with cancers arising less commonly in the transition zone and very rarely in the central zone (De Marzo et al., 2007).



Pathology	Prostate zone		
	Peripheral	Transition	Central
Benign prostatic hyperplasia	None	High prevalence	Low prevalence
High grade intra-prostatic neoplasia	Medium - high prevalence	Medium prevalence	Low prevalence
Prostate carcinoma	Medium - high prevalence	Medium prevalence	Absent

Figure 2. Zones of the prostate gland and incidence of hyperplasia, high grade intra-prostatic neoplasia and cancer occurring within these zones.

Modified from: (De Marzo et al., 2007).

1.2 Prostate cancer

Prostate cancer is the most frequently diagnosed cancer in men in the UK with 1 in 8 men receiving a diagnosis of prostate cancer at some point in their lives (Prostate cancer UK, 2015). In 2014 there were over 46 000 men diagnosed with prostate cancer in the UK and over 11 000 deaths from the disease (CRUK, 2014).

Internationally, prostate cancer represents one fifth of all male cancer diagnoses with over 1,100,000 men around the world diagnosed in 2012 (Ferlay et al., 2010; WCRF, 2015

) A proportion of patients who initially received curative treatment will relapse and a further group have advanced metastatic disease at presentation.

Standard initial treatment in this situation is hormone therapy with androgen deprivation therapy. This may be achieved either surgically with bilateral orchidectomy or more commonly medically with either luteinising hormone releasing hormone (LHRH) agonists or antagonists (Huggins, 1942; Klotz et al., 2008).

Typically, after a 2 – 3 years of hormone treatment, prostate cancer becomes resistant to androgen deprivation therapy (Sharifi et al., 2010). Advances in past decade with new agents such as abiraterone and enzalutamide have meant more systemic treatments are available for patients with castrate resistant prostate cancer (Beer et al., 2014; Ryan et al., 2013). Recent trials such as the STAMPEDE study have also demonstrated the benefit of augmentation of systemic therapy with the addition of abiraterone or docetaxel in the castrate sensitive setting in both progression free and overall survival (James et al., 2017; Sweeney et al., 2015).

However, a clinical need remains for effective, non-toxic, targeted therapies to treat and improve outcomes for men with high risk and metastatic prostate cancer.

1.3 Stem cells and cancer stem cells

1.3.1 Stem cells

Stem cells are undifferentiated cells which demonstrate an ability to undergo self-renewal and potency (Perin and Silva, 2006). The former relates to repeated cell division producing the same undifferentiated cell type. Potency is the ability to produce terminally differentiated cells of different lineages. Stem cells have been divided into two types: embryonic stem cells (totipotent or pluripotent) are isolated from the inner cell mass of blastocysts and adult stem cells (multipotent) found in various adult tissues (Evans and Kaufman, 1981).

1.3.2 Adult stem cells

Adult stem cells demonstrate self-renewal and potency - the potential to differentiate to form all the functional cell types within a tissue (Mackillop et al., 1983; Pittenger et al., 1999). Stem cells are maintained by symmetrical cell division producing two identical stem cell daughters (Mackillop et al., 1983). Asymmetric division of stem cells may occur and this produces 2 cells with different characteristics: one cell identical to the original stem cell and a second cell programmed to differentiation (Miller et al., 2005; Pittenger et al., 1999). Adult stem cells maintain organ homeostasis that involves continuous replacement of differentiated cells (Mackillop et al., 1983). Stem cells differentiate into transit amplifying cells which then differentiate further into multiple cell types depending on this cascade of differentiation (Miller et al., 2005). As these cells progressively differentiate they become irreversibly committed to one of that particular tissue's cell type. This hierarchal process of stem cell maintenance and differentiation is described in Figure 3.

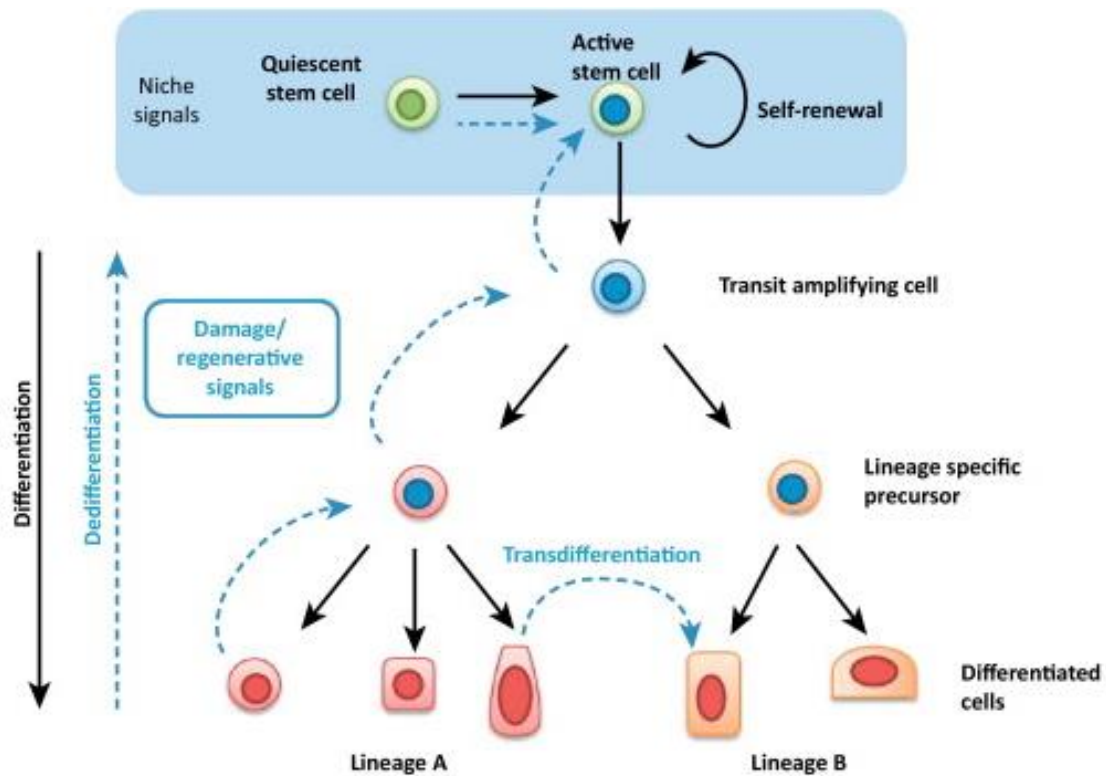


Figure 3. Adult stem cell hierarchy and the process of self-renewal of a stem cell and the process of differentiation through cell division into cells of distinct lineage.

Proliferating cells are indicated with a blue nucleus, differentiated cells with a red nucleus. Blue arrows represent cell damage and regeneration. Figure adapted from Tetteh et al (Tetteh et al., 2015).

1.3.3 Prostate stem cells

Stem cells and stem cell markers have been most extensively characterised in systems with active self - renewal and cell turnover, such as the haemopoietic system and gastrointestinal system (Scoville et al., 2008; Zon, 2008). However, since Professor Donald Coffey's important early work in the 1980s we now have a body of evidence for stem cells in the prostate.

The prostate gland increases in size with age. One theory states that with increasing age there may be an increase in the number of prostatic stem cells or in the clonal expansion of stem cells into amplifying and transit cells (Isaacs and Coffey, 1989). Early work suggesting the prostate gland has a subpopulation of cells capable of self-renewal and differentiation was in the prostate of rats, where androgen

suppression induced apoptosis of secretory epithelial cells and androgen replenishment induced cell proliferation (Evans and Chandler, 1987). This cycle of prostate regression and regeneration can be repeated more than 30 times, indicating the existence of a population of surviving stem cells (Isaacs et al., 1987).

Prostate stem cells are thought to differentiate into basal, luminal secretory and neuroendocrine distinct lineages (Kasper, 2008). Of these, prostate stem cells are thought to reside in the basal compartment (Rodgers CH, 1987). In human prostate tissue, the majority of proliferative cells are basal cells expressing Bcl-2 and cells where overexpressing of Bcl-2 gene protein had reduced levels of nuclear androgen receptor (Bonkhoff et al., 1998).

De Marzo et al (De Marzo et al., 1998) investigated the role expression of p27^{Kip1} may play in prostate carcinogenesis. In human benign epithelial prostate tissue widespread moderate to strong nuclear staining of p27^{Kip1} was observed whilst the potential stem cell harbouring basal cell compartment showed lower and more variable pattern of p27^{Kip1} expression. As well as basal cells, high-grade prostatic intraepithelial neoplasia and invasive carcinoma also demonstrated down-regulation of p27^{Kip1} compared with the surrounding normal secretory cells (De Marzo et al., 1998).

Shalken et al (Schalken and van Leenders, 2003) have described variability in expression of keratin (K) markers in the prostate based upon anatomical location as well as degree of cell differentiation. Basal cells strongly expressed K5, but only weakly expressed K18. Conversely, luminal cells strongly expressed K18. A proportion of basal cells coexpressed K5 and K14. Poorly differentiated stem cells in the basal layer were positive for K5 and K14, with weak expression for K18 whilst moderately differentiated cells expressed K5 and K18. The authors noted that prostate cancers demonstrated the same pattern of keratin expression as intermediate differentiated stem cells, potentially suggesting the role of these cells in prostate cancer carcinogenesis (Schalken and van Leenders, 2003).

In a mouse model, PTEN was found to regulate p63-positive prostatic basal cell proliferation without blocking differentiation (Wang et al., 2006). Basal cell proliferation was observed in this model with increased proliferation of a subpopulation of Sca-1 and Bcl-2-positive prostate stem/progenitor cells (Wang et al., 2006).

Prostate stem cells are therefore thought to demonstrate distinctive expression of proliferation markers including telomerase, p63 and p27Kip1 and identification of these markers may therefore potentially be used to identify stem cells (Kasper, 2008).

Prostate stem-like cells with increased prostate regenerative capacity have been identified with specific markers from mice (Xin et al., 2005). Using a single cell suspension derived from murine prostates, Sca-1+ cell fractions implanted under the kidney capsule of severe combined immunodeficient (SCID) mice produce much larger grafts with more prostatic structures than implantation of Sca-1- cell fractions (Xin et al., 2005). Other markers identifying cells with colony forming efficiency include $\alpha 2\beta 1$, CK5 / CK14 with lack of expression of markers prostate specific antigen and prostatic acid phosphatase (Collins et al., 2001) and CD133 expression within a cell population expressing $\alpha 2\beta 1$ (Richardson et al., 2004). Overexpression of the transcription factor NANOG in cancer cell lines Du145, LNCaP and MCF-7 have led to increased drug resistance and other pro-tumorigenic effects associated with upregulation of CD133 (Jeter et al., 2011).

Stem cell-like ability of self-renewal of murine prostate cells has been demonstrated *in vitro* using a sphere-forming assay as well as in mouse *in vivo* (Xin et al., 2007). Only a proportion of murine prostate epithelial cells were able to form spheroid structures when cultured in Matrigel, and when dissociated these cells were able to produce further spheres (Xin et al., 2007). Expression of CD24, CD49f, and Sca-1 was present in sphere forming cells. These sphere forming cells were tested in an *in vivo* assay and were able to form prostate murine tissue when injected subcutaneously into SCID mice (Xin et al., 2007).

Further work undertaken by my group aimed to determine which of these markers were most associated with cells which demonstrated stem-cell like characteristics such as spheroid colony-forming ability (Yamamoto et al., 2012). Subpopulations of cells positive for the previously noted markers: CD49f+, CD44+, and CD133+ differed in their propensity to behave as spheroid colony-forming cells. Expression of CD49f+ was highly accurate in identifying cells which were stem cell like in their spheroid colony-forming ability (Yamamoto et al., 2012).

1.3.4 Cancer stem cells and prostate cancer stem cells

The existence of cancer stem cells has also been proposed as a theory to explain a population of cancer cells with stem cell-like characteristics (Lapidot et al., 1994; Mani et al., 2008; Tai et al., 2005). Cancer stem cells are described as being a subpopulation of cells within a tumour able to self-renew and form a heterogeneous population of cancer cells (Clarke et al., 2006). The heterogeneity of cancer cells produced from cancer stem cells results in the disparate biology of cells observed within a tumour (Clarke et al., 2006; Reya et al., 2001a). There are parallels in the capabilities of self-renewal in stem cells and cancer stem cells (Reya et al., 2001a).

Putative prostate cancer stem cells have been sorted and enriched from a population of cells using their cell surface marker expression. Cells of primary human prostate cancers and prostate cancer cell lines isolated by fluorescence-activated cell sorting (FACS) for the presence of CD44+/ α 2 β 1hi/CD133+ demonstrate increased colony forming and sphere forming efficiency (Collins et al., 2005; Gu et al., 2007). For example, in experiments using cell lines and cells derived from human prostate cancer xenograft tumours, Patrawala et al (2006), reported that prostate cancer cells which are CD44(+) demonstrate increased proliferation and clonogenic, tumorigenic, and metastatic characteristics compared with CD44(-). CD44(+) cells also express elevated mRNA levels of stem cell genes such as Oct-3/4, BMI, and β -catenin (Patrawala et al., 2006). In addition, CD44(+) prostate cancer cells can produce CD44(-) cells *in vitro* and *in vivo* and CD44(+) cells which are AR(-) and can differentiate into AR(+) cells (Patrawala et al., 2006).

In experiments utilizing *in vitro* culturing techniques, the ability of a single cell to form a colony can be assessed (Puck and Marcus, 1955). Colony forming assays are commonly used to differentiate between cell types; it has been proposed that in cell culture cancer stem-like cells have the ability to form colonies derived from single cells (Pfeiffer and Schalken, 2010).

1.3.5 Prostate cancer cell line colonies

PC3 is a human prostate cancer cell line originating from a bone metastasis in a patient with advanced prostate cancer (Kaighn et al., 1979). The colony forming ability of PC3 cells and the differential behaviours of distinct colonies which are derived from single cells has been investigated (Li et al., 2008; Zhang and Waxman, 2010). Upon culturing PC3 cells at low density (1 cell / 32mm² clonal density), the emergence of distinctive colonies has been observed (Li et al., 2008; Zhang and Waxman, 2010). These colonies have been described to resemble colonies reminiscent of keratinocyte cultures that form holoclones, meroclones and paraclones (Barrandon and Green, 1987). Holoclones were colonies characterised as consisting of small tightly packed cells; paraclones were larger colonies comprised of less cells; meroclones were colonies in between in size and number of constituent cells (Li et al., 2008; Zhang and Waxman, 2010). Zhang et al (2010) reported appearances of these 3 colony types formed from single PC3 cells as shown in Figure 4.



Figure 4. Image showing 3 morphologically different colony types formed from culture of single cell plated PC3 cells.

Colony types were described as holoclones, meroclones and paraclones as shown (Zhang and Waxman, 2010).

Li et al (2008), describe and categorised colonies obtained from culturing PC3 cells at low density in single wells of a culture dish: 10% were holoclones, 22% meroclones and 68% paraclones (Li et al., 2008). As shown in table 1, cells of these 3 different colony types demonstrated different biological properties. Clones were followed and after 8 weeks, proliferative ability varied between colony types: 6 of 7 holoclones continued to proliferate well, 11 of 16 meroclones continued to proliferate well, but only 1 of 49 paraclones continued to proliferate well. Four weeks later, of these colonies investigated, only the 6 holoclones continued to proliferate and no meroclones or paraclones. In addition, cells of holoclones were able to produce colonies of all 3 types when re-plated at clonal density (Li et al., 2008).

Table 1. Survival of PC3 cell colonies.

Three colony types were described and cultured for 8 weeks by Li et al (2008). Holoclone colony type had the highest survival and paraclone colony type the lowest survival rate.

Colony Type	Survival	Aborted
Holoclone	6/7 (85.7%)	1/7 (14.3%)
Meroclone	11/16 (68.8%)	5/16 (31.2%)
Paraclone	1/49 (2.0%)	48/49 (98.0%)

Colonies derived from PC3 cells have a differential ability to initiate tumours and sustain serial tumour transplantation (Li et al., 2008). PC3 and PC3-GFP cells initiated tumours in a manner dependent on number of cells injected. A high incidence of tumours was induced when cells derived from 3 holoclones were injected into NOD/SCID mice. Cell populations derived from 2 meroclones did not induce tumours, and for paraclones it was difficult to yield a sufficient number of cells, but these did not induce tumours. When tumours induced by holoclone injected were harvested, these were able to serially induce secondary and tertiary tumours. Furthermore, Li et al, 2008, suggest that upon re-plating tumour derived cells at clonal density, all 3 colony morphologies were observed (Li et al., 2008). As such the

PC3 holoclones exhibited some characteristics of cancer stem cells whilst PC3 cells derived paraclones did not.

Plating cells at low density with the formation of distinct colonies has been used in *in-vitro* work as a surrogate stem cell assay (Li et al., 2008; Locke et al., 2005; Pfeiffer and Schalken, 2010). In Li et al's (2008) work discussed above, holoclones expressed the stem cell and progenitor marker proteins CD44, A2b1 and β -catenin whilst paraclones did not express these markers (Li et al., 2008).

The formation of 3 distinct colony types (holoclones, meroclones, and paraclones) has been demonstrated in other prostate cancer cell lines when plated at clonal density (Pfeiffer and Schalken, 2010). Cell lines DU145, 22Rv1, LAPC-4, DuCaP, and LNCaP form these morphologically distinct colony types. Examples of colonies formed by DU145 and LNCaP cells are shown in Figure 5 (Pfeiffer and Schalken, 2010).

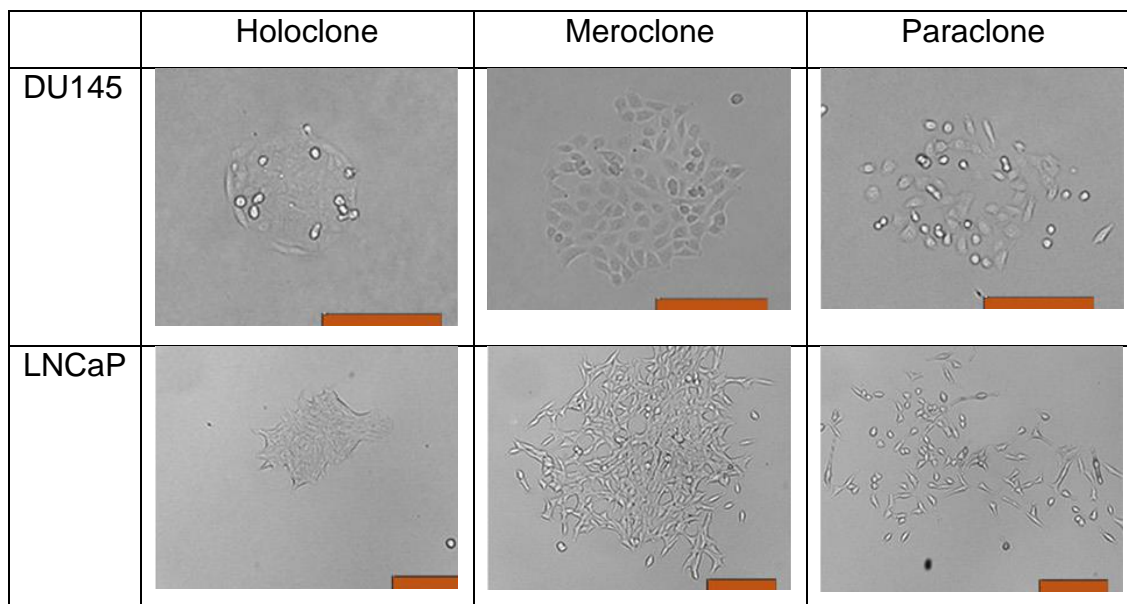


Figure 5. Colony morphologies observed in prostate cancer cell lines DU145 and LNCaP.

Pfeiffer et al reported that both DU145 and LNCaP formed three morphologically different colonies: holoclones, meroclones and paraclones (Pfeiffer and Schalken, 2010). Scale: Bar measures 200 μ m.

1.4 Wnt Signalling

Wnts (a name derived from *Drosophila wingless* and *int-1*) (Siegfried and Perrimon, 1994) are a family of secreted glycoprotein ligands that subsequent to binding to Frizzled (Fz) receptors activate a cascade of intracellular processes (Logan and Nusse, 2004; Niemann et al., 2004). The two major intracellular transducers of Wnt signalling are calcium (Ca^{2+}) and a transcription factor co-activator protein called β -catenin (CTNNB1). Wnt signalling is involved in the regulation of cellular processes such as proliferation, development and disease, including carcinogenesis (Boyden et al., 2002; Fearon and Vogelstein, 1990; Logan and Nusse, 2004; Niemann et al., 2004). Wnt signalling comprises several signal transduction pathways subsequent to the binding of a Wnt glycoprotein to a Fz receptor, which via the intracellular protein Dishevelled, transmits a downstream signalling cascade.

Wnt signalling plays an important role in stem cell functions such as self-renewal and differentiation (Reya and Clevers, 2005; Reya et al., 2003; Willert et al., 2003). The particular interest of investigation in this project was the role Wnt signalling may play in carcinogenesis. An early idea was that if active, Wnt signalling may regulate cancer stem cells or population of cells with stem like characteristics in cancer cell lines, known as cancer stem-like cells (Kondo, 2007).

1.4.1 Categorisation of Wnt pathways

A number of Wnts have been identified and Wnt signalling is implicated in a range of biological processes. Wnts have historically been categorised according to the physiological functions they exert.

Using a *Xenopus* embryo assay in which the expression of certain Wnts on the ventral aspect of the embryo induces the formation of a secondary dorsal body axis (Christian et al., 1991; McMahon and Moon, 1989). Injection of *Xenopus* embryo with murine Wnt 1 RNA was found to consistently produce a phenotype of embryonic axis duplication (McMahon and Moon, 1989). The same phenotype was observed in this

assay upon injection of ectopic mRNA encoding Xwnt 8 (Christian et al., 1991) and Xwnt3A (Wolda et al., 1993). However, overexpression of Xwnt 5A in *Xenopus* embryos results in a different phenotype with altered cell movements, malformations in the head and tail, but no duplication of the embryonic axis (Moon et al., 1993). Subsequently, mRNA Xwnt 4 and Xwnt 11 were found to produce an identical phenotype to Xwnt 5A. As such, Xwnt 1, 3A, and 8 were placed in one functional class and Xwnt 4, 5A, and 11 in another (Du et al., 1995).

Another important assay in the categorization of Wnts was based on their ability to induce transformation in a mammary epithelial cell line derived from normal mouse mammary tissue, C57MG (Wong et al., 1994). Expression constructs of murine Wnt genes were transfected into C57MG cells and transformation entailing cells becoming elongated and with disorganised growth pattern was assessed for each murine Wnt gene. Wnt 1, Wnt 3A, and Wnt 7A demonstrated frequent transformation to this morphology; Wnt 2, Wnt 5B, and Wnt 7B demonstrated a lower efficiency of transformation; Wnt 4 and Wnt 6 demonstrated little or no ability to induce transformation; and Wnt 5A demonstrated no ability at all to transform C57MG cells (Wong et al., 1994). As such, these findings were consistent with the observations in *Xenopus* embryos that Wnts may be categorised into functionally distinct groups, or “classes”.

Some Wnt ligands are able to induce release of intracellular Ca^{2+} ($[\text{Ca}^{2+}]_i$). In zebrafish embryos, injection of Xwnt 5A mRNA induces $[\text{Ca}^{2+}]_i$ release, whilst ectopic expression of Xwnt 8 does not (Slusarski et al., 1997b). Protein kinase C (PKC) isoforms respond to Ca^{2+} signalling and as such modulation of PKC by Wnts was investigated in *Xenopus* embryos, where again a differential effect is seen: Ectopic expression of Xwnt 5A was able to induce PKC localization and activity far more than Xwnt 8 (Sheldahl et al., 1999).

Cellular responses induced by Wnts, such as those described above have been found to be influenced by other factors such as Frizzled (Fz, see 1.2.1.1 below) receptors. In the *Xenopus* embryos assay, co-injection of Xwnt 5A RNA and hFz5 RNA induced secondary axis formation (He et al., 1997). In the early 1990s it was known that β -catenin played an important role in cell fate downstream of a Wnt

ligand receptor signal, and overexpression of β -catenin is also able to induce axis duplication (Guger and Gumbiner, 1995).

In addition, certain Wnts have been shown to antagonise the function of others. The interaction between the Wnt 5A class and Wnt 1 class signalling pathways by co-expressing members of both classes together was demonstrated in *Xenopus* embryos. Injection of RNAs encoding members of the Wnt 5A class antagonized the embryonic responses to ectopic expression of the Wnt 1 class (Torres et al., 1996).

This antagonistic effect of some Wnts on the functional effects of others supported the model of multiple Wnt signalling pathways responsible for disparate cellular responses.

1.4.2 Pathways of Wnt Signalling - The canonical (β -catenin) Wnt pathway

The key element of the canonical Wnt pathway is the regulation of β -catenin protein levels and thus regulation of transcription of β -catenin dependent target genes (Behrens et al., 1996) (Molenaar et al., 1996).

Wnt proteins bind to Fz receptors; there are 7 members of the Fz family of integral cell membrane proteins. Each Wnt may bind to a number of Fz receptors and one receptor may bind to several Wnt proteins. (Bhanot et al., 1996) With Wnt - Fz binding there is co-operation with co-receptors of the low-density lipoprotein receptor (LDLR)-related protein (LRP) family i.e. LRP5 or LRP6.

In the absence of Wnt ligand activation, levels of cytosolic and nuclear β -catenin are controlled via protein phosphorylation and ubiquitination. Essential to β -catenin degradation is a destruction complex composed of Axin / GSK-3 / APC. Scaffold proteins are often involved in the regulation of signalling pathways by interacting or binding with other members of a pathway and tethering them into complexes. Here, Axin is such a scaffold protein, interacting with GSK3, CK1 α and APC. CK1 α phosphorylates β -catenin at serine 45, which then leads to GSK3-mediated β -

catenin phosphorylation at threonine 41, serine 37 and serine 33 (Kimelman and Xu, 2006).

The S-phase kinase - associated protein 1 p19 (SKP1) / Cullin / F-box complex (SCF complex) is an ubiquitin ligase complex and the F-box component, B-TRCP, recognises phosphorylated β -catenin. This complex catalyses the ubiquitination of β -catenin, following which β -catenin degradation occurs (Kimelman and Xu, 2006). APC may also play a role in the β -catenin ubiquitination as in a colon cancer cell line, a truncated form of APC is functional in β -catenin phosphorylation but inhibited β -catenin ubiquitination and degradation (Yang et al., 2006).

On Wnt signalling activation, Dsh (Dishevelled) a cytoplasmic phosphoprotein is activated and interaction between LRP5/6 and Axin, a process mediated by phosphorylation of LRP by Casein kinase 1 γ (CK1 γ) (Gary et al., 2005). A significant consequence of Axin binding with LRP and Dsh with Fz, is that the APC complex becomes unable to function as a kinase for β -catenin.

As β -catenin is constitutively transcribed and translated, this inhibition in degradation leads to elevated cytosolic levels of unphosphorylated, stable β -catenin which may lead to its entry into the cell nucleus. Within the nucleus β -catenin binds to the N terminus of LEF/TCF (lymphoid enhancer factor/T cell factor) transcription factors resulting in expression of Wnt target genes (Behrens et al., 1996; Van de Wetering et al., 1997).

Functional APC is critical in the regulation of β -catenin by the destruction complex. The colon cell line SW480 with mutant APC has high levels of β -catenin. Transfection of SW480 cells with wild-type APC, results in a decrease of β -catenin staining on immunofluorescence. The ability of several APC constructs to down-regulate β -catenin was investigated and it was found that the presence of the central region of the protein was essential for the down regulation of β -catenin (Munemitsu et al., 1995). Consistent with these findings, mutant APC genes' protein products present in colorectal tumours have been found to be defective in their ability to reduce β -catenin activity (Morin et al., 1997).

The importance of the regulation of this pathway in cancer is critical as demonstrated by the fact that both Axin and APC are, likely, tumour suppressor genes and mutations in the latter are highly prevalent in colorectal carcinoma (He et al., 1998).

1.4.2.1 Translocation of β -catenin into nucleus

The mechanism by which stabilized β -catenin, a 92kDa protein, translocates from the cytoplasm to the nucleus is not yet fully understood (Thrasivoulou et al.). In general for eukaryotic cells, the size limit for molecules that can permeate the nuclear envelope through the nuclear pore complex (without a nuclear envelope specific translocation mechanism, e.g. expenditure of energy or receptor mediated translocation), is <10kDa (Mazzanti et al., 2001). Nuclear pore complexes are large proteins which span the nuclear envelope. The complex allows water soluble molecules such as metabolites and proteins with a diameter of ≤ 10 kDa to permeate through the nuclear membrane. However, proteins > 10kDa require a mediated mechanism for nuclear import (Gerace and Burke, 1988; Mazzanti et al., 2001). This process is dependent on nuclear location sequences (NLSs) - amino acid sequences - which are recognised by importins, or karyopherins proteins which dock the protein to the nuclear pore through which there is translocation of the protein into the nucleus in an energy dependent manner (Gerace and Burke, 1988), (Fagotto et al., 1998).

β -catenin has no NLS but shares functionally important Armadillo amino-acid repeats with importin / karyopherins. In colorectal cell lines, β -catenin has been shown to interact directly with nuclear pore complex components (Shitashige et al., 2008). The Armadillo sequence binds to specific regions of the NPC, and silencing of these regions of the NPC reduces the rate of both β -catenin import and export (Sharma et al., 2012). Nuclear import can be inhibited by importin (Fagotto et al., 1998; Kim et al., 2000). Through binding to β -catenin, cadherins have been found to inhibit β -catenin/TCF signalling (Fagotto et al., 1996; Gottardi et al., 2001). There may be inhibition of the transcriptionally active signalling pool of β -catenin without significantly reducing the protein's total levels in the cytosol or nucleus. In SW480, a colorectal cancer cell line, E-cadherin inhibits β -catenin/TCF signalling and SW480

tumour cell growth (Gottardi et al., 2001). In *Drosophila*, as well as its role in the destruction complex, axin has been found to retain β -catenin in the cytoplasm (Tolwinski and Wieschaus, 2001).

1.4.2.2 β -catenin mediated gene transcription

When there is a lack of nuclear β -catenin, TCF/LEF proteins act as inhibitors to transcription and bind to members of the Groucho/TLE family (Brantjes et al., 2001; Chen and Courey, 2000). In man there are four TCF transcription factors; TCF1, LEF1, TCF3 and TCF4 (Galceran et al., 2000; Kim et al., 2000; Korinek et al., 1998; Verbeek et al., 1995). There are four full-length human Groucho homologues: TLE - 1, -2, -3 and -4 (transducin-like enhancer of split) and one truncated variant: hAES (for amino-terminal enhancer of split) (Palaparti et al., 1997; Stifani et al., 1992). β -catenin accumulation in the nucleus results in its interaction with DNA-bound TCF/LEF transcription factors as a co-activator. In a number of benign and malignant cell lines, several TLE and TCF family members are expressed but there is no suggestion of specificity in the interaction between them (Brantjes et al., 2001). In fact, β -catenin and TLE appear to directly compete for LEF-1 binding and β -catenin is able to displace Groucho/TLE from TCF/LEF (Daniels and Weis, 2005).

Phosphorylation may also play an important role in mediating TCF transcriptional activity. NLK (NEMO-like kinase), through TAK1 (TGF- β -activated kinase) activation, phosphorylates TCF and represses activation of β -catenin mediated transcriptional activation in human embryonic kidney 293 cells (Ishitani et al., 1999). The kinase CK1 binds to and phosphorylates LEF-1 resulting in structural changes in the LEF1/DNA complex and disruption of the association of LEF1 with β -catenin, whilst not diminishing LEF1 DNA binding. Using reporter gene assays, in HEK293 cells, CK1e is found to have repressor and CK2 activator effects on the transcriptional activity of the LEF1/ β -catenin complex (Hämmerlein et al., 2005).

TCF/LEF may also be subject to ubiquitination. NARF, (a Nemo-like Kinase (NLK)-associated Ring Finger Protein) induces the ubiquitination of TCF/LEF and this is

enhanced by NLK. In 293 cells, NARF negatively regulates TCF/LEF-dependent transcriptional activity (Yamada et al., 2006).

Nuclear co-factors may also play a role in mediating Wnt transcription. In *Drosophila*, legless (lgs) and pygopus (pygo) mediate Wnt transcription, with lgs as a recruiter of pygo to β -catenin (Kramps et al., 2002). In man the human homolog of lgs is BCL9. In cell lines, BCL9 may act independently of pygo, and its effects are cell type specific; for example in lymphoid cells BCL9 enhances transcriptional activity significantly compared with its effect in fibroblastic cells (Sustmann et al., 2008).

1.4.2.3 Wnt- β -catenin target genes

There are numerous known target genes of Wnt / β -catenin mediated gene transcription. These are most notably and typically described as being functionally important in stem cell maintenance, terminal differentiation and carcinogenesis (Fevr et al., 2007; He et al., 1998; Kinzler et al., 1991; Nusse, 2008).

Wnt signalling target genes implicated in the aetiology of cancer are of particular research interest; understanding these processes may lead to the development of new therapies in the management or possibly prevention of the disease.

The literature regarding Wnt / β -catenin signalling target genes is summarised in table 2 and figure 6 below.

Table 2. Putative target genes under the transcriptional regulation of the β -catenin co-transcription factor.

The table below describes these genes, the system they have been studied in, and the mechanism by which their effect occurs.

Gene	System studied in	Effect	Up / down Regulated	Reference
c-myc	Human colon cancer	In colorectal cancer cell line HT29 (in which wild-type APC can be induced), APC mutations increase β -catenin / TCF 4 activity and lead to overexpression of c-myc. Wild type APC and a dominant-negative TCF 4 reduced c-myc expression.	up	(He et al., 1998)
n-myc	Vertebrate limb development	In mouse limb buds, n-myc expression is co-localized to the zone of proliferating cells in the limb; when n-myc is absent, cell division in this region decreases. Wnt 3a induces a proliferative effect in the forelimb bud of wild-type but not n-myc ^{-/-} limb buds.	up	(ten Berge et al., 2008a)
Cyclin D1	Human colon cancer	Cyclin D-1 is elevated in a third of human colon cancers. Cyclin D1 promoter has a LEF1	up	(Shtutman et al., 1999)

		binding site. In colorectal cancer cell line SW480, cyclin D1 is repressed by wild type APC.		
	HELA cells and human colon cancer	In HELA cells, β -catenin activates transcription from the cyclin D1 promoter, and transcription is augmented by p21ras. Mutant β -catenin cells constitutively produce elevated cyclin D1 mRNA and protein. Colorectal cancer cell line HCT116, dominant-negative TCF 4 inhibits cyclin D1 expression and arrests cells in G1 cell cycle phase, which is rescued by cyclin D1 expression.	up	(Tetsu and McCormick, 1999)
TCF 1	Human colon cancer	In colorectal cancer cell line HT29, APC expression decreases TCF 1. TCF 1 ^{-/-} mice develop intestinal and mammary adenomas. TCF 1 may provide negative feedback to regulate β -catenin / TCF target genes.	up	(Roose et al., 1999)
LEF1	Human colon cancer	LEF 1 is activated in colon cancer but not expressed in normal colonic tissue. β -catenin / TCF induces transcription from the	up	Hovanes et al., 2001

		LEF 1 promoter.		
	Human embryonic kidney cells	β -catenin / TCF induces transcription from the LEF 1 promoter.	up	(Filali et al., 2002)
PPARdelta	Human colon cancer	APC induction inhibits β -catenin / TCF 4 regulated transcription of PPAR δ .	up	(He et al., 1999)
c-jun	Human colon cancer	Colorectal cancer cell lines transfected with β -catenin increases gene expression of c-jun, fra-1 and urokinase-type plasminogen activator receptor (uPAR). c-jun is a component of the AP-1 transcription factor complex.	up	(Mann et al., 1999)
Fra 1	Human colon cancer	Colorectal cancer cell lines transfected with β -catenin increases gene expression of c-jun, fra-1 and urokinase-type plasminogen activator receptor (uPAR). Fra 1 is a component of the AP 1 transcription factor complex.	up	(Mann et al., 1999)
uPAR	Human colon cancer	Colorectal cancer cell lines transfected with β -catenin increases gene expression of c-jun, fra-1 and urokinase-type plasminogen activator receptor (uPAR). uPAR's transcription is activated by AP 1.	up	(Mann et al., 1999)

		In patients with primary colorectal cancer and liver metastases, uPAR and β -catenin expression levels are concomitantly increased in tissue from both sites.		
matrix metalloproteinase MMP-7	Human colon cancer	The promoter of the human invasion associated gene, MMP-7 has 2 TCF binding sites. The Human MMP-7 Promoter is activated by β -catenin / TCF 4 and suppressed by a dominant-negative TCF 4 mutant in colon cancer cells. MMP-7 expression correlates with that of β -catenin in tissue from patients with hereditary and sporadic colon cancer.	up	(Brabletz et al., 1999)
	Human colon cancer	In colon cancer cell lines, MMP-7 promoter activity is up-regulated by β -catenin, particularly in those cell lines with a low level of endogenous β -catenin /TCF, and is dependent on an optimal TCF 4 recognition site. Co-expression of E-cadherin (thought to be an inhibitor of Wnt signalling) reduces MMP-7 promoter activity.	up	(Crawford et al., 1999)
Axin-2 / Hnkd	Human colon cancer	In a colon cancer cell line with stabilised β -	up	(Yan et al.,

		<p>catenin due to truncated APC, reducing cytosolic β-catenin reduces levels of axin 2 and human naked cuticle (hnkd) mRNAs. Compared with benign colon cells, >60% of human colon cancers cells demonstrate elevated levels of axin 2 and hnkd mRNA.</p> <p>In cancer cells where expression of axin2 and hnkd mRNA was increased, mutations in APC were present.</p>		2001)
Nr-CAM	Various cell lines including human malignant melanoma and human colon cancer	Nr-CAM is induced by β -catenin in various cell types and LEF/TCF binding sites in the Nr-CAM promoter are required for this activation. Nr-CAM and β -catenin target gene, LEF 1 expression is increased in human colon cancer tissue and cell lines and malignant melanoma cell lines, but not in benign melanocyte cell lines or benign colon tissue.	up	(Conacci-Sorrell et al., 2002)
ITF-2	RK3E cell line (epithelial rat kidney), human ovarian cancer tissue	Mutant β -catenin promotes malignant transformation in the RK3E cell line. Class I bHLH protein ITF-2 is activated in these cells but not in cells transformed through other	up	(Kolligs et al., 2002)

		<p>pathways. β-catenin mediated induction of ITF-2 is inhibited by a mutant dominant negative TCF 4.</p> <p>In a colorectal cell line, APC activity suppresses ITF-2 expression. In human ovarian cancer tissue with defects in β-catenin regulation, there are increased levels of ITF-2A and ITF-2B transcripts compared to ovarian cancer without aberrant β-catenin regulation. ITF-2B induces neoplastic transformation in RK3E cells.</p>		
Gastrin	Human colon cancer	<p>In colorectal cell lines induction of wild-type APC reduces gastrin mRNA expression. In HELA cells, co-transfection of a constitutively active β-catenin expression construct increases gastrin promoter activity; this activity can be inhibited by a dominant-negative TCF 4 expression construct. In APC (min-/+) mice, an increase in colonic polyps is observed in those which overexpress a form of gastrin, whilst in mice lacking gastrin, a reduced number of polyps is observed.</p>	up	(Koh et al., 2000)

CD44	Human and mouse benign and cancerous colon	CD44 is overexpressed in human adenomas and carcinomas. In APC mutant mice, CD44 is expressed in the crypt epithelium of normal intestine, in adenomas and in invasive carcinomas. In APC-mutant mice, aberrant crypt foci with dysplasia overexpress CD44 and the same is observed in humans with familial adenomatous polyposis. In TCF 4 ^{-/-} mutant mice there is no expression of CD44 in the small intestine epithelium.	up	(Wielenga et al., 1999)
EphB/ephrin-B	Human colon cancer	EphB2/EphB3 are receptor tyrosine kinases. Gene expression of the ligand Ephrin-B1 is upregulated upon inhibition of β -catenin / TCF.	down	(van de Wetering et al., 2002)
BMP4	Human colon cancer	In a colorectal cell line, gene expression of BMP4 is lower in clones lacking β -catenin than in parental cells. In APC mutant colon cancer cell lines, BMP4 levels are high. BMP4 expression is elevated in colon cancer cell lines compared with benign colonic tissue.	up	(Kim et al., 2002)
claudin-1	Human colon cancer	In colon cancer cell lines, when β -catenin is reduced through introduction of wild-type APC	up	(Miwa et al., 2001)

		in APC-deficient cells, expression of CLDN1 is in turn reduced. CLDN1 transcription occurs through TCF 4 binding sites. There is increased expression of CLDN1 in human colorectal cancer compared with benign tissue.		
Survivin	Human colon cancer	In a colorectal cell line, induction of wild-type reduces survivin mRNA and protein expression. Dominant-negative TCF 4 reduces survivin expression.	up	(Zhang et al., 2001)
VEGF	Human colon cancer	A VEGF-pGL2-basic luciferase vector construct is active in colon cancer cell lines with endogenously activated Wnt signalling. In the same cell lines, dominant negative TCF 4 co-transfection reduces VEGF promoter activity. A similar suppression of VEGF is not observed in 293 kidney cells.	up	(Zhang et al., 2001)
FGF18	Human colon cancer	FGF18 gene expression is elevated in human colorectal cancer tissue compared with benign tissue. In colon cancer cell line SW480, FGF18 expression is reduced by dominant negative TCF 4.	up	(Shimokawa et al., 2003)

Hath1	Human colon cancer	Hath1 expression is relatively high in benign colon and small intestinal tissue but is down-regulated in cancers arising from these sites. Hath1 expression is low in colon cancer cell lines. In a colon cancer cell line, inhibition of Wnt signalling through transient expression of wild-type APC and dominant negative LEF 1 increases Hath1 expression.	down	(Leow et al., 2004)
Met	Human colon cancer	The receptor tyrosine kinase, met, is overexpressed in human dysplastic aberrant crypt foci, adenoma and in carcinoma of the colon. In colorectal cancer cell lines, dominant-negative TCF reduces met expression.	up	(Boon et al., 2002)
endothelin-1	Human colon cancer	In a colorectal cell line, when APC is induced, EDN1 mRNA levels are reduced. In another colorectal cancer cell line (HCT116), lithium treatment which inhibits GSK3B and stabilizes β -catenin increases EDN1 mRNA. Dominant-negative TCF 4 or β -catenin reduce EDN1 peptide secretion. EDN1 is overexpressed in human colon cancers.	up	(Jung and Kim, 2005)

c-myc binding protein	Human colon cancer, human corneal epithelial cell	In a colon carcinoma cell line (DLD-1) and a corneal epithelial cell line (HCE), LEF 1 overexpression up-regulates c-myc binding protein gene.	up	(Jung and Kim, 2005)
L1	Human colon cancer	L1, transmembrane cell adhesion molecule, is expressed in SW480 and HCT116 colorectal cell lines; sparsely growing cells express higher levels of L1 than densely growing cells. In 293 cells, L1 promoter activation is increased by mutant stabilized β -catenin and is inhibited by dominant negative LEF 1. In a colorectal cell line, β -catenin suppression results in reduction in L1.	up	(Gavert et al., 2005)
Id2	Human colon cancer	Id2 is expressed in human colonic adenomas but not in normal colonic tissue. There is a concordance in Id2 β -catenin expression in crypts. Colon cancer cell lines with TCF reporter TOPFLASH activity express Id2. Over-expression of β -catenin in HEK-293 cells increases expression of Id2. In colorectal cell line SW480 which has an APC	up	(Rockman et al., 2001)

		mutation and high nuclear β -catenin, reintroduction of wild type APC protein reduces Id2 promoter activity.		
Jagged	Human colon cancer	Notch is a family of transmembrane receptors. Wnt and notch inhibition in CRC cell line Ls174T down-regulate a number of genes. The Notch ligand, jagged, is highly expressed in Ls174T but dominant negative TCF 4 reduces jagged mRNA and protein, and activated Notch1. Jagged1 mRNA levels is elevated in human adenomas in those with FAP, compared with normal intestinal tissue. Pattern of expression correlates with regions also demonstrating nuclear β -catenin staining, together with Notch 1 and Notch2.	up	(Rodilla et al., 2009)
Msi1 translation inhibitor protein, Musashi1 (MSI1)	Human colon cancer	In colorectal cancer cell line HCT116 with wild-type allele of β -catenin (HCT116 β w), reducing APC mRNA and protein levels results in an increase in MSI1 mRNA and protein. APC mRNA is a target of translational inhibition by MSI1. Knockdown of MSI1 in HCT116 β w	up	(Spears and Neufeld, 2011)

		cells result in an increase in APC protein, and so in a negative feedback loop overexpression of wild-type Msi1 in HCT116 β w cells decreases APC protein.		
Tiam1	Human colon cancer	Tiam1 is a selective Rac GTPase activator expressed in cells at the base of small intestine crypts in wild type mice but uniformly in both polyps of APC mutant mice and in human colon adenomas. In human CRC cell line, DLD1, inhibition of TCF reduces Tiam1 mRNA and protein. Exogenous expression of both Wnt 1 and β -catenin in RIE (a rat intestinal epithelial cell line) cells increases Tiam1 protein.		(Malliri et al., 2006)
Nitric Oxide Synthase 2	Human colorectal cancer cell lines and a liver cancer cell line Hepg2 cells	There are 2 TCF 4-binding elements (TBE1 and TBE2) in the promoter of human inducible NO synthase 2 (NOS2). In human colorectal cancer cell lines and a liver cancer cell line, β -catenin /TCF 4 specifically binds to these TBES. Overexpression of β -catenin and TCF 4 expression plasmids increase NOS2 promoter activity. In colorectal cancer cell line HCT116,	up	(Du et al., 2006)

		overexpression of TCF 4 or β -catenin increases NOS2 mRNA and protein whilst dominant-negative TCF 4 decreases NOS2 mRNA and protein expression. Similarly, LiCl inhibition of GSK-3 β increases NOS2 protein expression in primary human hepatocytes.		
Telomerase	Mouse ES cells	TERT is part of the telomerase complex which controls telomere length. Tert mRNA and protein is reduced in β -catenin-deficient mouse ES cells. Wnt 3a stimulation of wild-type ES cells increases Tert expression. Reduction in Tert expression and telomerase activity produces shortened telomeres in β -catenin-deficient cells.	up	(Hoffmeyer et al., 2012)
Dickkopf	Various cells, tumours	DKK1 is known to be an inhibitor of Wnt signalling. There are 9 nine putative TCF-binding sites on the DKK1 promoter. In various cell lines (MCF-7, MDA-MB-453, HeLa) activation of canonical signalling by Wnt 1 or ectopic β -catenin or TCF 4 induces transcription of DKK-1. Non-canonical Wnt 5a does not	up	(Gonzalez-Sancho et al., 2005)

		activate DKK1. Inactivation of TCF4 suppresses DKK-1 promoter activation. However, DKK-1 is down-regulated in human colon tumours as compared to normal tissue.		
FGF9	Ovarian endometrioid adenocarcinoma	A proportion of primary ovarian endometrioid adenocarcinomas (OEA) have constitutive activation of Wnt signalling. FGF20 and FGF9 are up-regulated in OEAs with deregulated β -catenin / TCF signalling compared with those with intact signalling. Two OEA-derived cell lines demonstrate increased expression of FGF9. FGF9 is overexpressed by Wnt 1, β -catenin and LiCl GSK3 β inhibition, whilst dominant-negative TCF 4 reduces expression.	up	(Hendrix et al., 2006)
FGF20	293 cells, ovarian endometrioid adenocarcinoma, Xenopus	FGF20 RNA is normally only present in the adult central nervous, but is also present in several human colon cancers and in a β -catenin mutant ovarian endometrioid cell line. In 293 cells and primary ovarian endometrioid adenocarcinomas, stabilised β -catenin leads to overexpression of FGF20 and DKK1.	up	(Chamorro et al., 2005)

LBH	293 cells, breast cancer cells	In human 293T embryonic kidney epithelial cells, Wnt 3a induces Lbh and Dkk1 expression and is abrogated by depletion of β -catenin. Wnt 5a and Wnt 7a treatment reduce Lbh and Dkk1 expression. Mammary tumours from MMTV-Wnt 1 mice have elevated Lbh expression compared with normal mammary cells and HC11 mouse mammary epithelial cell line.	up	(Rieger et al., 2010)
LGR5 (Leucine-rich-repeat-containing G-protein-coupled receptor 5); Gpr49	Intestine	Dominant-negative TCF 4 suppresses expression of LGR5. There is some expression of LGR5 in the crypts of mouse small intestine.	up	(Barker et al., 2007)
Sox9	Intestine	SOX proteins are a family of high mobility group box transcription factors. In mouse neonate and adult intestine, of these SOX9 is over-expressed particularly in proliferative regions. SOX9 mRNA and protein are expressed in CRC cell lines. In colorectal cancer cell line LS174T, dominant negative TCF 4 suppresses SOX9 mRNA and protein expression. Additionally, SOX9 suppresses the intestinal differentiation genes	up	(Blache et al., 2004)

		CDX2 and MUC2.		
Sox17	Gastric and colonic tumours	Gan mice develop gastric tumours via Wnt / β -catenin signalling and such tumours express several Wnt target genes including Sox17. Sox17 is expressed in human gastric adenomas but less so in carcinomas. Similar findings are observed in colon polyps and carcinomas. Sox17 inhibits β -catenin / TCF activity in a human gastric cancer cell line. Wnt signalling induces Sox17 in early tumourigenesis.	up	(Du et al., 2009)
Runx2	Chick chondrocytes	In chick chondrocytes, Wnt 8c, Wnt 9a, and β -catenin overexpression up-regulates RunX2 mRNA and produces chondrocyte hypertrophy. β -catenin and LEF 1 over-expression induce Runx2 promoter activation whilst a mutation in the TCF / LEF binding site of Runx2 inactivates its response to β -catenin.	up	(Dong et al., 2006)
Gremlin	Human and mouse fibroblasts	In Wnt responsive human lung fibroblasts, Wnt 3a increases expression of GREMLIN2, the gene for secreted bone morphogenetic protein (BMP) antagonist.	up	(Klapholz-Brown et al., 2007)

SALL4	Check cell lines 2102 EP embryonal carcinoma cells and epithelial ovarian cancer OVCAR-3 cells. HEK293 cells	The product of SALL4 is thought to be a transcription factor, and mutations of the gene cause a rare syndrome (Okihiro/Duane-Radial Ray syndrome) associated with various malformations. In 2102 EP embryonal carcinoma cells and epithelial ovarian cancer OVCAR-3 cells, LEF 1 and TCF 4E activate the SALL4 promoter, whilst mutation of the TCF / LEF-binding site reduces activation.	up	(Böhm et al., 2006)
Osteoprotegerin	Mouse Osteoblasts	Osteoprotegerin (Opg), encodes a TNF α receptor which inhibits osteoclast differentiation. In mice with constitutively active canonical signalling in osteoblasts, osteoblastic expression of Opg is elevated in developing long bones. Opg expression is decreased in bones and osteoblasts of mutant mice deficient in β -catenin signalling.	up	(Glass li et al., 2005)
CCN1/Cyr61	Mouse mesenchymal stem cells	In a mouse mesenchymal progenitor line, CCN1/Cyr61, CCN2/connective tissue growth factor (CTGF), and CCN5/WISP2, are up-regulated in response to Wnt 3a.	up	(Si et al., 2006)

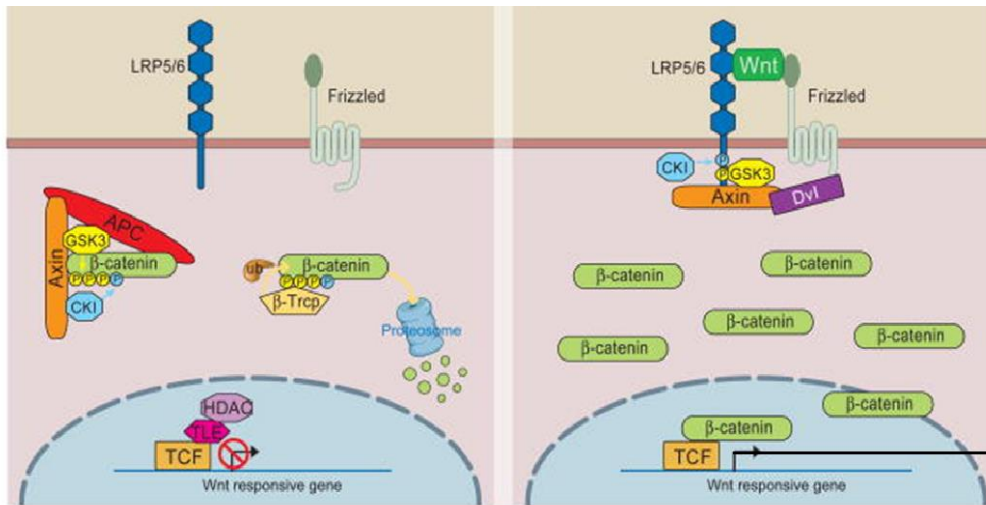
<p>Pituitary tumour transforming gene (PTTG)</p>	<p>Human oesophageal squamous cell carcinoma</p>	<p>PTTG mRNA is overexpressed in human oesophageal squamous cell carcinoma (ESCC), as well as human ESCC and other malignant cell lines. β-catenin is localised in the cytoplasm in malignant ESCC compared to on the membrane in benign tissue. Most ESCCs exhibiting cytoplasmic accumulation of β-catenin also demonstrate overexpression of PTTG. Mutant constitutively active β-catenin activates PTTG promoters, which are inhibited by dominant-negative TCF 4. Corresponding elevation and inhibition of PTTG mRNA and protein are observed.</p>	<p>up</p>	<p>(Zhou et al., 2005)</p>
<p>Delta-like 1</p>	<p>Somites</p>	<p>The Notch ligand Delta-like 1(Dll1) is a gene of the Notch-Delta signalling pathway, downstream of Wnt signalling. LEF 1 mutant mice exhibit a lowered expression of Mesp2, Notch 1 and Dll1. LEF 1 binding sites are present in Dll1. In a fibroblastic cell line, a LEF1-β-catenin fusion protein induces an elevation in the expression of Dll1.</p>	<p>up</p>	<p>(Galceran et al., 2004)</p>

FoxN1	Thymus	Proper development of the thymus requires expression of transcription factor FoxN1. Co-culture of TEC cell lines transfected with a reporter with thymocytes, activates TCF / LEF1 dependent transcription. Wnt 4 up-regulates FoxN1. Dominant-negative TCF 4 inhibits FoxN1 transcription.	up	(Balciunaite et al., 2002)
matrix metalloproteinase-26	Human lung cancer and fibrosarcoma cell lines	Matrix metalloproteinases (MMPs) are important in remodelling and motility and their expression is usually well regulated. MMP-26 is expressed in common human epithelial cancers including lung, breast, endometrium, prostate cancer and their cell lines. A TCF 4 site was identified in the MMP-26 promoter. In human lung cancer and fibrosarcoma cell lines, mutation in the TCF 4-binding site reduces transcriptional activity of the MMP-26 promoter.	up	(Marchenko et al., 2002)
nanog	ES	TCF 3 is highly expressed in murine ES cells where on TCF 3 knockdown there is increased expression of Oct4, Sox2, and Nanog. On treatment with Wnt 3a, Oct4 and Nanog gene	up	(Cole et al., 2008)

		expression increase. As such TCF 3 normally represses its target genes, with increased gene expression on Wnt stimulation.		
Oct 4	ES	As above	up	(Cole et al., 2008)
Snail	Embryoid bodies of mouse ESCs	In a Wnt reporter construct of embryoid bodies (aggregates of pluripotent stem cells), Wnt 3a up-regulates snail and fibronectin expression. Treatment with Wnt inhibitor Dkk1 reduces snail and fibronectin expression.	up	(ten Berge et al., 2008b)
Fibronectin	As above	As above	up	(ten Berge et al., 2008b)
Follistatin	Human embryonic carcinoma	On treating human teratocarcinoma cells with Wnt 3a, several genes including follistatin are up-regulated. In NCCIT cells, Wnt 3a activates the follistatin promoter. Activation does not occur in the presence of a mutation in the TCF binding site on the Follistatin promoter.	up	(Willert et al., 2002)
receptor activator of NFkappaB ligand (RANKL or TNFSF11)	Human and mouse osteoblastic cells	Treatment of osteoblastic cells with LiCl (increasing β -catenin signalling) inhibits RANKL mRNA and protein expression. Wnt 3a	down	(Spencer et al., 2006)

		produces the same response whilst non-canonical Wnt 5A has no effect of RANKL expression. Similarly, β -catenin overexpression reduces RANKL promoter activity.		
--	--	---	--	--

Figure 6. Figure summarising inactive canonical signalling (left) and active canonical signalling with target genes under the transcriptional regulation of the β -catenin (right). Modified from: (MacDonald et al., 2009).



- | | |
|--|---------------|
| c-myc | n-myc |
| Cyclin D1 | TCF 1 |
| LEF1 | PPARdelta |
| c-jun | Fra 1 |
| uPAR | MMP-7 |
| Axin-2 / Hnkd | Nr-CAM |
| ITF-2/ITF-2 | Gastrin |
| CD44 | EphB/ephrin-B |
| BMP4 | claudin-1 |
| Survivin | VEGF |
| FGF18 | Hath1 |
| Met | endothelin-1 |
| c-myc binding protein | L1 |
| Id2 | Jagged |
| Msl1 | Tiam1 |
| Nitric Oxide Synthase 2 | Telomerase |
| Dickkopf | FGF9 |
| FGF20 | LBH |
| Sox9 | Sox17 |
| Runx2 | Gremlin |
| Osteoprotegerin | SALL4 |
| CCN1/Cyr61 | PTTG |
| Delta-like 1 | FoxN1 |
| MMP-26 | nanog |
| Oct 4 | Snail |
| Fibronectin | Follistatin |
| receptor activator of NFkappaB ligand (RANKL or TNFSF11) | |

1.4.3 Pathways of Wnt signalling: The non - β -catenin mediated pathways

The most well described non-canonical pathway is the Wnt / Ca^{2+} pathway; a further non-canonical pathway is the Planar Cell Polarity (PCP) (Wnt – JNK) pathway.

Ligands which activate the non-canonical pathways are: Wnt 4, Wnt 5a, and Wnt 11 (Sheldahl et al., 1999; Slusarski et al., 1997a; Slusarski et al., 1997b).

1.4.3.1 Wnt / Calcium pathway

As discussed earlier in section 1.4.1, it was proposed that activation by some Wnts can induce free intracellular Ca^{2+} ($[\text{Ca}^{2+}]_i$) release, whilst other Wnts were only thought to mediate their effects through β -catenin signalling. Hence the designation of canonical and non-canonical pathways (Gonzalez-Sancho et al., 2005; Molenaar et al., 1996).

The ability of a Wnt protein to produce a cellular response mediated by a Ca^{2+} response was originally studied in zebrafish embryos and *Xenopus laevis*. Expression of Rfz-2 (rat protein Frizzled-2), but not Rfz-1 increased Ca^{2+} release above basal levels from internal stores in zebrafish embryos. $[\text{Ca}^{2+}]_i$ release has been shown to be elevated in response to Xwnt 5A (Slusarski et al., 1997a) but not Xwnt 8 (Slusarski et al., 1997b). Rfz-2 and Wnt 5A modulate Ca^{2+} flux through G proteins and phosphatidylinositol cycling, and their ability to induce Ca^{2+} release is sensitive to inhibition by G protein inhibitor pertussis toxin (Slusarski et al., 1997a). With regard to frizzled receptors, certain Fzs are associated with activation of either the canonical or non-canonical pathways. In *Xenopus*, ectopic expression of the homologs Rfz2, mouse Frizzled 3, mouse Frizzled 4 and mouse Frizzled 6 induced PKC membrane translocation in *Xenopus* but did not induce expression of β -catenin target genes siamois and Xnr3. Ectopic expression of mouse Frizzled 7 and mouse Frizzled 8, and Rfz1, did not induce PKC translocation, but did induce expression of siamois and Xnr3 (Sheldahl et al., 1999).

Wnt 5A interacts with its Fz receptors and also with receptor tyrosine kinase-like orphan receptor 2 (Ror2). The latter possess an extracellular cysteine rich domain

(CRD) similar to the Wnt binding site of Fz receptors. As such Ror2 is also a receptor for Wnt 5A through this CRD (Oishi et al., 2003). Interestingly, Ror2^{-/-} and Wnt 5a^{-/-} mice exhibit similar developmental abnormalities including dwarfism, facial abnormalities, and lung and genital dysplasia (Oishi et al., 2003). In NIH3T3 cells, both Wnt 5A and Ror2 increase activity of non-canonical mediator JNK. Co-expression of both Wnt 5A and Ror2 produces a further increase in JNK activity (Oishi et al., 2003).

Dishevelled is required for transduction of both canonical and non-canonical signalling (Theisen et al., 1994). Dsh's role in Ca²⁺ signalling has been demonstrated in *Xenopus* where a Dsh construct which is inactive in β -catenin signalling activates PKC, intracellular Ca²⁺ flux and Ca²⁺ / calmodulin-dependent protein kinase II. In *Xenopus* embryos, PKC activity enhanced by XFz-7 is inhibited by a domain of Dsh (Sheldahl et al., 2003). In the C-terminal DEP domain of the dsh¹ allele, there is a single amino acid point mutation required for JNK and planar cell polarity signalling but not required for β -catenin dependent signalling. As such, Wnt / Fz signalling employs Dsh, after which intracellular signalling may have divergent downstream pathways (Boutros et al., 1998).

In terms of Ca²⁺ signalling activating protein kinase C (PKC), Wnt and frizzled homologs have been found to differentially induce translocation of PKC to the plasma membrane and total PKC activity. For example, Xwnt 5A and Rfz2 induce PKC translocation with an increase in total PKC activity more than Xwnt 8 or Xwnt 3A or Rfz1 (Sheldahl et al., 1999).

Despite no direct measurement (e.g. the conventional approach of adding a ligand and measuring free cytosolic calcium release) of investigating this phenomenon, it was proposed that ability of certain Wnts and their Frizzled receptors to produce [Ca²⁺]_i release and activation of PKC led to the proposition that the non-canonical Wnts may activate other Ca²⁺ sensitive kinases such as Ca²⁺ / calmodulin-dependent protein kinase II (CamKII), a serine /threonine protein kinase. In man, CamKII activity is described in a range of biological processes including malignancy which will be discussed later. However, it is most abundantly present in the neuronal system where it is involved in long-term potentiation signalling between neurones (Hudmon

and Schulman, 2002) and is also described in arrhythmia in cardiac disease (Mohler and Hund, 2011). In *Xenopus* embryos Xwnt 5A, Xwnt 11 and Rfz2 induce CamKII activity. Conversely, Xwnt 8 and Rfz1, which signal through the β -catenin-dependent canonical pathway do not stimulate CamKII activity. Dominant negative Xwnt 11 inhibits CamKII activity. As discussed, Rfz2 and Xwnt 5a induction of Ca^{2+} release is sensitive to pertussis (Slusarski et al., 1997a) and as expected, activity of CamKII in response to Xwnt 5A is also sensitive to pertussis. CamKII autophosphorylates upon activation and elevated autophosphorylation is observed with Xwnt 5A and Rfz2. CamKII activity is elevated on the ventral aspect of the *Xenopus* embryo and also functions in axis formation (Kühl et al., 2000).

1.4.3.2 **Wnt/planar cell polarity pathway and Wnt / jun N-terminal kinase (JNK) pathways**

Planar cell polarity describes the feature many cells possess of being arranged in a polarized fashion in the plane of a tissue. Though initially studied in *Drosophila* (Gubb and Garcia, 1982; Wong and Adler, 1993), planar cell polarity occurs within both epithelial and mesenchymal human tissue.

The planar cell polarity pathway involves 2 sets of factors which are evolutionarily conserved: Frizzled (Fz) / Flamingo (Fmi) and Fat / Dachshous (Ds). In *Drosophila*, planar cell polarity activation involves asymmetric redistribution of its core proteins - frizzled, flamingo, dishevelled, Stbm/Vang and prickle. In *Drosophila* pupal wings, Dsh localization follows a particular pattern. Prickle acts to antagonize Fz and Dsh localization and magnifies the differences in Fz / Dsh activity between adjacent cell surfaces. (Tree et al., 2002)

In the *Drosophila* wing, Fat provides directional information to the Fz-associated polarity alignment mechanism (Ma et al., 2003). Fat is a large (> 5000 amino acids) transmembrane cadherin receptor protein (Mahoney et al., 1991). Dachshous (Ds) is also a large (> 3500 amino acids), transmembrane protein that binds to Ft and the two proteins stabilize one another on the cell surface (Matakatsu and Blair, 2004). In *Drosophila*, the gene four-jointed (Fj) encodes a protein kinase which

phosphorylates serine or threonine residues within extracellular cadherin domains of Fat and Dachsous, as such performing as a regulator of Fat signalling (Ishikawa et al., 2008).

1.4.4 Pathways of Wnt signalling - A convergent Wnt pathway

As discussed in section 1.4.2.1, the mechanism by which β -catenin, a negatively charged 92kDa protein, moves from the cytoplasm to the nucleus is not yet fully understood. Nuclear pore complexes are large proteins which span the nuclear envelope. The complex allows water soluble molecules such as metabolites and proteins with a diameter of ≤ 10 kDa to permeate through the nuclear membrane. However, proteins > 10 kDa require a mediated mechanism for nuclear import (Gerace and Burke, 1988; Mazzanti et al., 2001).

Recently, a new, convergent pathway of Wnt signalling has been proposed in prostate, breast and urothelial cancer cell lines (Thrasivoulou et al., 2013) that proposes a convergent Wnt signalling pathway in mammalian cells and may also explain how a large protein such as β -catenin may enter the nucleus through the nuclear envelope. The ratio of Fluo4 / FuraRed dyes was used to quantify $[Ca^{2+}]_i$. The addition of Wnts of different classes – Wnt 3A; Wnt 4; Wnt 5A; Wnt 7A; Wnt 9B and Wnt 10B all induced $[Ca^{2+}]_i$ release in whole populations of PC3 prostate cancer cell line. A similar response was seen in breast cell line MCF7 and urothelial cell line 253J and also COS7 (simian kidney cell line). Further to this, the “waveform” describing the rise, duration and fall of $[Ca^{2+}]_i$ could be measured. For example, at the same concentration, Wnt 9B induced a longer period of elevated $[Ca^{2+}]_i$ than Wnt 5a did. This $[Ca^{2+}]_i$ response to Wnts 5A, 9B and 10B was not observed when cells were prior treated with thapsigargin, an inhibitor of endoplasmic reticulum Ca^{2+} - ATPase which inhibits intracellular Ca^{2+} stores. An increase in $[Ca^{2+}]_i$ further resulted in elevated intranuclear Ca^{2+} concentration. Immunocytochemistry demonstrated increased expression of β -catenin in PC3 cells treated with Wnt 3A, Wnt 4, Wnt 5A, Wnt 9B, and Wnt 10B compared with untreated cells (Thrasivoulou et al., 2013).

Based on the above observations of $[Ca^{2+}]_i$ response to Wnts, Thrasivoulou et al proposed a novel convergent, electrogenic model for Wnt signalling and an explanation for β -catenin protein may traverse the nuclear envelope (Thrasivoulou et al., 2013). Wnt signalling induces an increase in intranuclear Ca^{2+} and depolarisation of the nuclear membrane and is associated with elevated expression of nuclear β -catenin (Thrasivoulou et al., 2013). Conversely, incubation of cells with thapsigargin reduced the translocation of β -catenin into the nucleus. This suggests that the regulation of the nuclear membrane potential regulation of through ions such as Ca^{2+} may control the translocation of β -catenin into the nucleus and Wnt signalling (Thrasivoulou et al., 2013). Patent (New British Patent Application no. 1318659.8).

1.5 Wnt signalling and cancer

Of all malignancies, the role of the Wnt pathway in the aetiology of colon cancer has been most researched and through mechanisms outlined below, significant numbers of colon cancers are initiated due to aberrant Wnt signalling. Much of our understanding of Wnt signalling and the consequences of deregulated signalling on tumourigenesis is derived from this system. However, Wnt signalling has now been implicated in a range of other solid tumours including lung, breast, head and neck, pancreas, ovarian, central nervous system, penile and prostate cancer.

1.5.1 De-regulated Wnt signalling and cancer

In 1925, Lockhart-Mummery, a surgeon at St Mark's hospital, London described the clinical features and family histories of 3 of his patients between the ages of 20-31 presenting with extensive benign adenomatous polyposis of the large bowel, each of whom had multiple family members who had died from colorectal cancer at a young age (Lockhart-Mummery, 1925). We now understand that this condition of familial adenomatous polyposis (FAP) is characterised by the development of multiple, benign, colonic polyps which develop into adenocarcinoma at an early age and is

caused by an autosomal dominant germline mutation of the APC gene on chromosome 5q21 (Kinzler et al., 1991; Nishisho et al., 1991).

The effects of mutant APC have been studied in colon cancer cell line SW480 which has mutant APC and high levels of β -catenin throughout the cell. Transfection of SW480 cells with wild-type APC, results in a decrease of β -catenin staining on immunofluorescence. The ability of several APC constructs to down-regulate β -catenin was investigated and it was found the presence of the central region of the protein was essential for the down regulation of β -catenin (Munemitsu et al., 1995). Consistent with these findings, mutant APC genes' protein products present in colorectal tumours have been found to be defective in their ability to reduce β -catenin activity (Morin et al., 1997).

As well as APC mutations, de-regulated β -catenin signalling may also occur from mutations in β -catenin itself (Morin et al., 1997). In 2 colorectal cell lines with full length APC, HCT116 and SW48, β -catenin / TCF-mediated transcription remains constitutively active, and is unaffected by wild-type APC. However, these cells were found to have mutations in the β -catenin gene: HCT116 a 3-bp deletion removing amino acid Ser45 and SW48 a missense mutation that changing Ser33 to Tyr. In a series of primary colorectal cancers without APC mutations, over half the cancers were found to have β -catenin mutations thought to affect their ability to become phosphorylated (Morin et al., 1997). β -catenin mutants are highly inductive of β -catenin / TCF mediated transcription (Morin et al., 1997).

β -catenin stabilization and resultant activation of TCF-dependent transcription can also, though less commonly, occur as a result of mutation in Axin 2. This functional effect of mutant Axin 2 has been demonstrated in cell lines. A series of human colorectal tumours demonstrated Axin 2 mutations in a third of tumours with defective DNA mismatch repair. These tumours had β -catenin accumulation, whilst not possessing mutations in APC or CTNNB (Liu et al., 2000).

The effect of APC in regulating β -catenin / TCF-mediated transcriptional activity has been investigated in colon cancer cell lines and several other systems. As discussed above in the description of Wnt target gene research, manipulation of the Wnt

signalling system by reducing APC function or treating with ectopic Wnts has led to the discovery of many Wnt target genes.

1.5.2 Wnt and solid cancers other than colorectal cancer

Wnt signalling has been investigated in prostate, colorectal, breast, lung, pancreatic, ovarian, gastric and penile cancer. Several studies have investigated Wnt signalling in prostate cancer tissue. Compared to benign prostate tissue, there is up-regulation of certain genes (SFRP4, Fz4, Fz6, DVL1, TCF4, and MYC) and down regulation of others (WNT2, WIF1, PPP2CB, CCND2, CD44) in prostate cancer. (Wissmann et al., 2003). Further work found Wnt 5a expression is elevated in prostate cancer tissue compared to benign tissue (Wang et al., 2010). Expression of Wnt 5A mRNA and Wnt5A protein was also increased in a prostate cancer cell line compared with a benign cell line. (Wang et al., 2010). Wnt 5A expression is greater in high grade cancers compared to cancers of lower grade Gleason 7 cancers or below. Wnt5a expression has been found to be prognostic and an independent predictor for prostate cancer relapse following radical prostatectomy (Yamamoto et al., 2010).

Table 3 below lists our current understanding of the role of Wnt signalling in cancer.

Table 3. Wnt signalling in solid cancers.

Tumour	Investigated in	Mechanism	Wnt abnormality
Prostate	Human prostate cancer and benign tissue	Cancer tissue demonstrates a differential in RNA expression of Wnt gene genes	Comparison of Wnt genes expressed in prostate cancer tissue compared with benign tissue demonstrated up-regulation of certain genes (SFRP4, Fz4, Fz6, DVL1, TCF4, and MYC) and down regulation of others (WNT2, WIF1, PPP2CB, CCND2, CD44). The most marked aberrant RNA expression in cancer were of Wnt inhibitory factor 1 (WIF1) and secreted frizzled related protein (SFRP4). SFRP4 was up-regulated in 81% of the tissues it was expressed in, whilst WIF1 was down regulated in 64%. There is also reduced expression of WIF1 protein in 23% of the prostate cancers analysed (Wissmann et al., 2003).
	Prostate cancer mouse model; human prostate cancer and benign tissue	Wnt 5A acts as an activator carcinogenesis, potentially via AR signalling	Using a mouse model, a mutation in the androgen receptor – AR T887A mutation – led to the formation of prostate cancer development. In such tumours, Wnt 5A was an activator for carcinogenesis. In human benign prostatic hyperplasia, Wnt 5A expression is normal whilst in prostate cancer tissue Wnt 5A levels are elevated. Co-localisation of AR proteins and Wnt 5A was specifically seen in in cancerous tissue (Takahashi et al., 2011).

<p>Human prostate cancer and benign tissue Prostate cancer cell lines and benign cell line</p>	<p>Wnt 5A is overexpressed in a prostate cancer cell line and prostate cancer tissue. mRNA of Wnt/β-catenin target genes mRNA is reduced in prostate cancer; Wnt5A induces a Ca^{2+} release in the PC3 cell line.</p>	<p>Wnt 5A protein is expressed in benign and malignant human prostate cancer tissue and semi-automated analysis demonstrates expression is significantly elevated in malignant compared to benign prostate tissue. Expression of Wnt 5A mRNA and Wnt 5A protein was increased in a prostate cancer cell line compared with a benign cell line. Wnt/β-catenin mediated TCF transcription target genes' mRNA is reduced in prostate cancer cells compared with benign cells, suggesting Wnt/β-catenin mediated TCF transcription may be of less significance in prostate cancer than other Wnt mechanisms such the Wnt / Ca^{2+} pathway. Wnt5A peptide induces Ca^{2+} release of up to 100s duration in prostate cancer cell line PC3 (Wang et al., 2010).</p>
<p>Human prostate cancer and benign tissue Prostate cancer cell lines and benign cell line</p>	<p>Wnt5a expression is increased in prostate cancer tissue; Wnt 5A is associated with invasion in prostate cancer cell lines; Wnt 5A expression is a prognostic factor for clinical relapse.</p>	<p>On immunohistochemistry of prostate cancer tissue, Wnt 5A expression is elevated in cancer tissue compared to benign tissue. A greater proportion of high grade cancers expressed Wnt 5A compared to cancers of lower grade Gleason 7 or below. On multivariate analysis, Wnt 5A staining was found to be an independent predictor for prostate cancer relapse following radical prostatectomy. Knockdown Wnt 5A in a prostate cancer cell line DU145 reduces invasion whilst Wnt 5A overexpression in prostate cancer cell line PC3 stimulates invasion. (Yamamoto et al., 2010)</p>

Colorectal	Human colorectal cancer; mouse model	Mutation in APC leads to loss of function and unregulated β -catenin causing aberrant Wnt signalling	As discussed earlier, most human colorectal cancers have a loss of function of APC, (Kinzler and Vogelstein, 1996) which usually functions as a tumour suppressor through its regulation of β -catenin. This regulation is required for both prevention of tumourigenesis as well as normal embryonic development (Smits et al., 1999).
	Colorectal cancer cell lines, human colorectal cancer	As well as APC mutations, de-regulated β -catenin signalling may also occur from mutations in β -catenin itself	In certain colorectal cancer cell lines, β -catenin / TCF-mediated transcription is constitutively active, and is unaffected by wild-type APC. However, these cells were found to have mutations in the β -catenin gene: HCT116 a 3-bp deletion. In a series of primary colorectal cancers without APC mutations, over half the cancers were found to have β -catenin mutations thought to affect their ability to become phosphorylated. β -catenin mutants are inductive of β -catenin / TCF mediated transcription (Morin et al., 1997).

Breast	Breast cancer cell lines	Upregulated β -catenin from autocrine expression of Wnt ligands	Breast and ovarian cancer cells lines with transcriptionally active β -catenin do not have mutations in β -catenin or APC, but express Wnt ligands in an autocrine fashion. Wnt antagonists FRP1 and DKK1 inhibit the upregulation of β -catenin in these cells (Bafico et al., 2004).
	Human breast cancer, breast cancer cell lines, breast cancer mouse model	LRP6 co-receptor activates Wnt signalling and its inhibition reduces carcinogenesis	The co-receptor LRP6 is upregulated in a proportion of breast cancer tissues and cell lines, particularly those which are receptor negative. Knockdown of LRP6 results in a reduction of β -catenin and Wnt gene transcription as measured by quantification of target genes as well as a TCF-dependent TOP Flash reporter. Overexpression of LRP6 increases cancer cell proliferation in a cell line and suppression of LRP6 reduces cancer growth in a breast cancer mouse model (Liu et al., 2010).
	Human breast tissue	Cytoplasmic and nuclear β -catenin is elevated in in-situ and invasive cancers and is indicative of poorer prognosis	Membrane β -catenin is found in normal tissue, but less frequently in in-situ and invasive carcinoma. Cytosolic and nuclear β -catenin is scarce / absent in benign breast tissue but seen in in-situ and invasive cancers. Elevated cytosolic or nuclear β -catenin expression is associated with poorer prognosis (Khramtsov et al., 2010).

Lung	Human lung cancer tissue and lung cancer cell lines	Dishevelled overexpression is important in Wnt signalling activation and colony formation in NSCLC	Dishevelled 3 is overexpressed in lung cancer. Transfection of siRNA results in selective inhibition of human dishevelled -1, -2 and -3 in non-small cell lung cancer (NSCLC) cell line H1703. This reduced β -catenin expression and TCF-dependent transcriptional activity and colony formation in H1703 (Uematsu et al., 2003).
Pancreas	Human pancreas cancer tissue	Elevated total β -catenin is found in adenocarcinoma of the pancreas, whilst mutation in β -catenin is rare	Analysis of human adenocarcinoma of the pancreas tissue and benign pancreatic tissue demonstrated elevated total β -catenin in malignant tissue. However, very few of these tumours demonstrated a β -catenin mutation.
Ovarian	Ovarian cancer cell lines	Upregulated β -catenin from autocrine expression of Wnt ligands	Breast and ovarian cancer cells lines with transcriptionally active β -catenin do not have mutations in β -catenin or APC, but express Wnt ligands in an autocrine fashion. Wnt antagonists FRP1 and DKK1 are able to inhibit the upregulation of β -catenin in these cells (Bafico et al., 2004).
Gastric	Human Gastric cancer	Nuclear β -catenin detected in proportion of gastric cancers, with frequent mutation in exon 3	Nuclear β -catenin was found in almost 30% of gastric cancers, and 26% had a mutation in exon 3 of β -catenin. In tumours where there was no nuclear β -catenin, none the cancers tested were found to have a mutation in β -

			catenin. This mutation in β -catenin may be important in carcinogenesis in gastric malignancy (Clements et al., 2002).
	Gastric cancer cell lines, human gastric cancer, <i>in vivo</i> mouse model	HMGA1 is a target of Wnt and is associated with nuclear β -catenin and increased proliferation of gastric cancer cells	High-mobility group A (HMGA) proteins are expressed in several cancers, including gastric cancer. Knockdown of cmyc or β -catenin in gastric cancer cell lines results in reduced HMGA1. Knockdown of HMGA1 with siRNAs results in reduced proliferation of gastric cancer cells. In gastric cancer tissue, increased detection of HMGA1 was associated with nuclear β -catenin in 30% of studied samples (Akaboshi et al., 2009).
Penile	Human penile cancer tissue and benign penile tissue	There is increased expression of Wnt protein in squamous cell carcinoma of the penis and benign / malignant tissue may be characterised by Wnt protein co-localisation	Protein expression of Wnt4 and of several downstream targets of β -catenin transcription activation - MMP7, cyclinD1 and c-MYC - are significantly increased in squamous cell carcinoma of the penis in comparison to non-malignant penile tissue. In addition, when protein co-localisation was analysed in control benign / grade 1 malignant / grade 2 malignant tissues, differences in co-localisation between certain proteins, such as MMP7/Wnt4, was between different tissues. These differences in Wnt protein expression may in the future be

			used as a biomarker in diagnosis or prognosis of squamous cell carcinoma of the penis. (Arya et al., 2015)
--	--	--	---

1.6 Wnt signalling in stem and cancer stem cells

Wnt signalling is involved in both the self-renewal and differentiation of stem cells and may play an important role in the behaviour of cancer stem cells. This is discussed below.

1.6.1 Wnt in stem cells

Crypts of the small intestine provide a physiological example of the importance of Wnt signalling and stem cell function. The epithelium of the small bowel epithelium is continuously undergoing self-renewal with the maintenance of several differentiated cell types. Stem cells reside towards the base of the crypts and produce progenitor cells (sometimes called transit amplifying cells), which differentiate as they move away from the crypt base towards the villi (Barker et al., 2012; Potten and Loeffler, 1990).

The key role of β -catenin / TCF transcription in maintaining stem cell function in the small intestine crypt has been demonstrated by studying TCF 712^{-/-} mice which lack TCF 4 activity. In the small intestine of control mouse embryo, various differences are observed in the morphology of cells on the villi compared with the inter-villi regions which were not found in TCF 712^{-/-} mice where cells of different compartments appeared the same. In normal mice, proliferation measured by Ki 67 staining was noted but restricted to the inter-villus regions whilst Tcf712^{-/-} mice demonstrated no Ki67 staining. Once neonatal, the intestinal epithelium of Tcf712^{-/-} mice consisted only of differentiated villus cells (Korinek et al., 1998). Similarly, in transgenic mice which ectopically express Wnt inhibitor Dickkopf1 (Dkk1), crypt and villus formation is greatly reduced and staining for β -catenin and proliferation markers is absent from crypt regions. Mutant mice also fail to produce secretory cell lineages in the intestine (Pinto et al., 2003).

In a study investigating Wnt target genes in colorectal cancer, nuclear β -catenin expression correlated with Wnt target gene expression in both cancer and the proliferative region of benign colon crypts using immunohistochemistry (van de Wetering et al., 2002). In addition, cells at the base of crypts demonstrate nuclear β -catenin staining which decreases in cells ascending up the crypt towards the surface. In colorectal cancer cell line Ls174T, genes down-regulated by dominant-negative TCF are those expressed by proliferating cells of the crypts, whilst differentiated epithelial cells express genes that were up-regulated when β -catenin / TCF transcription was suppressed (van de Wetering et al., 2002). Expression of the ligand ephrin-B1 and receptors EphB2/EphB3 are controlled by β -catenin / TCF transcription (Batlle et al., 2002; van de Wetering et al., 2002). *In vivo*, histological structure of crypts and villi in EphB2 /EphB3 mutant mice has been studied. Double mutant mice lack a clear boundary between proliferative and differentiated regions usually observed when proliferative cells are present in regions normally composed of differentiated cells (Batlle et al., 2002).

1.6.1.1 Wnt signalling in breast tumour initiating cells

The importance of Wnt β -catenin signalling has been demonstrated in breast tumour initiating cells, and further to this, the effect of inhibition of Wnt / β -catenin signalling on effectively suppressing tumourigenicity (Hallett et al., 2012).

In one such study, microarray analyses with global gene expression profiling were performed on tumourspheres (breast tumour inducing cells), mammospheres (mammary epithelial stem / progenitor cells), and mammospheres induced to differentiate *in vitro* (differentiated mammary epithelial cells). This demonstrated tumourspheres highly expressed transcripts of Wnt / β -catenin pathway genes compared with mammospheres or mammospheres induced to differentiate. Tumourspheres also highly expressed certain Wnt / β -catenin target genes such as Axin2, cyclinD1 and CD44. Mammospheres induced to differentiate express transcripts of inhibitors of Wnt / β -catenin signalling, such as Sfrp1, Sfrp2 and Dkk2. This pattern of expression between the three types of cells was confirmed with quantitative RT-PCR, which also demonstrated elevated expression of Wnt 7A, Wnt

7B, and Fz 4 and Fz 6 receptors in tumourspheres. In terms of clinical application of these findings, a Wnt breast tumour inducing cell gene signature of genes differentially expressed between tumourspheres and mammospheres induced to differentiate *in vitro* was used to categorise human tumour tissue into 2 groups. The group with expression of tumoursphere-related Wnt / β -catenin pathway gene expression had poorer overall and metastasis free survival when compared with the group with gene expression related to that of mammospheres induced to differentiate *in vitro* (Hallett et al., 2012).

1.7 Experimental aims

There is clear evidence of Wnt signalling being involved in carcinogenesis of many cancers including prostate cancer (section 1.5); the role of Wnt signalling is also well characterized in the maintenance of stem cells (section 1.6). Cancer is often suggested to be a disease of stem cells (Clarke et al., 2006; Reya et al., 2001a) and therefore I decided to establish an experimental system in which to investigate this notion. Ideally the role of Wnt signalling in prostate cancer would be studied *in vitro* models of human prostate cancer stem cells isolated from fresh tissue. There are numerous difficulties in executing such a plan, the primary one being the availability of human tissue and also the identification of putative stem (let alone cancer stem cells). Cell lines are thought to contain a fraction of cells that behave like stem cells (termed stem-like cells in cell lines).

The aim of this study was to characterise colonies formed from PC3 prostate cancer cells and investigate the properties of Wnt signalling in the cells of these colonies.

1.7.1 Hypothesis

PC3 cells at clonal density will form colonies with distinct morphology upon which they can be categorised. These colony types respond differently to Wnt signalling. Wnt signalling occurs in the cancer stem-like cells of holoclones, but not paraclones. Cells within these colonies will express β -catenin. Cells within these colonies will demonstrate an intracellular Ca^{2+} release following Wnt treatment which may make these amenable to compounds and mechanisms (e.g. regulation of cell membrane potential) that regulate Ca^{2+} homeostasis.

1.7.2 Key objectives

The following objectives test the hypothesis:

- To assess if PC3 prostate cancer cells form distinct colony types when cultured from single cells.
- To develop an objective, quantitative method for the assessment of these colonies.
- To characterize Wnt signalling with regards to intracellular Ca²⁺ release and expression and location of β -catenin in these colonies.

Chapter 2: Materials and methods

2.1 Cell culture

The PC3 cell line was used to study colonies formed from clonal expansion, in live cell imaging experiments and for immunocytochemistry. This cell line originated from a prostate cancer bone metastasis (Kaighn et al., 1979). Other cells used in this research project included prostate cancer cell lines LNCaP derived from a supraclavicular lymph node metastasis (Horoszewicz et al., 1983) and DU145 derived from a brain metastasis (Stone et al., 1978). Cell culture was performed as described below for all cell lines.

Cells were cultured in 75 cm² culture flasks (Nunc) in RPMI1640 (Invitrogen) supplemented with 2 mM L-Glutamine (Invitrogen) and 10% foetal bovine serum (FBS) (PAA, UK #A10409-1608); this will be referred as culture medium, henceforth. Cells were incubated at 37°C 5% CO₂. As a general practice cells were grown in culture to approximately 70% confluency. To passage cells, medium was aspirated from the culture flask using a glass pipette and suction device. Two millilitres of trypsin 0.25% (Invitrogen) was added to the empty flask, ensuring coverage of the base of the flask, and the flask then placed in an incubator at 37°C for 3-4 min. Following this period cells were inspected for detachment from the surface of the flask, and the cell suspension was transferred using a pipette into a 7ml Bijou bottle containing 2 ml culture medium. The number of cells / ml in this cell suspension was determined as outlined below. The cell suspension was used to set up fresh culture flasks or used in experiments.

2.1.1 Cell counting using a haemocytometer

The haemocytometer was to determine the number of cells / ml in a cell suspension following trypsinisation. The cell suspension was gently mixed by pipetting and 100 µL cell suspension added to 100 µL trypan blue (Sigma-Aldrich) in an Eppendorf

tube. 100 μ L of this blue cell suspension was loaded into the haemocytometer chambers. Using the 10X objective of the microscope, the number of viable cells in each of the 4 peripheral cells and the central square were counted.

The number of cells / ml = total counted cells / 5 x 10 000 x 2.

2.2 Clonal expansion

2.2.1 Clonal expansion in 6 well plates

Colonies formed from single cells were studied in a clonogenic assay (McCulloch et al., 1981; Pellegrini et al., 1999). A cell suspension was made through trypsinisation of a culture flask (not >70% confluent as described above). A cell count using trypan blue and a haemocytometer was used to determine the concentration of cells / ml in the cell solution. Serial dilution of the cell suspension was performed by diluting a small volume of cell suspension into a larger volume of supplemented RPMI medium, to achieve a final cell suspension of 40 cells / ml.

Six well plates (Nunc) were used to study colony formation. Cells were plated at clonal density, defined as 60 cells / well in 3 ml of culture medium (60 cells / 9.6cm²). Some plates were placed in the IncuCyte™ (Essen Bioscience), a live cell imaging apparatus, for cell division and colony formation studies. Cell culture medium was changed at day 5 with a fresh 3 ml of culture medium and colonies imaged and colony size measured at day 10.

2.2.2 Clonal expansion with cells grown on FluoroDishes

In order to study Wnt induced [Ca²⁺]_i release (Wang et al., 2010) and protein expression in colonies, further colonies were grown in 35-mm FluoroDishes (catalog no. FD35-100, World Precision Instruments). FluoroDishes were placed on a plastic surface to facilitate their handling and transfer. Cells were plated at clonal density on FluoroDishes defined as 40 cells in 1 ml culture medium / dish. After 1 day, once cells had become adherent, a further 1 ml RPMI was added to each dish. Culture

medium was changed on day 7. Colonies were used for live cell Ca^{2+} imaging or immunostaining at day 12.

2.3 Live cell free intracellular calcium ($[\text{Ca}^{2+}]_i$) imaging of colonies

Live cell Ca^{2+} imaging was performed based upon previous work from our group (Wang et al., 2010) An Olympus FluoView FV 1000 confocal microscope (Olympus KeyMed) with x10 and x20 dry objectives (numerical aperture = 0.75) was used. Ca^{2+} dyes Fluo-4 and FuraRed (Invitrogen) were used: Fluo4 binds free calcium and FuraRed detects bound calcium within the cells; in live calcium measurement assays, as the Ca^{2+} is released from the stores in response to a stimulus (e.g. Wnt ligand) the Fluo4 signal should increase while the FuraRed signal should simultaneously decrease. The ratio of the signal between Fluo4 and FuraRed represent the free intracellular calcium release (Thrasivoulou et al., 2013) (Wang et al., 2010). PC3 cells were plated at low density and cultured as described above for experiments. On day 12 after plating, FluoroDishes were carefully transported to the UCL core facility for confocal imaging where the Olympus system resides. For each dish, culture medium was discarded and replaced with just 1ml culture medium. 2 μl Fluo-4 and 2 μl FuraRed each at concentration 1ng / ml was added to the FluoroDish for 15 min.

The culture medium was then discarded, the dish washed with 2ml PBS and a further 1 ml of fresh culture medium added to the dish. The FluoroDish was placed into the chamber of an Olympus microscope with incubator set at 37°C. All live intracellular Ca^{2+} experiments were performed at 37°C.

Cells were viewed using x10 objective to identify an individual colony of cells. This colony was then observed at x20 and 20 cells were contoured (sampled) as separate regions of interest for further analysis. On Olympus settings, imaging was performed using excitation from an argon laser (488nm) with emissions recorded in green (510–580 nm) and red channels (600–700 nm) for Fluo-4 and FuraRed respectively (Wang

et al., 2010). The microscope was set at x20 objective; zoom x1; 512x512. Gain was appropriately adjusted so as the signal would have scope to potentially increase or decrease in intensity before being saturated or disappearing. Images were taken at intervals of 450ms. Excitation of Fluo-4 and FuraRed was recorded and exported into an excel file for analysis. Cells were imaged for a “run in” period of at least 30-60s before proceeding with the experiment. During this run-in period a plateau of intensity was observed. At this time, either 2 µl of PBS control, 2 µl of 100 ng/ml Wnt 5A (R&D Systems) or 2 µl of 100 ng/ml Wnt 9B (R&D Systems) was very carefully and gently pipetted onto the surface of the medium in the dish, at a distance of approximately 1cm from the colony being imaged. Imaging continued until no further response or change in plotted intensity was observed. Data from each experiment was saved as an OIF movie file and exported as an excel datasheet. Analysis of live cell imaging data is detailed in chapter 3.

2.4 Cell proliferation assays

Using PC3 cell line, cell culture, trypsinisation and cell counting was performed as described in sections 2.1.1. 50 000 cells were plated into each well of a 6 well plate (Nunc) with or without experimental compounds (see below). Plates were placed in an IncuCyte™ programmed to image a selection of areas of each well at a 4 hour time interval. Following 24 hours, once cells had become adherent, the control and experimental wells were treated with the appropriate agents and placed back in the IncuCyte™ for further imaging of cell proliferation. Compounds used, and details of this assay are described in section 4.2.

2.5 Immunocytochemistry

2.5.1 Cell fixation

Cells were washed with PBS and fixed with 1ml 4% paraformaldehyde (PFA) at room temperature for 20 min. Cells were then washed 3x with PBS for 5 min. Plates were sealed and stored at 4°C for up to 1 month.

2.5.2 Cell staining

A permeabilisation buffer of 0.2% bovine serum albumin (BSA) in PBS with 0.2% Triton x 100 (Sigma) was prepared. 1ml permeabilisation buffer was added to each dish and incubated for 40 min.

The permeabilisation buffer was removed and cells blocked with 10% normal goat serum (NGS) (PAA) in PBS for 30 minutes at room temperature to prevent non-specific binding. Primary antibody dilutions were prepared in 1% NGS in PBS and the blocking buffer was removed and replaced with the primary antibody and incubated overnight at 4°C in a humidity box, to prevent drying (see sections 3.2.4 and 4.2.2). For negative control, antibody diluent containing no antibody was added to the target well. Following an overnight incubation, the primary antibody was removed, and the wells were washed 4 times with PBS containing 1% NGS.

Secondary Ab was prepared at dilution 1:500 in 2% BSA in PBS and added to the dishes. The vessels were again placed upon a tray which was wrapped in foil and placed on a rocker at medium speed in a dark room for 60 min. Following this time, cells were washed in PBS for 3 x 5 min.

At the final wash extra care was taken to remove as much PBS as possible. A small drop of Vectorshield mounting medium with DAPI (vector laboratories) was placed on a glass round coverslip diameter 22 mm. The coverslip was gently placed onto

the surface of the Fluorodish using forceps. Care was taken to lower the coverslip onto the dish so as to avoid disruption of cells and formation of air bubbles. Dishes were placed on a tray and wrapped in foil and left at 4°C until imaging.

2.5.3 Imaging using confocal microscopy

Imaging of fixed and stained cells was performed using an Olympus confocal microscope. Cells were focussed upon and serial sections were imaged through the cells forming a Z-stack. Slices were imaged at 0.63 µm intervals such that each stack was formed of approximately 15 images. Images were taken using x10; x20; x40 objectives and sometimes with the combination of a zoom function. Z stack images are presented in subsequent chapters. Further details are described in section 3.3.

2.6 Polymerase Chain Reaction (PCR)

2.6.1 Primer design

Primer design was the first step in investigating gene expression in cells of interest. Several websites were used in the primer design process. <http://www.genecards.org/> was used in determining the correct nomenclature for genes and the NCBI/Primer-BLAST website was used for primer design. Primer lengths of 20 base pairs and product size 400-600 base pairs were requested parameters. Of those primer pairs suggested by the website, those with an appropriate GC content of 55%, and similar annealing temperatures of approximately 50°C were selected.

2.6.2 RNA extraction

RNA extraction from harvested cells was performed using Qiagen RNeasy Mini Kit (Qiagen, Manchester). The kit protocol was followed as detailed in the 06/2012 handbook. <http://www.qiagen.com/us/products/catalog/sample-technologies/rna-sample-technologies/total-rna/rneasy-mini-kit/>. As per the protocol, RNA was eluted using 50 µl RNase-free water. RNA concentration was measured using a spectrophotometer at 260 and 280 nm wavelengths. RNA extraction from cells of colonies and PCR of stem cell genes is detailed in chapter 3.

2.6.3 Reverse transcription of RNA into cDNA

RNA was synthesised to cDNA using a Qiagen Omniscript RT kit as per the 10/2010 handbook protocol: <http://www.qiagen.com/us/products/catalog/assay-technologies/end-point-pcr-and-rt-pcr-reagents/omniscript-rt-kit/>. For sufficient yield of cDNA for subsequent PCR, constituents were scaled up x 2 so that 4 µg template RNA was used and made up to a volume of 24 µl with RNase free water as indicated in table 4. Once the protocol was completed, the cDNA was frozen at -20C if for later use in PCR.

Table 4. Mixture composition used for reverse transcription reactions.

In each reaction 4 µg template RNA was used and made up to a volume of 24 µl with RNase free water as indicated. The reaction mixture was made up with the constituents as shown to a volume of 40 µl.

Reaction Component	Volume (µl)
10x Buffer RT	4
dNTP Mix	4
Oligo dT primer (8.4 µM)	4
RNase inhibitor	2
Omniscript reverse transcriptase	2
RNase free water + Template RNA	24

Total Volume	40
--------------	----

2.6.4 PCR

PCR was performed using Qiagen Taq PCR Master Mix kit and following the protocol handbook 10/2010. <http://www.qiagen.com/us/products/catalog/assay-technologies/end-point-pcr-and-rt-pcr-reagents/taq-pcr-master-mix-kit>. Prior to commencing PCR cDNA was thawed on ice and quantified using a spectrometer giving a concentration in $\mu\text{g/ml}$. 0.5 μg template cDNA was used in all PCR reactions per reaction tube. The volume of cDNA required for 0.5 μg was calculated and the volume of RNase free water to make a cDNA solution up to 12 μl was calculated as indicated in table 5. Reaction tubes were placed in a thermal cycler programmed as indicated in table 6. Following amplification, PCR product samples were stored at 4°C until agarose gel electrophoresis.

PCR of ion channel genes is detailed in section 4.2.1.

Table 5. Reaction mixture made up in each tube for PCR reaction.

For all PCR reactions 0.5 μg template cDNA was used in each reaction tube. The volume of cDNA required for 0.5 μg was calculated and the volume of RNase free water to make a cDNA solution up to 12 μl was calculated as indicated in table 5. The other constituents were added as in the table to a total volume of 30 μl .

Reaction Component	Volume (μl)
Taq PCR mastermix solution	15
Primer A (forward) 8.4 μM	1.5
Primer A (reverse) 8.4 μM	1.5
RNase-free water + Template DNA 0.5 μg	made up to 12
Total volume	30

Table 6. Programme for thermal cycler.

PCR reaction tubes were placed in a thermal cycler programmed as indicated below. Following amplification, PCR product samples were stored at 4°C until agarose gel electrophoresis.

Initial denaturation	3 min	94°C	
3-step cycling			
Denaturation:	0.5–1 min	94°C	Approximately 5°C below T _m of primers
Annealing:	0.5–1 min	55°C	
Extension:	1 min	72°C	
Number of cycles:	35		
Final extension			
Final extension	10 mins	72°C	
Following end of programme			
Following end of programme		4°C	

2.6.5 Agarose gel electrophoresis

A concentrated stock solution of TAE_x50 was diluted x50 using de-ionized water to TAE_x1. Agarose gel 1.1% was made up using 150 ml TAE_x1 with 1.65 g agarose in a conical flask. This mixture was heated at high power in a microwave for approximately 3 min, with swirling in between, until boiling and all agarose had dissolved. The flask was left to cool for approximately 10 min after which 10 µl 0.5 µg/ml ethidium bromide (Sigma-Aldrich) was added. The mixture was then gently poured in to an electrophoresis gel tray (Bio Rad) and 2 combs placed in the tray to create wells. The gel was left to set for approximately 20 min. Once set the combs were removed and the gel and tray placed in a bath of TAE_x1 in an electrophoresis machine. Care was taken to ensure TAE_x1 covered the surface of the gel. A template was created mapping which product was to be pipetted into which well. 10 µl of each PCR product was pipetted into wells with 1 µl 10x Blue Juice loading dye (Sigma-Aldrich). 2 µl of 1K base pair DNA ladder (ThermoFisher Scientific 10787-018) was also pipetted into a well in each column with <1 µl 10x Blue Juice loading dye.

For gel electrophoresis a current was applied at 110V for duration of 70 min. Following this time, the gel was imaged under UV light analysed for the presence of product bands at the expected sizes to be indicative of expression of that specific gene.

2.6.6 Sequencing

To confirm products visualised at the expected band size were amplified products of the genes being characterised, positive bands genes of interest were sent to for sequencing. Immediately after imaging a gel, a clean scalpel was used to carefully cut out a band from the gel. Each PCR product band was placed in an Eppendorf tube. DNA extraction from the gel was performed using a QIAquick[®] Gel Extraction Kit (Qiagen). The protocol handbook 10/2010 was followed:

<https://www.qiagen.com/gb/resources/resourcedetail?id=f4ba2d24-8218-452c-ad6f->

1b6f43194425&lang=en. The DNA was sent for sequencing to Beckman Coulter Genomics (now known as Genewiz Europe (Takeley, UK). The resultant sequences were read using Finch TV software and cross-referenced for the gene on the NCBI website.

Chapter 3: PC3 prostate cancer colony formation and characterisation

3.1 Introduction

The colony forming ability of PC3 cells and the differential behaviours of distinct colonies which are derived from single cells have been investigated (Li et al., 2008; Zhang and Waxman, 2010). Distinctive colonies - holoclones, meroclones and paraclones - have been observed when PC3 cells are cultured at low density (1 cell / 32mm² clonal density) (Li et al., 2008; Zhang and Waxman, 2010). Holoclones were colonies characterised as consisting of small tightly packed cells; paraclones were larger colonies comprised of fewer cells; meroclones were colonies in between in size and number of constituent cells (Li et al., 2008; Zhang and Waxman, 2010).

Cells of these different colony types have distinct biological properties. On serial passage, cells of the holoclone colony type had the highest survival and paraclone colony type the lowest survival rate (Li et al., 2008). Cells of holoclones are considered cancer stem cell-like in their properties and unlike cells of paraclones, are able to induce tumour in a xenograft model (Li et al., 2008; Locke et al., 2005; Pfeiffer and Schalken, 2010).

Wnt signalling occurs in stem-like cells (Reya and Clevers, 2005; (Reya et al., 2003; Willert et al., 2003). A physiological example of Wnt signalling in stem cell function is in the crypts of the small intestine of the human gastrointestinal tract (Barker et al., 2012; Potten and Loeffler, 1990). Wnt signalling occurs in cancer stem-like cells (Hallett et al., 2012; Holland et al., 2013; Reya and Clevers, 2005; Reya et al., 2001b). The importance of Wnt β -catenin signalling has been demonstrated in breast tumour initiating cells where inhibition of Wnt / β -catenin signalling suppressed tumourigenecity (Hallett et al., 2012).

Aim

The aim of the work described in this chapter was to assess if colonies are formed by a prostate cancer cell line (PC3) and if so, to characterise Wnt signalling by determining intracellular Ca^{2+} activation and β -catenin expression in different PC3 colonies.

3.1.1 Hypothesis

- 3.1.1.1 PC3 cells plated and cultured at clonal density, defined as 60 cells / well in 3 ml of culture medium (60 cells / 9.6cm²), will form distinct colonies of cells.
- 3.1.1.2 The colony types formed will resemble holoclones, meroclones and paraclones morphologically, but will also have objective features upon which they can be categorised.
- 3.1.1.3 Wnt signalling occurs in cells of PC3 colonies, but cells of different colonies will demonstrate differences in Wnt signalling with regards to Wnt induced intracellular Ca^{2+} release and expression of β -catenin, the two key transducers of Wnt signalling.

3.1.2 Objectives

- 3.1.2.1 To assess if PC3 prostate cancer cells form distinct colony types when cultured from single cells at clonal density.
- 3.1.2.2 To determine an objective, quantitative technique to describe these colonies formed from PC3 cells.
- 3.1.2.3 To characterise Wnt signalling with regards to intracellular Ca^{2+} release and expression and location of β -catenin in these colonies.

3.2 Materials and methods

3.2.1 Characterisation of colonies

The culturing of colonies was performed as outlined in section 2.3. Colonies were imaged at day 10 and exported as 'joint photographic expert group' (jpeg or jpg) files for further analysis. In order to calculate the cellularity of a colony, each image was processed using the Image J software (Murphy, 2012; Rasband, 2015) as follows:

- Image opened in Image J
- Image cropped so as to include colony only
- Image type converted to 8 bit greyscale
- Image thresholding applied to show cells; this is automated by processing and making the image binary
- Particles are analysed in image J
- Summary of area fraction of colony consisting of cells is given

3.2.2 Expression of stem cell genes in different populations of PC3 cells

PC3 cells in a single cell suspension were plated at clonal density (60 cells / well) in Nunc 6 well plates. Cells were cultured in 3 ml culture medium which was replaced after 5 days. For colonies grown for RNA extraction, 3 plates of cells were seeded for each experiment. Colonies were viewed using a microscope at x10 magnification and categorised as holo/meroclones or paraclones, initially, based upon the characteristics described previously (Li et al., 2008; Zhang and Waxman, 2010) and section 1.1.5. Cells were washed in PBS and replaced in 1 ml PBS/well. A 200 µl pipette was used to disrupt individual colonies and aspirate cells from individual colonies in a small volume of PBS. One centrifuge tube was used to collect cells aspirated from holo/meroclone colonies and another centrifuge tube used to collect cells from paraclone colonies. Cell suspensions were centrifuged at 350 x g for 5 min to obtain a cell pellet. RNeasy (Qiagen, Manchester) protocol was followed to extract RNA from pelleted cells. RNA was eluted into 50µl RNase-free water. The quantity

($\mu\text{g/ml}$) of isolated RNA was determined using a spectrometer machine. RNA was stored at -80°C until further use.

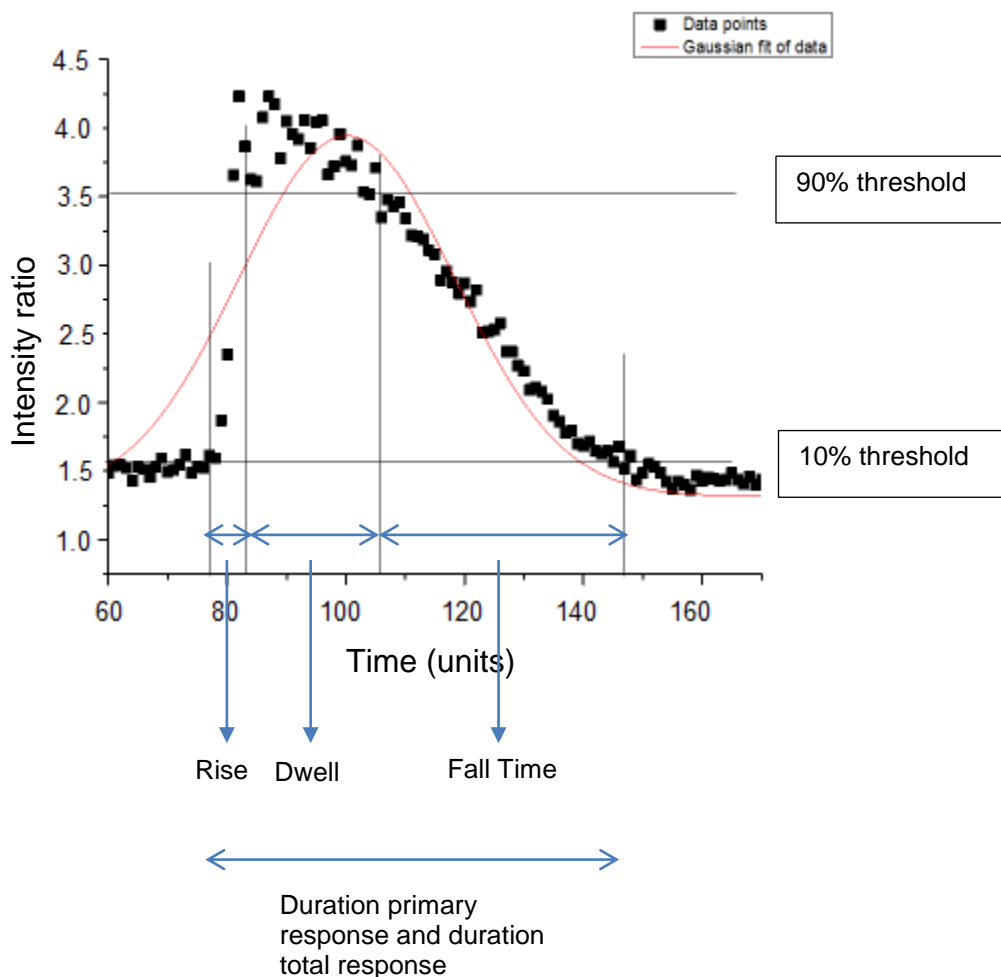
3.2.3 Live cell calcium imaging and data analysis

For methods of culture of PC3 colonies on FluoroDishes and intracellular calcium imaging on treatment with Wnt ligands see sections 2.2.2 and 2.3. For each cell, data points of intensity of signal were determined at 0.45s time intervals using Olympus FluoView 1000 software. Data from each experiment (after drawing regions of interest on cells within a colony) was saved as an Olympus (OIF) video file and also exported as an excel spreadsheet. Waveform graphs were created of Fluo-4 intensity: FuraRed intensity (y axis) against time (x axis) using Origin software. Graphs were used to determine the kinetics of $[\text{Ca}^{2+}]_i$ by calculating the rise, fall and dwell times of wave form for each cell.

A baseline (resting intensity) and maximum intensity reached for each waveform were determined and set as 0% and 100% excitation values for each specific cell. Using these values, 10% and 90% threshold values between the baseline and maximum were calculated and plotted on the waveform, and the time taken to reach these thresholds read from the graphs. The time interval between where the waveform rose intersected the 10% threshold until when it intersected with the 90% threshold was the rise time. The time the waveform was maintained above the 90% threshold was the dwell time. The time interval between the waveform falling from 90% to 10% threshold was the fall time. The time interval between the waveform rising above 10% to the initial fall to the 10% threshold was the duration of the primary response. The time interval between the waveform rising above 10% to the final fall to the 10% threshold was the duration of the total response. In many cases, where only a primary response was observed, the duration of the primary response was the same as the duration of the total response. These intervals of rise time, dwell time, fall time and duration primary and total response are as indicated in Figure 7 which shows a plotted waveform of intensity ratio against time obtained for one cell taken as a region of interest. Origin software was used to create graphs and test for statistical significance using the Mann-Whitney U test.

Figure 7. Plotted waveform of intensity ratio against time obtained for one cell taken as a region of interest.

For each cell, data points of intensity of signal were determined at 0.45 s time intervals using Olympus FluoView 1000 software. Data from each experiment (after drawing regions of interest on cells within a colony) was saved as an Olympus (OIF) video file and also exported as an excel spreadsheet. Waveform graphs were created of Fluo-4 intensity: FuraRed intensity (y axis) against time (x axis) using Origin software. The time interval between the waveform rose intersected the 10% threshold until when it intersected with the 90% threshold was the rise time. The time the waveform was maintained above the 90% threshold was the dwell time. The time interval between the waveform falling from 90% to 10% threshold was the fall time. The time interval between the waveform rising above 10% to the initial fall to the 10% threshold was the duration of the primary response. The time interval between the waveform rising above 10% to the final fall to the 10% threshold was the duration of the total response.



3.2.4 Immunocytochemistry for β -catenin

Colonies of PC3 cells were cultured on FluoroDishes and live cell Ca^{2+} imaging experiments performed as detailed in section 2.4. At the end of an experiment, the FluoroDish was left in the incubator at 37°C for 20 minutes. Medium was removed from the FluoroDish and cells fixed with 2ml paraformaldehyde (PFA) 4%. Following 20 minutes, PFA was removed from the FluoroDish and cells were washed in PBS 3x 5min. For each experiment day, 2 dishes were not treated with Wnt and the colonies cultured on these dishes were fixed as above.

Fluorodishes were labelled according to date, Wnt ligand, experiment number, and 1° and 2° antibody. Immunocytochemistry was performed as outlined in section 2.5.1. Primary mouse monoclonal antibody to beta catenin (abcam; ab22656) was prepared as indicated in Table 7. The permeabilisation buffer was removed and cells blocked with 10% normal goat serum (NGS) (PAA) in PBS for 30 minutes at room temperature to prevent non-specific binding. Primary antibody dilutions (Table 7) were prepared in 1% NGS in PBS and the blocking buffer was removed and replaced with the primary antibody and incubated overnight at 4°C in a humidity box, to prevent drying. For negative control, antibody diluent containing no antibody was added to the target well. Following an overnight incubation, the primary antibody was removed and the wells were washed 4 times with PBS containing 1% NGS. Secondary Ab was prepared at dilution 1:500 in 2% BSA in PBS and added to the dishes. The vessels were again placed upon a tray which was wrapped in foil and placed on a rocker at medium speed in a dark room for 60 min. Following this time, cells were washed in PBS for 3 x 5 min.

At the final wash extra care was taken to remove as much PBS as possible. A small drop of Vectorshield mounting medium with DAPI (vector laboratories) was placed on a glass round coverslip diameter 22 mm. The coverslip was gently placed onto the surface of the Fluorodish using forceps. Care was taken to lower the coverslip onto the dish so as to avoid disruption of cells and formation of air bubbles. Dishes were placed on a tray and wrapped in foil and left at 4°C until imaging.

Table 7. Antibodies and dilution used for β -catenin immunocytochemistry.

	Antibody	Dilution	Total Volume per Fluorodish
Primary	Mouse monoclonal to β -catenin (abcam ab22656)	1:250 in PBS BSA 2%	750 μ l
Secondary	Cy 5 Goat anti-mouse IgG (SouthernBiotech-1030-15)	1:500 in PBS BSA 2%	750 μ l

3.2.5 Imaging and analysis of β -catenin immunostaining

Colonies were imaged using an Olympus microscope system. The specific colony imaged in the live cell Ca^{2+} experiment was identified using 10x objective. Cells of this colony were then imaged using x40 objective at x3 zoom excited with a 647 nm wavelength. Serial images were taken at 0.63 μm intervals forming a Z stack. Z-stacks were visually assessed to explore differences in β -catenin expression following Wnt treatment and amongst cells in different colony types.

3.3 Results

3.3.1 Colony formation

Cells plated at clonal density (see section 2.2.1) in 6 well plates (Nunc), were cultured for 10 days and during this period formed clusters, or colonies that could be visually categorised into 2 types as shown in Figure 8. One type of colony consisted of tightly clustered, rounded cells and with a colony outline which could be well demarcated. Examples of the two types of colonies observed at day 10 are as shown in Figure 8.

This was consistent with holoclones or meroclone colonies previously described (Li et al., 2008; Pfeiffer and Schalken, 2010; Zhang and Waxman, 2010). A further type of colony was formed of cells with a greater inter-cellular distance, flattened in appearance and with a colony outline which was difficult to demarcate. The holoclone/meroclone packed colony is shown in figure 8A and the sparser, less distinct paraclone colony type shown in figure 8B.

PC3 cells plated on 6 well plates at 60 cells / well were incubated in an IncuCyte™ and imaged every 6 hours for 10 days as described in materials and methods (section 2.2.1). IncuCyte™ images around 25% of the well, which decreases the probability of focussing upon a single cell. Nonetheless, several single cells were captured at the start of imaging which went on to form colonies. Figure 9 shows representative images from IncuCyte™ at given time intervals which demonstrate the formation of a colony from a single cell. The images presented are representative of at least four independent experiments.

Figure 8. Image of 2 distinct PC3 cell colonies formed after 10 days culture at clonal density.

PC3 cells were plated on Nunc 6 well plates at clonal density, defined as 60 cells / well in 3 ml of culture medium (60 cells / 9.6cm²). Colonies were imaged, and colony size measured at day 10. Colony on the left (A) morphologically a holoclone or meroclone with tightly clustered cells and colony on the right (B) a paraclone with the appearance of more dispersed cells. Scale bar as shown. Representative image of experiments performed at least 10 times.

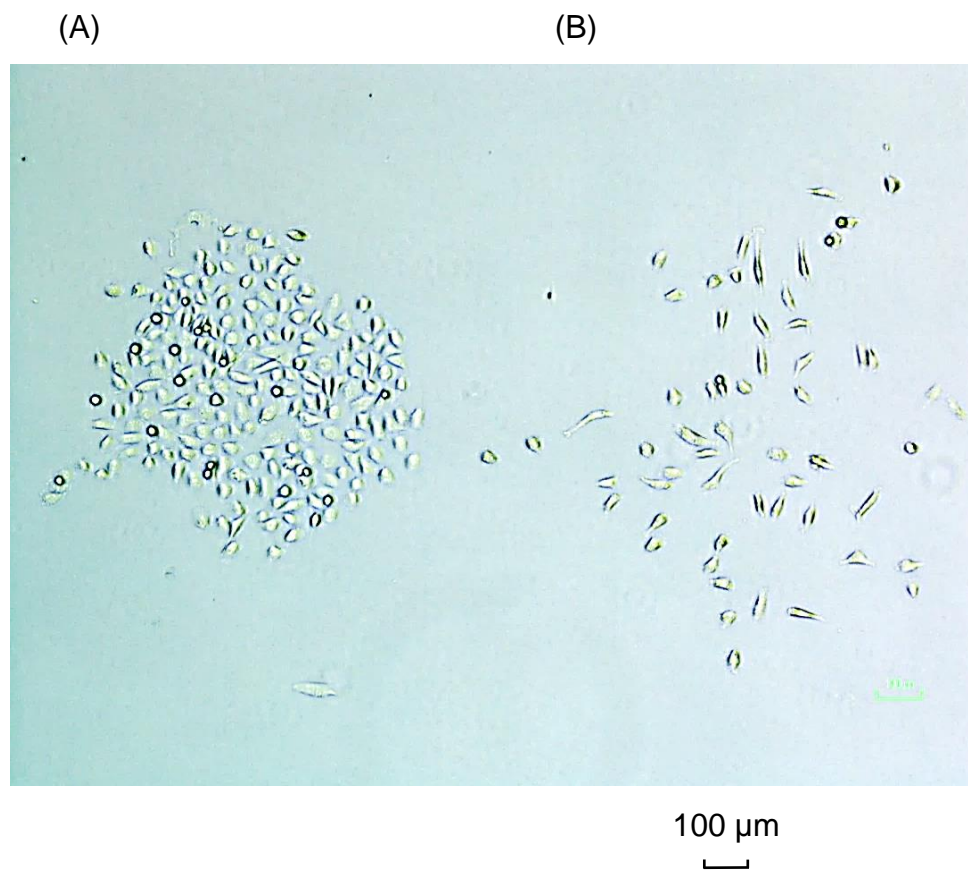
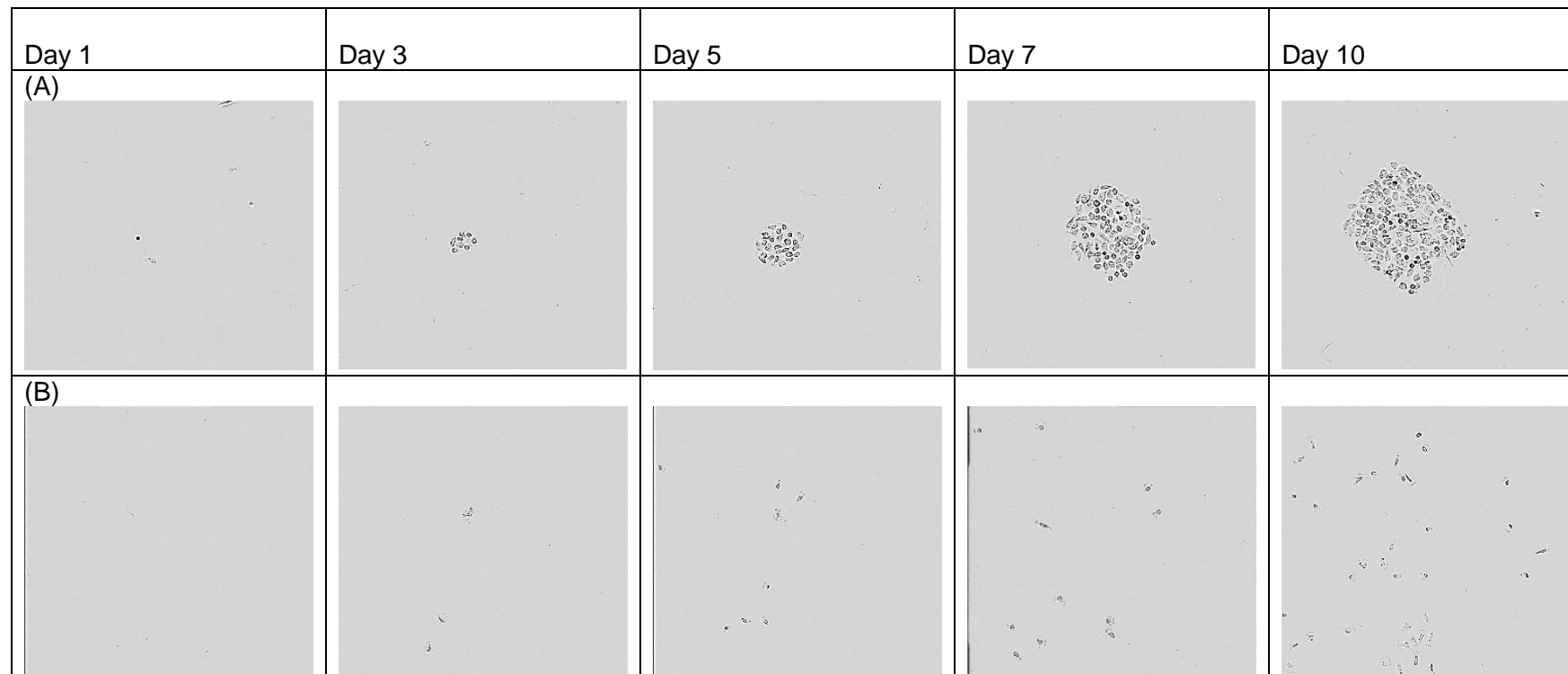


Figure 9. Sequential imaging using IncuCyte™ live image acquisition system showing colony formation by a single cell over a 10 period.

PC3 cells plated on 6 well plates (Nunc) at 60 cells / well in 3 ml of culture medium (60 cells / 9.6cm²). Plates were incubated in an IncuCyte™ and imaged every 6 hours for 10 days. Row (A) shows a single cell at day 1. This forms a colony of tightly clustered cells. (B) shows a single cell at day 1. This forms a colony of dispersed cells. Therefore, 2 morphologically distinct colony types are observed: (A) holo/meroclone and (B) paraclone.



0 400 μm

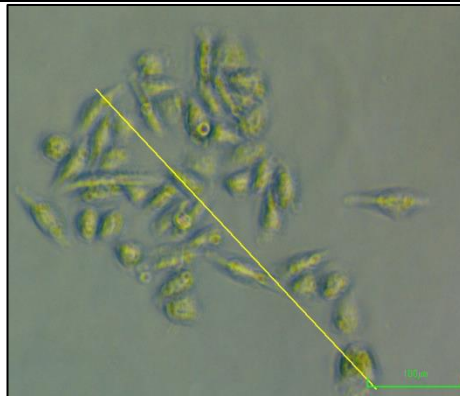

Colony formation by PC3 cells in 6 well plates was analysed. The experiment was repeated 4 times and data from 24 wells was obtained. A total of 198 colonies were observed at day 10 were and subjectively, morphologically categorised into 2 colony types: holo/meroclones or paraclones. Each colony was measured for diameter as shown in Figure 10A. This was defined as the greatest distance between 2 cells of a colony.

Figure 10B shows the automated conversion of an imaged colony into black and white for the calculation of an objective measure of how closely packed cells were in a colony, i.e. inter-cellular distance. This measure was defined as the “mean cell density” within each colony. Details regarding the processing of images and calculation of mean cell density are described in section 3.2.1.

Figure 10. Representative colony imaged using a bright field microscope.

(A) Shows a measurement made of the longest dimension of the colony. (B) Shows the image converted to a black and white 8 bit image by ImageJ for subsequent calculation of the % cellularity. PC3 cells were plated at cell density 60 cells / well in 3 ml of culture medium (60 cells / 9.6cm²) in 6 well plates (Nunc). Colony formation by PC3 cells was analysed.

(A) An example of a colony and the measured length as shown with a line. The length of the line is the colony diameter (434 μm)



(B) Image converted to 8-bit and proportion of total colony area covered by cells calculated (as described in section 3.2.5)



100 μM



Two, morphologically distinct, types of colonies were formed: holo/meroclones and paraclones. Table 8 describes parameters of almost 200 colonies analysed when PC3 cells were plated at clonal density. In a total of 24 wells, 102 colonies were formed and identified, morphologically, as holo/meroclones and 96 colonies as paraclones. Of the holo/meroclones, a mean number of 4.3 ± 0.4 colonies were formed with a mean diameter of $837.7 \pm 21.6 \mu\text{m}$. Of the paraclones, a mean number of 4.0 ± 0.4 colonies were formed with a mean diameter of $1191.3 \pm 28.3 \mu\text{m}$. Figure 10 shows the distribution of PC3 colony diameters. The diameters of all colonies formed are presented in Figure 11A and the distribution of colony diameter according to morphological type of colony (holo/meroclone or paraclone) is shown in Figure 11B.

There was no difference in the number of holo/meroclones formed and number of paraclones formed. An independent t-test performed for equality of means found that the diameter of paraclones was greater than the diameter of holo/meroclones ($p < 0.05$).

Thirteen colonies out of 120, comprising of both holo/meroclones and paraclones, were randomly selected and imaged at day 10 of culture and analysed for their % cellularity (summarized in Table 9). The mean cell density of holo/meroclones was 27.3 ± 3.2 ($n=8$, mean \pm SE) and the mean cell density of paraclones was 4.7 ± 0.4 ($n=5$). To enable valid statistical testing, mean cell densities (which were proportions ranging from 0-1.0) were transformed using an arcsine transformation. A Mann-Whitney U test was applied to transformed measurements. The mean cell density in holo/meroclones was significantly greater than in paraclones ($p < 0.05$).

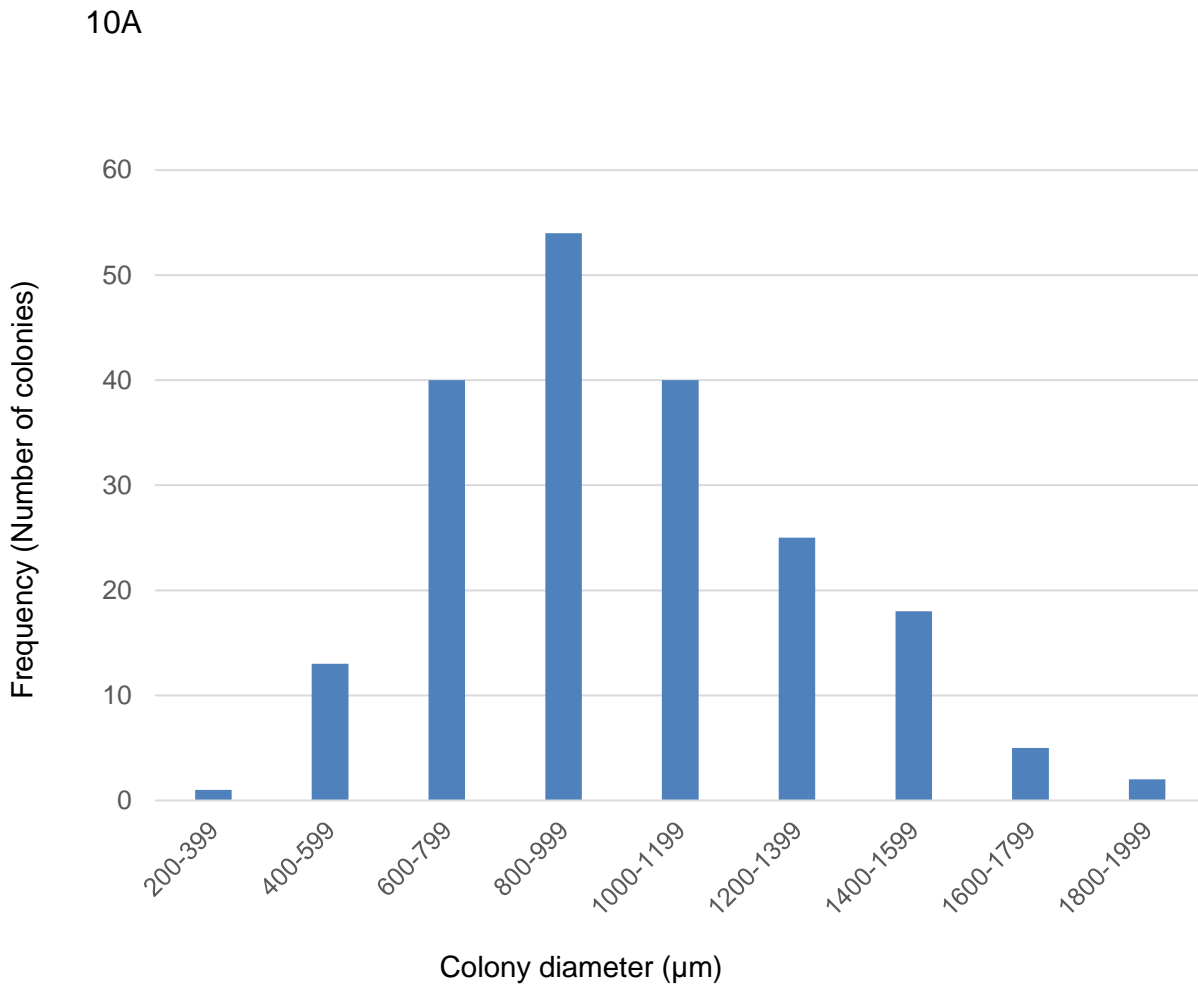
Table 8. Characteristics of colonies formed by PC3 cells.

Two, morphologically distinct, types of colonies are formed: holo/meroclones and paraclones. PC3 cells were plated at cell density 60 cells / well in 3 ml of culture medium (60 cells / 9.6cm²) in 6 well plates (Nunc). Colony formation by PC3 cells was analysed. The experiment was repeated 4 times and data from 24 wells was obtained. A total of 198 colonies were observed at day 10 and subjectively, morphologically categorised into 2 colony types: holo/meroclones or paraclones. Each colony was measured for diameter. The table shows numbers of colonies formed in a total of 24 wells; mean number of colonies formed per well and diameter of individual colony (data is presented as mean ± SE).

	Morphological holo/meroclones	Morphological paraclones
Number of colonies in 4 experiments (24 wells)	102	96
Mean number of colonies formed per well	4.3 ± 0.4	4.0 ± 0.4
Mean diameter of each colony (µm)	837.7 ± 21.6	1191.3 ± 28.3

Figure 11. Histogram showing the distribution of PC 3 colony diameters.

PC3 cells were plated at cell density 60 cells / well in 3 ml of culture medium (60 cells / 9.6cm²) in 6 well plates (Nunc). Colony formation by PC3 cells was analysed. 198 colonies were observed at day 10 were and subjectively, morphologically categorised into 2 colony types: holo/meroclones or paraclones. Each colony was measured for diameter. (A) Shows colony diameters of all colonies formed. (B) Shows colony diameter according to type of colony (holo/meroclone or paraclone).



10B

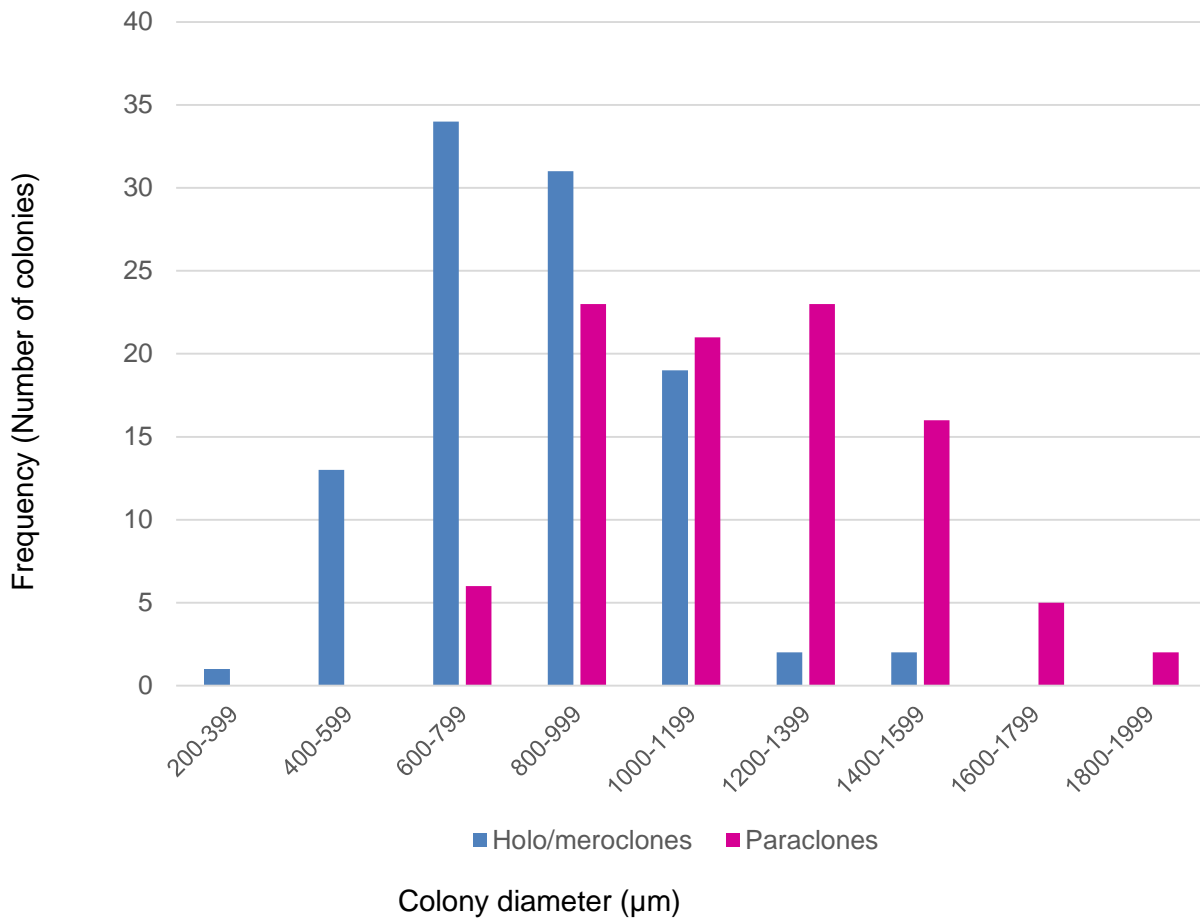


Table 9. Colony diameter; subjective morphology; % cellularity and the arc sin of these values for a random selection of 13 colonies observed and analysed at day 10 of culture.

PC3 cells were plated at cell density 60 cells / well in 3 ml of culture medium (60 cells / 9.6cm²) in 6 well plates (Nunc). Colony formation by PC3 cells was analysed. % cellularity describes the proportion of total colony area covered by cells and these values were transformed using an arc sin function for valid statistical analysis.

Colony diameter	Categorisation by morphology	% cellularity	arc sin of % cellularity
356	Holo/meroclone	36	37
434	Holo/meroclone	17	24
625	Holo/meroclone	31	34
650	Holo/meroclone	30	33
739	Holo/meroclone	41	40
896	Holo/meroclone	17	24
1086	Holo/meroclone	25	30
1124	Holo/meroclone	21	28
1108	Paraclone	5	12
1431	Paraclone	4	11
1664	Paraclone	4	12
1761	Paraclone	6	14
1868	Paraclone	5	12

3.3.2 Expression of stem cell genes in different populations of PC3 cells

As described in section 2.7, RNA was extracted from colonies and following reverse transcription, cDNA PCR was performed to test for expression of stem cell genes. PCR was performed on 3 separate passages of colonies formed. Results for gene expression in holo/meroclones and paraclones are shown in Table 10. The results show that there was a differential expression of the 4 stem cell genes between

holo/meroclones and paraclones. Whilst both holo/meroclones and paraclones expressed BMI1, only holo/meroclones expressed Oct 4 whilst paraclones did not express Oct 4. These results were consistent in 3 passages of experimental repeats. Expression of two stem cell genes was not detected in cells of either colony type – these were BCRP and hSOX. Example agarose gel images of product electrophoresis are shown in Figure 12.

Table 10. Summary of expression of 4 stem cell genes: BM1, Oct 4, BCRP and hSOX in cells of holo/meroclones and paraclones with 3 experimental repeats.

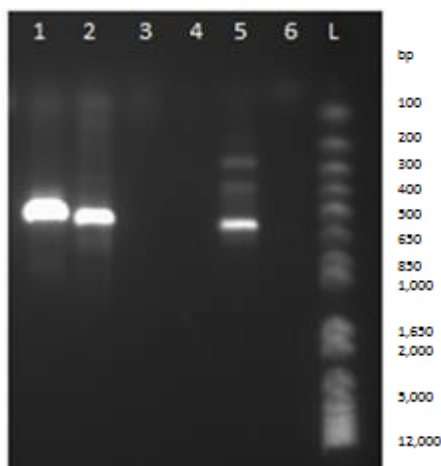
PC3 cells in a single cell suspension were plated at clonal density (60 cells / well) in Nunc 6 well plates. Cells were cultured in 3ml culture medium which was replaced after 5 days. Colonies were viewed using a microscope at x10 magnification and categorised as holo/meroclones or paraclones, based upon morphology. Cells were washed in PBS and replaced in 1ml PBS/well. A 200µl pipette was used to disrupt individual colonies and aspirate cells from individual colonies in a small volume of PBS. One centrifuge tube was used to collect cells aspirated from holo/meroclone colonies and another centrifuge tube used to collect cells from paraclone colonies. Cell suspensions were centrifuged at 350 x g for 5 min to obtain a cell pellet. RNA was extracted from colonies and following reverse transcription, cDNA PCR was performed to test for expression of stem cell genes.

		Holo/meroclones	Paraclones
(1)	BMI 1	Positive	Positive
(2)	Oct 4	Positive	Absent
(3)	BCRP	Absent	Absent
(4)	hSOX	Absent	Absent
(5)	GAPDH	Positive	Positive
(6)	GAPDH - control (no cDNA)	Absent	Absent

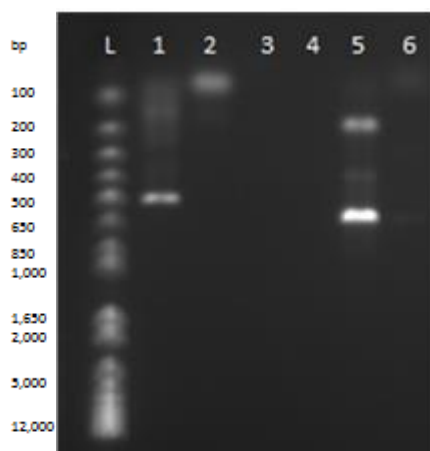
Figure 12. Agarose gel electrophoresis of PCR products from holo/meroclones (A) and paraclones (B).

0.5 µg template cDNA was used in all PCR reactions per reaction tube. The volume of cDNA required for 0.5 µg was calculated and made up to a volume of 12 µl with RNase free water. A reaction mixture of Taq PCR mastermix solution, Primer A (forward) 8.4 µM, Primer A (reverse) 8.4 µM, RNase-free water + Template DNA 0.5 µg was made up to a total volume of 30 µl. Agarose gel 1.1% was made up using 150 ml TAEx1 with 1.65g agarose and 10 µl 0.5 µg/ml ethidium bromide (Sigma-Aldrich) for visualisation. 10 µl of each PCR product was pipetted into wells with 1µl 10x Blue Juice loading dye (Sigma-Aldrich). 2 µl of 1K base pair DNA ladder (ThermoFisher Scientific 10787-018) was also pipetted into a well in each column with <1 µl 10x Blue Juice loading dye. Gel electrophoresis was performed using a current was applied at 110V for 70 min followed by the gel imaging under UV light. Presence of product bands at the expected sizes is indicative of expression of that specific gene. 1=BMI 1; 2=Oct 4; 3=BCRP; 4=hSOX; 5=GAPDH; 6=GAPDH negative control (no cDNA); L=ladder.

(A)



(B)



3.3.3 Wnt induced $[Ca^{2+}]_i$ release in PC3 cell line derived colonies

As described in section 3.2.3, intensity ratio of Fluo-4 : FuraRed was measured in cells defined as regions of interest (ROI). An example of a view of cells defined as regions of interest following staining with Fluo-4 and FuraRed is shown in Figure 13. Intensity ratios were observed and analysed from over a period of up to 15min during which cells were treated with PBS control or Wnt. There was no change in intensity ratios of the stained cells following treatment with PBS control. There was a change in intensity ratios following the addition of Wnt ligands to the plate. A representative example of changing Fluo-4 intensity in cells of a colony over time following treatment with Wnt5A is shown in Figure 14.

Waveform graphs were created of intensity ratio of Fluo-4 : FuraRed against time indicating changes in $[Ca^{2+}]_i$. As described in section 3.2.3, the kinetics of $[Ca^{2+}]_i$ within each cell analysed was determined using graphs to calculate rise, fall and dwell times of $[Ca^{2+}]_i$ (Thrasivoulou et al., 2013).

There was no change in intensity ratios of the stained cells following treatment with PBS control on 3 experimental repeats. A total of 104 cells within holo/meroclones and a total of 109 cells within paraclones were analysed for intracellular response to Wnts. These cells were in colonies cultured and tested in 3 experimental repeats. All holo/meroclone colonies demonstrated an $[Ca^{2+}]_i$ response to treatment with Wnt5A and to treatment with Wnt 9B. The majority of paraclones tested demonstrated an $[Ca^{2+}]_i$ response to both Wnt 5A and Wnt 9B. A representative waveform of intensity ratio of Fluo-4 : FuraRed in a single cell region of interest against time following Wnt treatment with a Gaussian fit curve is shown in Figure 15A.

Following an initial (primary) $[Ca^{2+}]_i$ response and a return to baseline, a number of cells of holo/meroclones, particularly those treated with Wnt 9B, demonstrated a second rise in $[Ca^{2+}]_i$. An example of such a waveform with a primary and secondary response is shown in Figure 15B.

Figure 13. A holo/meroclone imaged for intensities of (A) Fluo-4 and (B) FuraRed with a selection of cells sampled as regions of interest for analysis.

Cells were plated at clonal density (40 cells in 1 ml culture medium / dish) on 35-mm FluoroDishes (see methods). After 1 day, once cells had become adherent, a further 1 ml RPMI was added to each dish. Culture medium was changed on day 7. Colonies were used for live cell Ca^{2+} imaging at day 12. Intensity ratio of Fluo-4 : FuraRed was measured in cells defined as regions of interest (ROI).

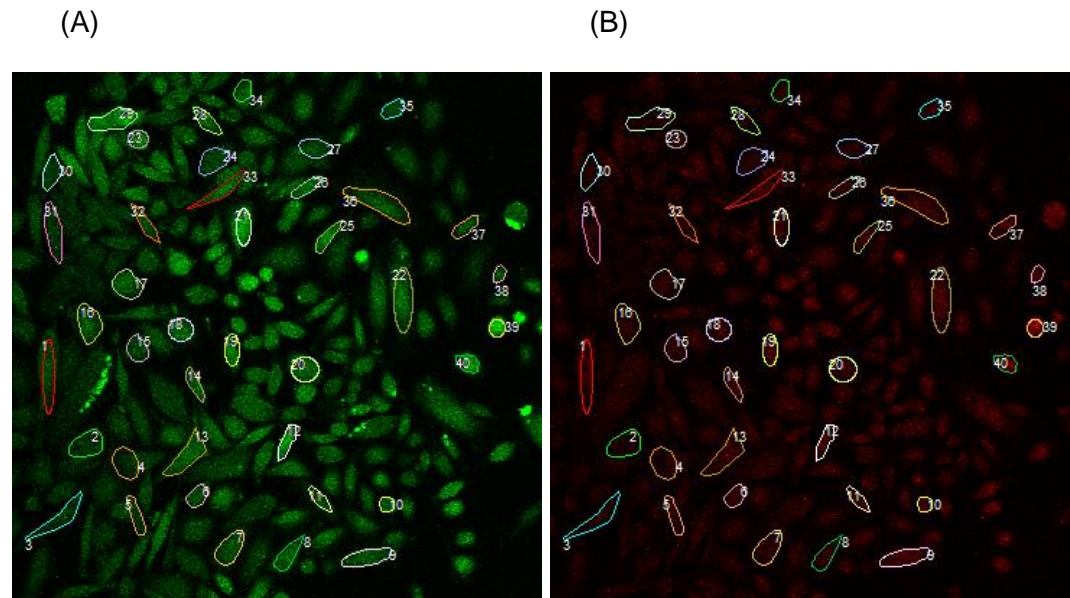


Figure 14. Changing intensity of Fluo-4 in cells of a holo/meroclone colony over time following treatment with Wnt5A.

Cells were plated at clonal density (40 cells in 1 ml culture medium / dish) on 35-mm FluoroDishes (see methods). After 1 day, a further 1 ml RPMI was added to each dish. Culture medium was changed on day 7. Colonies were used for live cell Ca^{2+} imaging at day 12. Cells of colonies cultured on a Fluorodish were treated with 100 ng/ml Wnt 5A, 100 ng/ml Wnt 9B or control. Intensity in cells demarcated as regions of interest. Intensity ratios of Fluo-4 and FuraRed were measured for up to 15 min during which cells were treated with PBS control or Wnt.

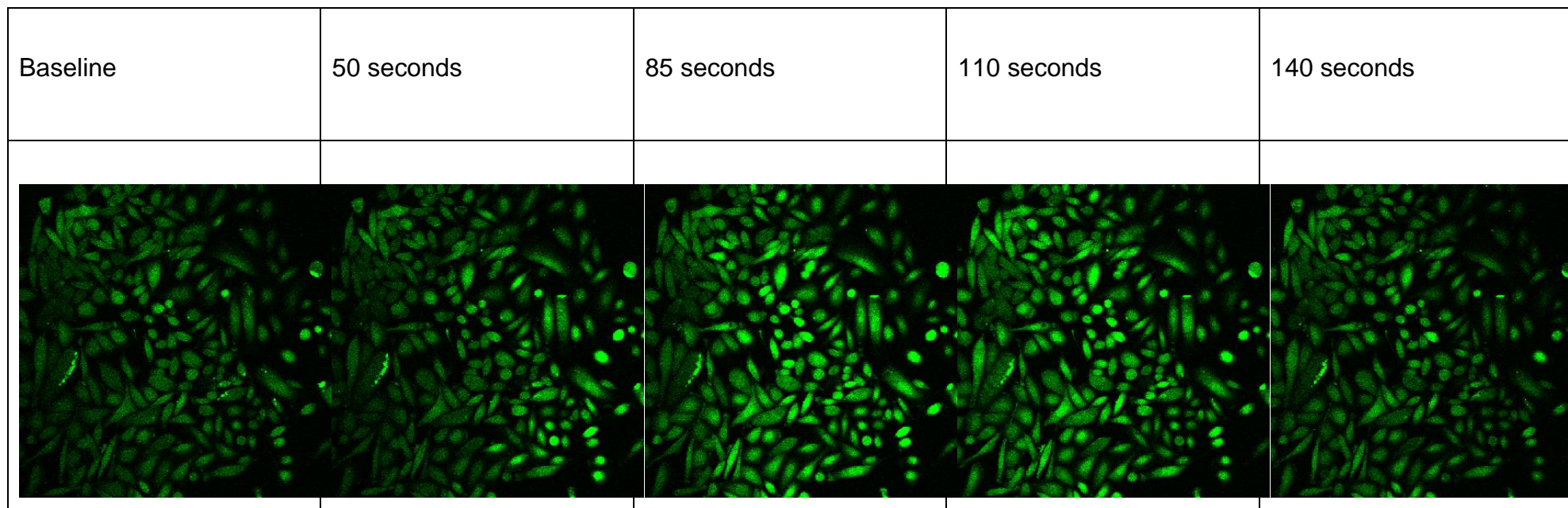
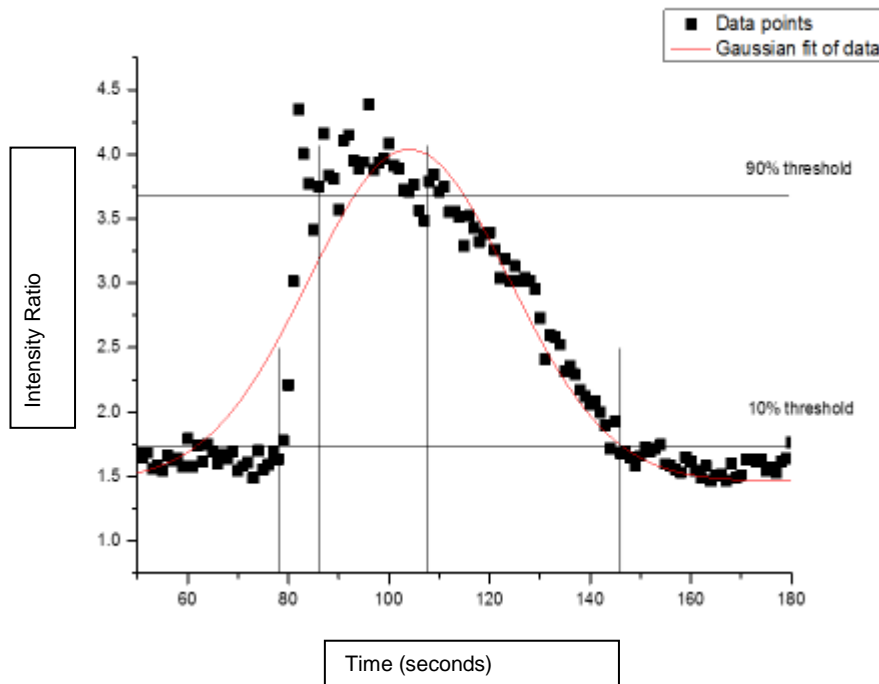


Figure 15. Intensity ratio of Fluo-4 : FuraRed in a single cell region of interest against time following Wnt treatment with a Gaussian fit curve.

Cells were plated at clonal density (1 cell / 32mm²) on 35-mm FluoroDishes. Colonies were used for live cell [Ca²⁺]_i imaging at day 12. Cells of colonies cultured on a Fluorodish were treated with Wnt 5A, Wnt 9B or control. Intensity in cells was demarcated as regions of interest. Intensity ratios of Fluo-4 and FuraRed were observed and analysed from over a period of up to 15 min during which cells were treated with PBS control or Wnt. Intensity ratio of Fluo-4 : FuraRed in single cell regions of interest when imaged using live cell imaging were calculated and plotted against time following treatment with Wnt. (A) shows a representative waveform of intensity ratio of Fluo-4 : FuraRed in a single cell region of interest when imaged using live cell imaging against time following treatment with Wnt. (B) shows a representative waveform of intensity ratio of Fluo-4 : FuraRed in a single cell region of interest against time following treatment with Wnt with an initial rise followed by a second rise in intensity ratio. In (B) a primary response is observed and a longer total response time.

(A)



(B)

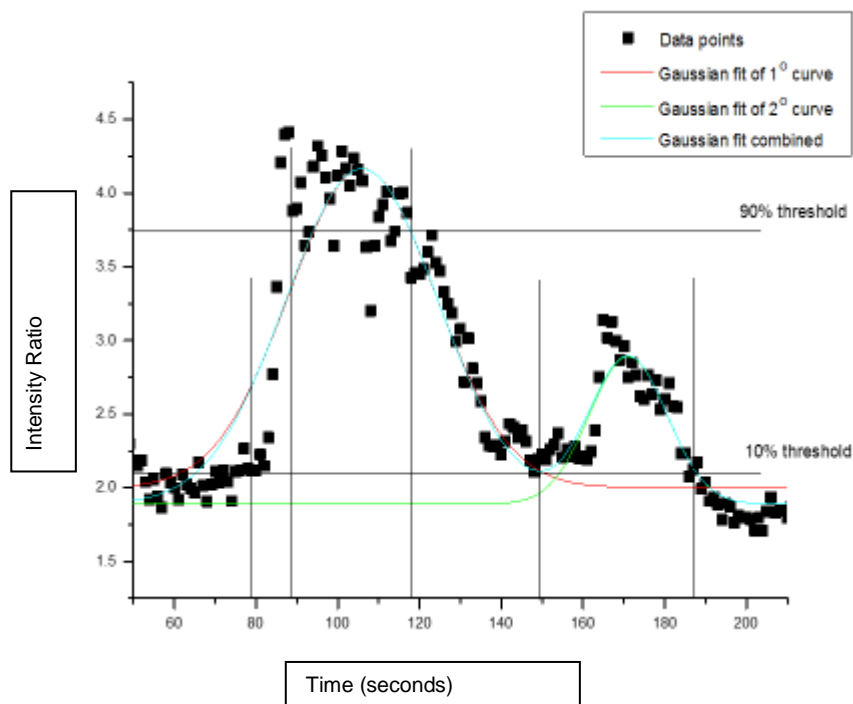


Table 11 summarizes the numbers of cells within holo/meroclones and cells within paraclones in which Wnt 5A and Wnt 9B induced $[Ca^{2+}]_i$ was observed and the numbers in which either response single waveform only or a primary or secondary waveform was observed. Figure 16 shows these results graphically. In paraclone colonies Wnts (5A or 9B) did not induce $[Ca^{2+}]_i$ in some cells; as a control, other cells within the same colonies were observed to have Wnt induced $[Ca^{2+}]_i$ release. A smaller proportion of cells within paraclones showed a secondary waveform to Wnt 9B and Wnt 5A. Chi squared statistical tests were performed on the data using IBM SPSS. With regards to $[Ca^{2+}]_i$ release observed with Wnt 5A treatment (n=103), this was more likely to occur in cells of holo/meroclones than in paraclones ($p < 0.05$). $[Ca^{2+}]_i$ release was also more likely to occur in cells of holo/meroclones than in cells of paraclones following treatment with Wnt 9B (n=110). Cells of holo/meroclones were also more likely than cells of paraclones to demonstrate a secondary response in $[Ca^{2+}]_i$ release (n= 213, $p < 0.05$). Amongst all cells, Wnt 9B was more likely to produce a secondary response in $[Ca^{2+}]_i$ release than Wnt 5A (n=213, $p < 0.05$).

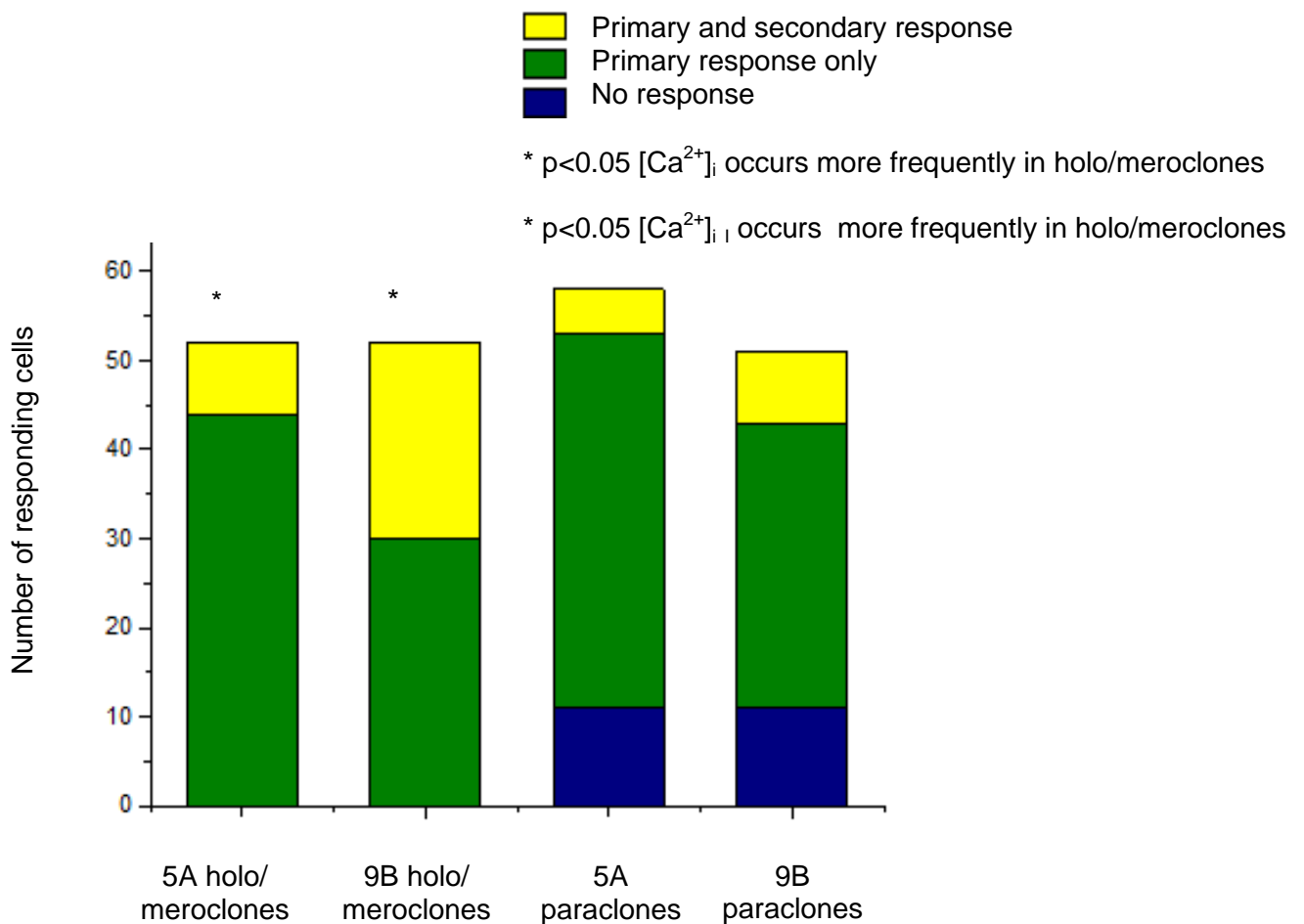
Table 11. Response of cells within holo/meroclones and paraclones to Wnt 5A and Wnt 9B.

Cells of colonies cultured on a Fluorodish were treated with Wnt 5A, Wnt 9B or control. Intensity in cells were demarcated as regions of interest. Intensity ratios of Fluo-4 and FuraRed were observed and analysed from over a period of up to 15 min during which cells were treated with PBS control or Wnt. Intensity ratio of Fluo-4 : FuraRed in single cell regions of interest when imaged using live cell imaging were calculated and plotted against time following treatment with Wnt. Either no response, primary response only or both primary and secondary response waveforms were observed as shown below.

Wnt and colony type	No response	Primary response only	Primary and secondary response
5A Holo/meroclones	0	44	8
9B Holo/meroclones	0	30	22
5A Paraclones	11	42	5
9B Paraclones	11	32	8

Figure 16. Numbers of cells within holo/meroclones and paraclones demonstrating a Wnt induced free intracellular calcium release $[Ca^{2+}]_i$ following treatment with Wnt 5A and Wnt 9B.

Intensity ratio of Fluo-4 : FuraRed in single cell regions of interest when imaged using live cell imaging were calculated and plotted against time following treatment with Wnt. For $[Ca^{2+}]_i$ release, either no response, primary response only or both primary and secondary response waveforms were observed. All analysed cells in holo/meroclones responded to Wnt 5A with a proportion of cells demonstrating a primary response and others a primary and secondary response; All analysed cells in holo/meroclones responded to Wnt 9B with a proportion of cells demonstrating a primary response and others a primary and secondary response; not all cells in paraclones responded to Wnt 5A but a proportion demonstrated a primary response and others a primary and secondary response; not all cells in paraclones responded to Wnt 9B but a proportion demonstrated a primary response and others a primary and secondary response. With regards to $[Ca^{2+}]_i$ release observed with Wnt 5A treatment (n=103), this was more likely to occur in cells of holo/meroclones than in paraclones ($p < 0.05$). $[Ca^{2+}]_i$ release was also more likely to occur in cells of holo/meroclones than in cells of paraclones following treatment with Wnt 9B (n=110). Cells of holo/meroclones were also more likely than cells of paraclones to demonstrate a secondary response in $[Ca^{2+}]_i$ release (n= 213, $p < 0.05$). (see asterisk below).



Rise, dwell, fall and total duration of response times of cells within holo/meroclones and cells within paraclones in response to Wnt 5A and Wnt 9B were calculated. Table 12 summarises these results. The duration of the 1° responses and the duration of the entire responses, taking into account the duration of any 2° responses observed are presented in Table 12. Results are presented as mean ± standard error. Significance tests are presented in text below using the Mann-Whitney Test.

Table 12. Summary of the rise, dwell and fall times for $[Ca^{2+}]_i$ of cells within holo/meroclones and paraclones in response to Wnt 5A and Wnt 9B presented as mean ± SE.

Intensity ratio of Fluo-4 : FuraRed in single cell regions of interest when imaged using live cell imaging were calculated and plotted against time following treatment with Wnt. Either no response, primary response only or both primary and secondary response waveforms were observed. The table below summarises findings by colony type and Wnt.

	Holo/meroclones		Paraclones	
Wnt	5A	9B	5A	9B
n	52	52	47	40
Rise time seconds	13.8 ± 1.8*	32.3 ± 4.2	23.5 ± 4.0*	45.8 ± 10.6
	5A: rise time for paraclones longer than holo/meroclones $p < 0.05$ 9B: no difference in rise times between colony types $p = 0.08$ Holo/meroclones: rise time with Wnt 5A shorter than Wnt 9B $p < 0.05$ Paraclones: rise time with Wnt 5A shorter than Wnt 9B $p < 0.05$			

Dwell time seconds	38.0 ± 4.3*	45.3 ± 2.6	93.9 ± 8.6*	84.3 ± 10.5
	<p>5A: dwell time for paraclones longer than holo/meroclones p<0.05</p> <p>9B: dwell time for paraclones longer than holo/meroclones p<0.05</p> <p>Holo/meroclones: dwell time with Wnt 5A shorter than Wnt 9B p<0.05</p> <p>Paraclones: no difference in dwell time between Wnt type p=0.23</p>			
Fall time seconds	96.5 ± 7.0	85.5 ± 7.4	114.8 ± 10.2*	179.8 ± 17.7*
	<p>5A: no difference in fall times between colony types</p> <p>9B: fall time for paraclones was longer than holo/meroclones <0.05</p> <p>Holo/meroclones: no difference in fall time between Wnt type p=0.10</p> <p>Paraclones: fall time with Wnt 5A shorter than Wnt 9B p<0.05</p>			
Duration primary response	148.2 ± 8.6	146.5 ± 6.4	232.3 ± 20.3*	309.9 ± 23.3*
	<p>5A: duration of primary response longer in paraclones than holo/meroclones p<0.05</p> <p>9B: duration of primary response longer in paraclones than holo/meroclones p<0.05</p> <p>Holo/meroclones: no difference in duration of primary response between Wnt type p=0.90</p> <p>Paraclones: duration of primary response with Wnt 5A shorter than Wnt 9B p<0.05</p>			

Duration total response	185.2 ± 17.7*	405.7 ± 40.2	272.2 ± 27.1*	350.4 ± 25.7
	<p>5A: duration total response longer in paraclones than holo/meroclones p<0.05</p> <p>9B: no difference in duration of total response between colony types p=0.68</p> <p>Holo/meroclones: duration total response shorter with Wnt 5A than Wnt9B p<0.05</p> <p>Paraclones: duration total response shorter with Wnt 5A than Wnt9B p<0.05</p>			

This data was further analysed to ascertain if there were any differences in how cells of holo/meroclones compared to cells of paraclones responded to Wnts, in terms of rise time, dwell time, fall time, duration of primary response or the duration of total response. As shown below, Mann Whitney U tests were performed on the data for any differences in these Ca²⁺ responses with regards to colony type (Figure 17).

A similar analysis was performed to establish if there were differences in rise time, dwell time, fall time, duration of primary response or the duration of total response for free [Ca²⁺]_i when cells of the same colony type were treated either Wnt 5A or Wnt 9B. I.e., if cells of holo/meroclones demonstrated a different response when treated with Wnt 5A compared to Wnt 9B, and similarly if cells of paraclones demonstrated a different response when treated with Wnt 5A compared to Wnt 9B. These analyses are summarised in Figure 18.

When comparing [Ca²⁺]_i following Wnt 5A treatment by colony type, significant differences between cells of holo/meroclones and cells of paraclones were observed. Both rise time and dwell times for paraclones (n=47) were longer than holo/meroclones (n=52) p<0.05. In addition, durations of both primary and total response were longer than in cells of paraclones (n=47) than holo/meroclones (n=52) p<0.05. Following treatment with Wnt 9B, dwell time and fall time in cells of

paraclones (n=40) were longer than in cells of holo/meroclones (n=52) $p < 0.05$. Duration of primary response in cells of paraclones (n=40) was also longer than in cells of holo/meroclones (n=52) $p < 0.05$.

When comparing responses of the same cell type to Wnts, both cells of holo/meroclones (n=52) and cells of paraclones (n=47) had a shorter rise time following treatment with Wnt 5A than with Wnt 9B (n=52; n=40) $p < 0.05$. Compared with Wnt 9B (n=52), Wnt 5A (n=52) induced a shorter dwell time in holo/meroclones. $p < 0.05$. In cells of holo/meroclones, the durations of dwell time and total response following treatment were shorter with Wnt 5A (n=52) than following treatment with Wnt9B (n=52) $p < 0.05$. Similarly, in cells of paraclones, the duration of the total response following treatment with Wnt 5A (n=47) was shorter than following treatment with Wnt9B (n=40) $p < 0.05$.

Figure 17. $[Ca^{2+}]_i$ response rise time (A), dwell time (B), fall time (C), duration primary response (D), and duration total response (E) in holo/meroclones compared to in paraclones following treatment with Wnt 5A (left column) and Wnt 9B (right column).

Intensity ratio of Fluo-4 : FuraRed in single cell regions of interest when imaged using live cell imaging were calculated and plotted against time following treatment with Wnt. Either no response, primary response only or both primary and secondary response waveforms were observed. Each waveform was analysed for the duration, in seconds, of rise time, dwell time, fall time the duration of the initial (primary response) and the duration of the total response when intensity ratios were plotted against time. The figure below summarises findings by colony type and Wnt.

	Wnt 5A treatment	Wnt 9B treatment
(A) Rise time	<p>Figure shows rise time of $[Ca^{2+}]_i$ in holo/meroclones compared to in paraclones following treatment with Wnt 5A. Rise time for paraclones (n=47) was longer than for cells of holo/meroclones (n=52) p<0.05 designated by an asterisk.</p>	<p>Figure shows rise time of $[Ca^{2+}]_i$ in holo/meroclones compared to in paraclones following treatment with Wnt 9B. There was no difference in rise times between holo/meroclones (n=52) and paraclones (n=40) p=0.08.</p>

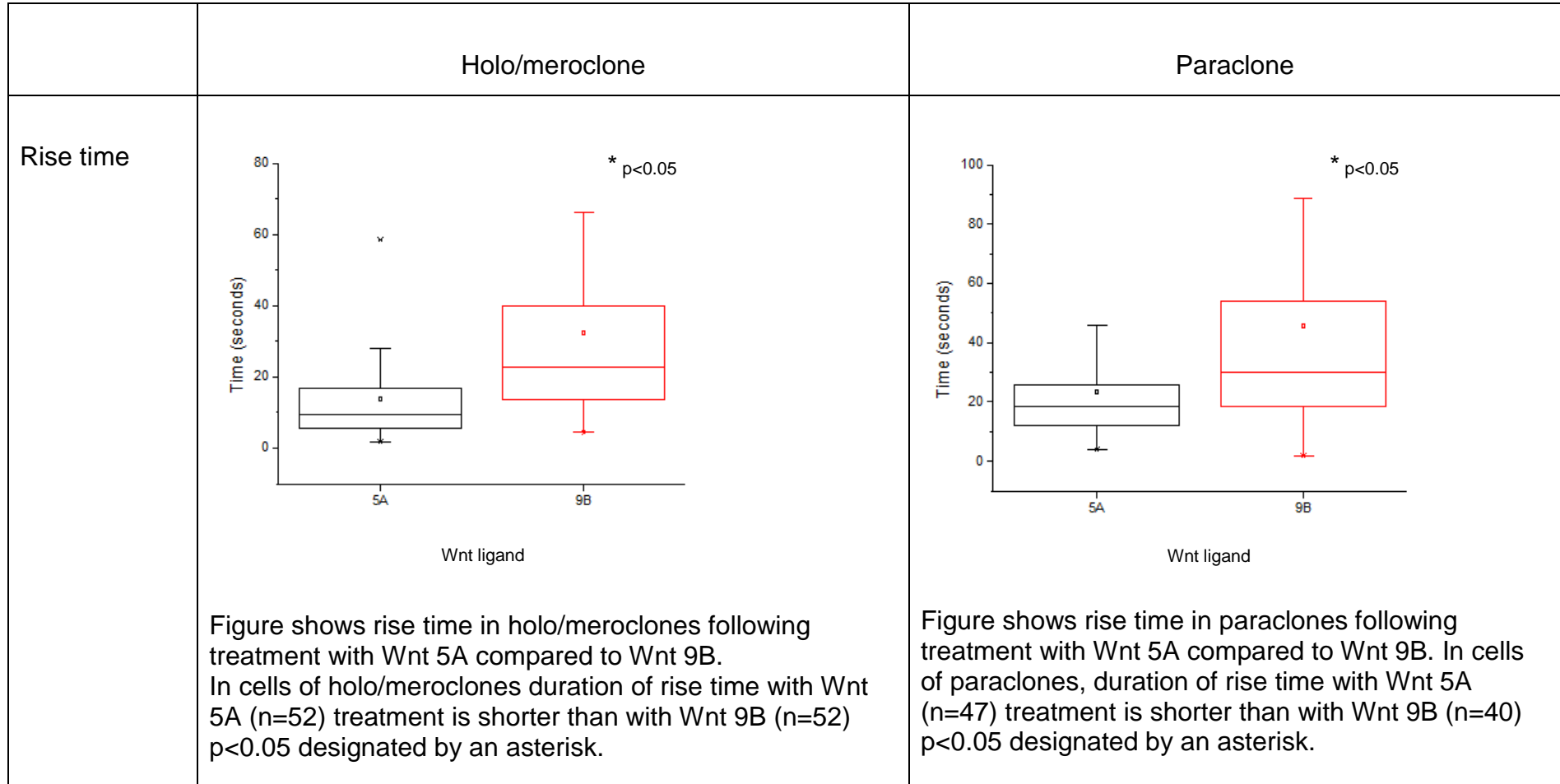
	Wnt 5A treatment	Wnt 9B treatment
(B) Dwell time	<p>Figure shows dwell time of $[Ca^{2+}]_i$ in holo/meroclonal compared to in paraclonal following treatment with Wnt 5A. Dwell time for paraclonal (n=47) was longer than for cells of holo/meroclonal (n=52) $p<0.05$ designated by an asterisk.</p>	<p>Figure shows dwell time of $[Ca^{2+}]_i$ in holo/meroclonal compared to in paraclonal following treatment with Wnt 9B. Following treatment with Wnt 9B, dwell time for paraclonal (n=40) was longer than for cells of holo/meroclonal (n=52) $p<0.05$ designated by an asterisk.</p>

	Wnt 5A treatment	Wnt 9B treatment
(C) Fall time	<p>n.s.</p>	<p>* p<0.05</p>
	<p>Figure shows fall time of $[Ca^{2+}]_i$ in holo/meroclones compared to in paraclones following treatment with Wnt 5A. Fall time in cells of holo/meroclones (n=52) is no different than cells of paraclones (n=47).</p>	<p>Figure shows fall time of $[Ca^{2+}]_i$ in holo/meroclones compared to in paraclones following treatment with Wnt 9B. Following treatment with Wnt 9B, fall time for paraclones (n=40) was longer than for cells of holo/meroclones (n=52) p<0.05 designated by an asterisk.</p>

	Wnt 5A treatment	Wnt 9B treatment
(D) Duration primary response	<p>Figure shows duration of primary response, as defined by time from rising above the 10% intensity threshold to the first fall back to the 10% intensity threshold. Following treatment with Wnt 5A, duration of primary response in cells of paraclones (n=47) is longer than in cells of holo/meroclonal (n=52) p<0.05 designated by an asterisk.</p>	<p>Figure shows duration of primary response, as defined by time from rising above the 10% intensity threshold to the first fall back to the 10% intensity threshold. Following treatment with Wnt 9B, duration of primary response in cells of paraclones (n=40) is longer than in cells of holo/meroclonal (n=52) p<0.05 designated by an asterisk.</p>

	Wnt 5A treatment	Wnt 9B treatment
(E) Duration total response	<p>* $p < 0.05$</p>	<p>n.s.</p>
	<p>Figure shows duration of total response, as defined by time from rising above the 10% intensity threshold to the final fall back to the 10% intensity threshold. Following treatment with Wnt 5A, duration of total response in cells of paraclones (n=47) is longer than in cells of holo/meroclones (n=52) $p < 0.05$ designated by an asterisk.</p>	<p>Figure shows duration of total response, as defined by time from rising above the 10% intensity threshold to the final fall back to the 10% intensity threshold. Following treatment with Wnt 9B, there is no difference in duration of total response between cells of holo/meroclones (n=52) and cells of paraclones (n=40) $p = 0.68$.</p>

Figure 18. Calcium response rise time (A), dwell time (B), fall time (C), duration primary response (D), and duration total response (E) following treatment with Wnt 5A compared to Wnt 9B in holo/meroclones (left) and paraclones (right).



	Holo/meroclone	Paraclone
Dwell time	<p>Figure shows dwell time in holo/meroclones following treatment with Wnt 5A compared to Wnt 9B. In cells within holo/meroclones, dwell time of following treatment with Wnt 5A (n=52) is shorter than compared with Wnt 9B (n=52) ($p < 0.05$).</p>	<p>Figure shows dwell time in paraclones following treatment with Wnt 5A compared to Wnt 9B. In cells of paraclones, there is no difference in dwell time following treatment with Wnt 5A (n=40) or 9B (n=47) ($p = 0.23$).</p>

	Holo/meroclone	Paraclone
Fall time	<p>n.s.</p> <p>Time (seconds)</p> <p>Wnt ligand</p> <p>5A 9B</p>	<p>* $p < 0.05$</p> <p>Time (seconds)</p> <p>Wnt ligand</p> <p>5A 9B</p>
	<p>Figure shows fall time in holo/meroclones following treatment with Wnt 5A compared to Wnt 9B. In cells of holo/meroclones, there is no difference in fall time following treatment with Wnt 5A (n=52) compared with Wnt 9B (n=52) ($p=0.10$).</p>	<p>Figure shows fall time in paraclones following treatment with Wnt 5A compared to Wnt 9B. In cells of paraclones, duration of fall time following treatment with Wnt 5A (n=47) is shorter than with Wnt 9B (n=40) ($p < 0.05$).</p>

	Holo/meroclone	Paraclone
Duration primary response	<p>n.s.</p> <p>Time (seconds)</p> <p>Wnt ligand</p> <p>Figure shows duration of primary response in holo/meroclones following treatment with Wnt 5A compared to Wnt 9B. In cells of holo/meroclones, there is no difference in duration of the primary response following treatment with Wnt 5A (n=52) or with Wnt 9B (n=52) ($p=0.90$).</p>	<p>* $p<0.05$</p> <p>Time (seconds)</p> <p>Wnt ligand</p> <p>Figure shows duration of primary response in paraclones following treatment with Wnt 5A compared to Wnt 9B. In cells of paraclones, duration of primary response following treatment with Wnt 5A (n=47) is shorter than following treatment with Wnt 9B (n=40) ($p<0.05$).</p>

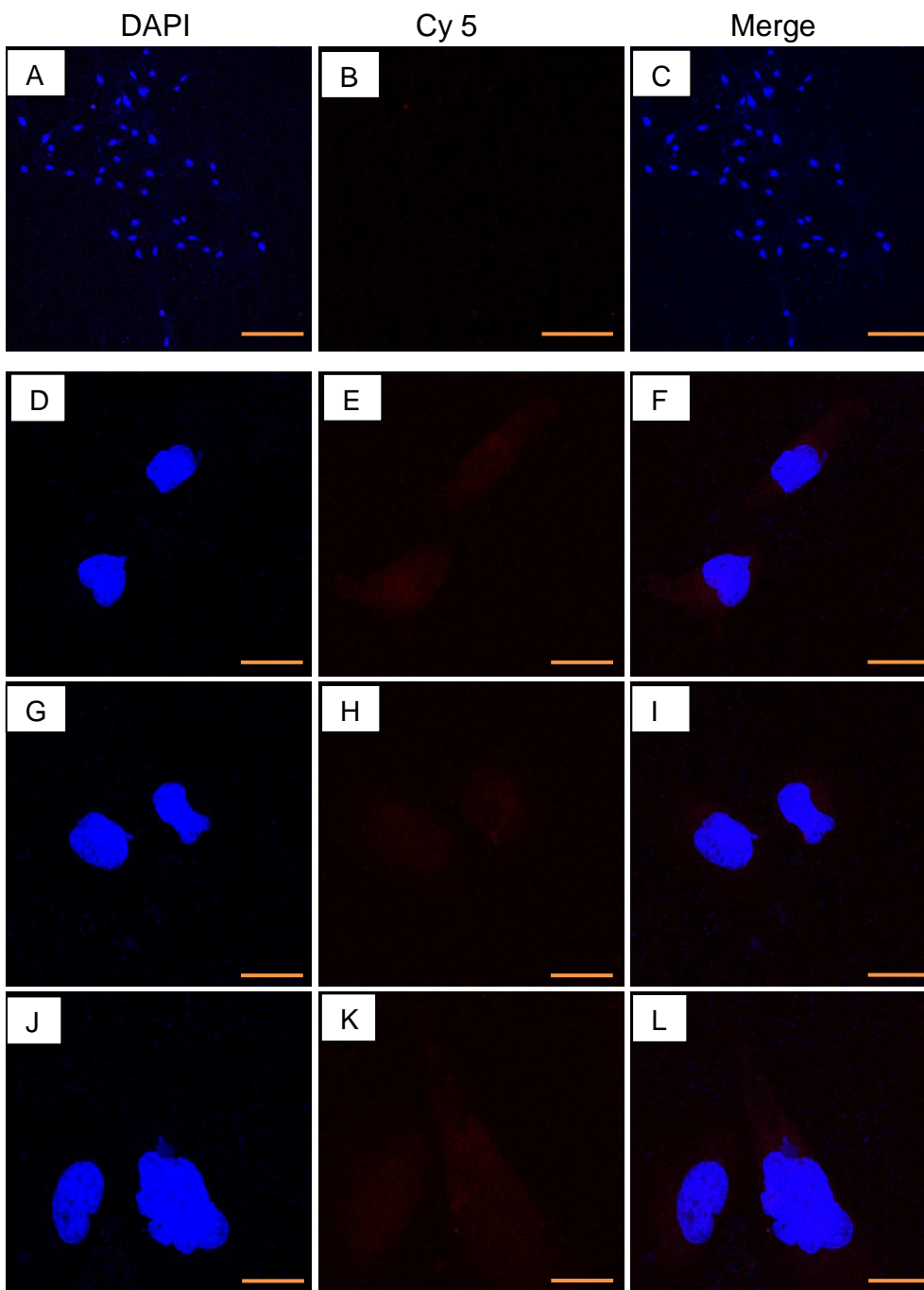
	Holo/meroclone	Paraclone
Duration total response	<p>Figure shows duration of total response in holo/meroclones following treatment with Wnt 5A compared to Wnt 9B. In cells of holo/meroclones, the duration of the total response following treatment with Wnt 5A (n=52) is shorter than following treatment with Wnt 9B (n=52) (p<0.05) designated by an asterisk.</p>	<p>Figure shows duration of total response in paraclones following treatment with Wnt 5A compared to Wnt 9B. In cells of paraclones, the duration of the total response following treatment with Wnt 5A (n=47) is shorter than following treatment with Wnt 9B (n=40) (p<0.05) designated by an asterisk.</p>

3.3.4 Expression of β -catenin in colonies with and without Wnt treatment and co-localisation of β -catenin in the nucleus

Negative controls for immunostaining were performed using no primary antibody (section 3.2.4). With no primary antibody to bind the secondary antibody, lack of signal in negative controls demonstrates specificity of the primary antibody in subsequent experiments. Negative controls demonstrated no secondary antibody signal as shown in Figure19 below.

Figure 19. Experiments conducted as negative controls using no primary antibody and a flurophore secondary antibody (Cy 5 Goat anti-mouse IgG) counter stained with DAPI (blue) show that there was no non-specific binding of the secondary antibody.

A-L show signal observed at excitation 647 nm, emission 667 nm. A-C show the same whole colony: A shows DAPI staining, B signal observed for flurophore secondary antibody Cy 5, C shows A+B merge. D,E,F,G,H,I,J,K,L show higher magnification of cells within this colony. D,G,J show DAPI staining, E,H,K show signal observed for flurophore secondary antibody Cy 5; F,I,L show respective merge images. Z-stacks obtained using an Olympus confocal system are shown. Representative image following at least 10 repeats. Scale Bar A,B,C: 180 μ m; D,E,F,G,H,I,J,K,L: 15 μ m.



As outlined in section 3.2.4, PC3 cells in holo/meroclones were tested for Wnt 5A and Wnt 9B induced $[Ca^{2+}]_i$ release and then underwent immunostaining for expression of β -catenin. As a control for the expression of β -catenin in cells of holo/meroclones without Wnt ligand treatment, cells were treated with PBS control and then fixed and stained for β -catenin (section 3.2). Figures 20-22 below show the expression of β -catenin by immunocytochemistry in cells of holo/meroclones in the experiments as indicated: figure 20 shows cells of a holo/meroclone treated with PBS control; figure 21 shows cells of a holo/meroclone treated with Wnt 5A and Figure 22 shows cells of a holo/meroclone treated with Wnt 9B. Figure 20 shows all imaged cells of holo/meroclones treated with PBS control expressed β -catenin. However, comparatively, Figures 21 and 22 show cells of holo/meroclones treated with Wnt 5A or Wnt 9B respectively have markedly stronger staining for β -catenin than control cells treated with PBS. Cells of both holo/meroclones and paraclones treated with Wnt 5A and with Wnt 9B demonstrate strong nuclear staining for β -catenin. This can particularly be observed in images in figure 21 F,I,L (holo/meroclone) and figure 22 F,I, L (paraclone). These results indicate that in cells of holo/meroclones and cells of paraclones, Wnt signal activation via Wnt 5A and Wnt 9B is associated with apparent increased β -catenin expression, and suggestive of translocation of β -catenin into the nucleus.

Figure 20. Immunocytochemistry shows presence of β -catenin in PBS treated cells of PC3 holo/meroclones.

Primary antibody mouse monoclonal to β -catenin concentration 1:250 detected with a flurophore secondary antibody (Cy 5 Goat anti-mouse IgG) concentration 1:500 (red) and counter stained with DAPI (blue). A-L show signal observed at excitation 647 nm, emission 667 nm. A-C show the same whole colony: A shows DAPI staining, B signal observed for flurophore secondary antibody Cy 5, C shows A+B merge. D,E,F,G,H,I,J,K,L show higher magnification of cells within this colony. D,G,J show DAPI staining, E,H,K show signal observed for flurophore secondary antibody Cy 5; F,I,L show respective merge images. Images F,I,L show a relatively moderate level of β -catenin staining. Z-stacks obtained using an Olympus confocal system are shown. Representative images following at least 10 repeats. Scale Bar A,B,C:180 μ m; D,E,F,G,H,I,J,K,L:15 μ m.

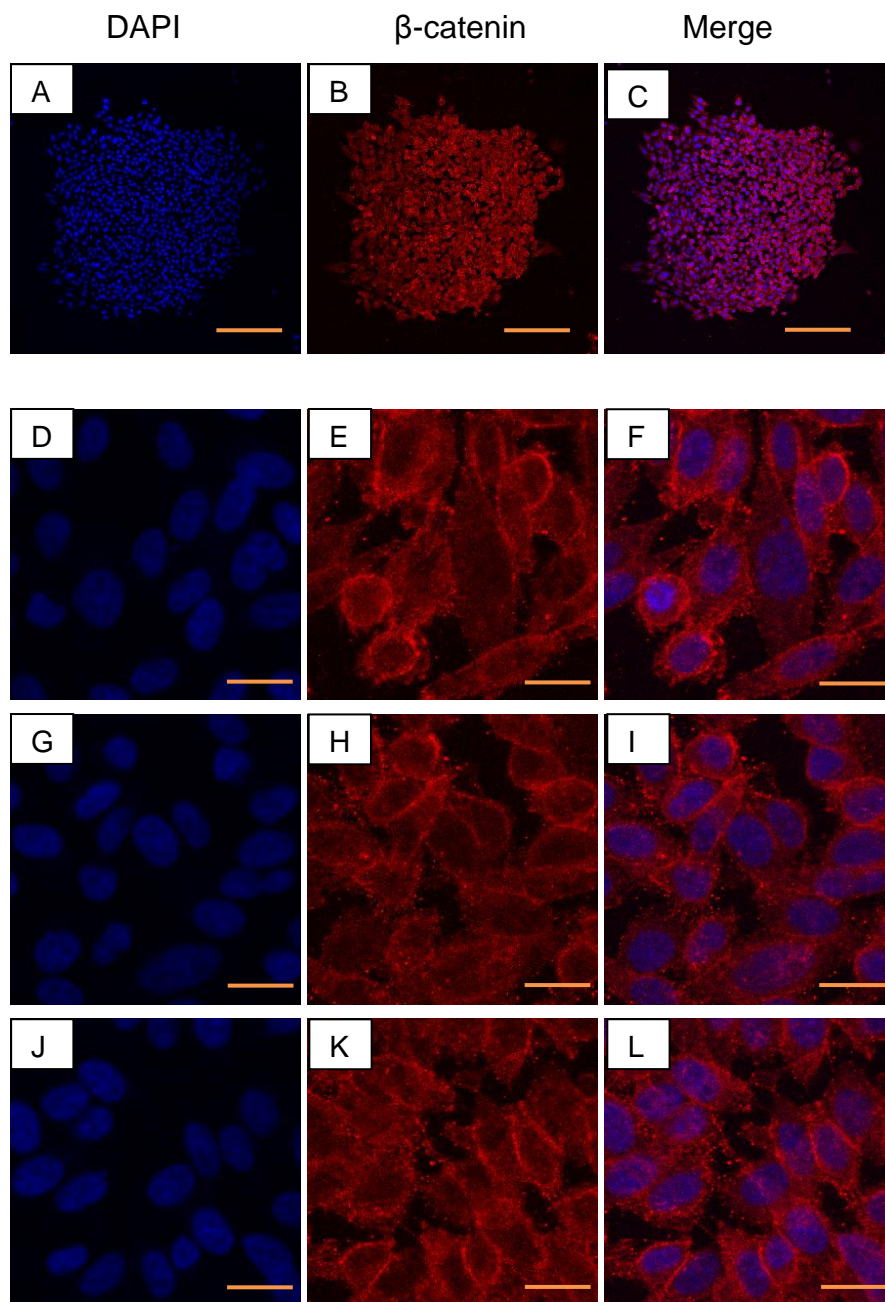


Figure 21. Immunocytochemistry on cells of PC3 holo/meroclones shows strong staining of β -catenin, and suggests increased nuclear β -catenin following treatment with Wnt 5A.

Images suggest there is increased nuclear β -catenin following treatment with Wnt 5A ligand (100 ng/ml) compared with cells treated with PBS control. Primary antibody mouse monoclonal to β -catenin concentration 1:250 detected with a flurophore secondary antibody (Cy 5 Goat anti-mouse IgG) concentration 1:500 (red) and counter stained with DAPI (blue). Signal observed at excitation 647 nm, emission 667 nm. A-C show the same whole colony: A shows DAPI staining, B signal observed for flurophore secondary antibody Cy 5, C shows A+B merge. D,E,F,G,H,I,J,K,L show higher magnification of cells within this colony. D,G,J show DAPI staining, E,H,K show signal observed for flurophore secondary antibody Cy 5; F,I,L show respective merge images. Images F,I,L show the suggestion of increased β -catenin staining relative to control images in figure 20, as well as punctate staining over the nucleus. Z-stacks obtained using an Olympus confocal system are shown. Representative images following at least 10 repeats. Scale Bar A,B,C:180 μ m; D,E,F,G,H,I,J,K,L:15 μ m.

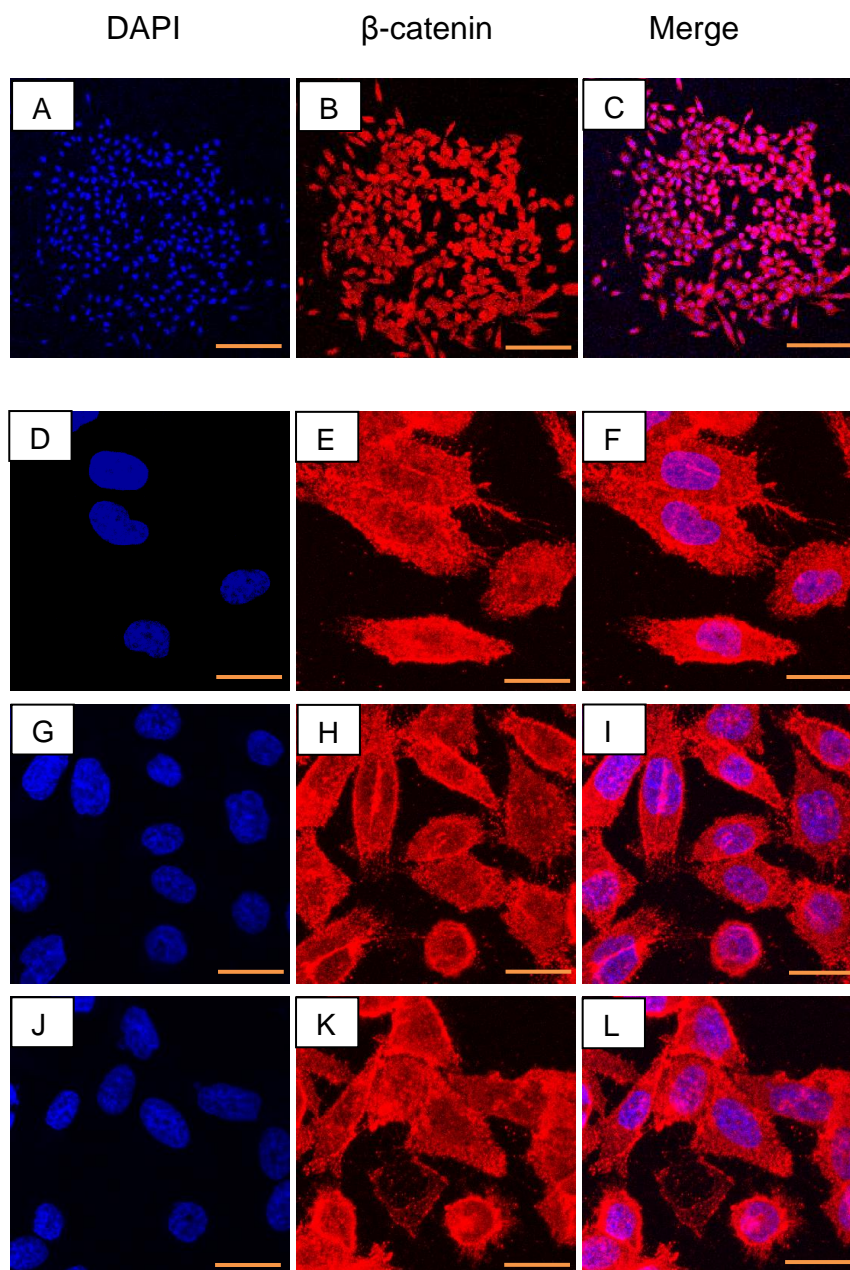
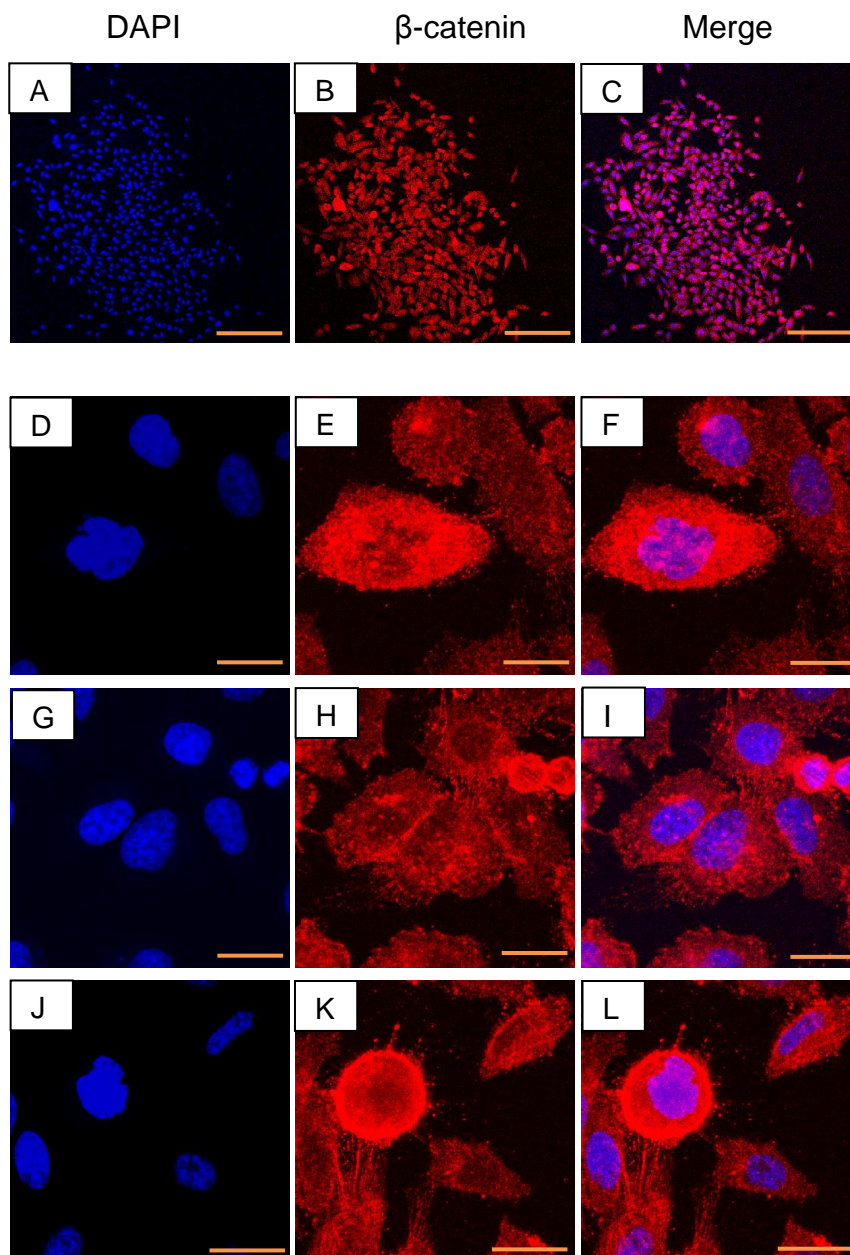


Figure 22. Immunocytochemistry on cells of PC3 holo/meroclones shows strong staining of β -catenin and suggests increased nuclear β -catenin following treatment with Wnt 9B ligand.

Images suggest there is increased nuclear β -catenin following treatment with Wnt 9B ligand (100 ng/ml) compared with cells treated with PBS control. Primary antibody mouse monoclonal to β -catenin concentration 1:250 detected with a flurophore secondary antibody (Cy 5 Goat anti-mouse IgG) concentration 1:500 (red) and counter stained with DAPI (blue). Signal observed at excitation 647 nm, emission 667 nm. A-C show the same whole colony: A shows DAPI staining, B signal observed for flurophore secondary antibody Cy 5, C shows A+B merge. D,E,F,G,H,I,J,K,L show higher magnification of cells within this colony. D,G,J show DAPI staining, E,H,K show signal observed for flurophore secondary antibody Cy 5; F,I,L show respective merge images. Images F,I,L show the suggestion of increased β -catenin staining relative to control images in figure 20, as well as punctate staining over the nucleus. Z-stacks obtained using an Olympus confocal system are shown. Representative images following at least 10 repeats. Scale Bar A,B,C:180 μ m; D,E,F,G,H,I,J,K,L:15 μ m.



Paraclones were cultured for 10 days, treated with PBS control and stained for β -catenin as outlined in section 3.2.4. Figures 23-25 below show the expression of β -catenin by immunocytochemistry in cells of paraclones in the experiments as indicated: figure 23 shows cells of a paraclone treated with PBS control; figure 24 shows cells of a paraclone treated with Wnt 5A and Figure 25 shows cells of a paraclone treated with Wnt 9B. Expression of β -catenin PC3 cells of paraclones treated with PBS control was compared with staining observed in Wnt 5A and Wnt 9B treated cells. Figure 23 shows β -catenin is expressed in cells of paraclones treated with PBS control (no Wnt ligand). The staining observed is similar to staining observed in cells of holo/meroclones treated with PBS control. Figures 24 D-L and 24 D-L demonstrate that compared to control cells, there is increased staining for β -catenin following Wnt 5A and Wnt 9B treatment in paraclone cells and increased staining over the nucleus. This suggests that just as in cells of holo/meroclones, Wnt activation via Wnt 5A and 9B appears to result in increased expression of β -catenin and nuclear translocation.

Figure 23. Immunocytochemistry shows presence of β -catenin in PBS treated control cells of PC3 paraclones.

Immunocytochemistry shows presence of β -catenin in control cells though staining is less than in paraclone cells treated with Wnts 5A or 9B (see figures 24 D-L and 25 D-L for comparison). Primary antibody mouse monoclonal to β -catenin concentration 1:250 detected with a flurophore secondary antibody (Cy 5 Goat anti-mouse IgG) concentration 1:500 (red) and counter stained with DAPI (blue). A-L show signal observed at excitation 647 nm, emission 667 nm. A-C show the same whole colony: A shows DAPI staining, B signal observed for flurophore secondary antibody Cy 5, C shows A+B merge. D,E,F,G,H,I,J,K,L show higher magnification of cells within this colony. D,G,J show DAPI staining, E,H,K show signal observed for flurophore secondary antibody Cy 5; F,I,L show respective merge images. Images F,I,L relatively moderate level of β -catenin staining . Z-stacks obtained using an Olympus confocal system are shown. Representative images following at least 10 repeats. Scale Bar A,B,C:180 μ m; D,E,F,G,H,I,J,K,L:15 μ m.

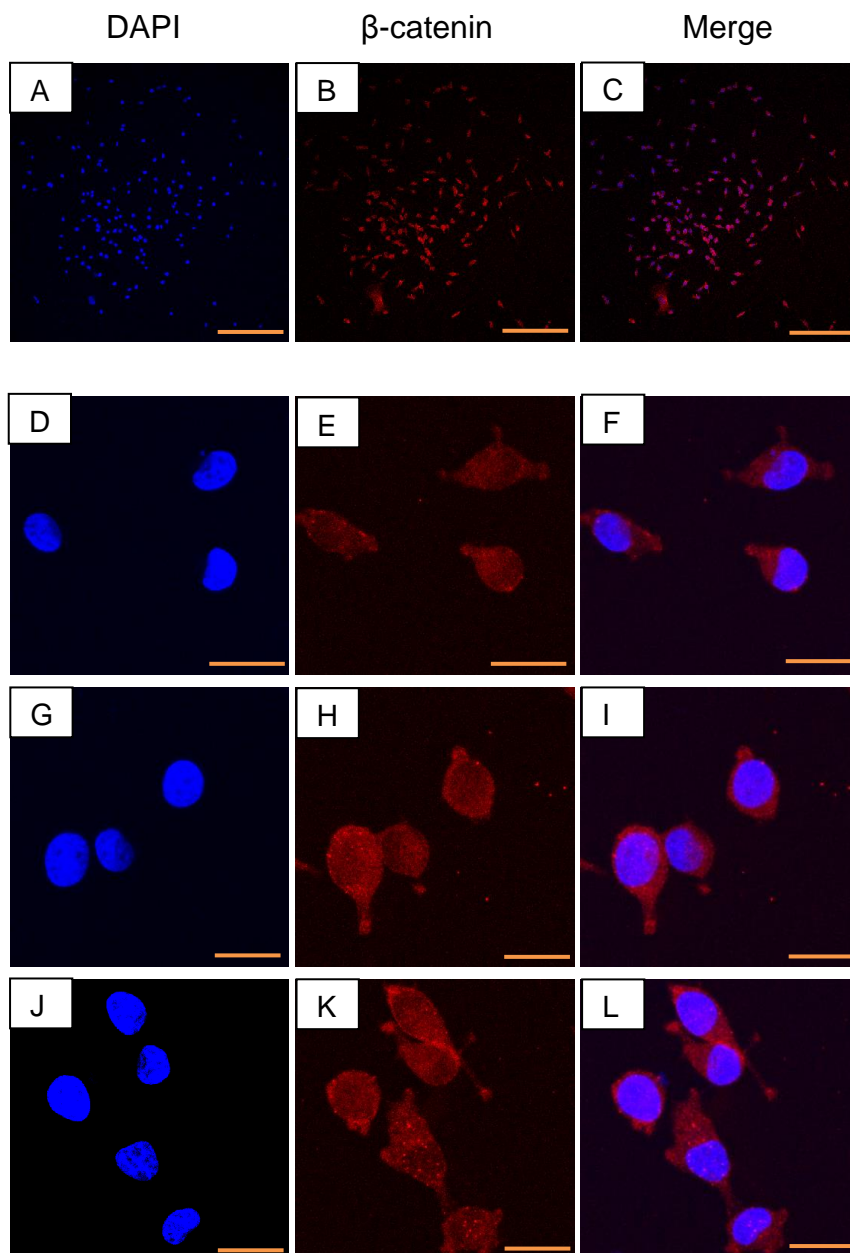


Figure 24. Immunocytochemistry on cells of PC3 paraclones shows strong staining of β -catenin, and suggests increased nuclear β -catenin following treatment with Wnt 5A.

Images suggest there is increased nuclear β -catenin following treatment with Wnt 5A ligand (100 ng/ml) compared with PBS treated control cells in figure 23. Primary antibody mouse monoclonal to β -catenin concentration 1:250 detected with a flurophore secondary antibody (Cy 5 Goat anti-mouse IgG) concentration 1:500 (red) and counter stained with DAPI (blue). Signal observed at excitation 647 nm, emission 667 nm. A-C show the same whole colony: A shows DAPI staining, B signal observed for flurophore secondary antibody Cy 5, C shows A+B merge. D,E,F,G,H,I,J,K,L show higher magnification of cells within this colony. D,G,J show DAPI staining, E,H,K show signal observed for flurophore secondary antibody Cy 5; F,I,L show respective merge images. Images F,I,L are suggestive of increased β -catenin staining, as well as punctate staining over the nucleus relative to control images in figure 23. Z-stacks obtained using an Olympus confocal system are shown. Representative images following at least 10 repeats. Scale Bar A,B,C:180 μ m; D,E,F,G,H,I,J,K,L:15 μ m.

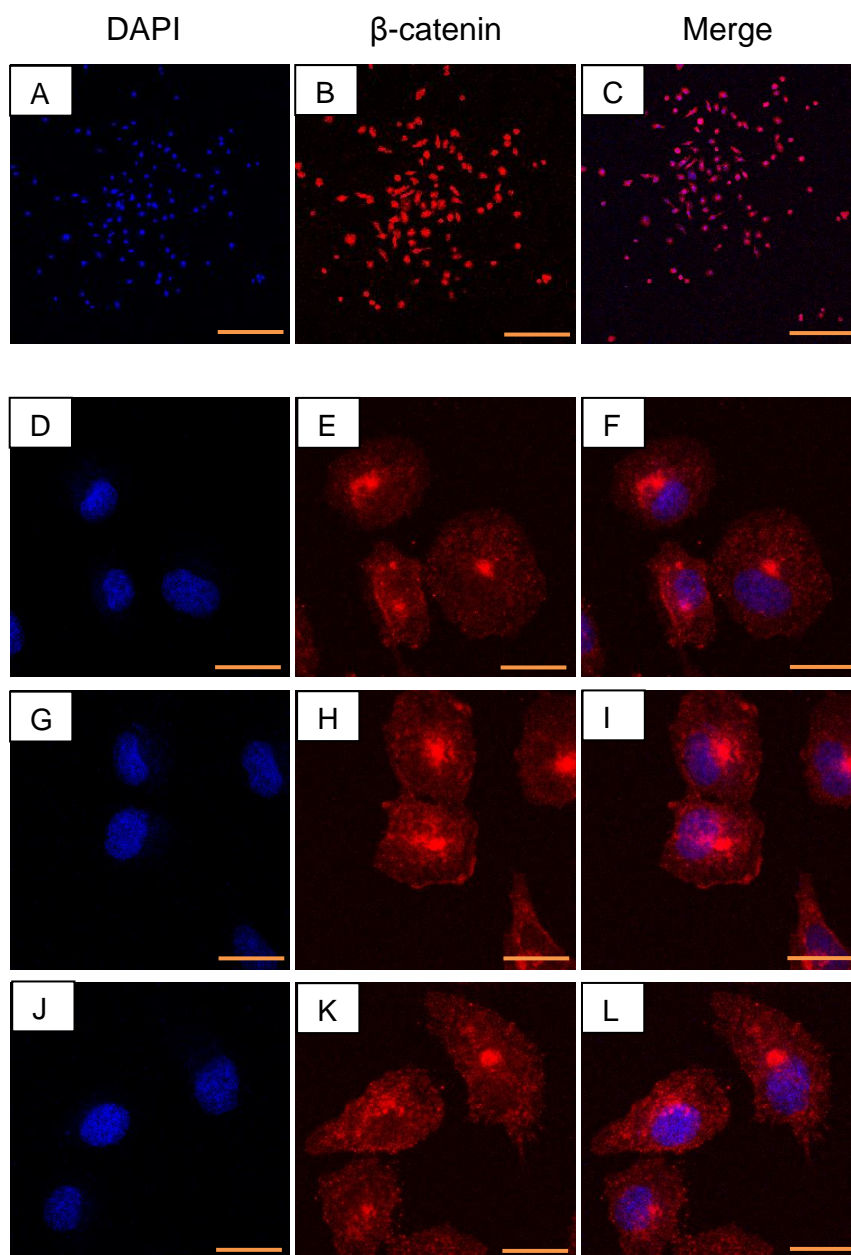
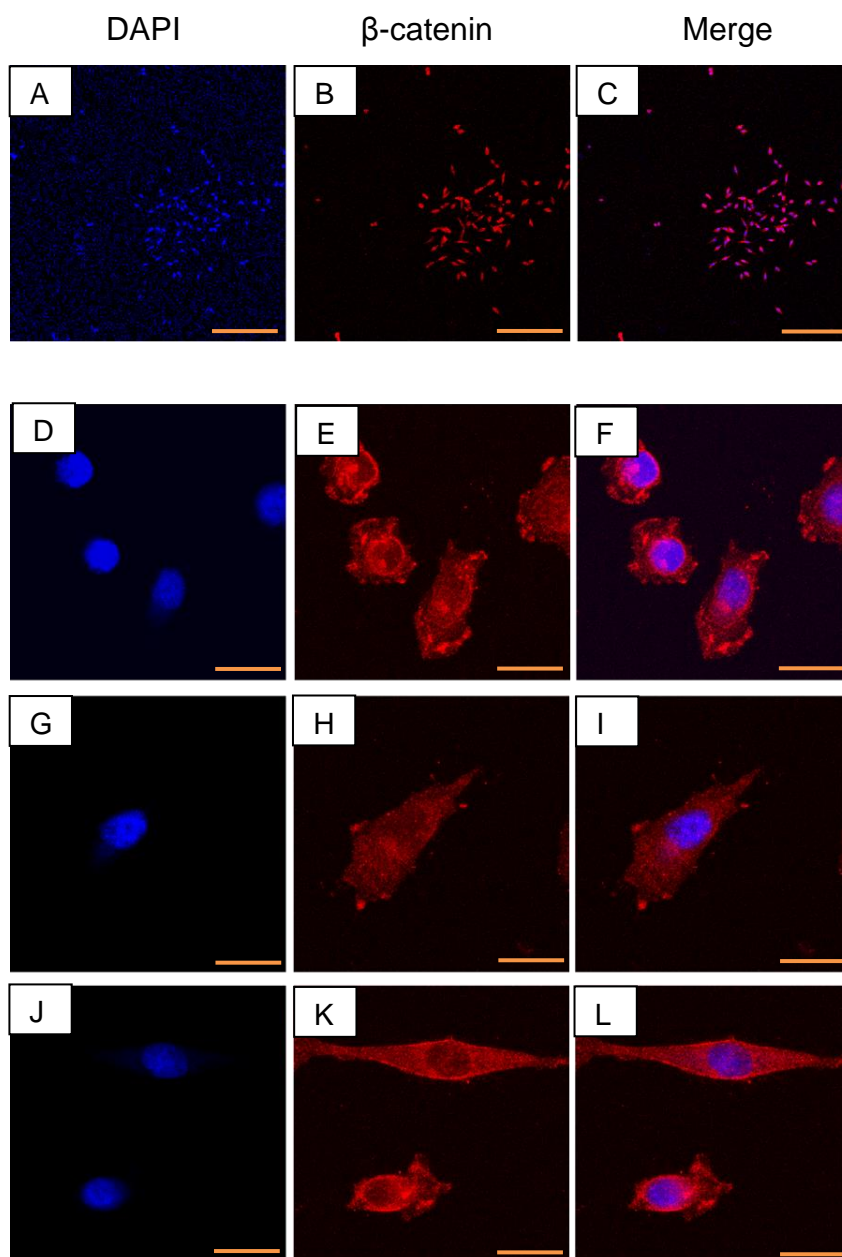


Figure 25. Immunocytochemistry on cells of PC3 paraclones shows significant staining of β -catenin, and suggests increased nuclear β -catenin following treatment with Wnt 9B ligand.

Images suggest there is increased nuclear β -catenin following treatment with Wnt 9B ligand (100 ng/ml) compared with PBS treated control cells in figure 23. Primary antibody mouse monoclonal to β -catenin concentration 1:250 detected with a flurophore secondary antibody (Cy 5 Goat anti-mouse IgG) concentration 1:500 (red) and counter stained with DAPI (blue). Signal observed at excitation 647 nm, emission 667 nm. A-C show the same whole colony: A shows DAPI staining, B signal observed for flurophore secondary antibody Cy 5, C shows A+B merge. D,E,F,G,H,I,J,K,L show higher magnification of cells within this colony. D,G,J show DAPI staining, E,H,K show signal observed for flurophore secondary antibody Cy 5; F,I,L show respective merge images. Images F,I,L are suggestive of increased β -catenin staining, as well as punctate staining over the nucleus compared to holo/meroclones untreated with Wnt as shown in figure 20. Z-stacks obtained using an Olympus confocal system are shown. Representative images following at least 10 repeats. Scale Bar A,B,C: 180 μ m; D,E,F,G,H,I,J,K,L: 15 μ m.



3.4 Discussion

The first aim of the work described in this chapter was to assess if colonies are formed by a prostate cancer cell line (PC3). A further aim was to characterize Wnt signalling as measured by a live cell imaging Ca^{2+} assay for $[\text{Ca}^{2+}]_i$ response in these colonies.

3.4.1 Colony formation by PC3 cells

The first hypothesis in this study was that cultured from single cells at clonal density, defined as 60 cells / well in 3 ml of culture medium (60 cells / 9.6cm^2), will form distinct colonies of cells. I formed a hypothesis that the colony types formed will resemble holoclones, meroclones and paraclones morphologically, as has been described previously in keratinocytes, and a number of cancer cell lines including prostate, breast, pancreatic and head and neck (Barrandon and Green, 1987; Harper et al., 2007; Liu et al., 2013; Pfeiffer and Schalken, 2010). In addition, the colony types formed by PC3 cells will also have objective features upon which they can be categorised.

In this study, cells plated at clonal density formed colonies that could be categorised into 2 types, visually (Davda et al., 2015). One type of colony consisted of tightly clustered, rounded cells and with a colony outline which could be well demarcated. This was similar to two colony types - holoclones and meroclones - previously described (Li et al., 2008; Pfeiffer and Schalken, 2010; Zhang and Waxman, 2010). A further type of colony was formed of cells with a greater inter-cellular distance, flattened in appearance and with a colony outline which was difficult to demarcate. This colony type was morphologically consistent with paraclones previously reported by Li et al and others (Li et al., 2008; Pfeiffer and Schalken, 2010; Zhang and Waxman, 2010).

Unlike findings in this study, Li et al and Zhang and Waxman (Li et al., 2008; Zhang and Waxman, 2010) reported 3 distinct colony types formed by single cell culture of

PC3 cells - holoclones, meroclones and paraclones (see Figure 4). However, in my work presented here, holoclones and meroclones were not clearly identified as two distinct colony types, morphologically. Paraclones were identified as a distinct colony type, morphologically. Similar to the observations presented in this thesis, the formation of just 2 rather than 3 colony types from single cell plating of PC3 cells in this study was also reported by Pfeiffer and Schalken as shown in figure 26 below.

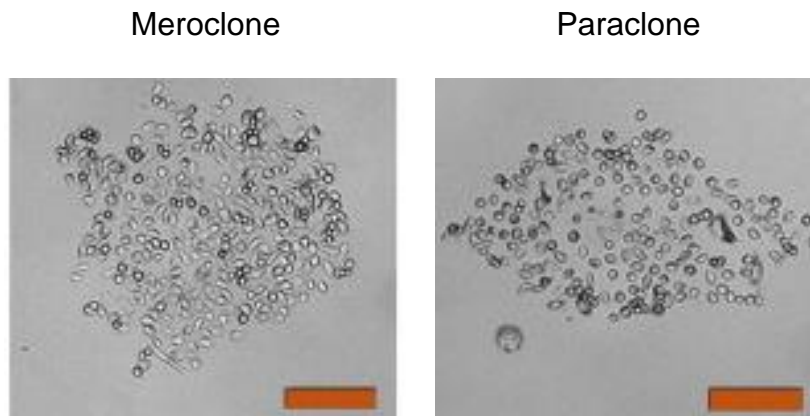


Figure 26. Two PC3 colonies in a colony forming assay.

Pfeiffer and Schalken reported that with a PC3 colony forming assay, typical holoclone phenotype was not observed, only 2 colony types : meroclones and paraclones (Pfeiffer and Schalken, 2010). Scale: Bar measures 200 μ m.

Morphological segregation, as employed by Li et al 2008, (Li et al., 2008) appears to hold visually, for holo- and paraclones, but does not appear to hold for meroclones (section 1.3.5 Figure 4). For visual only classification of biological phenomenon, the differences need to be obvious (e.g. holo- and para-clones) and anything that is in between is difficult to categorize and subject to inaccuracy of observer interpretation (Motoyoshi et al., 2007). Such classification is not a quantitative measure. One specific issue that I attempted to address in this thesis was to develop some quantitative measure of analysis for the observed colonies. Surprisingly, previous studies (Barrandon and Green, 1987; Harper et al., 2007; Liu et al., 2013; Pfeiffer and Schalken, 2010) did not provide any quantitative analysis. At day 10 post-plating, colonies with morphological appearances of holoclones and meroclones consisted of tightly clustered cells and colonies with morphological appearances of paraclones consisted of dispersedly spread cells. In addition to a morphological

description alone, this study aimed to describe disparate colony types by quantifiable measurements. At a specified time point of 10 days post cell plating, colonies were imaged and the longest diameter measured. Colonies with the morphological appearances of holo/meroclones had a mean diameter of $837 \pm 21 \mu\text{m}$. Those morphologically paraclones had a mean diameter of $1191.3 \pm 28.3 \mu\text{m}$. The diameter of paraclones was greater than that of holo/meroclones ($p < 0.05$).

A further difference between the colony types was the how closely cells were packed together within the colonies. Publications using prostate (Li et al., 2008; Pfeiffer and Schalken, 2010) and breast (Liu et al., 2013) cancer cell lines, as well as murine keratinocytes (Tudor et al., 2006) have described holoclones to consist of “closely packed cells”. This again has been a subjective description not quantified in studies. Analysis of colony images in my study found colonies mean cell density of colonies could be quantified, and mean cell density of holo/meroclones was greater than mean cell density of paraclones $p < 0.05$ (27.3 ± 3.2 vs 4.7 ± 0.4). This manner in which cells of holoclones grow densely adjacent to each other may represent a function of their characteristics. For example, there may be altered intercellular communication between cells of holoclones which enhances their stem cell-like characteristics compared with intercellular communication between more dispersed cells of paraclones.

3.4.2 Stem cell gene expression in prostate cancer cell line colonies

The colony types have previously been associated with their possible identity as stem cells (Li et al., 2008; Pfeiffer and Schalken, 2010; Zhang and Waxman, 2010). I measured the expression of four putative stem cell genes was assessed in the 2 colony types formed by PC3 cells. There was a differential expression in the stem cell gene Oct 4 between the 2 types of colonies formed as shown in section 3.3.2 (Fig 10). In this study holo/meroclones expressed the stem cell gene Oct 4, but paraclones did not. However, BMI 1 was expressed by cells of both holo/meroclones and cells of paraclones in this study. A limitation of this work was that the PCR products were not sequenced and therefore lack absolute confirmation of being the expected products. Zhang and Waxman tested expression of stem cell markers

CD44⁺ and $\alpha 2\beta 1$ ⁺ using flow cytometry and found that expression of these 2 markers was prevalent in the majority of PC3 cells, regardless of colony type. Through microarray and qPCR analysis to determine genes differentially expressed in cells of holoclones, Zhang and Waxman identified FAM65B was strongly up regulated in holoclones compared to paraclones and MFI2, LEF1 and IL18R1 were down regulated in holoclones compared to paraclones. The expression of these genes was not investigated in my study (Zhang and Waxman, 2010).

Expression of stem cell markers has also been investigated in DU145 cell line derived colonies. Beaver et al, (2014) used immunocytochemistry to determine expression of four stem cell markers CD44, $\alpha 2\beta 1$ integrin, Oct4 and BMI-1 in DU145 colonies (Beaver et al., 2014). Most cells within holoclones stained for all these markers whilst paraclones were negative for $\alpha 2\beta 1$ integrin, BMI-1 and Oct-4 and had fewer CD44 expressing cells than the holoclones and meroclones (Beaver et al., 2014). Pfeiffer and Schalken investigated the expression of stem cell markers by immunocytochemistry in DU145 holoclones and paraclones (Pfeiffer and Schalken, 2010) . Converse to finding by Beaver et al (2014) $\alpha 2$ -integrin and BRCP staining was observed in both holoclones and paraclones (Pfeiffer and Schalken, 2010). These results suggest that stem cell markers may be expressed in both holoclone and paraclone colony types, in colonies derived from prostate cancer cell lines PC3 and DU145.

3.4.3 Differential response to Wnts in cells of holo/meroclones and cells of paraclones

A further aim study was to characterise PC3 colonies according to their response to Wnt signalling. This is the first study to investigate the free $[Ca^{2+}]_i$ release in cells of holo/meroclones and paraclones in response to Wnt 5A and Wnt 9B ligands. These two Wnts were selected as they are typical Wnt ligands of the non-canonical Wnt / Ca^{2+} pathway (Sheldahl et al., 1999) and canonical Wnt pathways (Dong et al., 2006) respectively, as described in section 1.4.

Analysis of cells within the 2 different colony types demonstrated that as shown in Table 11 and Figure 16, whilst all cells of holo/meroclones demonstrated an $[Ca^{2+}]_i$ response to Wnt 5A and to Wnt 9B, 11 of 58 cells analysed within paraclones did not respond to Wnt 5A and 11 of 51 cells analysed within paraclones did not respond to Wnt 9B. This observation occurred consistently in all 3 experimental repeats. Cells within holo/meroclones were more likely to respond to Wnt 5A (n=103), than cells within paraclones (p<0.05). Holo/meroclones were also more likely than paraclones to respond to Wnt 9B (n=110) (Davda et al., 2015).

As shown in Table 11 and Figure 16, a secondary response to Wnts 5A was observed in 8 of 52 cells within holo/meroclones and 5 of 58 cells of paraclones. A secondary response to Wnt 9B was observed in 22 of 52 cells within holo/meroclones and 8 of 51 cells of paraclones. Cells of holo/meroclones were therefore more likely than cells of paraclones to demonstrate a secondary response (n= 213, p<0.05) to Wnt 5A or Wnt 9B. This phenomenon may be a characteristic of putative stem-like cells with an increased amount of Ca^{2+} released in response to Wnt ligands.

These findings support my initial hypothesis that cells of holo/meroclones are more *stem cell like*, and the hypothesis that these more stem cell-like cells would be more responsive to Wnt ligand stimulation, which could be demonstrated by an $[Ca^{2+}]_i$ response. Cells of holo/meroclones may have more receptors able to interact and be activated by ligand exposure or may have more significant downstream signalling by Wnt mediators. Cells within paraclones may be more heterogeneous in their response to Wnt 5A and 9B. Alternatively, cells within paraclones may in fact demonstrate a uniform response to these Wnt ligands but there may have been an artefactual effect leading to these results. For example, a cell not fully within the plane of focus may have appeared to not have demonstrated a response. Although this may particularly have been a possibility in cells of paraclones, which by definition are more dispersed over a larger area from each other, when selecting cells for analysis cells were chosen across an individual colony in both colony types i.e. centrally and peripherally but within focus.

An interesting secondary observation relates to appearance of two calcium peaks in some experiments (e.g. Fig 15 B). It could be speculated that in these stem-like colonies, there is a bimodal response due to activation of different $[Ca^{2+}]_i$ response. The secondary response may also be attributable to extracellular calcium entry into the cell through store-operated Ca^{2+} entry (SOCE). As discussed, Ca^{2+} levels in the cytosol are controlled bSOCE, mediated by store-operated channels (SOCs) (Flourakis et al., 2010; Williams et al., 2001). Findings reported above have shown that ORAI-1 (a calcium selective ion channel and component of SOCE) is expressed in both PC3 colony types. However, a detailed and systematic analysis of this phenomenon is needed and was not within the scope of this project.

Free intracellular calcium is involved in key functions including modulation of enzyme activity and gene regulation, proliferation and migration (Bading, 2013; M L Villereal and Palfrey, 1989; Melchionda et al., 2016; Monteith et al., 2012). Dwell time of released free intracellular calcium is a key determinant of how much and for how long free calcium is available in the cytosol for such processes. Analyses were performed on the differences in $[Ca^{2+}]_i$ response to Wnt 5A and Wnt 9B between cells of holo/meroclones and cells of paraclones which responded (as summarised in Table 12). When comparing response to Wnt 5A by colony type, significant differences between cells of holo/meroclones and cells of paraclones were observed. Both rise time and dwell times for paraclones were longer than holo/meroclones (section 3.3.3 Table 12, Fig 16). In addition, durations of both primary and total response were longer than in cells of paraclones than holo/meroclones $p < 0.05$. As $[Ca^{2+}]_i$ is involved in key cellular functions cells, a potential explanation for these findings is that holo/meroclones are more stem cell-like and therefore cells in holo/meroclones induce a different pattern of $[Ca^{2+}]_i$ response to Wnt ligand stimulation than cells of paraclones. This is consistent with the proposed theory that cells of holo/meroclones behave differently to cells of paraclones on Wnt activation.

Cells in holo/meroclones induce a faster elevation of $[Ca^{2+}]_i$ in response to Wnt signalling, whilst the response seen in cells of paraclones is slower. This slower response in cells of paraclones may possibly be due to less activation either by reduced FZ activation or downstream by β -catenin or other mediators.

When comparing the same cell type to Wnts, both cells of holo/meroclones and cells of paraclones had a shorter rise time following treatment with Wnt 5A than with Wnt 9B $p < 0.05$ (Table 12). The short rise time following treatment with Wnt5A is consistent with previous findings in whole populations of PC3 cells which were not clonal (Thrasivoulou et al., 2013). In cells of holo/meroclones, the durations of dwell time and total response following treatment were shorter with Wnt 5A than following treatment with Wnt 9B $p < 0.05$ (Table 12). Similarly, in cells of paraclones, the duration of the total response following treatment with Wnt 5A was shorter than following treatment with Wnt 9B $p = 0 < 05$. Similarly, in whole populations of PC3 cells, Thrasivoulou et al found a short dwell time following treatment with Wnt 5A compared with treatment with Wnt 9B (dwell time < 15 seconds vs > 30 seconds $p < 0.05$) (Thrasivoulou et al., 2013). It could be speculated that the one of the determinants of cellular characteristic or function (e.g. stemness vs differentiation) could be the result of release, and availability of free $[Ca^{2+}]_i$ and also of the Wnt ligand availability (e.g. Wnt 5A or Wnt 9B). For example, shorter dwell time in holo/meroclones in response to Wnt 5A in this study and in whole populations of PC3 cells may indicate that availability of Wnt 5A ligand is usually tightly regulated.

3.4.4 Expression and co-localisation of β -catenin in different colony types

This is the first study to investigate the effect of Wnts on β -catenin expression in cells of PC3 colonies. The effect of Wnts on β -catenin expression has been investigated in a population of cells not in colonies (Thrasivoulou et al., 2013). In work by Thrasivoulou et al., (2013), there was little or no expression of β -catenin in the nucleus of PC3 control cells, as most of the β -catenin is considered to be sequestered in the cytosol. However, expression was increased, particularly in the nucleus, in cells treated with Wnts 5A, 9B, and 10B (Thrasivoulou et al., 2013). Thrasivoulou et al., (2013) confirmed the visual appearances nuclear co-localization with objective quantification and additionally found that inhibition of Wnt induced $[Ca^{2+}]_i$ release also reduced nuclear translocation of β -catenin.

In my study expression of β -catenin was visually observed in cells of both holo/meroclone and paraclone colony types (Davda et al., 2015). This is in contrast

with other studies reporting β -catenin protein expression to be absent in paraclone PC3 colonies and present in holoclone PC3 colonies (Li et al., 2008). Although cells of both colony types expressed β -catenin in the absence of Wnt ligand treatment, staining appeared relatively increased throughout the cells following treatment with Wnt 5A and following treatment with Wnt 9B in both colony types. Visually there appeared to be increased expression β -catenin on Wnt 5A and Wnt 9B activation and nuclear and peri-nuclear punctate staining. The findings suggest nuclear translocation of β -catenin on Wnt activation in PC3 holo/meroclone and paraclone colonies. Further work to objectively demonstrate this would be to perform image deconvolution and quantitative analyses of nuclear co-localisation of β -catenin using colocalization co-efficients. This could be performed on single imaged slices rather than the Z-stacks presented above.

3.5 Chapter 3 Conclusions

This chapter investigated colony formation from single cell culture of PC3 cells and aimed to characterise the colonies formed by subjective parameters and characterise differences in their response to Wnts. PC3 cells cultured in a clonogenic assay form 2 colony types: holo/meroclones and paraclones. There are differences in these 2 types of colonies which can be described by parameters of colony diameter and cell density. Both colony types respond to Wnt 5A and Wnt 9B as determined by $[Ca^{2+}]_i$ response. However, there are differences in Wnt induced increase in $[Ca^{2+}]_i$ between the 2 colony types: a greater proportion of cells in holo/meroclones respond to Wnts 5A and 9B, a greater proportion demonstrate a secondary elevation in $[Ca^{2+}]_i$, and there is a shorter rise time compared to cells in paraclones. These differences between holo/meroclones and paraclones are possibly attributable to cells in the former being more stem cell like.

This study shows for the first time that Wnt mediated $[Ca^{2+}]_i$ release occur in response to both Wnt 5A and Wnt 9B in both colony types. Both colony types also expressed β -catenin and both colony types expressed increased expression β -

catenin on Wnt activation on visual interpretation of the images. The images suggest nuclear translocation of β -catenin on Wnt activation, with strong punctate staining observed in the nucleus and around it, in cells of both colony types.

Chapter 4: Expression of ion channels in prostate cancer cell lines and PC3 colonies

4.1 Introduction

All colonies formed from single cells of PC3 cells respond to Wnt ligands (5A and 9B) by inducing free $[Ca^{2+}]_i$ release, confirming previous observations that both canonical and non-canonical ligands can induce calcium release in mammalian cells (Thrasivoulou et al., 2013). There is also visual evidence that there is translocation of β -catenin in response to Wnt signal activation particularly in holo/meroclones (see above). Thrasivoulou et al (Thrasivoulou et al., 2013) further demonstrated it is possible to inhibit at least one component of the calcium release with thapsigargin, indicating the involvement of store operated calcium entry (SOCE) (Flourakis et al., 2010; Williams et al., 2001).

Such elevations in free $[Ca^{2+}]_i$ are important in cell signalling and mediate key processes such proliferation, metabolism and gene transcription (Berridge, 1995; Berridge, 2005; Berridge et al., 2003; Clapham, 2007). In addition, the Ahmed laboratory has also shown a number of known compounds that regulate cell membrane potential (membrane potential regulating compounds, MPRCs) also modulate Wnt induced calcium release (New British Patent Application no. 1318659.8 and US-2016-16-0271157-A1). Further to this, they have demonstrated that some MPRCs also activate $[Ca^{2+}]_i$ stores (Petrou et al., 2017). The wide range of effects of ion channels and the Wnt induced calcium response suggests that ion channels may be involved in the Wnt signalling pathway. At the time of conducting this project the identity of the specific membrane ion channel that may be involved in the Wnt signalling regulation was not known. It was decided therefore to lay some foundation work by investigating the expression of a large number of ion channels that have been previously described in cancer in the literature (Table 13).

Ca²⁺ levels in the cytosol are controlled by SOCE, mediated by store-operated channels (SOCs) (Flourakis et al., 2010; Williams et al., 2001). Calcium release-activated calcium channel protein 1 (ORAI-1) is a calcium selective ion channel and component of SOCE in prostate cancer cell line LNCaP where influx of Ca²⁺ leads to apoptosis, whilst downregulation of ORAI-1, and SOCE function, reduces apoptosis (Flourakis et al., 2010).

Over the past decade there has been interest in expression of ion channel genes in cancer, their relevance in malignancy and potential effects of their manipulation in clinical practice. The expression of ion channel families has been studied in a number of tumour types including prostate cancer, breast cancer, melanoma, cervical cancer, ovarian cancer and astrocytoma. Table 13 below gives a summary of the important findings to date regarding ion channels and solid cancers.

In addition to the role of ion transporters in the cell membrane in cancer, described above, recent observations pertinent to this thesis, have been made in our laboratory, very recently. These indicate that various compounds that are known to act on a variety of ion channels, receptors and transporters, may be able to regulate Wnt signalling (Ahmed A., International Patent Application PCT/GB2014/053138; British patent application No. 1318659.8; USPTO 2016/0271157A1).

Table 13. Expression of ion channel genes in solid cancers.

	Ion channel gene	Summary of channel function	Experimental model	Mechanism
ORAI-1	ORAI-1	Calcium release-activated calcium channel protein 1 (ORAI-1) is a calcium selective ion channel and component of the	Prostate cancer cell lines	Thapsigargin triggers Ca ²⁺ -dependent apoptosis. Knocking down ORAI with si ORAI results in resistance to

		<p>ICRAC system: calcium release activated calcium currents. The ion channel is activated when internal calcium stores are low. STIM 1 protein detects low concentration of calcium in the endoplasmic reticulum.</p>		<p>thapsigargin induced apoptosis, chemotherapy induced apoptosis following treatment with strong alkylating agents, and resistance to a physiological model of apoptosis (Flourakis et al., 2010).</p>
			<p>Breast cell lines Breast cancer tissue</p>	<p>Breast cancer cell lines have elevated levels of ORAI-1 whilst STIM1 and STIM2 are not overexpressed. ORAI-1 siRNA reduces store-operated calcium entry. Further analysis of STIM1 and STIM2 expression found that from transcriptional data from almost 300 breast cancers, poorer prognostic histology sub-type was associated with the presence of high</p>

				STIM1 : low STIM2 ratio (McAndrew et al., 2011).
Kv 1.3	KCNA3	Potassium channel, voltage gated shaker related subfamily A, member 3	Human osteosarcoma cell line; mouse melanoma cell line	Potassium membrane-permeable Kv 1.3 inhibitors psora-4, PAP-1 and clofazimine target mitochondrial Kv 1.3 channels. These inhibitors induced apoptosis in mouse melanoma cell line B16F10 and human sarcoma cell line SAOS-2, both of which were demonstrated to express Kv 1.3. The same effect was not observed in HEK293 cells, understood to highly express Kv channels. Downregulation of Kv 1.3 via siRNA removed the inhibitors' effects (Leanza et al., 2012).
			Melanoma mouse model	In an orthotopic melanoma B16F10

				<p>mouse model, clofazimine administered intraperitoneally markedly reduced tumour size when animals were sacrificed at day 16. Examination of the internal organs of the mice demonstrated no obvious other pathology on comparison to non-treated mice (Leanza et al., 2012).</p>
EAG1 / Kv 10.1 / h-eag1	KCNH1	ether à go-go (Eag1) potassium channel	Human colorectal cancer tissue and control benign tissue	<p>In normal tissues, EAG mRNA is specifically expressed in the brain.</p> <p>Analysis of Eag1 protein in human colorectal cancer tissue and benign tissue found that mRNA and protein was present in the majority of malignant samples, but not detected in benign</p>

				tissue. Eag1 protein expression was associated with clinical tumour stage (Ding et al., 2007).
			Primary culture of cervical tissue	Eag1 gene and protein expression was found in all cervical cancer primary cultures derived from human biopsies, whilst expression was present in 1/3 of benign tissues (Farias et al., 2004).
KCa 2.3 / SK 3	KCNN3	SK channels or Small conductance calcium-activated potassium channels are a subfamily of Ca ²⁺ -activated K ⁺ channels	Breast cancer cell lines	SK2 was expressed in all breast cancer cell lines tested, whilst SK3 was only expressed in one cell line. SK2 was found in both benign and malignant breast cancer tissue whilst SK3 was only in cancerous tissue. SK3 expression increased migration in cell lines, whilst proliferation was not affected (Potier et al., 2006).

<p>KCa 3.1 / SK4</p>	<p>KCNN4</p>	<p>Intermediate conductance Ca²⁺ activated K(+) channel</p>	<p>Glioma cell lines. Glioma mouse model</p>	<p>Using data from the National Cancer Institute database, KCa 3.1 was upregulated in 32% of patient cancers; KCa 3.1 expression was associated with reduction in survival.</p> <p>KCa 3.1, if present, enhances cell migration. Several glioma lines tested with a migration assay found that cell lines with high KCa 3.1 expression had reduced migration upon treatment with channel inhibitor. Cell lines with low KCa 3.1 expression demonstrated no change in migration following inhibition. Loss of KCa 3.1 function also inhibited invasion. Further to this, tumour invasion was reduced when KCa 3.1 was inhibited in</p>
----------------------	--------------	--	---	---

				SCID mice (Turner et al., 2014).
KCa 1.1	KCNMA1	Pore forming α -subunit of BK _{Ca} channels (Large conductance calcium-activated potassium channels)	Breast cancer cell lines	Breast cancer cell lines from brain metastases have a higher expression of KCNMA1 than those cell lines from other metastatic sites. BKCa channels are active in breast cancer cell lines and their inhibition reduces invasion and migration (Khaitan et al., 2009).
TASK3	KCNK 9	Potassium channel, subfamily K,	Colorectal cancer	Analysis of 124 colorectal cancers found expression of KCNK9 in 46% of tumours (Kim et al., 2004).
			Ovarian cancer tissue and ovarian cancer cell lines	TASK-3 is expressed in ovarian cancer cell line, as well as normal ovarian tissue and ovarian cancer tissue. Using a tissue array, expression was found in almost all

				tumours and increased staining was associated with improved prognosis. Inhibition of TASK-3 in 2 cell lines resulted in reduced cell proliferation and apoptosis (Innamaa et al., 2013b).
TREK-1 and TREK-2	KCNK 2 and KCNK10	Potassium channel, subfamily K	Ovarian cancer tissue and ovarian cancer cell lines	TREK-1 and TREK-2 are expressed in ovarian cancer cell lines, benign ovarian tissue and the majority of ovarian cancer tissue. A TREK-1 inhibitor reduced cell proliferation, in a dose dependent manner, and increased apoptosis (Innamaa et al., 2013).
hERG / Kv 11.1	KCNH2	Human ether-a-go-go-related gene K ⁺ channels	human embryonic kidney cells Glioblastoma cell line	Doxazosin is an inhibitor of hERG and reduces hERG current in human embryonic kidney (HEK) cells. Doxazosin induces apoptosis in 2

				<p>human glioblastoma cell lines.</p> <p>Knockdown hERG via si RNA also reduces cell viability of a glioblastoma cell line (Staudacher et al., 2014).</p>
<p>Ear 2 / Kv 10.2</p>	KCNH 5	<p>Potassium channel, voltage gated eag related subfamily H, member 5.</p>	<p>Mouse and human medulloblastoma tissue</p>	<p>Analysis of a mouse medulloblastoma model found mRNA of Eag 2 elevated and Eag 1 reduced in tumour compared with normal cerebellum. Eag 2 expression was also elevated in the majority of tissue samples from primary and recurrent human tumours, compared with control tissue. Further to this, Eag2 knockdown reduced growth of medulloblastoma and tumourigenicity in a mouse model (Huang et al., 2012).</p>
Kir 4.1	KCNJ10	Inwardly-	Human	Analysis of human

channel subunit		rectifying K+ channel	astrocytoma tissue	astrocytomas found Kir 4.1 mRNA and protein to be expressed. Increased expression was associated with pathologic tumour grade (Tan et al., 2008).
-----------------	--	-----------------------	--------------------	---

Based upon this literature review, several classes of ion channels which may be important in cancer cell signalling were chosen for further investigation in this project with a view that these might be useful targets to regulate the activity of Wnt signalling (Petrou et al., 2017). Table 14 summarises the ion channels which are investigated in this project. The expression of ion channel families has been studied in a number of tumour types including prostate cancer. Key families of ion channels associated with malignancy have been identified in the literatures. Both Wnt 5A and Wnt 9B produce a $[Ca^{2+}]_i$ response in a population of PC3 cells, and in cells cultured in a colony forming assay in holo/meroclones and in paraclones. The aim of this study was to characterise ion channel expression in prostate cancer cell lines and cells of PC3 colonies.

Table 14. Summary of ion channel genes known to be associated with malignancy and characterised further in this study.

Family	Genes
KCNJ	KCNJ1 var1, KCNJ2, KCNJ3 var1, KCNJ4 var1, KCNJ5, KCNJ6, KCNJ8, KCNJ9, KCNJ10, KCNJ11, KCNJ12, KCNJ13 var1, KCNJ14, KCNJ15, KCNJ16
KCNA	KCNA1, KCNA2, KCNA3, KCNA4, KCNA5, KCNA6, KCNA7, KCNA10
KCNK	KCNK1, KCNK2 var1, KCNK3, KCNK4, KCNK5, KCNK6, KCNK 7 var C, KCNK9 var1, KCNK10 var1, KCNK12, KCNK13, KCNK15, KCNK16 var1, KCNK17 var1, KCNK 18
ORAI	ORAI1, ORAI2 var1, ORAI2 var2, ORAI3
STIM	STIM1 var1, STIM1 var2, STIM2 var1, STIM2 var2
KCNH	KCNH1 var1, KCNH2 var1, KCNH2var2, KCNH5 var1
KCNMA	KCNMA1 var1
KCNN3	KCNN3 var1, KCNN4
CACNA	CACNA1C var2

A number of MPRCs are commonly and safely routinely used in clinical practice, mainly for cardiovascular conditions. Such MPRCs include amlodipine and isradipine. These MPRCs, as well as cadmium chloride were chosen as a selection of MPRC to test their effects on cancer cell line proliferation. Rather than specific MPRCs, broad-channel blockers, and known regulators of the cell membrane potential were selected for use in this project. Table 15 below describes several calcium channel blockers, their physiological effect and clinical indications.

Table 15. Calcium channel blockers, their physiological effect and clinical indications.

Calcium channel blockers have been in widespread clinical use for decades for therapeutic use in cardiovascular disease as summarised below.

Calcium channel blocker	Physiological effect and clinical indication
Isradipine	Similar effects to those of nifedipine. Clinical indications: Hypertension (RSPGB, 2015).
Amlodipine	No effect on myocardial contraction and can be used in cardiac failure. Improves coronary vasospasm. Clinical indications: Angina; hypertension (RSPGB, 2015).
Nifedipine	Relaxation of vascular smooth muscle leading to dilatation of coronary and peripheral arteries. Compared with verapamil, there is greater effect on vasculature and it is not an anti-arrhythmic. Infrequently causes heart failure. Clinical indications: Hypertension; angina (RSPGB, 2015).
Nimodipine	Similar to nifedipine but primary effect on coronary artery smooth muscle. Clinical indications: Prevention of vascular spasm following aneurysmal subarachnoid haemorrhage (RSPGB, 2015).
Verapamil	Reduces cardiac output, slows the heart rate, and may impair atrioventricular conduction. Clinical indications: Angina; hypertension; arrhythmias (RSPGB, 2015).
Diltiazem	Less negative inotropic effect than verapamil and significant myocardial depression occurs rarely. Clinical indications: Angina; hypertension (RSPGB, 2015).

Nicorandil	Promotes potassium efflux leading to inhibition of voltage gated calcium channels. Acts a vasodilator and is used in the treatment of angina (RSPGB, 2015).
------------	---

Experimental Aims

The aim of this chapter is to investigate ion channel gene expression in prostate cancer cell lines and ion channel protein expression. A further aim is that if channels are identified, to perform provisional work on the inhibition by MPRCs.

4.1.1. Hypothesis

Ion channel genes are expressed in prostate cancer cell lines.

Ion channels are expressed in both cells of PC3 holo/meroclones and cells of PC3 paraclones.

4.1.2 Objectives

The following objectives test the hypothesis:

1. To characterise ion channel expression in prostate cancer cell lines by gene expression.
2. To confirm ion channel protein expression, for some channels that are putative targets of MPRCs in cells of PC3 holo/meroclones and cells of PC3 paraclones.

A further objective was to establish cell growth conditions \pm MPRCs to assess if inhibition of MPRCs affects proliferation of cancer cells in whole populations of the PC3 prostate cancer cell line.

4.2 Materials and methods

4.2.1 Ion channel genes

Primer sequences were designed for ion channel genes identified as being overexpressed in cancer. The method of primer sequence design was as outlined in section 2.6, using sequence of interest information from the NCBI website (<https://www.ncbi.nlm.nih.gov/tools/primer-blast/> date of accession 6th March 2014). Each primer sequence was allocated a PCR reaction number, as indicated in Table 16.

For gene expression in whole populations, prostate cancer cell lines PC3, DU145 and LNCaP were cultured in T75 flasks. Cells were harvested, and RNA extraction performed using RNeasy kit as outlined in section 2.6. RNA was quantified for each cell line and reverse transcription was performed as outlined in section 2.6. RNA was synthesised to cDNA using a Qiagen Omniscript RT kit as per the 10/2010 handbook protocol: <http://www.qiagen.com/us/products/catalog/assay-technologies/end-point-pcr-and-rt-pcr-reagents/omniscript-rt-kit/>. For sufficient yield of cDNA for subsequent PCR, constituents were scaled up x 2 so that 4µg template RNA was used and made up to a volume of 24 µl with RNase free water as indicated in table 4. Once the protocol was completed, the cDNA was frozen at -20C if for later use in PCR. PCR was performed using Qiagen Taq PCR Master Mix kit and following the protocol handbook 10/2010. <http://www.qiagen.com/us/products/catalog/assay-technologies/end-point-pcr-and-rt-pcr-reagents/taq-pcr-master-mix-kit>. Prior to commencing PCR cDNA was thawed on ice and quantified using a spectrometer giving a concentration in µg/ml. 0.5 µg template cDNA was used in all PCR reactions per reaction tube. The volume of cDNA required for 0.5 µg was calculated and the volume of RNase free water to make a cDNA solution up to 12 µl was calculated as indicated in table 5. Reaction tubes were placed in a thermal cycler programmed as indicated in table 6. Following amplification, PCR product samples were stored at 4°C until agarose gel electrophoresis.

Table 16. Oligonucleotide sequences designed for PCR of ion channel genes, and expected size for each product.

PCR reaction number	Oligonucleotide sequence (5' to 3')	Oligonucleotide name	Expected size
1	GTGGACATCTGGACAACGGT	KCNJ1 var1 F	418
	CTCCCCGTTTGCTGATCACT	KCNJ1 var1 R	
2	CCGCTACAGCATCGTCTCTT	KCNJ2 F	446
	TTGGGCATTCATCCGTGACA	KCNJ2 R	
3	GGCATTGTGGAAACAACCTGGG	KCNJ3 var1 F	508
	AATCAGCCACAGACTGGCTC	KCNJ3 var1 R	
4	GCTCTTTTTTCGGCCTCCTCT	KCNJ4 var1F	620
	CCTTGCCCATGCCATAAAGC	KCNJ4 var1 R	
5	AGATCAGCCAGCCCAAGAAG	KCNJ5 F	799
	CCCCCAAACAGCACACTCAA	KCNJ5 R	
6	CAGCACCCCATCCCTTAGTG	KCNJ6 F	684
	TGTAAGTGGCACACCCACAT	KCNJ6 R	
7	ATCTCAGCAACTGACCTGGC	KCNJ8 F	690
	CCCACCCCTGCACATAACTT	KCNJ8 R	
8	CACGGGAATGACATGCCAAG	KCNJ9 F	534
	TCCCTGAAATCAGGACCCCT	KCNJ9 R	
9	CACACCTGCCATCTCACTGT	KCNJ10 F	497
	GCATGGCTGAGGCCTTCTAA	KCNJ10 R	
10	TGTGCCCATTTAGCTGAGG	KCNJ11 F	559
	AGAGTGTGGCTGGTCAATCG	KCNJ11 R	
11	CCTACAGACGGGAGTCAGAGA	KCNJ12 F	680
	GCTCGTGAGCTCGATGAAGT	KCNJ12 R	
12	CTCTGTTGACCCGAGGTTCC	KCNJ13 F	592
	CACCCAGGGAGCTAGGTTTG	KCNJ13 R	
13	AGTCTAGTTTCCCCGGCTCT	KCNJ14 F	510

	GCTTCTCACCCCTGGTCAACA	KCNJ14 R	
14	CCCTGGAATCCCAGACAACC	KCNJ15 F	796
	AGGGTTAAACCTGGATGGCG	KCNJ15 R	
15	CAAGGCGAGACGAAGGTCAT	KCNJ16 F	479
	GCCTCCTTCCTGCCTTCATT	KCNJ16 R	
16	CGGTGATGTCTGGGGAGAACG	KCNA1 F	598
	GTGCCCGTGAAGTCCTTGT	KCNA1 R	
17	ACATGCATGGTAGTGGGGTG	KCNA2 F	579
	PCCCCAATGGTAGTCGGAACC	KCNA2 R	
18	TCGCAGGACTCATTCTGAAGC	KCNA3 F	556
	TGGTCACTGGGTGCATATCG	KCNA3 R	
19	GCCTGAAGAGGCCAGTCAAT	KCNA4 F	640
	CGGAATACTCGGACCAGACG	KCNA4 R	
20	TGCCATGACCGTCAGAGGAG	KCNA5 F	467
	TGCGGTCTGAAGAAGTACTCG	KCNA5 R	
21	GGAGGGAGAGCAACAGGATG	KCNA6 F	562
	ACCTCGACCATCTACACGGA	KCNA6 R	
22	TTCCCGGACACTCTGCTAGG	KCNA7 F	743
	CGGATGACTCTCAGGATGGC	KCNA7 R	
23	GACTTCGACTCAACCAGCCC	KCNA10 F	646
	CCCTATCCTCCCGGA ACTCT	KCNA10 R	
24	CAACTCGGTCAAGGAGTCCC	ORAI1 F	381
	TCCTGTAAGCGGGCAA ACTC	ORAI1 R	
25	ACCTCTAACCACCACTCGGT	ORAI2 F	495
	GATGATGGTGGACACCAGGG	ORAI2 R	
26	GAGTGACCACGAGTACCCAC	ORAI3 F	554
	AGGAGCGGTAGAAATGCAGG	ORAI3 R	
27	GTTCTGAAGGCTACGGGACC	STIM1 F	574
	GATGGTGTGTCTGGGTCTGG	STIM1 R	
28	CAACTGCCGCCTCCTCTC	STIM2 F	535
	GGGCGTGTTAGAGGTCCAAA	STIM2 R	
31	ATGCTTCCAGTCGGAATGTGT	KCNJ1 var1 F	528

	TGGCCCCACACATGAAAGAA	KCNJ1 var 1 R	
32	CAAATGGCTTTGGGAACGGG	KCNJ2 var1 F	433
	ATGATGCAGCCCACGATTGA	KCNJ2 var1 R	
33	GCATTGTGGAAACAACCTGGG	KCNJ3 var1 F	438
	AGTTGCCCGGAACTGAACTT	KCNJ3 var1 R	
34	GCTCTTTTTTCGGCCTCCTCT	KCNJ4 var1 F	597
	CTGTCCTCGTCGATCTCGTG	KCNJ4 var1 R	
35	AAGAGAGCGGAGACCCTCAT	KCNJ5 F	543
	CCGGCCTTCCCTCTTCATTT	KCNJ5 R	
36	CTGGACCGCATCTTTCTGGT	KCNJ12 F	521
	TCTGACTCCCGTCTGTAGGG	KCNJ12 R	
37	GGAGGATGGTCACCAAGGAT	KCNJ13 var1 F	424
	TTCGCCACAAAAGCACCTGT	KCNJ13 var1 R	
38	GGACACTCTGCTAGGGGACC	KCNA7 var1 F	546
	ATACACAGCGTCTCCACCAC	KCNA7 var1 R	
39	ACCTGGAACCTGGTCACCTCT	ORAI2 var1 F	565
	AGGGAGCGGTAGAAGTGGAT	ORAI2 var1 R	
40	ACCTGGAACCTGGTCACCTCT	ORAI2 var2 F	565
	AGGGAGCGGTAGAAGTGGAT	ORAI2 var2 R	
41	TGTGCACCTCTTTGCACTCA	ORAI3 F	524
	GTTCTGCTTGTAGCGGTCT	ORAI3 R	
42	GACAAGCCGGGTATCTCTGC	STIM1 var1 F	470
	TGTCAGGCAGTTTCTCCACC	STIM1 var1 R	
43	CACATGAGGTGGAGGTGCAA	STIM1 var2 F	498
	CGGAATGGGTCAAATCCCTCT	STIM1 var2 R	
44	TTTGGACCTCTAACACGCC	STIM2 var1 F	548
	GCAGCAACCTCATCTTTAGCA	STIM2 var1 R	
45	CGACTTTTTTCGCTGGCAACA	STIM2 var2 F	493
	CTGTGTCTGGCACTTCCCAT	STIM2 var2 R	
51	GAACCTGGGACTTCACCTCCG	KCNK1 F	409
	GCCTTCCCCAGGCACATAAT	KCNK1 R	
52	AACCCACGAGCAAAAAGGGA	KCNK2 var1 F	485

	TCTGTGCGTGGTGAGATGTT	KCNK2 var1 R	
53	TCATCGTGTGCACCTTCACCTA	KCNK3 F	527
	GAAGGTCCAGTGCTCGTAGTG	KCNK3 R	
54	TTTATGCGCTGGTGGGGATT	KCNK4 F	417
	ACACTACTCGCAGCCAGTTC	KCNK4 R	
55	GAGGTGTGAGTCTGCGGAAG	KCNK5 F	593
	GGAGTAGACTACCAGGGGCA	KCNK5 R	
56	AGTGACCGTCTGCTTTCTGG	KCNK6 F	402
	TACCTGGGGATGGAAGCGTA	KCNK6 R	
57	CTTCCAGGCAGAGCATAGGG	KCNK 7 var C F	594
	GCTGTTAGGTGGCTGGACTT	KCNK 7 varC R	
58	CCATAGGTTATGGGCACGCT	KCNK9 var1 F	488
	CCGCTCATCCTCACTGTTCA	KCNK9 var1 R	
59	TTTCTTTCTTGGTGGCCGT	KCNK10 var1 F	404
	CCTATTGGACTGACTCCCGC	KCNK10 var1 R	
60	GCTGGGACCATCCTGTTCTT	KCNK12 F	417
	CGAGTAAATGCAGCACACGC	KCNK12 R	
61	GGGTGTTCCAGCACCATCTT	KCNK13 F	531
	GCGTGATCGCAAGAGTCCT	KCNK13 R	
62	CTCGAGTCCGAGGCGGAAAG	KCNK15 F	593
	AGGAAGCTGAAGGCCACGTA	KCNK15 R	
63	AGAGCCTTTCCAAACACCCC	KCNK16 var1 F	419
	GAAGCGTCTAGGCTGTGTG	KCNK16 var1 R	
64	GAGCTGTTGCAGAACTTCACG	KCNK17 var1 F	524
	TGGGAGGGGTTTATTCCAATC	KCNK17 var1 R	
65	TGGCTACATCTACCCCGTCA	KCNK 18 F	474
	TCCACCTGCTGTCCAACCTC	KCNK 18 R	
66	GCGTGCAAAAAGGCGAGAAT	KCNH1 var1 F	450
	AGGCACTAACCTCATCCACG	KCNH1 var1 R	
67	GTTTCATCATCGCCAACGCTC	KCNH2 var1 F	570
	ATGGCTGTCACTTCGTCCAG	KCNH2 var1 R	
68	ACTTCACCTTCAGCAGCCTC	KCNH2var2 F	591

	AGGGCATTTCAGTCCAGTG	KCNH2 var2 R	
69	GCACTGACGTACTGTGACCT	KCNH5 var1 F	458
	AGTTCCATGGCATCACGGTT	KCNH5 var1 R	
70	AGAACTGTACCTCACGCAGC	KCNMA1 var1 F	421
	AAACTCATAGGGCGGGTTGG	KCNMA1 var1 R	
71	CACACGTGAAGTCCAGCTCT	KCNN3 var1 F	435
	CTTTCACAGACACGGACGGT	KCNN3 var1 R	
72	CTCATCGTGGCCTTTCATGC	KCNN4 F	479
	GTGGCATTAAACAGCCTGCCT	KCNN4 R	
73	GGCCCCATCTACAACCTACCG	CACNA1C var2 F	436
	AACCCTTGGGTTTGAAGGCA	CACNA1C var2 R	

4.2.2 Immunostaining for ion channel proteins

Following PCR experiments, ORAI-3 and KCNK-1 protein ion channel expression was investigated by immunocytochemistry. Whole cell populations of PC3 cells were grown on 8-well chamber slides (Nunc Lab-Tek Chamber Slide System). Cells at day 5 of culture were trypsinised, counted and plated at a concentration of 500 cells in each well with 200 μ L of medium. After 3 days of culture, the cells were fixed with 4% PFA and immunocytochemistry was performed as outlined in Chapter 2.

ORAI-3 and KCNK-1 antibodies for immunocytochemistry were available commercially. As the primary antibodies, anti-ORAI-3 Ab (Sigma product number HPA015022) and anti- KCNK1 (abcam; sigmaaldrich) were used at dilutions of 1:50-1:200 and 1:200-1:500, respectively, as recommended by the manufacturer. Primary antibody dilutions and concentrations are as indicated in Tables 17 and 18 below. Negative control experiments, in which no primary antibody was added, were used to determine non-specific reaction. Experiments with no primary antibody were used as a negative control.

An optimisation process was performed, as summarised in Tables 17 and 18 and Figures 29 and 30 to establish basic specificity and concentration dependence of antigen-antibody interactions (Burry, 2000; sigmaaldrich, 2017). The secondary antibody used was goat anti-rabbit IgG-FITC (Southern Biotech- 4030-02) at a dilution of 1:500.

Table 17. Concentrations of primary antibody anti-ORAI-3 tested in optimisation process for immunocytochemistry.

	Dilution
Concentration 1 Anti-ORAI-3	1:50 (4 μ g/ml)
Concentration 2 Anti-ORAI-3	1:100 (2 μ g/ml)
Concentration 3 Anti-ORAI-3	1:200 (1 μ g/ml)

Table 18. Concentrations of primary antibody anti-KCNK1 tested in optimisation process for immunocytochemistry.

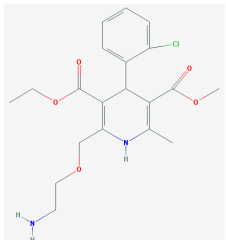
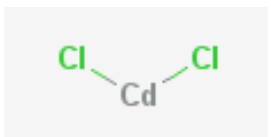
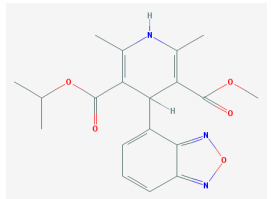
	Dilution
Negative control with no 1° antibody	0 µg/ml
Concentration 1 anti-KCNK1	1:200 (1 µg/ml)
Concentration 2 anti-KCNK1	1:350 (0.57 µg/ml)
Concentration 3 anti-KCNK1	1:500 (0.4 µg/ml)

4.2.3 Assessment of MPRCs on proliferation of cancer cell lines in whole populations of cells

A number of MPRCs are commonly and safely routinely used in clinical practice, mainly for cardiovascular conditions (see section 3.1). Such MPRCs include amlodipine, nicorandil and isradipine. These MPRCs, as well as cadmium chloride were chosen as a selection of MPRC to test their effects on cancer cell line proliferation. Rather than specific MPRCs, broad-channel blockers, and known regulators of the cell membrane potential were chosen for this preliminary investigation on PC3 proliferation in whole populations.

Table 19 below shows the molecular formula, mass, 2-dimensional structure and concentration used in experiments for amlodipine (Sigma-Aldrich A5606), cadmium chloride (Sigma-Aldrich 202908), nicorandil (Sigma-Aldrich N3539) and isradipine (Sigma-Aldrich I6658). Dose-response was analysed for isradipine at concentrations of 5 µM, 10 µM and 100 µM.

Table 19. MPRCs used in cell proliferation experiments and their molecular formula, mass, structure and concentrations tested in proliferation experiments.

Drug	Molecular Formula	Molecular mass (g/mol)	2-Dimensional structure	Concentration tested
Amlodipine	$C_{20}H_{25}ClN_2O_5$ (PubChem, 2017)	408.9	 (PubChem, 2017)	530 nM
Cadmium chloride	$CdCl_2$ (PubChem, 2017)	183.3	 (PubChem, 2017)	1 mM
Isradipine	$C_{19}H_{21}N_3O_5$ (PubChem, 2017)	371.4	 (PubChem, 2017)	5 μ M, 10 μ M and 100 μ M

Experiments were performed in whole populations of PC3 cells (not on colonies) as initial work to potentially form the foundation for future studies on holo/meroclones and paraclones.

PC3 prostate cancer cells were cultured in T80 flasks, as described in Chapter sections 2.1. Cells were trypsinised, counted and subjected to serial dilution to 50,000 cells/ml. Then, 50,000 cells were pipetted into each well of a 6-well plate (Nunc), with 2 ml RPMI with supplements (see section 2.1. The plates were placed in a 37°C, CO₂ incubator in an IncuCyte™ (Essen Bioscience) live cell imaging system, which acquired images every 4 hours for later analysis of confluence. After 24 hours, the plates were removed, treated with MPRCs and control plates received vehicle only, phosphate buffered saline or dimethylsulfoxide, DMSO. Control wells were treated with the same volume of DMSO control used in the experiment wells. Plates were placed back in an IncuCyte™ and experiments were terminated once the control wells had reached confluence (>90% growth in the vessel), or after a maximum of 144 hours (6 days). Experiments were performed in triplicate.

Statistical analyses were performed on numerical cell confluence data obtained from the IncuCyte™ at the time intervals specified above. An independent t-test was used to assess if there were differences in cell proliferation between the control experiments (no MPRC) and experimental arms. IPSS software was used for statistical analysis.

4.3 Results

4.3.1 Characterisation of ion channel gene expression in 3 prostate cancer cell lines

4.3.1.1 Ion channel genes expressed on RT-PCR

Numerous ion channel genes are expressed in the prostate cancer cell lines PC3, LNCaP and DU145. PCR was performed on 3 cell passages for each of the cell lines PC3, LNCaP and DU145. Figure 27 (A-D) below shows representative agarose gel electrophoresis images from PC3 cell PCR reactions for the expression of channel genes. Experiments were performed in RNA isolated from three different passages of the cell lines.

Figure 27. Agarose gel electrophoresis images from PC3 cell PCR reactions.

0.5 µg template cDNA was used in all PCR reactions per reaction tube. The volume of cDNA required for 0.5 µg was calculated and made up to a volume of 12 µl with RNase free water. A reaction mixture of Taq PCR mastermix solution, Primer A (forward) 8.4 µM, Primer A (reverse) 8.4 µM, RNase-free water + Template DNA 0.5 µg was made up to a total volume of 30 µl. Agarose gel 1.1% was made up using 150 ml TAE_x1 with 1.65g agarose and 10 µl 0.5 µg/ml ethidium bromide (Sigma-Aldrich) for visualisation. 10 µl of each PCR product was pipetted into wells with 1 µl 10x Blue Juice loading dye (Sigma-Aldrich). 2 µl of 1K base pair DNA ladder (ThermoFisher Scientific 10787-018) was also pipetted into a well in each column with <1 µl 10x Blue Juice loading dye. Gel electrophoresis was performed using a current was applied at 110V for 70 min followed by the gel imaging under UV light. Presence of product bands at the expected sizes is indicative of expression of that specific gene.

Figure (A) shows 1kb plus DNA ladder with labelled base pairs (bp) size bands on ladder and PCR products 1–15 with expected size of respective products (bp). Left to right the products are: (1) KCNJ1 (418); (2) KCNJ2 (446); (3) KCNJ3 (508); (4) KCNJ4 (620); (5) KCNJ5 (799); (6) KCNJ6 (684); (7) KCNJ8 (690); (8) KCNJ9 (534); (9) KCNJ10 (497); (10) KCNJ11 (559); (11) KCNJ12 (680); (12) KCNJ13 (592); (13) KCNJ14 (510); (14) KCNJ15 (796); (15) KCNJ16 (479).

(A)

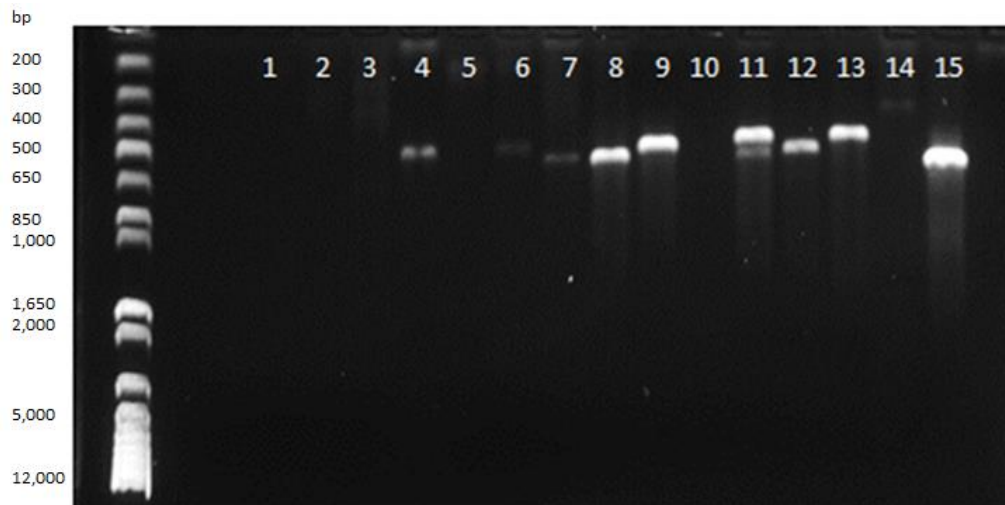


Figure (B) shows 1kb plus DNA ladder with labelled base pairs (bp) size bands on ladder and PCR products 16–30 with expected size of respective products (bp). Left to right the products are: (16) KCNA1 var 1 (598); (17) KCNA2 (579); (18) KCNA3 var 1 (556); (19) KCNA4 var 1 (640); (20) KCNA5 (467); (21) KCNA6 (562); (22) KCNA7 (743); (23) KCNA10 (646); (24) ORAI1 (381); (25) ORAI2 (495); (26) ORAI3 (554); (27) STIM1 (574); (28) STIM2 (535); (29) GAPDH + DNA (568); (30) GAPDH no DNA.

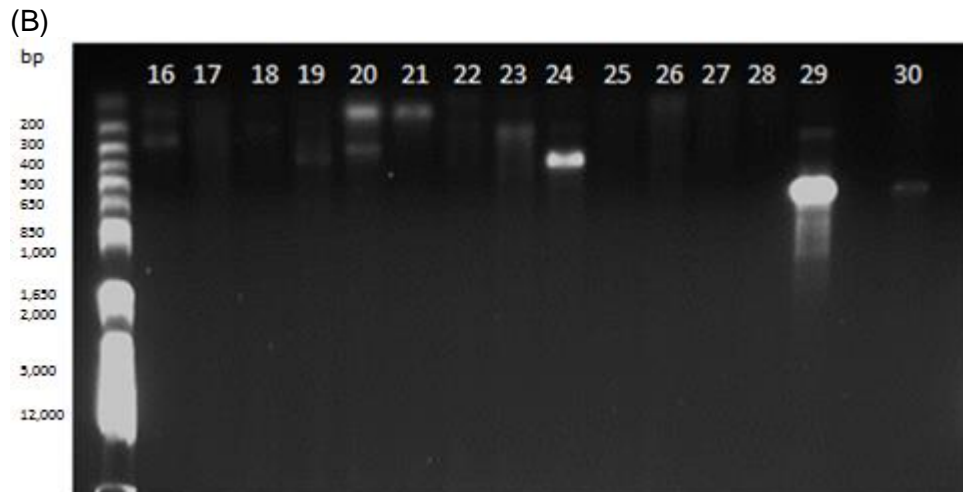


Figure C shows 1kb plus DNA ladder with labelled base pairs (bp) size bands on ladder and PCR products 31–45 and 66-69 with expected size of respective products (bp). Left to right the products are: (31) KCNJ1 var1 (528); (32) KCNJ2 var1 (433); (33) KCNJ3 var1 (438); (34) KCNJ4 var1 (597); (35) KCNJ5 (543); (36) KCNJ12 (521); (37) KCNJ13 var1 (424); (38) KCNA7 var1 (546); (39) ORAI2 var1 (565); (40) ORAI2 var2 (565); (41) ORAI3 (524); (42) STIM1 var1 (470); (43) STIM1 var2 (498); (44) STIM2 var1 (548); (45) STIM2 var2 (493); (66) KCNH1 var1 (450); (67) KCNH2 var1 (570); (68) KCNH2 var2 (591); (69) KCNH5 var1 (458).

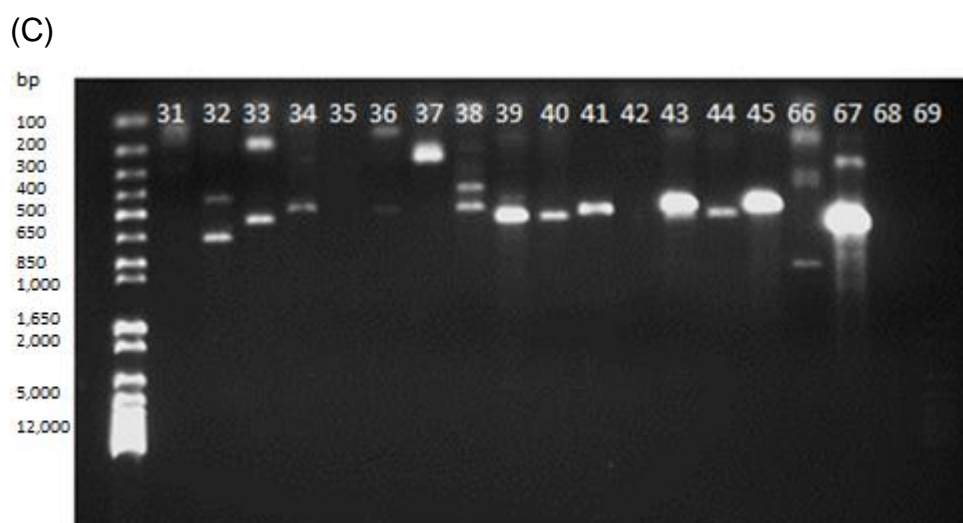
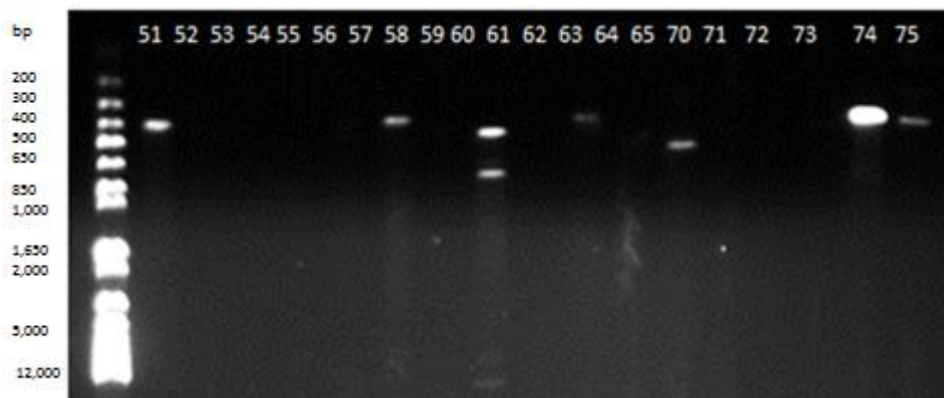


Figure D shows 1kb plus DNA ladder with labelled base pairs (bp) size bands on ladder and PCR products 51–65 and 70-75 with expected size of respective products (bp). Left to right the products are: (51) KCNK1 (409); (52) KCNK2 var1 (485); (53) KCNK3 (527); (54) KCNK4 (417); (55) KCNK5 (593); (56) KCNK6 (402); (57) KCNK 7 var C (594); (58) KCNK9 var1 (488); (59) KCNK10 var1 (404); (60) KCNK12 (417); (61) KCNK13 (531); (62) KCNK15 (593); (63) KCNK16 var1 (419); (64) KCNK17 var1 (524); (65) KCNK 18 (474); (70) KCNMA1 var1 (421); (71) KCNN3 var1 (435); (72) KCNN4 (479); (73) CACNA1C var2 (436); (74) GAPDH + DNA (568); (75) GAPDH no DNA.

(D)



The results of PCR gene expression are summarised in Tables 20 and 21.

Table 20. Gene expression detected in the three cell lines PC3, DU145 and LNCaP, performed in triplicate in 3 cell passages.

* Denotes appropriate band size detected on agarose gel electrophoresis following PCR; + denotes gene confirmed on sequencing.

Gene	Reaction number	Band Size	PC3	DU145	LNCaP
KCNJ1	1	418			
KCNJ2	2	446			
KCNJ3	3	508			
KCNJ4	4	620			
KCNJ5	5	799			
KCNJ6	6	684			
KCNJ8	7	690	* +		
KCNJ9	8	534			
KCNJ10	9	497	* +		
KCNJ11	10	559		* +	
KCNJ12	11	680	*		
KCNJ13	12	592		*	* +
KCNJ14	13	510		*	*
KCNJ15	14	796			
KCNJ16	15	479			
KCNA1 var 1	16	598			
KCNA2	17	579			
KCNA3 var 1	18	556			
KCNA4 var 1	19	640			
KCNA5	20	467			
KCNA6	21	562			* +
KCNA7	22	743			

KCNA10	23	646			
ORAI1	24	381	* +	*	
ORAI2	25	495			
ORAI3	26	554			
STIM1	27	574			
STIM2	28	535			
GAPDH + DNA	29	568	*	*	*
GAPDH no DNA	30				
KCNJ1 var1	31	528			
KCNJ2 var1	32	433	Band not expected size		
KCNJ3 var1	33	438			* +
KCNJ4 var1	34	597	Band not expected size		
KCNJ5	35	543			
KCNJ12	36	521	*		* +
KCNJ13 var1	37	424			*
KCNA7 var1	38	546	Band not expected size		
ORAI2 var1	39	565	*	*	* +
ORAI2 var2	40	565	*	*	
ORAI3	41	524	*	*	*
STIM1 var1	42	470			
STIM1 var2	43	498	*	*	*
STIM2 var1	44	548	*	*	* +
STIM2 var2	45	493	*	*	* +
KCNK1	51	409	*	*	* +
KCNK2 var1 F	52	485		*	
KCNK3	53	527			
KCNK4	54	417			
KCNK5	55	593			
KCNK6	56	402			
KCNK 7 var C	57	594			
KCNK9 var1	58	488			

KCNK10 var1	59	404			
KCNK12	60	417			
KCNK13	61	531	*	*	* +
KCNK15	62	593		*	
KCNK16 var1	63	419			
KCNK17 var1	64	524			
KCNK 18	65	474			* +
KCNH1 var1	66	450			
KCNH2 var1	67	570			
KCNH2 var2	68	591			
KCNH5 var1	69	458			
KCNMA1 var1	70	421	*	*	* +
KCNN3 var1	71	435	*	*	* +
KCNN4	72	479			
CACNA1C var2	73	436			
GAPDH + DNA	74	568	*	*	*
GAPDH no DNA	75				

Table 21. Summary of identified ion channel genes detected in 3 prostate cancer cell lines.

* Denotes predicted band size detected on agarose gel electrophoresis following PCR.

Gene	PC 3	DU 145	LNCaP
KCNJ3 var1			*
KCNJ8	*		
KCNJ10	*		
KCNJ11		*	
KCNJ12	*		
KCNJ12	*		*
KCNJ13		*	*
KCNJ14		*	*
KCNA6			*
KCNA7			*
ORAI1	*	*	
ORAI2 var1	*	*	
ORAI2 var2	*	*	
ORAI3	*	*	*
STIM1 var2	*	*	*
STIM2 var1	*	*	*
STIM2 var2	*	*	*
KCNK1	*	*	*
KCNK13	*	*	*
KCNK15		*	
KCNK 18			*
KCNMA1 var1	*	*	*
KCNN3 var1	*	*	*

4.3.1.2 Validation of the PCR products

A number of ion channel genes were expressed in all 3 cell lines PC3, LNCaP and DU145. A PCR product of the predicted size is only an indication of the presence of the gene of interest in the sample (Bevan et al., 1992). To validate these results, some of the PCR products were sequenced using commercial sequencing facilities. DNA extraction from agarose gel was performed for these genes, and the purified DNA was sequenced by Beckman Coulter Genomics. Finch TV software was used to review the results. The NCBI website (<http://www.ncbi.nlm.nih.gov/>) was used to cross-reference the DNA sequence found against the gene it represented. Table 22 below lists these genes expressed in all 3 cell lines and confirmed on sequencing.

Table 22. Ion channel genes expressed in all 3 cell lines PC3, LNCaP and DU145 and confirmed on sequencing.

Orai1
Orai2 var1
Orai3
STIM1 var2
STIM2 var1
STIM2 var2
KCNK1
KCNK13
KCNMA1 var1
KCNN3 var1

Assessment of gene expression in cells of PC3 colonies holo/meroclones and paraclones would be of interest. However, due to time constraints it was not possible to assess gene expression by colony type.

After PCR and sequencing, I also sought to analyse the expression of selected ion channel proteins to validate the PCR results.

4.3.2 Ion channel protein expression of KCNK-1 and ORAI-3 in PC3 colonies

As detailed in section 4.3.1.1, characterisation of gene expression found a number of ion channels to be expressed in all 3 prostate cancer cell lines. KCNK-1 and ORAI-3 are 2 such genes. Expression of KCNK-1 and ORAI-3 proteins in PC3 colonies was also investigated by immunocytochemistry. In addition to the commercial availability of these antibodies, KCNK1 and ORAI-3 were chosen for further investigation as both genes were expressed in all 3 prostate cancer cell lines PC3, LNCaP and DU 145. KCNK family have been found to be expressed in colorectal cancer (Kim et al., 2004) and have been implicated, indirectly, in the proliferation of ovarian cancer tissue (Innamaa et al., 2013). The ORAI family of genes have been found to be involved with resistance to apoptosis in prostate cancer cell lines apoptosis (Flourakis et al., 2010) and a more aggressive phenotype in breast cancer cell lines (McAndrew et al., 2011).

Optimisation of primary antibodies was performed, as described in the Methods section of Chapter 4. Results are shown in Figures 28 and 29. Negative controls for immunostaining were performed using no primary antibody. Figures 28A and 29A show negative controls demonstrated no staining. Concentration of KNCK-1 primary antibody 1:200 (1 µg/ml) is shown in figure 28B and was selected for further immunocytochemistry as staining could be seen most clearly using this concentration. Similarly, staining for ORAI-3 was visualised most clearly using concentration of Anti-ORAI-3 1:50 (4 µg/ml) as shown in figure 29B.

Figure 28. Immunocytochemistry and optimisation of primary antibody demonstrating expression of KNCK-1 in PC3 cells.

KNCK-1 was detected with a FITC conjugated secondary antibody (green) and counter stained with DAPI (blue) and merge images are presented. (A) Negative control (no primary antibody); (B) Primary antibody concentration 1:200 (1 $\mu\text{g/ml}$); (C) Primary antibody concentration 1:350 (0.57 $\mu\text{g/ml}$). (D) Primary antibody concentration 1:500 (0.4 $\mu\text{g/ml}$); Excitation and emission 495 nm and 525 nm respectively. There is no non-specific staining in the negative control (A). Staining is seen using various primary antibody concentrations as shown with clear staining in all PC3 cells (B). Cells were grown in eight-well chamber slides, fixed, and stained for KNCK-1 using protocols described in section 1.2.2. Z-stacks obtained using an Olympus confocal system are shown. Representative images of at least 10 repeats are shown. Scale bar A-D: 45 μm .

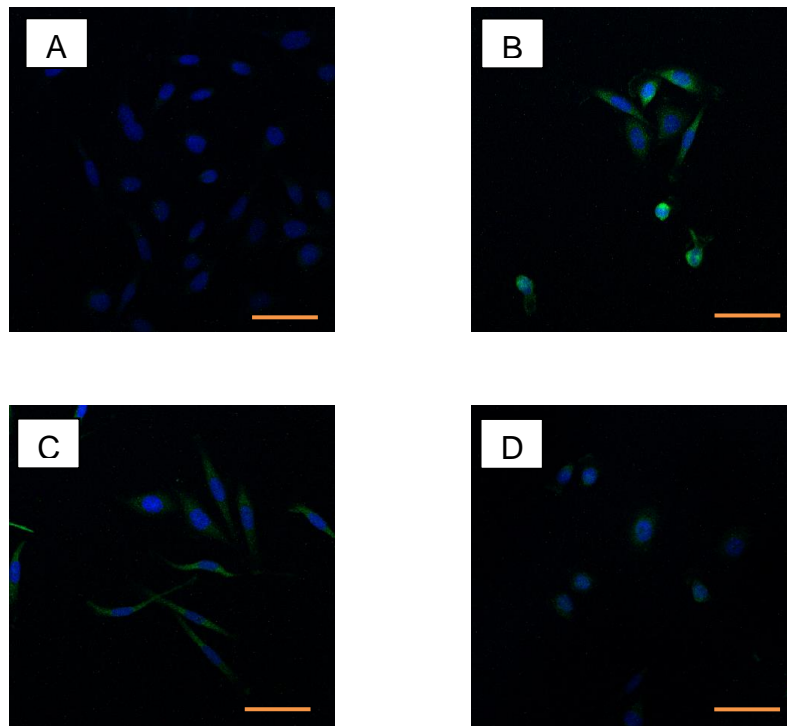
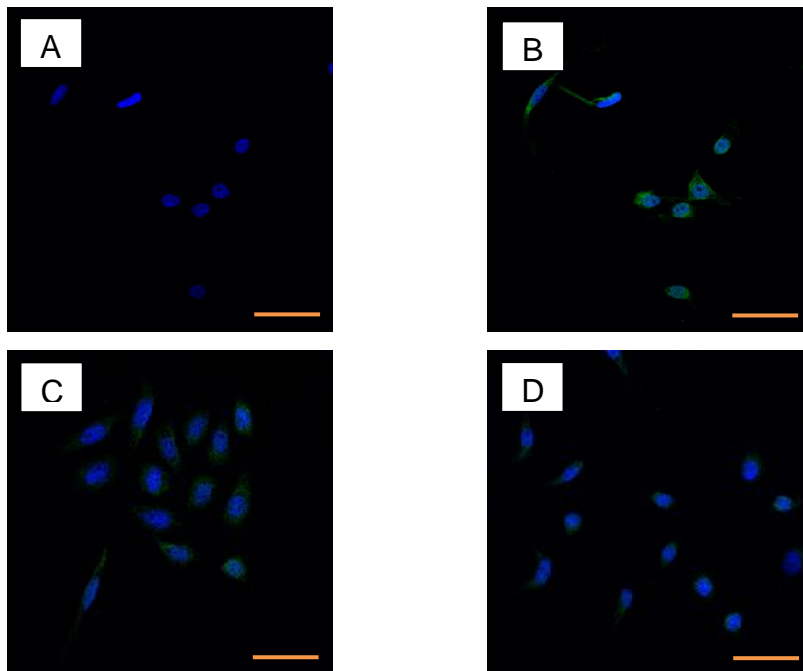


Figure 29. Immunocytochemistry and optimisation of primary antibody demonstrating expression of ORAI-3 in PC3 cells.

ORAI-3 was detected with a FITC conjugated secondary antibody (green) and counter stained with DAPI (blue) and merge images are presented. (A) Negative control; (B) Primary antibody concentration 1:50 (4 µg/ml); (C) Primary antibody concentration 1:100 (2 µg/ml); (D) Primary antibody concentration 1:200 (1 µg/ml). Excitation and emission wavelengths 495 nm and 525 nm respectively. There is no non-specific staining in the negative control (A). Staining is seen using various primary antibody concentrations as shown with clear staining in all PC3 cells (B). Cells were grown in eight-well chamber slides, fixed, and stained for ORAI-3 using protocols described in section 1.2. Z-stacks obtained using an Olympus confocal system are shown. Representative images of at least 10 repeats are shown. Scale bar A-D: 45µm.



Immunostaining for expression of KCNK-1 in PC3 holo/meroclone and paraclone cells was performed. Figures 30 and 31 show a representative holo/meroclone and paraclone respectively. All imaged cells in both colony types express KCNK-1.

Immunostaining for expression of ORAI-3 in PC3 holo/meroclone and paraclone cells was performed. Figure 32 and 33 show a representative holo/meroclone and paraclone respectively. All imaged cells in both colony types express ORAI-3.

Figure 30. Immunocytochemistry showing expression of KCNK-1 (green) in PC3 cells of a holo/meroclone colony.

Primary antibody mouse monoclonal to KCNK-1 concentration 1:200 detected with a flurophore secondary antibody (goat anti-rabbit IgG-FITC 1:500, green) and counter stained with DAPI (blue). A-C show the same whole colony: A shows DAPI staining, B signal observed for flurophore secondary antibody, C shows A+B merge. D,E,F,G,H,I,J,K,L show higher magnification of cells within this colony. D,G,J show DAPI staining, E,H,K show signal observed for flurophore secondary antibody; F,J,L show respective merge images. KCNK-1 is expressed in all cells of holo/meroclones. Cells were grown in eight-well chamber slides, fixed, and stained for KCNK-1 using protocols described in section 1.2.2. Excitation and emission wavelengths 495 nm and 525 nm respectively. Z-stacks obtained using an Olympus confocal system are shown. Representative images of at least 10 repeats are shown. Scale bar A: 180 μm ; B-D: 15 μm .

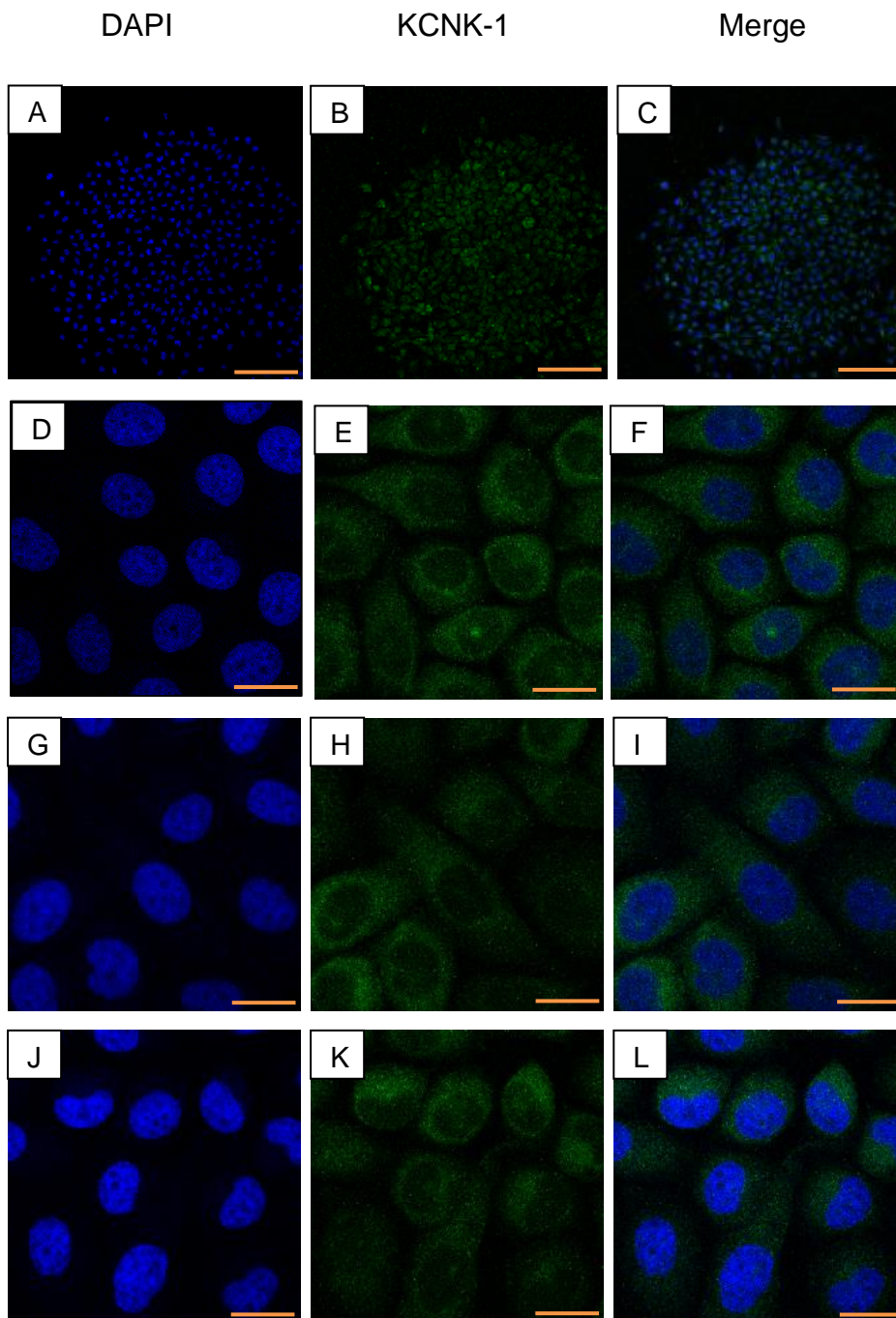


Figure 31. Immunocytochemistry showing expression of KCNK-1 (green) in PC3 cells of a paraclone colony.

Primary antibody mouse monoclonal to KCNK-1 concentration 1:200 detected with a flurophore secondary antibody (goat anti-rabbit IgG-FITC 1:500, green) and counter stained with DAPI (blue). A-C show the same whole colony: A shows DAPI staining, B signal observed for flurophore secondary antibody, C shows A+B merge. D,E,F,G,H,I,J,K,L show higher magnification of cells within this colony. D,G,J show DAPI staining, E,H,K show signal observed for flurophore secondary antibody; F,J,L show respective merge images. KCNK-1 is expressed in all cells of paraclones. Cells were grown in eight-well chamber slides, fixed, and stained for KCNK-1 using protocols described in section 1.2.2. Excitation and emission wavelengths 495 nm and 525 nm respectively. Z-stacks obtained using an Olympus confocal system are shown. Representative images of at least 10 repeats are shown. Scale bar A: 180 μm ; B-D: 15 μm .

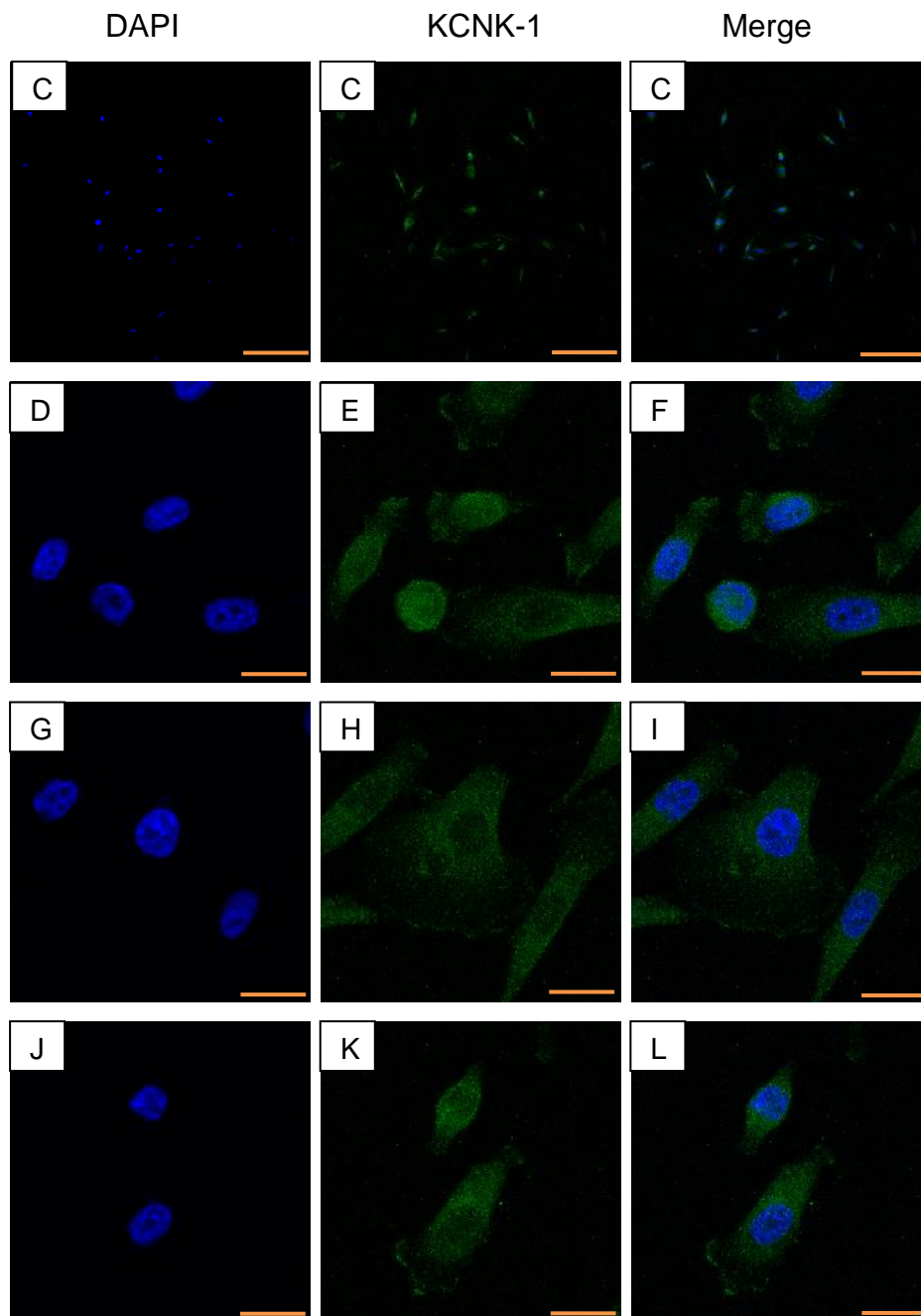


Figure 32. Immunocytochemistry showing expression of ORAI-3 (green) in PC3 cells of a holo/meroclone colony.

Primary antibody mouse monoclonal to ORAI-3 concentration 1:200 detected with a flurophore secondary antibody (goat anti-rabbit IgG-FITC 1:500, green) and counter stained with DAPI (blue). A-C show the same whole colony: A shows DAPI staining, B signal observed for flurophore secondary antibody, C shows A+B merge. D,E,F,G,H,I,J,K,L show higher magnification of cells within this colony. D,G,J show DAPI staining, E,H,K show signal observed for flurophore secondary antibody; F,J,L show respective merge images. ORAI-3 is expressed in all cells of holo/meroclones. Cells were grown in eight-well chamber slides, fixed, and stained for ORAI-3 using protocols described in section 1.2.2. Excitation and emission wavelengths 495 nm and 525 nm respectively. Z-stacks obtained using an Olympus confocal system are shown. Representative images of at least 10 repeats are shown. Scale bar A: 180 μm ; B-D: 15 μm .

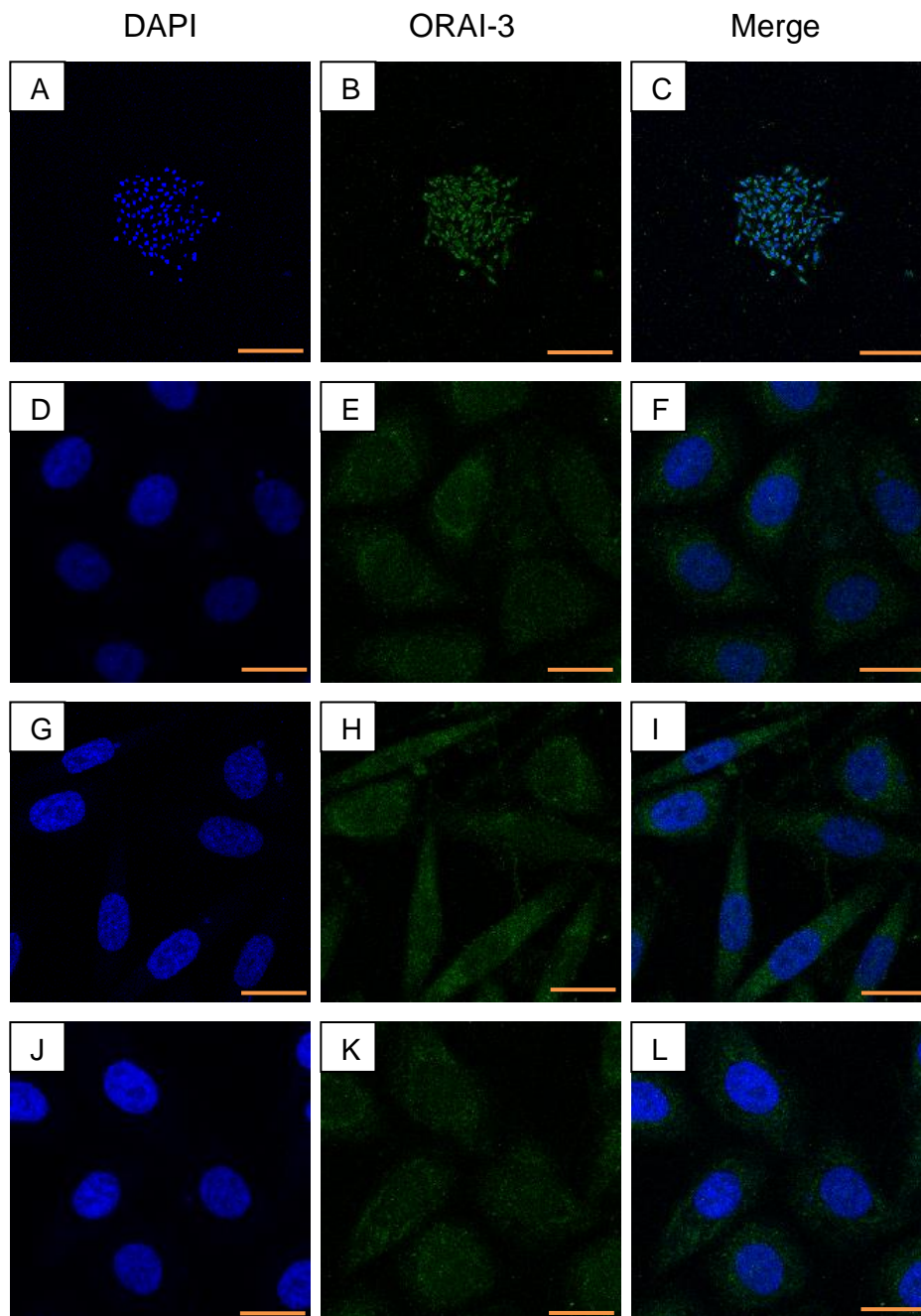
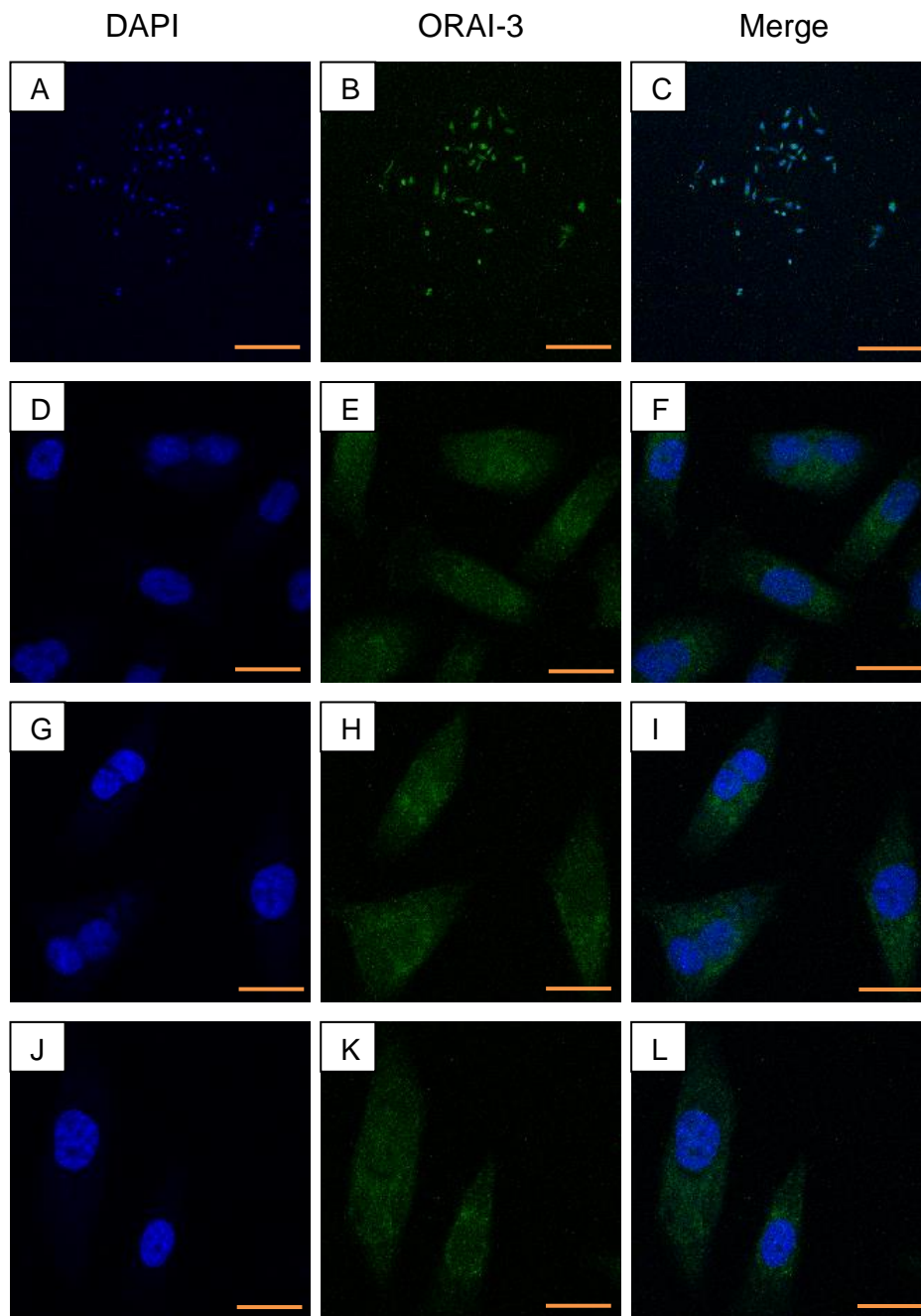


Figure 33. Immunocytochemistry showing expression of ORAI-3 (green) in PC3 cells of a paraclone colony.

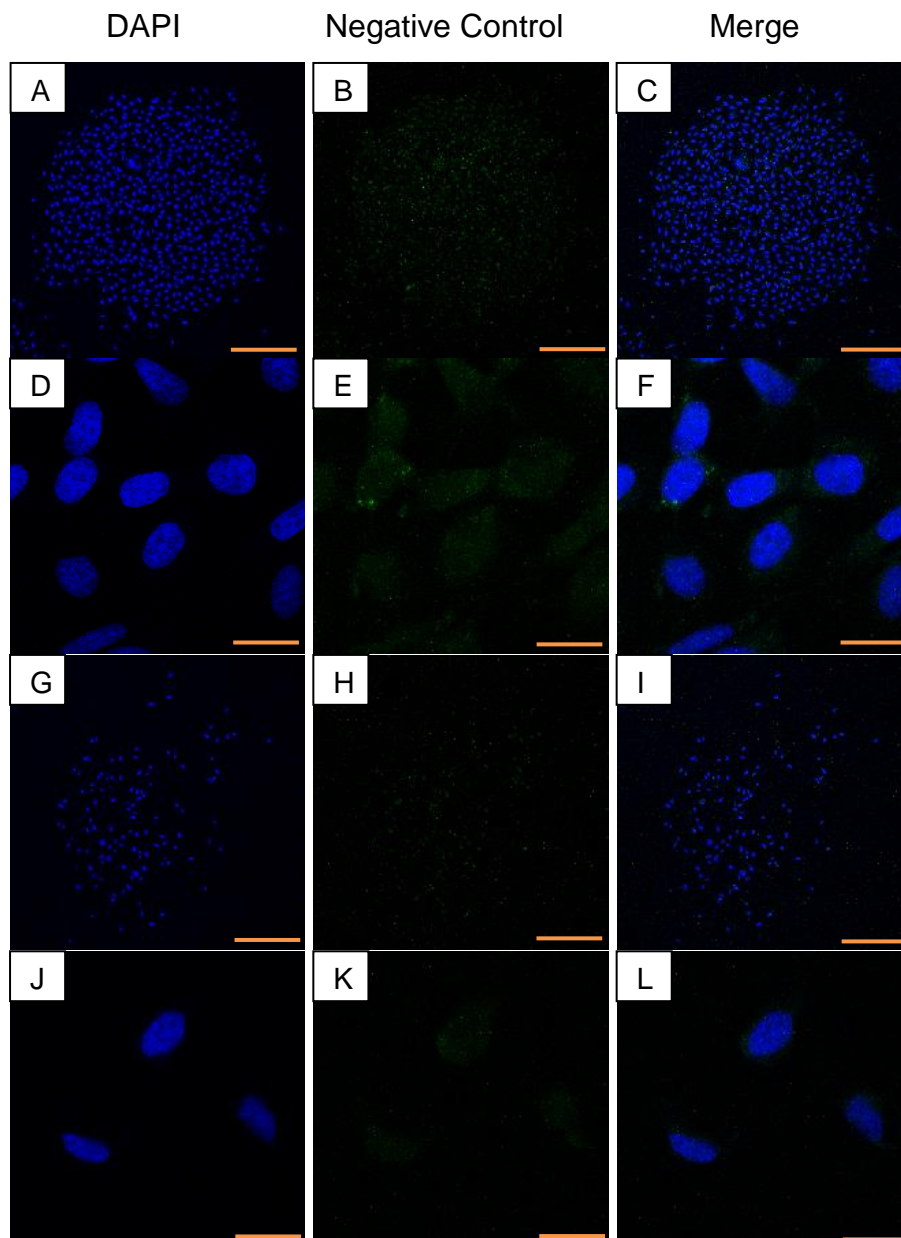
Primary antibody mouse monoclonal to ORAI-3 concentration 1:200 detected with a flurophore secondary antibody (goat anti-rabbit IgG-FITC 1:500, green) and counter stained with DAPI (blue). A-C show the same whole colony: A shows DAPI staining, B signal observed for flurophore secondary antibody, C shows A+B merge. D,E,F,G,H,I,J,K,L show higher magnification of cells within this colony. D,G,J show DAPI staining, E,H,K show signal observed for flurophore secondary antibody; F,J,L show respective merge images. ORAI-3 is expressed in all cells of paraclones. Cells were grown in eight-well chamber slides, fixed, and stained for ORAI-3 using protocols described in section 1.2.2. Excitation and emission wavelengths 495 nm and 525 nm respectively. Z-stacks obtained using an Olympus confocal system are shown. Representative images of at least 10 repeats are shown. Scale bar A: 180 μm ; B-D: 15 μm .



To determine if there was non-specific staining of secondary antibody in PC3 cells, which could be affecting these results, negative control experiments without primary antibody were performed. Figure 34 below shows in the absence of primary antibody there is no non-specific staining in cells of a holo/meroclone (A-F) or cells of a paraclone (G-L) for secondary antibody.

Figure 34. Immunocytochemistry showing negative controls with lack of flurophore secondary antibody signal in absence of primary antibody in a PC3 holo/meroclone and PC3 paraclone.

No significant flurophore secondary antibody signal (goat anti-rabbit IgG-FITC 1:500, green) is seen in absence of primary antibody in PC3 holo/meroclones and PC3 paraclones counter stained with DAPI (blue). A-C show a holo/meroclone colony: A shows DAPI staining, B signal observed for flurophore secondary antibody, C shows A+B merge. D,E,F show higher magnification of cells within this colony for DAPI, flurophore secondary antibody, and merge respectively. There is no non-specific staining in the holo/meroclone negative control without primary antibody. G,H,I show a paraclone colony: G shows DAPI staining, H signal observed for flurophore secondary antibody, I shows A+B merge. J,K,L show higher magnification of cells within this colony for DAPI, flurophore secondary antibody, and merge respectively. There is no non-specific staining in the paraclone negative control without primary antibody. Cells were grown in eight-well chamber slides, fixed, and stained using protocols described in section 3.7.2. Excitation and emission wavelengths 495 nm and 525 nm respectively. Z-stacks obtained using an Olympus confocal system are shown. Representative images of at least 10 repeats are shown. Scale bar A-C, G-I: 180 μm ; D-F, J-L: 15 μm .



4.3.3 Effect of treatment of MPRCs on proliferation of a population of PC3 cells

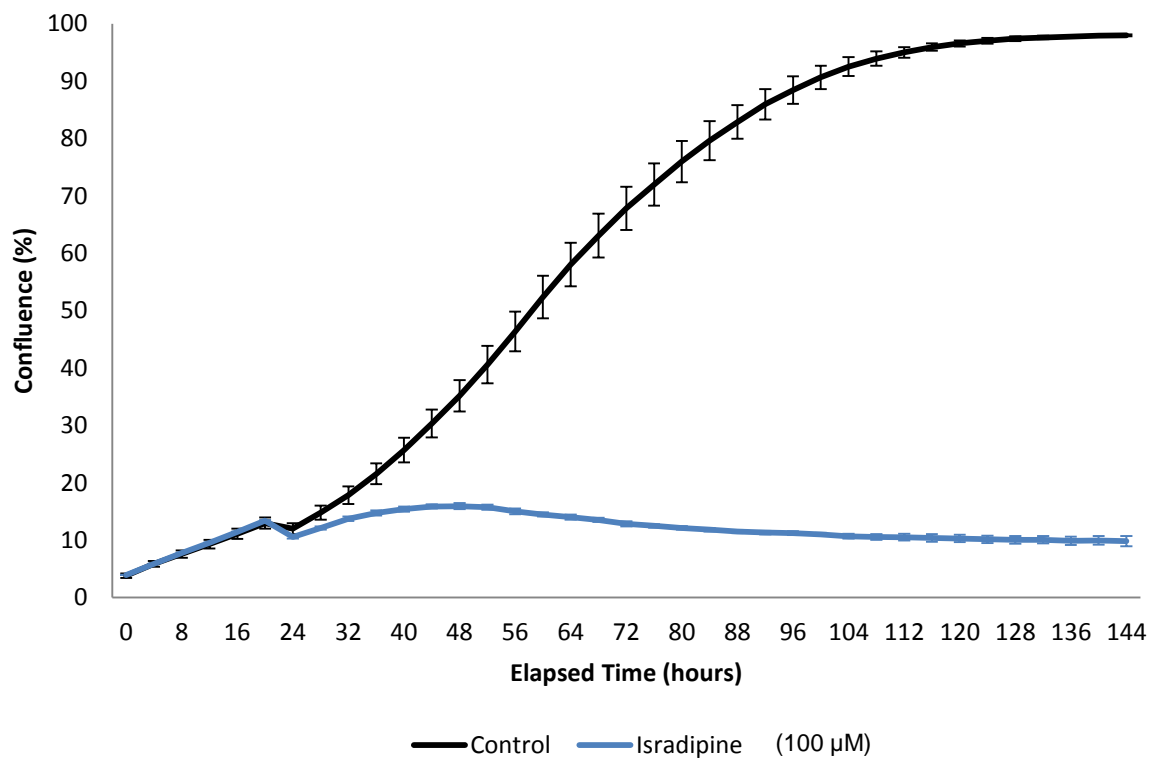
Experiments were performed to test the effect of MPRCs isradipine, amlodipine and cadmium chloride on the proliferation of PC3 cells in a whole population. PC3 cells were plated in 6-well plates, as described in Chapter section 4.2.3. Cell confluence data obtained from Incucyte™ is presented below.

4.3.3.1 Effect of isradipine on proliferation of PC3 cells

Data on cell proliferation in 6-well plates was obtained by imaging using an Incucyte™ live cell imaging system every 4 hours. Imaging was commenced 4 hours after plating and continued for 144 hours (6 days). Control wells were treated with DMSO and experimental wells were treated with isradipine 100µM, 24 hours after plating. A growth curve with and without the drug is shown in Figure 35. Confluence was observed to be similar in the control and experimental wells until 24 hours (Figure 35), after which time the curves diverge as can be seen by the shift in the slope of the growth curve ± drugs (Figure 35). The control arm proliferation continued, whilst confluence in the treated wells failed to increase. At 144 hours, mean confluence in the control well was 97.9% ± 0.1 (n=3) whilst mean confluence in isradipine treated wells was lower at 9.8% ± 0.9 (n=3). Statistical testing using an independent t-test for the confluence at the end of assay (144h), demonstrates percentage of confluence in the wells treated with isradipine was significantly less than that in the control wells (p<0.05).

Figure 35. Graph showing the % confluence against time of population of PC3 cells when treated with isradipine or DMSO control.

The increase in % confluence is arrested following treatment with isradipine (100 μ M). PC3 prostate cancer cells were cultured in T80 flasks, trypsinised, counted and subjected to serial dilution to 50,000 cells/ml. 1 ml of cell solution (50,000 cells) was pipetted into each well of a 6-well plate (Nunc), with 2 ml RPMI. The plates were placed in a 37°C, CO₂ incubator in an IncuCyte™ (Essen Bioscience) live cell imaging system, which acquired images every 4 hours for later analysis of confluence. After 24 hours, the plates were removed, treated with isradipine (control plates received vehicle only), and placed back in IncuCyte™ for further imaging. Experiments were terminated after 144 hours (6 days). Experiments were performed in triplicate.

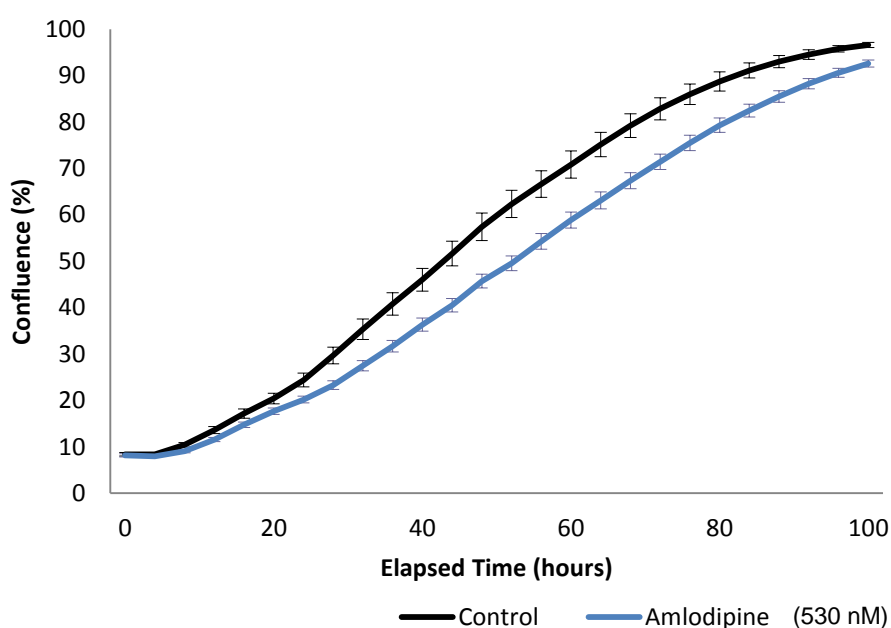


4.3.3.2 Effect of amlodipine on proliferation of PC3 cells

Similarly, the effect of another MPRC, amlodipine on proliferation of a population of PC3 cells was assessed. Figure 36 shows the proliferation in 3 control wells and 3 wells treated with amlodipine 530 nM 24 hours following plating. Proliferation does continue in cells treated with amlodipine 540 nM but is slower than that observed in control cells. At 60 hours, mean confluence in control wells was $70.8\% \pm 2.9$ (n=3) compared with mean confluence $58.9\% \pm 1.7$ (n=3) in amlodipine treated wells ($p < 0.05$). By 100 hours there was still a lower level of confluence in the amlodipine treated wells ($92.6\% \pm 0.7$) (n=3) compared with control wells ($96.6\% \pm 0.5$) (n=3) $p < 0.05$. It should be noted that very low concentration of the drug was used here as part of preliminary, proof of concept experiments.

Figure 36. Graph showing the % confluence against time of population of PC3 cells when treated with amlodipine or DMSO control.

The increase in % confluence is arrested following treatment with amlodipine 530 nM. PC3 prostate cancer cells were cultured in T80 flasks, trypsinised, counted and subjected to serial dilution to 50,000 cells/ml. 1 ml of cell solution (50,000 cells) was pipetted into each well of a 6-well plate (Nunc), with 2 ml RPMI. The plates were placed in a 37°C, CO₂ incubator in an IncuCyte™ (Essen Bioscience) live cell imaging system, which acquired images every 4 hours for later analysis of confluence. After 24 hours, the plates were removed, treated with amlodipine (control plates received vehicle only), and placed back in IncuCyte™ for further imaging. Experiments were terminated after 144 hours (6 days). Experiments were performed in triplicate. Graph showing the confluence % against time of PC3 cells when treated with amlodipine 530 nM or DMSO control. Wells treated with amlodipine have a reduction in % confluence compared with control wells $p < 0.05$.

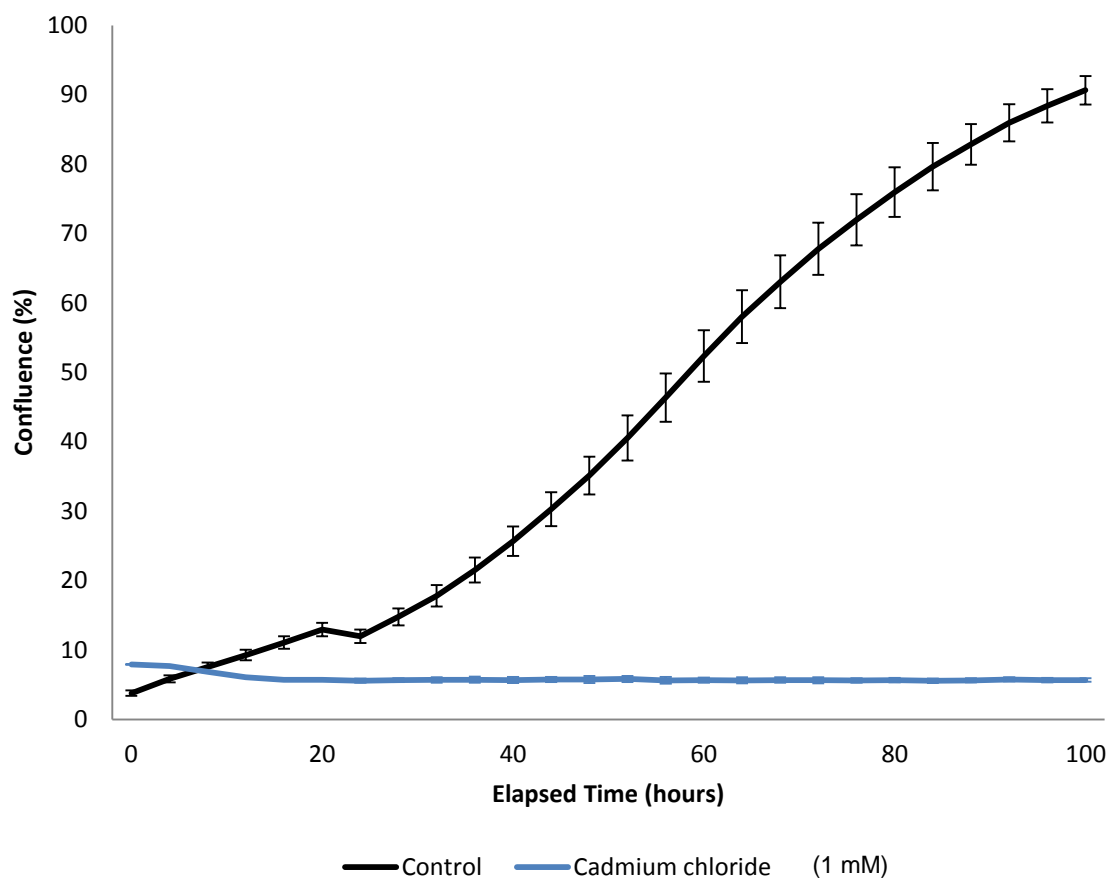


4.3.3.3 Effect of cadmium chloride on proliferation of PC3 cells

The effect on PC3 cell proliferation of cadmium chloride 1 mM was similarly tested using Incucyte™. Figure 37 below shows that treatment of cadmium chloride to wells at 24 hours following plating completely stopped proliferation of PC3 cells. Figure 37 shows the consistent results of 3 experimental repeats. Independent t-test for significance confirmed that at 100 hours following cell plating, there was a significant difference in the confluence reached by control wells (mean 90.6% \pm 2.0 n=3) and those treated with cadmium chloride (mean 5.7% \pm 0.4 n=3), $p < 0.05$.

Figure 37. Graph showing the % confluence against time of PC3 cells when treated with cadmium chloride or DMSO control.

As shown, proliferation of cells is inhibited following treatment with cadmium chloride 1 mM. PC3 prostate cancer cells were cultured in T80 flasks, trypsinised, counted and subjected to serial dilution to 50,000 cells/ml. 1 ml of cell solution (50,000 cells) was pipetted into each well of a 6-well plate (Nunc), with 2 ml RPMI. The plates were placed in a 37°C, CO₂ incubator in an IncuCyte™ (Essen Bioscience) live cell imaging system, which acquired images every 4 hours for later analysis of confluence. After 24 hours, the plates were removed, treated with cadmium chloride 1mM (control plates received vehicle only), and placed back in IncuCyte™ for further imaging. Experiments were terminated after 144 hours (6 days). Experiments were performed in triplicate. Graph showing the confluence % against time of PC3 cells when treated with cadmium chloride 1 mM or DMSO control. Wells treated with cadmium chloride have a reduction in % confluence compared with control wells $p < 0.05$.

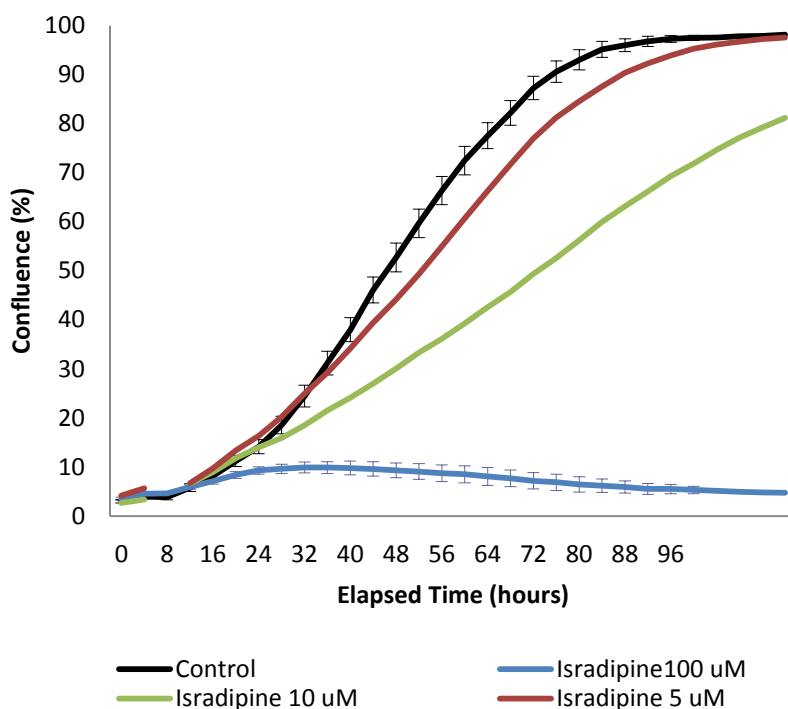


4.3.3.4 Dose–response effect of isradipine on proliferation of PC3 cells

Following these preliminary experiments further investigation of a possible dose-response relationship between MPRC concentration and effect on reduction of proliferation was explored. Dose response experiments were conducted as they are suggestive of a cause and effect relationship between isradipine and reduction in proliferation. Further experiments were therefore performed using isradipine, comparing 3 differing concentrations: isradipine 5 μM , isradipine 10 μM and isradipine 100 μM with DMSO control treated wells. Experiments were performed in triplicate. Figure 38 below shows the effect of isradipine at these 3 concentrations on PC3 cell proliferation. The figure demonstrates that at 100 hours, the % confluence is reduced when wells are treated with either isradipine 5 μM , 10 μM or 100 μM . Following incubation to a longer time to 173 hours, there was no difference in confluence between isradipine 5 μM and control wells' confluence ($p=0.29$) ($n=3$). As observed in the initial experiment, cell proliferation is halted following treatment of isradipine 100 μM at 24 hours. These results show that isradipine inhibits cell proliferation in a concentration dependent manner with an IC_{50} between 10 and 100 μM .

Figure 38. Graph showing the confluence % against time of PC3 cells when treated with isradipine 100 μ M, isradipine 10 μ M and isradipine 5 μ M or DMSO control.

Increasing concentration of isradipine reduced proliferation of PC3 cells.



4.4 Discussion

The aim of the work presented in this chapter was to begin the characterisation of ion channel expression in prostate cancer cell lines and cells of PC3 colonies holo/meroclones and paraclones. As there was significant expression of ion channels in all 3 prostate cancer cell lines investigated and in cells of both colony types, I then also investigated whether the inhibition of expressed channels, by known inhibitors, may affect the proliferation of the PC3 prostate cancer cell line using 3 broad MPRCs isradipine, amlodipine and cadmium chloride.

4.4.1 Expression of ion channel genes

After conducting a review of the published literature as summarised in Chapter section 4.1, ion channel families which have been identified in carcinogenesis and cancer proliferation in other tumour types, were selected for investigation in prostate cancer cell lines. Their expression level in 3 prostate cancer cell lines (PC3, DU145 and LNCaP) was determined. The profile of expression differed between them, though expression of several ion channel proteins was detected in all 3 cell lines. In the cases of PC3 cells expression of KCNJ2 var1 and KCNJ4 var1, bands were seen but not of the sizes expected (500 base pairs with expected size 597, 700 base pairs with expected size 433 respectively). In PC3 expression of KCNA7 var 1, two bands were seen at size 400 and 480 with expected band size of 546. These findings may be due to splice variants. However, I have not reported these genes as being expressed as they were not sent for sequencing confirmation. Gene expression was most diverse in the LNCaP cell line, with 15 out of 65 of the tested genes being expressed in this cell line. Several ion channel genes e.g. ORAI1, ORAI2 var1, ORAI3, STIM1 var2, STIM2 var1, STIM2 var2, KCNK1, KCNK13, KCNMA1 var1 and KCNN3 var1 were expressed in all the 3 cell lines. A limitation of this work was the lack of a positive control for each primer set used. This would have indicated if a gene was not expressed rather than the primer pair developed not functioning.

Although the gene expression is indicative of the presence of mRNA, however, to be functionally relevant the protein must be expressed. Testing the presence of proteins for all the genes expressed in the 3 prostate cell lines was not planned at the start of this research to be within the scope of this project. This scale of analysis could be performed using automated protein expression analysis (Symes, PLOS ONE et al 2013), which was not planned to be undertaken and would have entailed excessive costs. As such, I performed immunocytochemistry protein expression of 2 of these genes *ORAI* and *KCNK* for assessment in holo/meroclones and paraclones types.

Cells within both holo/meroclones and paraclones expressed ion channel proteins *ORAI* and *KCNK*.

4.4.2 Effect of MPRCs on cell proliferation

Ion channel genes were widely expressed in all the 3 prostate cancer cell lines investigated, and in cells of holo/meroclonal and paraclonal PC3 colonies. Further investigation was undertaken to determine whether the inhibitors of ion channel functions may affect cell proliferation, as proposed for the MPRCs in the patent by Ahmed et al (Ahmed et al., 2016) and as shown previously *in vitro* studies in other prostate, melanoma, glioblastoma and ovarian cancer cell lines, the latter in a dose dependent manner (Flourakis et al., 2010; Innamaa et al., 2013; Leanza et al., 2012; Staudacher et al., 2014). Rather than specific MPRCs, broad-channel blockers, and known regulators of the cell membrane potential were used that are frequently used in clinical practice were chosen for this preliminary investigation. Concentrations of drugs used were physiological. These were calculated from clinical dose concentration data from British National Formulary for the volume of the solutions used. Experiments were performed with whole cell populations rather than stem cell colonies. Due to time constraints it was not possible to perform experiments in stem cell-like cells in this study. However, more recent experiments however have shown that some of the MPRCs do inhibit putative prostate stem-like cells from cell lines (personal communications; experiments in Ahmed laboratory).

PC3 prostate cancer cells were treated with the MPRCs isradipine, amlodipine, cadmium chloride, nicorandil. IncuCyte™ imaging of cells was performed from plating to confluence. The compounds isradipine, amlodipine and cadmium chloride were found to cause a reduction in the proliferation of cells and the percentage of confluence.

A possible dose–response effect on proliferation was briefly explored with isradipine. The results suggested that treatment with increasing concentration of isradipine was associated with further reduction in the extent of cell proliferation.

4.5 Chapter 4 Conclusions

This chapter investigated the expression of several families of ion channel genes in 3 prostate cancer cell lines and foundational work was performed that can be carried on in other projects in the laboratory. With reference to the literature, ion channels thought to be potentially expressed and important in prostate cancer were identified. This study provides a relatively comprehensive characterisation of ion channel gene expression in 3 prostate cancer cell lines for the first time. This work is not only relevant for the purposes of the stated objectives of this thesis, but also generally for the investigations of the fundamental role the ion channels play in physiology. This study demonstrates that these genes are expressed in all the 3 cell lines tested: PC3, DU145 and LNCaP. However, the profile of expression differs between the cell lines. Such analyses could be useful for researchers interested in specific ion channel function in prostate and prostate cell lines. This study demonstrates that cells within both holo/meroclones and paraclones of PC3 colonies expressed ion channel proteins ORAI and KCNK.

Given these findings, investigation was undertaken to determine whether the inhibition of ion channel signalling may affect cell proliferation, albeit in whole populations. The exploratory experiments performed in this study found that treatment of PC3 cells with broad MPRCs was associated with a reduction in cell proliferation. Whether this is directly related to the inhibition of Wnt signalling could be explored further. Evidence from the laboratory experiments conducted independently of this project in the host laboratory indicates that this may indeed be the case.

With regards to the published literature of ion channel and cancer, a range of mechanisms have been identified in various tumour types as summarised in Table 13 (section 4.1). On review of the literature, several studies have investigated the effect of MPRCs on cancer cell proliferation or apoptosis *in vitro*.

TREK-1 and TREK-2 are potassium channels, subtype family K, expressed in ovarian cancer cell lines, benign ovarian tissue and the majority of ovarian cancer tissue (Innamaa et al., 2013). *In vitro*, a TREK-1 inhibitor reduced cell proliferation,

in a dose dependent manner, and increased apoptosis (Innamaa et al., 2013). Although the assay used differed to my experiments, the results are consistent with the effects of broad MPRCs isradipine and cadmium chloride found in my study. Innamaa et al proposed further work to investigate the therapeutic potential of TREK-1 blockers is warranted (Innamaa et al., 2013).

Breast cancer cell lines from brain metastases have a higher expression of ion channel KCa1.1(KCNMA1), a pore forming α -subunit of BK_{Ca} channels (large conductance calcium-activated potassium channels), than those cell lines from other metastatic sites (Khaitan et al., 2009). Increased BK_{Ca} channel activity leads to greater invasiveness and migration. The BK_{Ca} channel may be a key target of downstream Wnt signalling as Wnts induce free $[Ca^{2+}]_i$ release in prostate cells (Thrasivoulou et al., 2013) which acts as an activator of these ion channels. Iberiotoxin is an ion channel inhibitor of large-conductance calcium-activated potassium channels. Cell migration was reduced in breast cancer cell lines MCF-7, MDA-MB-231 and MDA-MB-361 by blocking *KCNMA1* by either treatment of cells with siRNA that targeted the *KCNMA1* gene or by treatment of cells with iberiotoxin (Khaitan et al., 2009).

A further study with results consistent with my work was based upon inhibition of Human ether-a-go-go-related gene K⁺ channel hERG / Kv11.1 in human embryonic kidney cells and glioblastoma cell lines (Staudacher et al., 2014). hERG is inhibited by doxazosin (Staudacher et al., 2014). Doxazosin induced apoptosis in 2 human glioblastoma cell lines and knockdown hERG via si RNA also reduced cell viability of a glioblastoma cell line (Staudacher et al., 2014).

Further work in gliomas using the National Cancer Institute reported that KCa 3.1 was upregulated in 32% of patient cancers and KCa 3.1 expression was associated with reduction in survival (Turner et al., 2014). Work in glioma cell lines and a glioma mouse model found cell lines with high KCa 3.1 expression had reduced migration upon treatment with a channel inhibitor. Cell lines with low KCa3.1 expression demonstrated no change in migration following inhibition. Loss of KCa 3.1 function also inhibited invasion. Further to this, tumour invasion was reduced when KCa 3.1 was inhibited in SCID mice (Turner et al., 2014).

In a mouse medulloblastoma model, there was found to be increased mRNA of Eag 2 (Potassium channel, voltage gated eag related subfamily H, member 5.) and low levels of Eag 1 in tumour compared with normal cerebellum (Huang et al., 2012). Eag 2 expression was elevated in the majority of both primary and recurrent human tumours, compared with control tissue (Huang et al., 2012). Eag2 knockdown reduced growth of medulloblastoma and tumourigenicity in a mouse model (Huang et al., 2012).

Inhibition of the Kv 1.3 Potassium channel, voltage gated shaker related subfamily A, member 3 in a human osteosarcoma cell line and mouse melanoma cell line has investigated using Kv 1.3 inhibitors psora-4, PAP-1 and clofazimine (Leanza et al., 2012). These inhibitors induced apoptosis in mouse melanoma cell line B16F10 and human sarcoma cell line SAOS-2, both of which were demonstrated to express Kv 1.3. Downregulation of Kv1.3 via siRNA removed the inhibitors' effects (Leanza et al., 2012). Further to this, in an orthotopic melanoma B16F10 mouse model, clofazimine administered intraperitoneally markedly reduced tumour size when animals were sacrificed at day 16. Examination of the internal organs of the mice demonstrated no obvious other pathology on comparison to non-treated mice (Leanza et al., 2012).

Chapter 5: Discussion and conclusions

5.1 Summary of findings

- Colonies formed from single PC3 cells can be classified into 2 different classes - holo/meroclones and paraclones - by their morphological appearances unlike 3 distinct colony types reported previously.
- Colonies formed from single PC3 cells can also be classified into holo/meroclones and paraclones by objective characteristics such as cell density.
- Colonies of both types respond to 2 classes of Wnt ligands - Wnt 5A and 9B - with an intracellular calcium response.
- Calcium response is likely to be a key mediator of Wnt signalling in both colony types and in response to both Wnt 5A and Wnt 9B.
- There are differences in Wnt induced increase in $[Ca^{2+}]_i$ between the 2 colony types. In particular, a greater proportion of cells in holo/meroclones respond to Wnts 5A and 9B, a greater proportion demonstrate a secondary elevation in $[Ca^{2+}]_i$, and there is a shorter rise time compared to cells in paraclones. These differences between holo/meroclones and paraclones are possibly attributable to cells in the former being more *stem cell like*.
- β -catenin is expressed in cells of both colony types with and without Wnt activation.
- β -catenin translocation appears to occur in response to Wnt 5A and Wnt 9B activation in cells of both holo/meroclones and paraclones.

- In the literature, ion channels have been shown to be expressed in a range of solid cancers and inhibition of such channels have reduced cell proliferation in ovarian cancer, glioblastoma, osteosarcoma and melanoma cell lines.
- Prostate cancer cell lines express a number of ion channels genes from a range of families. Investigated ion channels proteins are expressed in cells of both PC3 holo/meroclones and PC3 paraclones.
- MPRCs tested reduce proliferation of PC3 cells. Isradipine suppresses whole cell population growth, drastically.
- Further investigation of the effects of MPRCs on cell proliferation in cells of holo/meroclones and cells of paraclones is of interest.
- If MPRCs can inhibit the proliferation of holo/meroclones or a subpopulation of cells driving a cancer *in vivo*, this mechanism could lead to novel therapies using ion channel inhibition as strategy to treat prostate cancer.

5.2 Wnt signalling in PC3 colonies

As discussed in Chapter 1.6, Wnt signalling plays a key role in the self-renewal of stem cells and in the human body, the crypts of the small intestine provide an example of this maintenance of stem cells and production of differentiated cell types (Barker et al., 2012; Potten and Loeffler, 1990). Dysregulated Wnt signalling occurs in cancer, most notably in colorectal cancer (Kinzler et al., 1991; Nishisho et al., 1991).

Cells plated at clonal density are reported to form colonies (Barrandon and Green, 1987), and cells of holoclones possess cancer stem cell-like characteristics (Li et al., 2008; Pfeiffer and Schalken, 2010; Zhang and Waxman, 2010), including the ability to induce tumour in a xenograft model (Li et al., 2008; Locke et al., 2005; Pfeiffer and Schalken, 2010).

Unlike 3 distinct colony types reported previously (Li et al., 2008), my study found that PC3 cells form 2 colony types, namely holo/meroclones and paraclones. However, the colonies reported by Li et al were only morphologically described and not objectively characterised to be distinct, as shown in this work. My study investigated Wnt signalling in holo/meroclones and paraclones in PC3 cells. My research found both holo/meroclones and paraclones express β -catenin. This differs from the findings of Li et al showing that paraclones lack the expression of β -catenin. However, in my work, the colonies were fixed and stained at an earlier time point as compared to that reported by Li et al (2 weeks); this may explain the difference observed. In my study, β -catenin was expressed in both colony types after treatment with Wnt 5A and Wnt 9B. These findings indicate that the Wnt pathway involving β -catenin is active in both colony types and that β -catenin Wnt signalling is active after treatment with both Wnt 9B and Wnt 5A.

There are no published studies investigating a calcium response in Wnt signalling in different colony types in any cell line. Cells within holo/meroclones demonstrate an increase in $[Ca^{2+}]_i$ on exposure to both Wnt5A and Wnt 9B. All cells analysed demonstrated such a response. These findings are consistent with my initial hypothesis that cells of holo/meroclones being more stem cell-like would be more responsive to Wnt ligand stimulation, demonstrated by an $[Ca^{2+}]_i$ response. Cells of holo/meroclones may have more receptors able to interact and be activated by ligand exposure, or may have more significant downstream signalling by Wnt mediators. Cells of paraclones also demonstrate a calcium response to Wnt5A and Wnt 9B but a proportion of cells do not. Cells within paraclones may be more heterogeneous in their response to Wnt 5A and 9B.

Cells of paraclones may be more heterogeneous in their expression of Wnt signalling target genes. The expression of Wnt target genes in cells of holo/meroclones and cells of paraclones, and any differential expression between cells was not investigated in this study. As this study has shown that cells of both holo/meroclones and cells of paraclones respond to Wnt signalling, an analysis of Wnt target genes in different colony types would be of interest.

5.3 Ion channels and cancer

Over the past decade there has been interest in expression of ion channel genes in cancer, their relevance in malignancy and potential effects of their manipulation in clinical practice. The expression of ion channel families has been studied in a number of solid cancers, including breast cancer, melanoma, cervical cancer, ovarian cancer and astrocytoma.

As discussed in Chapter 4.4.3, several *in vitro* studies using cancer cell lines have demonstrated that specific inhibition of ion channels TREK-1 and TREK-2, K⁺ channel hERG and Kv 1.3 Potassium channel resulted in reduced cell proliferation (Innamaa et al., 2013),(Staudacher et al., 2014) (Leanza et al., 2012). Little *in vivo* work has been performed investigating the effect of MPRCs on cancer cell proliferation. One study utilised an orthotopic melanoma B16F10 mouse model, to test clofazimine administered intraperitoneally (Leanza et al., 2012). Clofazimine markedly reduced tumour size when animals were sacrificed at day 16. Examination of the internal organs of the mice demonstrated no obvious other pathology compared to control non-treated mice (Leanza et al., 2012).

5.4 Ion channels in prostate cancer cell lines and cancer stem cells

The expression of a number of ion channel families has been investigated and characterised in this study. Expression of ion channels in cells of different colony types - PC3 holo/meroclones and paraclones has been demonstrated.

This work adds to the literature on the limited body of work on ion channel signalling in prostate cancer. One study has investigated whether PC3 cells have a differing physiological profile of potassium channel as compared to LNCaP cells. Patch clamp

testing with characterisation of effects of external calcium levels and compounds was performed on PC3 and LNCaP cell lines. Different profiles were observed with LNCaP cells demonstrating greater voltage-gated potassium current density. Unlike LNCaP cells, a proportion of potassium channels in PC3 cells were Ca^{2+} -sensitive and, therefore, more excitable (Laniado et al., 2001). A subsequent study further investigated the expression of a subunit of voltage-gated Na^{+} channels thought to be important in prostate cancer metastases. When PC3 and LNCaP cell lines were tested for expression of the subunits by PCR, expression was found to be greater in the former than in the less aggressive LNCaP cell line (Diss et al., 2001).

In my study, some variation was noted in the ion channel genes expressed in the 3 cell lines tested. In contrast to the findings of Diss et al, the results of this study showed that the LNCaP cell line expressed the greatest number of the ion channel genes tested. The selection of families tested in this study was based upon a literature review of the classes of ion channels that have been detected in other cancer solid types and those that have been found to have functional significance, for example, with regard to the prognosis or associated with inhibition of proliferation *in vitro*.

The discovery that Wnt signalling is electrogenic and could be inhibited by MPRCs is a new discovery (Ahmed et al., 2016). Since the termination of this project a clear link between ion channels and Wnt signalling has been established (Ahmed, A personal communication). In that context the characterisation of multiple ion channel genes could be very helpful in progressing this emerging field. This would be of particular importance if this work is further explored in prostate cancer stem cells.

There is limited published work on ion channels in cancer stem-like cells. This project investigated the expression of ion channel genes in PC3 colonies. Cells of colonies described to be more cancer stem cell-like (holo/meroclones) expressed ion channel proteins as did cells of paraclones. A clear difference in expression was not demonstrated in cells of different colonies. Conversely, a study on glioblastoma cells found that a differential pattern in ion channel gene expression exists in cells which are more cancer stem cell-like. Benign neural and glial tissue does not express the ion channel KCa3.1 , whilst the glioblastoma cell line U87MG does. In addition, levels

of KCa3.1 mRNA and protein are increased in a stem cell-like sub-population of U87MG cells, as compared to the parent population (Ruggieri et al., 2012).

The findings of this study suggest that ion channels may play an important role in signalling in prostate cancer cell lines in cells of both holo/meroclones and cells of paraclones. Ion channel signalling may be important in prostate cancer and its inhibition may provide a mechanism via which proliferation of prostate cancer cells may be reduced. There has been limited data on ion channel inhibition in prostate cancer. One study investigating the expression of voltage-gated potassium channels detected the expression of Kv1.3 on immunostaining of all prostate cancer and benign specimens tested. This study demonstrated that the potassium channel agonists minoxidil, 1-ethyl-2-benzimidazolinone (EBIO) and diazoxide increased PC3 cell proliferation. Conversely, treatment with potassium channel-blockers dequalinium, amiodarone and glibenclamide, resulted in reduced proliferation and apoptosis of PC3 cells (Abdul and Hoosein, 2002).

5.5 MPRCs as a therapy

If effective in reducing proliferation of populations of cancer cells, the potential lack of toxicity of MPRCs makes them an attractive therapeutic strategy compared to conventional cancer treatments such as chemotherapy which have many side effects. Ion channel blockers are a class of compounds in widespread clinical use. The expression of ion channel families has been studied in a number of solid cancers, including breast cancer, melanoma, cervical cancer, ovarian cancer and glioma. Several studies have demonstrated cell proliferation can be reduced *in vitro* by the inhibition of ion channels found to be active or over-expressed in that particular cancer. Examples include inhibition of TREK-1 inhibitor in an ovarian cancer cell line (Innamaa et al., 2013); inhibition of *KCNMA1* in breast cancer cell lines by either treatment of cells with siRNA that targeted the *KCNMA1* gene or by treatment of cells with iberiotoxin (Khaitan et al., 2009); inhibition of Human ether-a-go-go-related gene K⁺ channel hERG / Kv11.1 in glioblastoma cell lines using either doxazocin or via si RNA also reduced cell viability of a glioblastoma cell line (Staudacher et al., 2014); inhibition of KCa3.1 in glioma cell lines (Turner et al., 2014); inhibition of Eag2 in medulloblastoma (Huang et al., 2012); inhibition of Kv 1.3 in a human osteosarcoma cell line and mouse melanoma cell line (Leanza et al., 2012).

5.6 Further research

In this study I have shown effects on $[Ca^{2+}]_i$ on Wnt signalling in PCR colonies and MPRC inhibition of cell proliferation. There are several strands of interest in further investigating the possible differential response of cells in holo/meroclones and cells of paraclones to Wnts and in particular, in investigation of the effects of MPRCs on Wnt signalling directly in colonies.

Cells of paraclones may be more heterogeneous in their expression of Wnt signalling target genes. The expression of Wnt target genes in cells of holo/meroclones and cells of paraclones, and any differential expression were not investigated in this study. As this study has shown that cells of both holo/meroclones and cells of paraclones respond to Wnt signalling, an analysis of Wnt target genes in different colony types would be of interest.

Further work may involve investigating the effect of Wnt signalling in cells of colonies treated with MPRCs. Any differences in $[Ca^{2+}]_i$ response, or Wnt target gene expression between cells of different colony types could be investigated. One would hypothesise that treatment with MPRCs would inhibit the $[Ca^{2+}]_i$ response seen in this study observed when cells within colonies were treated with Wnt 5A and Wnt 9B. Inhibition of Wnt signalling by MPRCs may suppress Wnt target gene expression. Such work would strengthen the proposed relationship between Wnt signalling, $[Ca^{2+}]_i$ response and inhibition of cell proliferation by MPRCs proposed in this study.

Initial, exploratory experiments performed in this study found MPRCs currently used in clinical practice reduced the proliferation of PC3 cells. Further research on the specific and any differential effects of MPRCs on cells of holo/meroclones and cells of paraclones, and effects on proliferation is of interest. It is possible that a profile of ion channel expression in cells of holo/meroclones is associated with malignant proliferation, invasion and metastases, and it may be possible to target this profile of channels with specific inhibitors. These concepts and profiling require further investigations both *in vitro* and *in vivo*. MPRCs may provide a targeted, relatively well-tolerated therapy for men with prostate or other cancers. MPRCs with a relatively low toxicity profile compared with chemotherapy would therefore be attractive for further study.

5.7 Conclusions

Although significant advances have been made in the management of prostate cancer over the past decade, there is a lack of targeted therapies. There is a particular need to improve treatments for use in advanced, castrate-resistant disease. The effects on the PC3 castrate resistant cell line are highly important since novel treatment strategies are required for this population of men who currently have limited treatment options available to them.

In this study, PC3 colonies were characterised into 2 types: holo/meroclones and paraclones. I also show, for the first time, that Wnt signalling is active in both colony types was observed in response to 2 Wnts ligands: 5A and 9B.

Ion channel signalling may be regulator of the Wnt pathway and several other cellular processes. It is known that Wnt signalling is important in prostate cancer. The body of work to date suggests that ion channels are expressed in various cancers, but there is little in the literature regarding prostate cancer. This study, for the first time, characterises the expression of ion channels in 3 prostate cancer cell lines and ORAI3 and KCNK protein expression in cells of both holo/meroclones and paraclones. Inhibition of ion channels with a selection of MPRCs resulted in reduced PC3 cell proliferation. Targeting a profile of ion channels may provide a mechanism against prostate cancer cell proliferation. This may lead to the development of a new, novel therapy with limited toxicity for the treatment of prostate and other cancers.

References

- Ahmed, A., Thrasivoulou, C., and Masters, J. (2016). Beta-catenin Google Patents (Google Patents).
- Akaboshi, S.-i., Watanabe, S., Hino, Y., Sekita, Y., Xi, Y., Araki, K., Yamamura, K.-i., Oshima, M., Ito, T., Baba, H., *et al.* (2009). HMGA1 Is Induced by Wnt/ β -Catenin Pathway and Maintains Cell Proliferation in Gastric Cancer. *The American Journal of Pathology* 175, 1675-1685.
- Arya, M., Thrasivoulou, C., Henrique, R., Millar, M., Hamblin, R., Davda, R., Aare, K., Masters, J.R., Thomson, C., Muneer, A., *et al.* (2015). Targets of Wnt/ss-catenin transcription in penile carcinoma. *PLoS One* 10, e0124395.
- Bading, H. (2013). Nuclear calcium signalling in the regulation of brain function. *Nat Rev Neurosci* 14, 593-608.
- Bafico, A., Liu, G., Goldin, L., Harris, V., and Aaronson, S.A. (2004). An autocrine mechanism for constitutive Wnt pathway activation in human cancer cells. *Cancer Cell* 6, 497-506.
- Balciunaite, G., Keller, M.P., Balciunaite, E., Piali, L., Zuklys, S., Mathieu, Y.D., Gill, J., Boyd, R., Sussman, D.J., and Hollander, G.A. (2002). Wnt glycoproteins regulate the expression of FoxN1, the gene defective in nude mice. *Nat Immunol* 3, 1102-1108.
- Barker, N., van Es, J.H., Kuipers, J., Kujala, P., van den Born, M., Cozijnsen, M., Haegebarth, A., Korving, J., Begthel, H., Peters, P.J., *et al.* (2007). Identification of stem cells in small intestine and colon by marker gene Lgr5. *Nature* 449, 1003-1007.
- Barker, N., van Oudenaarden, A., and Clevers, H. (2012). Identifying the Stem Cell of the Intestinal Crypt: Strategies and Pitfalls. *Cell Stem Cell* 11, 452-460.
- Barranton, Y., and Green, H. (1987). Three clonal types of keratinocyte with different capacities for multiplication. *Proceedings of the National Academy of Sciences of the United States of America* 84, 2302-2306.
- Batlle, E., Henderson, J.T., Beghtel, H., van den Born, M.M., Sancho, E., Huls, G., Meeldijk, J., Robertson, J., van de Wetering, M., Pawson, T., *et al.* (2002). Beta-catenin and TCF mediate cell positioning in the intestinal epithelium by controlling the expression of EphB/ephrinB. *Cell* 111, 251-263.
- Beaver, C.M., Ahmed, A., and Masters, J.R. (2014). Clonogenicity: holoclones and meroclones contain stem cells. *PLoS One* 9.

- Beer, T.M., Armstrong, A.J., Rathkopf, D.E., Loriot, Y., Sternberg, C.N., Higano, C.S., Iversen, P., Bhattacharya, S., Carles, J., Chowdhury, S., *et al.* (2014). Enzalutamide in metastatic prostate cancer before chemotherapy. *N Engl J Med* 371, 424-433.
- Behrens, J., von Kries, J.P., Kuhl, M., Bruhn, L., Wedlich, D., Grosschedl, R., and Birchmeier, W. (1996). Functional interaction of beta-catenin with the transcription factor LEF-1. *Nature* 382, 638-642.
- Bevan, I.S., Rapley, R., and Walker, M.R. (1992). Sequencing of PCR-amplified DNA. *PCR Methods Appl* 1, 222-228.
- Bhanot, P., Brink, M., Samos, C.H., Hsieh, J.C., Wang, Y., Macke, J.P., Andrew, D., Nathans, J., and Nusse, R. (1996). A new member of the frizzled family from *Drosophila* functions as a Wingless receptor. *Nature* 382, 225-230.
- Blache, P., van de Wetering, M., Duluc, I., Domon, C., Berta, P., Freund, J.N., Clevers, H., and Jay, P. (2004). SOX9 is an intestine crypt transcription factor, is regulated by the Wnt pathway, and represses the CDX2 and MUC2 genes. *J Cell Biol* 166, 37-47.
- Böhm, J., Sustmann, C., Wilhelm, C., and Kohlhase, J. (2006). SALL4 is directly activated by TCF/LEF in the canonical Wnt signaling pathway. *Biochemical and Biophysical Research Communications* 348, 898-907.
- Boon, E.M.J., van der Neut, R., van de Wetering, M., Clevers, H., and Pals, S.T. (2002). Wnt Signaling Regulates Expression of the Receptor Tyrosine Kinase Met in Colorectal Cancer. *Cancer Research* 62, 5126-5128.
- Boutros, M., Paricio, N., Strutt, D.I., and Mlodzik, M. (1998). Dishevelled Activates JNK and Discriminates between JNK Pathways in Planar Polarity and wingless Signaling. *Cell* 94, 109-118.
- Boyden, L.M., Mao, J., Belsky, J., Mitzner, L., Farhi, A., Mitnick, M.A., Wu, D., Insogna, K., and Lifton, R.P. (2002). High bone density due to a mutation in LDL-receptor-related protein 5. *N Engl J Med* 346, 1513-1521.
- Brabletz, T., Jung, A., Dag, S., Hlubek, F., and Kirchner, T. (1999). beta-catenin regulates the expression of the matrix metalloproteinase-7 in human colorectal cancer. *Am J Pathol* 155, 1033-1038.
- Brantjes, H., Roose, J., van de Wetering, M., and Clevers, H. (2001). All Tcf HMG box transcription factors interact with Groucho-related co-repressors. *Nucleic Acids Research* 29, 1410-1419.
- Burry, R.W. (2000). Specificity controls for immunocytochemical methods. *J Histochem Cytochem* 48, 163-166.

- Chamorro, M.N., Schwartz, D.R., Vonica, A., Brivanlou, A.H., Cho, K.R., and Varmus, H.E. (2005). FGF-20 and DKK1 are transcriptional targets of beta-catenin and FGF-20 is implicated in cancer and development. *EMBO J* 24, 73-84.
- Chen, G., and Courey, A.J. (2000). Groucho/TLE family proteins and transcriptional repression. *Gene* 249, 1-16.
- Christian, J.L., McMahon, J.A., McMahon, A.P., and Moon, R.T. (1991). Xwnt-8, a Xenopus Wnt-1/int-1-related gene responsive to mesoderm-inducing growth factors, may play a role in ventral mesodermal patterning during embryogenesis. *Development* 111, 1045-1055.
- Clarke, M.F., Dick, J.E., Dirks, P.B., Eaves, C.J., Jamieson, C.H., Jones, D.L., Visvader, J., Weissman, I.L., and Wahl, G.M. (2006). Cancer stem cells-- perspectives on current status and future directions: AACR Workshop on cancer stem cells (Cancer Res. 2006 Oct 1;66(19):9339-44. Epub 2006 Sep 21.).
- Clements, W.M., Wang, J., Sarnaik, A., Kim, O.J., MacDonald, J., Fenoglio-Preiser, C., Groden, J., and Lowy, A.M. (2002). beta-Catenin mutation is a frequent cause of Wnt pathway activation in gastric cancer. *Cancer Res* 62, 3503-3506.
- Cole, M.F., Johnstone, S.E., Newman, J.J., Kagey, M.H., and Young, R.A. (2008). Tcf3 is an integral component of the core regulatory circuitry of embryonic stem cells. *Genes Dev* 22, 746-755.
- Collins, A.T., Berry, P.A., Hyde, C., Stower, M.J., and Maitland, N.J. (2005). Prospective identification of tumorigenic prostate cancer stem cells. *Cancer Res* 65, 10946-10951.
- Collins, A.T., Habib, F.K., Maitland, N.J., and Neal, D.E. (2001). Identification and isolation of human prostate epithelial stem cells based on $\alpha 2\beta 1$ -integrin expression. *Journal of Cell Science* 114, 3865-3872.
- Conacci-Sorrell, M.E., Ben-Yedidia, T., Shtutman, M., Feinstein, E., Einat, P., and Ben-Ze'ev, A. (2002). Nr-CAM is a target gene of the beta-catenin/LEF-1 pathway in melanoma and colon cancer and its expression enhances motility and confers tumorigenesis. *Genes Dev* 16, 2058-2072.
- Crawford, H.C., Fingleton, B.M., Rudolph-Owen, L.A., Goss, K.J., Rubinfeld, B., Polakis, P., and Matrisian, L.M. (1999). The metalloproteinase matrilysin is a target of beta-catenin transactivation in intestinal tumors. *Oncogene* 18, 2883-2891.
- CRUK (2014). Cancer Research UK.
- Daniels, D.L., and Weis, W.I. (2005). [beta]-catenin directly displaces Groucho/TLE repressors from Tcf/Lef in Wnt-mediated transcription activation. *Nat Struct Mol Biol* 12, 364-371.

- Davda, R., Thrasivoulou, C., Masters, J., and Ahmed, A. (2015). Abstract 2230: Wnt signaling in prostate cancer stem like cells. *Cancer Research* 75, 2230-2230.
- De Marzo, A.M., Meeker, A.K., Epstein, J.I., and Coffey, D.S. (1998). Prostate Stem Cell Compartments: Expression of the Cell Cycle Inhibitor p27Kip1 in Normal, Hyperplastic, and Neoplastic Cells. *The American Journal of Pathology* 153, 911-919.
- De Marzo, A.M., Platz, E.A., Sutcliffe, S., Xu, J., Gronberg, H., Drake, C.G., Nakai, Y., Isaacs, W.B., and Nelson, W.G. (2007). Inflammation in prostate carcinogenesis. *Nat Rev Cancer* 7, 256-269.
- Ding, X.W., Yan, J.J., An, P., Lu, P., and Luo, H.S. (2007). Aberrant expression of ether a go-go potassium channel in colorectal cancer patients and cell lines. *World J Gastroenterol* 13, 1257-1261.
- Diss, J.K., Archer, S.N., Hirano, J., Fraser, S.P., and Djamgoz, M.B. (2001). Expression profiles of voltage-gated Na(+) channel alpha-subunit genes in rat and human prostate cancer cell lines. *Prostate* 48, 165-178.
- Dong, Y.F., Soung do, Y., Schwarz, E.M., O'Keefe, R.J., and Drissi, H. (2006). Wnt induction of chondrocyte hypertrophy through the Runx2 transcription factor. *J Cell Physiol* 208, 77-86.
- Du, Q., Park, K.S., Guo, Z., He, P., Nagashima, M., Shao, L., Sahai, R., Geller, D.A., and Hussain, S.P. (2006). Regulation of human nitric oxide synthase 2 expression by Wnt beta-catenin signaling. *Cancer Res* 66, 7024-7031.
- Du, S.J., Purcell, S.M., Christian, J.L., McGrew, L.L., and Moon, R.T. (1995). Identification of distinct classes and functional domains of Wnts through expression of wild-type and chimeric proteins in *Xenopus* embryos. *Mol Cell Biol* 15, 2625-2634.
- Du, Y.C., Oshima, H., Oguma, K., Kitamura, T., Itadani, H., Fujimura, T., Piao, Y.S., Yoshimoto, T., Minamoto, T., Kotani, H., *et al.* (2009). Induction and down-regulation of Sox17 and its possible roles during the course of gastrointestinal tumorigenesis. *Gastroenterology* 137, 1346-1357.
- Evans, G.S., and Chandler, J.A. (1987). Cell proliferation studies in the rat prostate: II. The effects of castration and androgen-induced regeneration upon basal and secretory cell proliferation. *Prostate* 11, 339-351.
- Evans, M.J., and Kaufman, M.H. (1981). Establishment in culture of pluripotential cells from mouse embryos. *Nature*.
- Fagotto, F., Funayama, N., Gluck, U., and Gumbiner, B.M. (1996). Binding to cadherins antagonizes the signaling activity of beta-catenin during axis formation in *Xenopus*. *The Journal of Cell Biology* 132, 1105-1114.

- Fagotto, F., Glück, U., and Gumbiner, B.M. (1998). Nuclear localization signal-independent and importin/karyopherin-independent nuclear import of β -catenin. *Current Biology* 8, 181-190.
- Fearon, E.R., and Vogelstein, B. (1990). A GENETIC MODEL FOR COLORECTAL TUMORIGENESIS. *Cell* 61, 759-767.
- Ferlay, J., Shin, H.R., Bray, F., Forman, D., Mathers, C., and Parkin, D.M. (2010). Estimates of worldwide burden of cancer in 2008: GLOBOCAN 2008. *Int J Cancer* 127, 2893-2917.
- Fevr, T., Robine, S., Louvard, D., and Huelsken, J. (2007). Wnt/ β -Catenin Is Essential for Intestinal Homeostasis and Maintenance of Intestinal Stem Cells. *Molecular and Cellular Biology* 27, 7551-7559.
- Filali, M., Cheng, N., Abbott, D., Leontiev, V., and Engelhardt, J.F. (2002). Wnt-3A/ β -Catenin Signaling Induces Transcription from the LEF-1 Promoter. *Journal of Biological Chemistry* 277, 33398-33410.
- Flourakis, M., Lehen'kyi, V., Beck, B., Raphael, M., Vandenberghe, M., Abeele, F.V., Roudbaraki, M., Lepage, G., Mauroy, B., Romanin, C., *et al.* (2010). Orai1 contributes to the establishment of an apoptosis-resistant phenotype in prostate cancer cells. *Cell Death Dis* 16, 52.
- Galceran, J., Miyashita-Lin, E.M., Devaney, E., Rubenstein, J.L., and Grosschedl, R. (2000). Hippocampus development and generation of dentate gyrus granule cells is regulated by LEF1. *Development* 127, 469-482.
- Galceran, J., Sustmann, C., Hsu, S.C., Folberth, S., and Grosschedl, R. (2004). LEF1-mediated regulation of Delta-like1 links Wnt and Notch signaling in somitogenesis. *Genes Dev* 18, 2718-2723.
- Gary, D., Wei, W., Jinlong, S., Josipa, B., Ursula, F., Peter, S., Andrei, G., and Christof, N. (2005). Casein kinase 1 γ couples Wnt receptor activation to cytoplasmic signal transduction. *Nature* 438, 867-872.
- Gavert, N., Conacci-Sorrell, M., Gast, D., Schneider, A., Altevogt, P., Brabletz, T., and Ben-Ze'ev, A. (2005). L1, a novel target of beta-catenin signaling, transforms cells and is expressed at the invasive front of colon cancers. *J Cell Biol* 168, 633-642.
- Gerace, L., and Burke, B. (1988). Functional organization of the nuclear envelope. *Annual review of cell biology* 4, 335-374.
- Glass Ii, D.A., Bialek, P., Ahn, J.D., Starbuck, M., Patel, M.S., Clevers, H., Taketo, M.M., Long, F., McMahon, A.P., Lang, R.A., *et al.* (2005). Canonical Wnt Signaling in

Differentiated Osteoblasts Controls Osteoclast Differentiation. *Developmental Cell* 8, 751-764.

- Gonzalez-Sancho, J.M., Aguilera, O., Garcia, J.M., Pendas-Franco, N., Pena, C., Cal, S., Garcia de Herreros, A., Bonilla, F., and Munoz, A. (2005). The Wnt antagonist DICKKOPF-1 gene is a downstream target of beta-catenin/TCF and is downregulated in human colon cancer. *Oncogene* 24, 1098-1103.
- Gottardi, C.J., Wong, E., and Gumbiner, B.M. (2001). E-Cadherin Suppresses Cellular Transformation by Inhibiting β -Catenin Signaling in an Adhesion-Independent Manner. *The Journal of Cell Biology* 153, 1049-1060.
- Griffiths, J. (1889). Observations on the Anatomy of the Prostate. *Journal of Anatomy and Physiology* 23, 374-386.
- Gu, G., Yuan, J., Wills, M., and Kasper, S. (2007). Prostate cancer cells with stem cell characteristics reconstitute the original human tumor in vivo. *Cancer Res* 67, 4807-4815.
- Gubb, D., and Garcia, B. (1982). A genetic analysis of the determination of cuticular polarity during development in *Drosophila melanogaster*. *Journal of Embryology and Experimental Morphology* Vol. 68, 37-57.
- Guger, K.A., and Gumbiner, B.M. (1995). β -Catenin Has Wnt-like Activity and Mimics the Nieuwkoop Signaling Center in *Xenopus* Dorsal–Ventral Patterning. *Developmental Biology* 172, 115-125.
- Hallett, R.M., Kondratyev, M.K., Giacomelli, A.O., Nixon, A.M., Girgis-Gabardo, A., Ilieva, D., and Hassell, J.A. (2012). Small molecule antagonists of the Wnt/beta-catenin signaling pathway target breast tumor-initiating cells in a Her2/Neu mouse model of breast cancer. *PLoS One* 7, 28.
- Hämmerlein, A., Weiske, J., and Huber, O. (2005). A second protein kinase CK1-mediated step negatively regulates Wnt signalling by disrupting the lymphocyte enhancer factor-1/ β -catenin complex. *CMLS, Cell Mol Life Sci* 62, 606-618.
- Harper, L.J., Piper, K., Common, J., Fortune, F., and Mackenzie, I.C. (2007). Stem cell patterns in cell lines derived from head and neck squamous cell carcinoma. *Journal of Oral Pathology & Medicine* 36, 594-603.
- He, T.-C., Chan, T.A., Vogelstein, B., and Kinzler, K.W. (1999). PPAR δ Is an APC-Regulated Target of Nonsteroidal Anti-Inflammatory Drugs. *Cell* 99, 335-345.
- He, T.-C., Sparks, A.B., Rago, C., Hermeking, H., Zawel, L., da Costa, L.T., Morin, P.J., Vogelstein, B., and Kinzler, K.W. (1998). Identification of c-MYC as a Target of the APC Pathway. *Science* 281, 1509-1512.

- He, X., Saint-Jeannet, J.P., Wang, Y., Nathans, J., Dawid, I., and Varmus, H. (1997). A member of the frizzled protein family mediating axis induction by Wnt- 5A. *Science* 275, 1652-1654.
- Hendrix, N.D., Wu, R., Kuick, R., Schwartz, D.R., Fearon, E.R., and Cho, K.R. (2006). Fibroblast growth factor 9 has oncogenic activity and is a downstream target of Wnt signaling in ovarian endometrioid adenocarcinomas. *Cancer Res* 66, 1354-1362.
- Hoffmeyer, K., Raggioli, A., Rudloff, S., Anton, R., Hierholzer, A., Del Valle, I., Hein, K., Vogt, R., and Kemler, R. (2012). Wnt/beta-catenin signaling regulates telomerase in stem cells and cancer cells. *Science* 336, 1549-1554.
- Holland, J.D., Klaus, A., Garratt, A.N., and Birchmeier, W. (2013). Wnt signaling in stem and cancer stem cells. *Curr Opin Cell Biol* 25, 254-264.
- Horoszewicz, J.S., Leong, S.S., Kawinski, E., Karr, J.P., Rosenthal, H., Chu, T.M., Mirand, E.A., and Murphy, G.P. (1983). LNCaP model of human prostatic carcinoma. *Cancer Res* 43, 1809-1818.
- <http://www.salisbury.nhs.uk>.
<http://www.salisbury.nhs.uk/InformationForPatients/Departments/Urology/urologyproblems/PublishingImages/Lower%20Urinary%20Tract%20and%20the%20Prostate.jpg>
.
- Huang, X., Dubuc, A.M., Hashizume, R., Berg, J., He, Y., Wang, J., Chiang, C., Cooper, M.K., Northcott, P.A., Taylor, M.D., *et al.* (2012). Voltage-gated potassium channel EAG2 controls mitotic entry and tumor growth in medulloblastoma via regulating cell volume dynamics. *Genes & Development* 26, 1780-1796.
- Hudmon, A., and Schulman, H. (2002). Neuronal CA2+/calmodulin-dependent protein kinase II: the role of structure and autoregulation in cellular function. *Annu Rev Biochem* 71, 473-510.
- Huggins, C. (1942). EFFECT OF ORCHIECTOMY AND IRRADIATION ON CANCER OF THE PROSTATE. *Ann Surg* 115, 1192-1200.
- Innamaa, A., Jackson, L., Asher, V., van Schalkwyk, G., Warren, A., Keightley, A., Hay, D., Bali, A., Sowter, H., and Khan, R. (2013). Expression and effects of modulation of the K2P potassium channels TREK-1 (KCNK2) and TREK-2 (KCNK10) in the normal human ovary and epithelial ovarian cancer. *Clin Transl Oncol* 15, 910-918.
- Isaacs, J.T., Schulze, H., and Coffey, D.S. (1987). Development of androgen resistance in prostatic cancer. *Prog Clin Biol Res* 243A, 21-31.

- Ishikawa, H.O., Takeuchi, H., Haltiwanger, R.S., and Irvine, K.D. (2008). Four-jointed Is a Golgi Kinase That Phosphorylates a Subset of Cadherin Domains. *Science* 321, 401-404.
- Ishitani, T., Ninomiya-Tsuji, J., Nagai, S., Nishita, M., Meneghini, M., Barker, N., Waterman, M., Bowerman, B., Clevers, H., Shibuya, H., *et al.* (1999). The TAK1-NLK-MAPK-related pathway antagonizes signalling between beta-catenin and transcription factor TCF. *Nature* 399, 798-802.
- James, N.D., de Bono, J.S., Spears, M.R., Clarke, N.W., Mason, M.D., Dearnaley, D.P., Ritchie, A.W.S., Amos, C.L., Gilson, C., Jones, R.J., *et al.* (2017). Abiraterone for Prostate Cancer Not Previously Treated with Hormone Therapy. *New England Journal of Medicine* 377, 338-351.
- Jeter, C.R., Liu, B., Liu, X., Chen, X., Liu, C., Calhoun-Davis, T., Repass, J., Zaehres, H., Shen, J.J., and Tang, D.G. (2011). NANOG promotes cancer stem cell characteristics and prostate cancer resistance to androgen deprivation. *Oncogene* 30, 3833-3845.
- Jung, H.-C., and Kim, K. (2005). Identification of MYCBP as a β -catenin/LEF-1 target using DNA microarray analysis. *Life Sciences* 77, 1249-1262.
- Kaighn, M.E., Narayan, K.S., Ohnuki, Y., Lechner, J.F., and Jones, L.W. (1979). Establishment and characterization of a human prostatic carcinoma cell line (PC-3). *Invest Urol* 17, 16-23.
- Kasper, S. (2008). Exploring the Origins of the Normal Prostate and Prostate Cancer Stem Cell. *Stem Cell Reviews* 4, 193.
- Khaitan, D., Sankpal, U.T., Weksler, B., Meister, E.A., Romero, I.A., Couraud, P.O., and Ningaraj, N.S. (2009). Role of KCNMA1 gene in breast cancer invasion and metastasis to brain. *BMC Cancer* 9, 1471-2407.
- Khramtsov, A.I., Khramtsova, G.F., Tretiakova, M., Huo, D., Olopade, O.I., and Goss, K.H. (2010). Wnt/beta-catenin pathway activation is enriched in basal-like breast cancers and predicts poor outcome. *Am J Pathol* 176, 2911-2920.
- Kim, C.H., Oda, T., Itoh, M., Jiang, D., Artinger, K.B., Chandrasekharappa, S.C., Driever, W., and Chitnis, A.B. (2000). Repressor activity of Headless/Tcf3 is essential for vertebrate head formation. *Nature* 407, 913-916.
- Kim, C.J., Cho, Y.G., Jeong, S.W., Kim, Y.S., Kim, S.Y., Nam, S.W., Lee, S.H., Yoo, N.J., Lee, J.Y., and Park, W.S. (2004). Altered expression of KCNK9 in colorectal cancers. *Apmis* 112, 588-594.

- Kim, J.S., Crooks, H., Dracheva, T., Nishanian, T.G., Singh, B., Jen, J., and Waldman, T. (2002). Oncogenic beta-catenin is required for bone morphogenetic protein 4 expression in human cancer cells. *Cancer Res* 62, 2744-2748.
- Kimelman, D., and Xu, W. (2006). β -Catenin destruction complex: insights and questions from a structural perspective. *Oncogene* 25, 7482-7491.
- Kinzler, K., Nilbert, M., Su, L., Vogelstein, B., Bryan, T., Levy, D., Smith, K., Preisinger, A., Hedge, P., McKechnie, D., *et al.* (1991). Identification of FAP locus genes from chromosome 5q21. *Science* 253, 661-665.
- Kinzler, K.W., and Vogelstein, B. (1996). Lessons from hereditary colorectal cancer. *Cell* 87, 159-170.
- Klapholz-Brown, Z., Walmsley, G.G., Nusse, Y.M., Nusse, R., and Brown, P.O. (2007). Transcriptional Program Induced by Wnt Protein in Human Fibroblasts Suggests Mechanisms for Cell Cooperativity in Defining Tissue Microenvironments. *PLoS One* 2, e945.
- Klotz, L., Boccon-Gibod, L., Shore, N.D., Andreou, C., Persson, B.E., Cantor, P., Jensen, J.K., Olesen, T.K., and Schroder, F.H. (2008). The efficacy and safety of degarelix: a 12-month, comparative, randomized, open-label, parallel-group phase III study in patients with prostate cancer. *BJU Int* 102, 1531-1538.
- Koh, T.J., Bulitta, C.J., Fleming, J.V., Dockray, G.J., Varro, A., and Wang, T.C. (2000). Gastrin is a target of the beta-catenin/TCF-4 growth-signaling pathway in a model of intestinal polyposis. *J Clin Invest* 106, 533-539.
- Kolligs, F.T., Nieman, M.T., Winer, I., Hu, G., Van Mater, D., Feng, Y., Smith, I.M., Wu, R., Zhai, Y., Cho, K.R., *et al.* (2002). ITF-2, a downstream target of the Wnt/TCF pathway, is activated in human cancers with beta-catenin defects and promotes neoplastic transformation. *Cancer Cell* 1, 145-155.
- Kondo, T. (2007). Stem cell-like cancer cells in cancer cell lines. *Cancer Biomark* 3, 245-250.
- Korinek, V., Barker, N., Moerer, P., van Donselaar, E., Huls, G., Peters, P.J., and Clevers, H. (1998). Depletion of epithelial stem-cell compartments in the small intestine of mice lacking Tcf-4. *Nat Genet* 19, 379-383.
- Kramps, T., Peter, O., Brunner, E., Nellen, D., Froesch, B., Chatterjee, S., Murone, M., Züllig, S., and Basler, K. (2002). Wnt/Wingless Signaling Requires BCL9/Legless-Mediated Recruitment of Pygopus to the Nuclear β -Catenin-TCF Complex. *Cell* 109, 47-60.
- Kühl, M., Sheldahl, L.C., Malbon, C.C., and Moon, R.T. (2000). Ca²⁺/calmodulin-dependent protein kinase II is stimulated by Wnt and Frizzled homologs and

promotes ventral cell fates in *Xenopus*. *Journal of Biological Chemistry* 275, 12701-12711.

- Lapidot, T., Sirard, C., Vormoor, J., Murdoch, B., Hoang, T., Caceres-Cortes, J., Minden, M., Paterson, B., Caligiuri, M.A., and Dick, J.E. (1994). A cell initiating human acute myeloid leukaemia after transplantation into SCID mice. *Nature* 367, 645-648.
- Leanza, L., Henry, B., Sassi, N., Zoratti, M., Chandy, K.G., Gulbins, E., and Szabo, I. (2012). Inhibitors of mitochondrial Kv1.3 channels induce Bax/Bak-independent death of cancer cells. *EMBO Mol Med* 4, 577-593.
- Leow, C.C., Romero, M.S., Ross, S., Polakis, P., and Gao, W.Q. (2004). Hath1, down-regulated in colon adenocarcinomas, inhibits proliferation and tumorigenesis of colon cancer cells. *Cancer Res* 64, 6050-6057.
- Li, H., Chen, X., Calhoun-Davis, T., Claypool, K., and Tang, D.G. (2008). PC3 Human Prostate Carcinoma Cell Holoclonal Contain Self-renewing Tumor-Initiating Cells. *Cancer Research* 68, 1820-1825.
- Liu, C.C., Prior, J., Piwnica-Worms, D., and Bu, G. (2010). LRP6 overexpression defines a class of breast cancer subtype and is a target for therapy. *Proc Natl Acad Sci U S A* 107, 5136-5141.
- Liu, T.J., Sun, B.C., Zhao, X.L., Zhao, X.M., Sun, T., Gu, Q., Yao, Z., Dong, X.Y., Zhao, N., and Liu, N. (2013). CD133+ cells with cancer stem cell characteristics associates with vasculogenic mimicry in triple-negative breast cancer. *Oncogene* 32, 544-553.
- Liu, W., Dong, X., Mai, M., Seelan, R.S., Taniguchi, K., Krishnadath, K.K., Halling, K.C., Cunningham, J.M., Boardman, L.A., Qian, C., *et al.* (2000). Mutations in AXIN2 cause colorectal cancer with defective mismatch repair by activating beta-catenin/TCF signalling. *Nat Genet* 26, 146-147.
- Locke, M., Heywood, M., Fawell, S., and Mackenzie, I.C. (2005). Retention of Intrinsic Stem Cell Hierarchies in Carcinoma-Derived Cell Lines. *Cancer Research* 65, 8944.
- Lockhart-Mummery, P. (1925). CANCER AND HEREDITY. *The Lancet* 205, 427-429.
- Logan, C.Y., and Nusse, R. (2004). THE WNT SIGNALING PATHWAY IN DEVELOPMENT AND DISEASE. *Annual Review of Cell and Developmental Biology* 20, 781-810.
- M L Villereal, a., and Palfrey, H.C. (1989). Intracellular Calcium and Cell Function. *Annual Review of Nutrition* 9, 347-376.

- Ma, D., Yang, C.-h., McNeill, H., Simon, M.A., and Axelrod, J.D. (2003). Fidelity in planar cell polarity signalling. *Nature* 421, 543-547.
- MacDonald, B.T., Tamai, K., and He, X. (2009). Wnt/beta-catenin signaling: components, mechanisms, and diseases. *Dev Cell* 17, 9-26.
- Mackillop, W.J., Ciampi, A., Till, J.E., and Buick, R.N. (1983). A stem cell model of human tumor growth: implications for tumor cell clonogenic assays. *J Natl Cancer Inst* 70, 9-16.
- Mahoney, P.A., Weber, U., Onofrechuk, P., Biessmann, H., Bryant, P.J., and Goodman, C.S. (1991). The fat tumor suppressor gene in *Drosophila* encodes a novel member of the cadherin gene superfamily. *Cell* 67, 853-868.
- Malliri, A., Rygiel, T.P., van der Kammen, R.A., Song, J.Y., Engers, R., Hurlstone, A.F., Clevers, H., and Collard, J.G. (2006). The rac activator Tiam1 is a Wnt-responsive gene that modifies intestinal tumor development. *J Biol Chem* 281, 543-548.
- Mani, S.A., Guo, W., Liao, M.-J., Eaton, E.N., Ayyanan, A., Zhou, A.Y., Brooks, M., Reinhard, F., Zhang, C.C., and Shipitsin, M. (2008). The epithelial-mesenchymal transition generates cells with properties of stem cells. *Cell* 133, 704-715.
- Mann, B., Gelos, M., Siedow, A., Hanski, M.L., Gratchev, A., Ilyas, M., Bodmer, W.F., Moyer, M.P., Riecken, E.O., Buhr, H.J., *et al.* (1999). Target genes of β -catenin–T cell-factor/lymphoid-enhancer-factor signaling in human colorectal carcinomas. *Proceedings of the National Academy of Sciences* 96, 1603-1608.
- Marchenko, G.N., Marchenko, N.D., Leng, J., and Strongin, A.Y. (2002). Promoter characterization of the novel human matrix metalloproteinase-26 gene: regulation by the T-cell factor-4 implies specific expression of the gene in cancer cells of epithelial origin. *Biochem J* 363, 253-262.
- Matakatsu, H., and Blair, S.S. (2004). Interactions between Fat and Dachshaus and the regulation of planar cell polarity in the *Drosophila* wing. *Development* 131, 3785-3794.
- Mazzanti, M., Bustamante, J.O., and Oberleithner, H. (2001). Electrical dimension of the nuclear envelope. *Physiol Rev* 81, 1-19.
- McAndrew, D., Grice, D.M., Peters, A.A., Davis, F.M., Stewart, T., Rice, M., Smart, C.E., Brown, M.A., Kenny, P.A., Roberts-Thomson, S.J., *et al.* (2011). ORAI1-Mediated Calcium Influx in Lactation and in Breast Cancer. *Molecular Cancer Therapeutics* 10, 448-460.

- McCulloch, E.A., Buick, R.N., Curtis, J.E., Messner, H.A., and Senn, J.S. (1981). The heritable nature of clonal characteristics in acute myeloblastic leukemia. *Blood* 58, 105-109.
- McMahan, A.P., and Moon, R.T. (1989). Ectopic expression of the proto-oncogene int-1 in *Xenopus* embryos leads to duplication of the embryonic axis. *Cell* 58, 1075-1084.
- McNeal, J.E. (1988). Normal histology of the prostate. *Am J Surg Pathol* 12, 619-633.
- Melchionda, M., Pittman, J.K., Mayor, R., and Patel, S. (2016). Ca^{2+}/H^{+} exchange by acidic organelles regulates cell migration in vivo. *The Journal of Cell Biology* 212, 803-813.
- Miller, S.J., Lavker, R.M., and Sun, T.T. (2005). Interpreting epithelial cancer biology in the context of stem cells: tumor properties and therapeutic implications. *Biochim Biophys Acta* 1756, 25-52.
- Miwa, N., Furuse, M., Tsukita, S., Niikawa, N., Nakamura, Y., and Furukawa, Y. (2001). Involvement of claudin-1 in the beta-catenin/Tcf signaling pathway and its frequent upregulation in human colorectal cancers. *Oncol Res* 12, 469-476.
- Mohler, P.J., and Hund, T.J. (2011). Role of CaMKII in cardiovascular health, disease, and arrhythmia. *Heart Rhythm* 8, 142-144.
- Molenaar, M., van de Wetering, M., Oosterwegel, M., Peterson-Maduro, J., Godsave, S., Korinek, V., Roose, J., Destree, O., and Clevers, H. (1996). XTcf-3 transcription factor mediates beta-catenin-induced axis formation in *Xenopus* embryos. *Cell* 86, 391-399.
- Monteith, G.R., Davis, F.M., and Roberts-Thomson, S.J. (2012). Calcium Channels and Pumps in Cancer: Changes and Consequences. *Journal of Biological Chemistry* 287, 31666-31673.
- Moon, R.T., Campbell, R.M., Christian, J.L., McGrew, L.L., Shih, J., and Fraser, S. (1993). Xwnt-5A: a maternal Wnt that affects morphogenetic movements after overexpression in embryos of *Xenopus laevis*. *Development* 119, 97-111.
- Morin, P.J., Sparks, A.B., Korinek, V., Barker, N., Clevers, H., Vogelstein, B., and Kinzler, K.W. (1997). Activation of β -Catenin-Tcf Signaling in Colon Cancer by Mutations in β -Catenin or APC. *Science* 275, 1787-1790.
- Motoyoshi, I., Nishida, S., Sharan, L., and Adelson, E.H. (2007). Image statistics and the perception of surface qualities. *Nature* 447, 206-209.
- Munemitsu, S., Albert, I., Souza, B., Rubinfeld, B., and Polakis, P. (1995). Regulation of intracellular beta-catenin levels by the adenomatous polyposis coli (APC) tumor-

suppressor protein. *Proceedings of the National Academy of Sciences* 92, 3046-3050.

- Murphy, R. (2012). The quest for quantitative microscopy. *Nat Meth* 9, 627-627.
- Niemann, S., Zhao, C., Pascu, F., Stahl, U., Aulepp, U., Niswander, L., Weber, J.L., and Muller, U. (2004). Homozygous WNT3 mutation causes tetra-amelia in a large consanguineous family. *Am J Hum Genet* 74, 558-563.
- Nishisho, I., Nakamura, Y., Miyoshi, Y., Miki, Y., Ando, H., Horii, A., Koyama, K., Utsunomiya, J., Baba, S., and Hedge, P. (1991). Mutations of chromosome 5q21 genes in FAP and colorectal cancer patients. *Science* 253, 665-669.
- Nusse, R. (2008). Wnt signaling and stem cell control. *Cell Res* 18, 523-527.
- Oishi, I., Suzuki, H., Onishi, N., Takada, R., Kani, S., Ohkawara, B., Koshida, I., Suzuki, K., Yamada, G., Schwabe, G.C., *et al.* (2003). The receptor tyrosine kinase Ror2 is involved in non-canonical Wnt5a/JNK signalling pathway. *Genes to Cells* 8, 645-654.
- Palaparti, A., Baratz, A., and Stifani, S. (1997). The Groucho/Transducin-like Enhancer of split Transcriptional Repressors Interact with the Genetically Defined Amino-terminal Silencing Domain of Histone H3. *Journal of Biological Chemistry* 272, 26604-26610.
- Patrawala, L., Calhoun, T., Schneider-Broussard, R., Li, H., Bhatia, B., Tang, S., Reilly, J.G., Chandra, D., Zhou, J., Claypool, K., *et al.* (2006). Highly purified CD44+ prostate cancer cells from xenograft human tumors are enriched in tumorigenic and metastatic progenitor cells. *Oncogene* 25, 1696-1708.
- Pellegrini, G., Golisano, O., Paterna, P., Lambiase, A., Bonini, S., Rama, P., and De Luca, M. (1999). Location and clonal analysis of stem cells and their differentiated progeny in the human ocular surface. *J Cell Biol* 145, 769-782.
- Perin, E.C., and Silva, G.V. (2006). What are stem cells and what do they do? An essential guide to cardiac cell therapy, 3-12.
- Petrou, T., Olsen, H.L., Thrasivoulou, C., Masters, J.R., Ashmore, J.F., and Ahmed, A. (2017). Intracellular Calcium Mobilization in Response to Ion Channel Regulators via a Calcium-Induced Calcium Release Mechanism. *Journal of Pharmacology and Experimental Therapeutics* 360, 378-387.
- Pfeiffer, M.J., and Schalken, J.A. (2010). Stem cell characteristics in prostate cancer cell lines. *Eur Urol* 57, 246-254.
- Pinto, D., Gregorieff, A., Begthel, H., and Clevers, H. (2003). Canonical Wnt signals are essential for homeostasis of the intestinal epithelium. *Genes & Development* 17, 1709-1713.

- Pittenger, M.F., Mackay, A.M., Beck, S.C., Jaiswal, R.K., Douglas, R., Mosca, J.D., Moorman, M.A., Simonetti, D.W., Craig, S., and Marshak, D.R. (1999). Multilineage Potential of Adult Human Mesenchymal Stem Cells. *Science* 284, 143-147.
- Potier, M., Joulin, V., Roger, S., Besson, P., Jourdan, M.L., Leguennec, J.Y., Bougnoux, P., and Vandier, C. (2006). Identification of SK3 channel as a new mediator of breast cancer cell migration. *Mol Cancer Ther* 5, 2946-2953.
- Potten, C.S., and Loeffler, M. (1990). Stem cells: attributes, cycles, spirals, pitfalls and uncertainties. Lessons for and from the crypt. *Development* 110, 1001-1020.
- Prostate cancer UK (2015).
- PubChem (2017).
- Puck, T.T., and Marcus, P.I. (1955). A RAPID METHOD FOR VIABLE CELL TITRATION AND CLONE PRODUCTION WITH HELA CELLS IN TISSUE CULTURE: THE USE OF X-IRRADIATED CELLS TO SUPPLY CONDITIONING FACTORS. *Proceedings of the National Academy of Sciences of the United States of America* 41, 432-437.
- Rasband, W.S. (2015). ImageJ.
- Reya, T., and Clevers, H. (2005). Wnt signalling in stem cells and cancer. *Nature* 434, 843-850.
- Reya, T., Duncan, A.W., Ailles, L., Domen, J., Scherer, D.C., Willert, K., Hintz, L., Nusse, R., and Weissman, I.L. (2003). A role for Wnt signalling in self-renewal of haematopoietic stem cells. *Nature* 423, 409-414.
- Reya, T., Morrison, S.J., Clarke, M.F., and Weissman, I.L. (2001a). Stem cells, cancer, and cancer stem cells. *Nature* 414, 105-111.
- Reya, T., Morrison, S.J., Clarke, M.F., and Weissman, I.L. (2001b). Stem cells, cancer, and cancer stem cells. *Nature* 414, 105-111.
- Richardson, G.D., Robson, C.N., Lang, S.H., Neal, D.E., Maitland, N.J., and Collins, A.T. (2004). CD133, a novel marker for human prostatic epithelial stem cells. *J Cell Sci* 117, 3539-3545.
- Rieger, M.E., Sims, A.H., Coats, E.R., Clarke, R.B., and Briegel, K.J. (2010). The embryonic transcription cofactor LBH is a direct target of the Wnt signaling pathway in epithelial development and in aggressive basal subtype breast cancers. *Mol Cell Biol* 30, 4267-4279.
- Rockman, S.P., Currie, S.A., Ciavarella, M., Vincan, E., Dow, C., Thomas, R.J., and Phillips, W.A. (2001). Id2 is a target of the beta-catenin/T cell factor pathway in colon carcinoma. *J Biol Chem* 276, 45113-45119.

- Rodgers CH, C.D., Cunha G, Grayhack JT, Hinman F Jr, Horton R, ed. (1987). Control of cell proliferation and cell death in the normal and neoplastic prostate: a stem cell model. (Washington, DC, US Department of Health and Human Services).
- Rodilla, V., Villanueva, A., Obrador-Hevia, A., Robert-Moreno, A., Fernandez-Majada, V., Grilli, A., Lopez-Bigas, N., Bellora, N., Alba, M.M., Torres, F., *et al.* (2009). Jagged1 is the pathological link between Wnt and Notch pathways in colorectal cancer. *Proc Natl Acad Sci U S A* 106, 6315-6320.
- Roose, J., Huls, G., Beest, M.v., Moerer, P., Horn, K.v.d., Goldschmeding, R., Logtenberg, T., and Clevers, H. (1999). Synergy Between Tumor Suppressor APC and the β -Catenin-Tcf4 Target Tcf1. *Science* 285, 1923-1926.
- RSPGB, B. (2015). British National Formulary. (London, BMJ Group and Pharmaceutical Press.).
- Ruggieri, P., Mangino, G., Fioretti, B., Catacuzzeno, L., Puca, R., Ponti, D., Miscusi, M., Franciolini, F., Ragona, G., and Calogero, A. (2012). The Inhibition of KCa3.1 Channels Activity Reduces Cell Motility in Glioblastoma Derived Cancer Stem Cells. *PLoS One* 7.
- Ryan, C.J., Smith, M.R., de Bono, J.S., Molina, A., Logothetis, C.J., de Souza, P., Fizazi, K., Mainwaring, P., Piulats, J.M., Ng, S., *et al.* (2013). Abiraterone in metastatic prostate cancer without previous chemotherapy. *N Engl J Med* 368, 138-148.
- Schalken, J.A., and van Leenders, G. (2003). Cellular and molecular biology of the prostate: stem cell biology. *Urology* 62, 11-20.
- Scoville, D.H., Sato, T., He, X.C., and Li, L. (2008). Current view: intestinal stem cells and signaling. *Gastroenterology* 134, 849-864.
- Sharifi, N., Gulley, J.L., and Dahut, W.L. (2010). An update on androgen deprivation therapy for prostate cancer. *Endocr Relat Cancer* 17, R305-315.
- Sharma, M., Jamieson, C., Johnson, M., Molloy, M.P., and Henderson, B.R. (2012). Specific Armadillo Repeat Sequences Facilitate β -Catenin Nuclear Transport in Live Cells via Direct Binding to Nucleoporins Nup62, Nup153, and RanBP2/Nup358. *Journal of Biological Chemistry* 287, 819-831.
- Sheldahl, L.C., Park, M., Malbon, C.C., and Moon, R.T. (1999). Protein kinase C is differentially stimulated by Wnt and Frizzled homologs in aG-protein-dependent manner. *Current Biology* 9, 695-S691.
- Sheldahl, L.C., Slusarski, D.C., Pandur, P., Miller, J.R., Kühl, M., and Moon, R.T. (2003). Dishevelled activates Ca²⁺ flux, PKC, and CamKII in vertebrate embryos. *The Journal of Cell Biology* 161, 769-777.

- Shimokawa, T., Furukawa, Y., Sakai, M., Li, M., Miwa, N., Lin, Y.M., and Nakamura, Y. (2003). Involvement of the FGF18 gene in colorectal carcinogenesis, as a novel downstream target of the beta-catenin/T-cell factor complex. *Cancer Res* 63, 6116-6120.
- Shitashige, M., Satow, R., Honda, K., Ono, M., Hirohashi, S., and Yamada, T. (2008). Regulation of Wnt signaling by the nuclear pore complex. *Gastroenterology* 134, 1961-1971.
- Shtutman, M., Zhurinsky, J., Simcha, I., Albanese, C., D'Amico, M., Pestell, R., and Ben-Ze'ev, A. (1999). The cyclin D1 gene is a target of the β -catenin/LEF-1 pathway. *Proceedings of the National Academy of Sciences* 96, 5522-5527.
- Si, W., Kang, Q., Luu, H.H., Park, J.K., Luo, Q., Song, W.-X., Jiang, W., Luo, X., Li, X., Yin, H., *et al.* (2006). CCN1/Cyr61 Is Regulated by the Canonical Wnt Signal and Plays an Important Role in Wnt3A-Induced Osteoblast Differentiation of Mesenchymal Stem Cells. *Molecular and Cellular Biology* 26, 2955-2964.
- Siegfried, E., and Perrimon, N. (1994). *Drosophila wingless*: A paradigm for the function and mechanism of Wnt signaling. *BioEssays* 16, 395-404.
- sigmaaldrich (2017).
- Slusarski, D.C., Corces, V.G., and Moon, R.T. (1997a). Interaction of Wnt and a Frizzled homologue triggers G-protein-linked phosphatidylinositol signalling. *Nature* 390, 410-413.
- Slusarski, D.C., Yang-Snyder, J., Busa, W.B., and Moon, R.T. (1997b). Modulation of Embryonic Intracellular Ca²⁺ Signaling by Wnt-5A. *Developmental Biology* 182, 114-120.
- Smits, R., Kielman, M.F., Breukel, C., Zurcher, C., Neufeld, K., Jagmohan-Changur, S., Hofland, N., van Dijk, J., White, R., Edelmann, W., *et al.* (1999). Apc1638T: a mouse model delineating critical domains of the adenomatous polyposis coli protein involved in tumorigenesis and development. *Genes & Development* 13, 1309-1321.
- Spears, E., and Neufeld, K.L. (2011). Novel double-negative feedback loop between adenomatous polyposis coli and Musashi1 in colon epithelia. *J Biol Chem* 286, 4946-4950.
- Spencer, G.J., Utting, J.C., Etheridge, S.L., Arnett, T.R., and Genever, P.G. (2006). Wnt signalling in osteoblasts regulates expression of the receptor activator of NFkappaB ligand and inhibits osteoclastogenesis in vitro. *J Cell Sci* 119, 1283-1296.
- Staudacher, I., Jehle, J., Staudacher, K., Pledl, H.-W., Lemke, D., Schweizer, P.A., Becker, R., Katus, H.A., and Thomas, D. (2014). Herg K⁺ Channel-

Dependent Apoptosis and Cell Cycle Arrest in Human Glioblastoma Cells. *PLoS One* 9, e88164.

- Stifani, S., Blaumueller, C.M., Redhead, N.J., Hill, R.E., and Artavanis-Tsakonas, S. (1992). Human homologs of a *Drosophila* Enhancer of split gene product define a novel family of nuclear proteins. *Nat Genet* 2, 119-127.
- Stone, K.R., Mickey, D.D., Wunderli, H., Mickey, G.H., and Paulson, D.F. (1978). Isolation of a human prostate carcinoma cell line (DU 145). *Int J Cancer* 21, 274-281.
- Sustmann, C., Flach, H., Ebert, H., Eastman, Q., and Grosschedl, R. (2008). Cell-Type-Specific Function of BCL9 Involves a Transcriptional Activation Domain That Synergizes with β -Catenin. *Molecular and Cellular Biology* 28, 3526-3537.
- Sweeney, C.J., Chen, Y.-H., Carducci, M., Liu, G., Jarrard, D.F., Eisenberger, M., Wong, Y.-N., Hahn, N., Kohli, M., Cooney, M.M., *et al.* (2015). Chemohormonal Therapy in Metastatic Hormone-Sensitive Prostate Cancer. *New England Journal of Medicine* 373, 737-746.
- Tai, M.-H., Chang, C.-C., Olson, L.K., and Trosko, J.E. (2005). Oct4 expression in adult human stem cells: evidence in support of the stem cell theory of carcinogenesis. *Carcinogenesis* 26, 495-502.
- Takahashi, S., Watanabe, T., Okada, M., Inoue, K., Ueda, T., Takada, I., Watabe, T., Yamamoto, Y., Fukuda, T., Nakamura, T., *et al.* (2011). Noncanonical Wnt signaling mediates androgen-dependent tumor growth in a mouse model of prostate cancer. *Proceedings of the National Academy of Sciences* 108, 4938-4943.
- Tan, G., Sun, S.Q., and Yuan, D.L. (2008). Expression of Kir 4.1 in human astrocytic tumors: correlation with pathologic grade. *Biochem Biophys Res Commun* 367, 743-747.
- ten Berge, D., Brugmann, S.A., Helms, J.A., and Nusse, R. (2008a). Wnt and FGF signals interact to coordinate growth with cell fate specification during limb development. *Development* 135, 3247-3257.
- ten Berge, D., Koole, W., Fuerer, C., Fish, M., Eroglu, E., and Nusse, R. (2008b). Wnt Signaling Mediates Self-Organization and Axis Formation in Embryoid Bodies. *Cell Stem Cell* 3, 508-518.
- Tetsu, O., and McCormick, F. (1999). β -Catenin regulates expression of cyclin D1 in colon carcinoma cells. *Nature* 398, 422-426.
- Tetteh, P.W., Farin, H.F., and Clevers, H. (2015). Plasticity within stem cell hierarchies in mammalian epithelia. *Trends Cell Biol* 25, 100-108.

- Theisen, H., Purcell, J., Bennett, M., Kansagara, D., Syed, A., and Marsh, J.L. (1994). *dishevelled* is required during wingless signaling to establish both cell polarity and cell identity. *Development* 120, 347-360.
- Thrasivoulou, C., Millar, M., and Ahmed, A. (2013). Activation of intracellular calcium by multiple Wnt ligands and translocation of beta-catenin into the nucleus: a convergent model of Wnt/Ca²⁺ and Wnt/beta-catenin pathways. *J Biol Chem* 288, 35651-35659.
- Tolwinski, N.S., and Wieschaus, E. (2001). Armadillo nuclear import is regulated by cytoplasmic anchor Axin and nuclear anchor dTCF/Pan. *Development* 128, 2107-2117.
- Torres, M.A., Yang-Snyder, J.A., Purcell, S.M., DeMarais, A.A., McGrew, L.L., and Moon, R.T. (1996). Activities of the Wnt-1 class of secreted signaling factors are antagonized by the Wnt-5A class and by a dominant negative cadherin in early *Xenopus* development. *Journal of Cell Biology* 133, 1123-1137.
- Tree, D.R.P., Shulman, J.M., Rousset, R., Scott, M.P., Gubb, D., and Axelrod, J.D. (2002). Prickle Mediates Feedback Amplification to Generate Asymmetric Planar Cell Polarity Signaling. *Cell* 109, 371-381.
- Tudor, D., Locke, M., Owen-Jones, E., and Mackenzie, I.C. (2006). Intrinsic Patterns of Behavior of Epithelial Stem Cells. *Journal of Investigative Dermatology Symposium Proceedings* 9, 208-214.
- Turner, K.L., Honasoge, A., Robert, S.M., McFerrin, M.M., and Sontheimer, H. (2014). A proinvasive role for the Ca⁽²⁺⁾-activated K⁽⁺⁾ channel KCa3.1 in malignant glioma. *Glia* 62, 971-981.
- Uematsu, K., He, B., You, L., Xu, Z., McCormick, F., and Jablons, D.M. (2003). Activation of the Wnt pathway in non small cell lung cancer: evidence of *dishevelled* overexpression. *Oncogene* 22, 7218-7221.
- Van de Wetering, M., Cavallo, R., Dooijes, D., Van Beest, M., Van Es, J., Loureiro, J., Ypma, A., Hursh, D., Jones, T., Bejsovec, A., *et al.* (1997). Armadillo coactivates transcription driven by the product of the *Drosophila* segment polarity gene dTCF. *Cell* 88, 789-799.
- van de Wetering, M., Sancho, E., Verweij, C., de Lau, W., Oving, I., Hurlstone, A., van der Horn, K., Batlle, E., Coudreuse, D., Haramis, A.-P., *et al.* (2002). The β -Catenin/TCF-4 Complex Imposes a Crypt Progenitor Phenotype on Colorectal Cancer Cells. *Cell* 111, 241-250.
- Verbeek, S., Izon, D., Hofhuis, F., Robanus-Maandag, E., te Riele, H., van de Wetering, M., Oosterwegel, M., Wilson, A., MacDonald, H.R., and Clevers, H. (1995).

An HMG-box-containing T-cell factor required for thymocyte differentiation. *Nature* 374, 70-74.

- Walker, J.W.T. (1904). The Surgical Anatomy of the Normal and Enlarged Prostate, and the Operation of Suprapubic Prostatectomy. *British Medical Journal* 2, 62-66.
- Wang, Q., Symes, A.J., Kane, C.A., Freeman, A., Nariculam, J., Munson, P., Thrasivoulou, C., Masters, J.R.W., and Ahmed, A. (2010). A Novel Role for Wnt/Ca(2+) Signaling in Actin Cytoskeleton Remodeling and Cell Motility in Prostate Cancer. *PLoS One* 5, e10456.
- Wang, S., Garcia, A.J., Wu, M., Lawson, D.A., Witte, O.N., and Wu, H. (2006). Pten deletion leads to the expansion of a prostatic stem/progenitor cell subpopulation and tumor initiation. *Proc Natl Acad Sci U S A* 103, 1480-1485.
- WCRF (2015
-). Prostate cancer statistics.
- Wielenga, V.J., Smits, R., Korinek, V., Smit, L., Kielman, M., Fodde, R., Clevers, H., and Pals, S.T. (1999). Expression of CD44 in Apc and Tcf mutant mice implies regulation by the WNT pathway. *Am J Pathol* 154, 515-523.
- Willert, J., Epping, M., Pollack, J.R., Brown, P.O., and Nusse, R. (2002). A transcriptional response to Wnt protein in human embryonic carcinoma cells. *BMC Dev Biol* 2, 8.
- Willert, K., Brown, J.D., Danenberg, E., Duncan, A.W., Weissman, I.L., Reya, T., Yates, J.R., and Nusse, R. (2003). Wnt proteins are lipid-modified and can act as stem cell growth factors. *Nature* 423, 448-452.
- Williams, R.T., Manji, S.S., Parker, N.J., Hancock, M.S., Van Stekelenburg, L., Eid, J.P., Senior, P.V., Kazenwadel, J.S., Shandala, T., Saint, R., *et al.* (2001). Identification and characterization of the STIM (stromal interaction molecule) gene family: coding for a novel class of transmembrane proteins. *Biochem J* 357, 673-685.
- Wissmann, C., Wild, P.J., Kaiser, S., Roepcke, S., Stoehr, R., Woenckhaus, M., Kristiansen, G., Hsieh, J.C., Hofstaedter, F., Hartmann, A., *et al.* (2003). WIF1, a component of the Wnt pathway, is down-regulated in prostate, breast, lung, and bladder cancer. *J Pathol* 201, 204-212.
- Wolda, S.L., Moody, C.J., and Moon, R.T. (1993). Overlapping Expression of Xwnt-3A and Xwnt-1 in Neural Tissue of *Xenopus laevis* Embryos. *Developmental Biology* 155, 46-57.
- Wong, G.T., Gavin, B.J., and McMahon, A.P. (1994). Differential transformation of mammary epithelial cells by Wnt genes. *Molecular and Cellular Biology* 14, 6278-6286.

- Wong, L.L., and Adler, P.N. (1993). Tissue polarity genes of *Drosophila* regulate the subcellular location for prehair initiation in pupal wing cells. *Journal of Cell Biology* 123, 209-221.
- Xin, L., Lawson, D.A., and Witte, O.N. (2005). The Sca-1 cell surface marker enriches for a prostate-regenerating cell subpopulation that can initiate prostate tumorigenesis. *Proceedings of the National Academy of Sciences of the United States of America* 102, 6942-6947.
- Xin, L., Lukacs, R.U., Lawson, D.A., Cheng, D., and Witte, O.N. (2007). Self-Renewal and Multilineage Differentiation In Vitro from Murine Prostate Stem Cells. *STEM CELLS* 25, 2760-2769.
- Yamada, M., Ohnishi, J., Ohkawara, B., Iemura, S., Satoh, K., Hyodo-Miura, J., Kawachi, K., Natsume, T., and Shibuya, H. (2006). NARF, an Nemo-like Kinase (NLK)-associated Ring Finger Protein Regulates the Ubiquitylation and Degradation of T Cell Factor/Lymphoid Enhancer Factor (TCF/LEF). *Journal of Biological Chemistry* 281, 20749-20760.
- Yamamoto, H., Masters, J.R., Dasgupta, P., Chandra, A., Popert, R., Freeman, A., and Ahmed, A. (2012). CD49f is an efficient marker of monolayer- and spheroid colony-forming cells of the benign and malignant human prostate. *PLoS One* 7, 12.
- Yamamoto, H., Oue, N., Sato, A., Hasegawa, Y., Matsubara, A., Yasui, W., and Kikuchi, A. (2010). Wnt5a signaling is involved in the aggressiveness of prostate cancer and expression of metalloproteinase. *Oncogene* 29, 2036-2046.
- Yan, D., Wiesmann, M., Rohan, M., Chan, V., Jefferson, A.B., Guo, L., Sakamoto, D., Caothien, R.H., Fuller, J.H., Reinhard, C., *et al.* (2001). Elevated expression of axin2 and hnk2 mRNA provides evidence that Wnt/beta-catenin signaling is activated in human colon tumors. *Proc Natl Acad Sci U S A* 98, 14973-14978.
- Yang, J., Zhang, W., Evans, P.M., Chen, X., He, X., and Liu, C. (2006). Adenomatous Polyposis Coli (APC) Differentially Regulates β -Catenin Phosphorylation and Ubiquitination in Colon Cancer Cells. *Journal of Biological Chemistry* 281, 17751-17757.
- Zhang, K., and Waxman, D.J. (2010). PC3 prostate tumor-initiating cells with molecular profile FAM65B(high)/MFI2(low)/LEF1(low) increase tumor angiogenesis. *Molecular Cancer* 9, 319-319.
- Zhang, X., Gaspard, J.P., and Chung, D.C. (2001). Regulation of Vascular Endothelial Growth Factor by the Wnt and K-ras Pathways in Colonic Neoplasia. *Cancer Research* 61, 6050-6054.

- Zhou, C., Liu, S., Zhou, X., Xue, L., Quan, L., Lu, N., Zhang, G., Bai, J., Wang, Y., Liu, Z., *et al.* (2005). Overexpression of human pituitary tumor transforming gene (hPTTG), is regulated by beta-catenin /TCF pathway in human esophageal squamous cell carcinoma. *Int J Cancer* 113, 891-898.
- Zon, L.I. (2008). Intrinsic and extrinsic control of haematopoietic stem-cell self-renewal. *Nature* 453, 306-313.

Reflection

I have learnt a great deal from undertaking this research project. I have vastly extended my knowledge of cell biology, improved my writing and statistical skills and gained experience in time management and team working. I have a greater appreciation of, and huge admiration for scientists working on cancer biology around the world to further our understanding of, and develop therapies for this disease. I hope this work has extended evidence for calcium release in Wnt signalling, and set a basis for further exploration of the use of MPRCs in malignancy.